

**INVESTIGATION INTO THE  
IMMUNOLOGICAL EFFECTS OF  
CHROMIUM AND COBALT IONS AND  
WEAR DEBRIS RELEASED FROM METAL-  
ON-METAL HIP IMPLANTS**

by

**MOEED AKBAR**

2011

THIS THESIS IS SUBMITTED IN PARTIAL FULFILMENT  
FOR THE DEGREE OF  
**DOCTOR OF PHILOSOPHY IN BIOENGINEERING**

BIOENGINEERING UNIT  
WOLFSON CENTRE  
106 ROTTENROW  
UNIVERSITY OF STRATHCLYDE  
GLASGOW G4 0NW

THIS THESIS IS THE RESULT OF THE AUTHOR'S ORIGINAL RESEARCH. IT HAS BEEN COMPOSED BY THE AUTHOR AND HAS NOT BEEN PREVIOUSLY SUBMITTED FOR EXAMINATION, WHICH HAS LEAD TO THE AWARD OF A DEGREE.

THE COPYRIGHT OF THIS THESIS BELONGS TO THE AUTHOR UNDER THE TERMS OF THE UNITED KINGDOM COPYRIGHT ACTS AS QUALIFIED BY UNIVERSITY OF STRATHCLYDE REGULATION 3.50. DUE ACKNOWLEDGEMENT MUST ALWAYS BE MADE OF THE USE OF ANY MATERIAL CONTAINED IN, OR DERIVED FROM, THIS THESIS.

**MOEED AKBAR**

## Acknowledgements

I would like to thank my supervisors Professors MH Grant and JM Brewer for their advice, encouragement, insight and support. I am extremely grateful for the valuable time they spared throughout this project. I am also indebted to Mr. Dominic Meek and Sister Helen Murray for arranging the delivery of the samples and collating patient data as well as their support and advice.

I would also like to thank Mrs C Henderson, Mr. B Cartlidge, and Mrs E Goldie for their technical support and advice. I am tremendously grateful to Mrs C Henderson, in particular, for the continuous support and A-Z assistance within the lab. I would also like to thank my colleagues within the lab for their support, friendship and laughter. In particular, I would like to thank Dr G Afolaranmi for the metal ion analysis. I also wish to express my heartfelt gratitude to my former colleagues in the CFB and now at the University of Glasgow. Whilst the humour was extremely poor, the level of assistance and knowledge was exceptional.

In addition, I am also immensely appreciative of the help, support and guidance Dr A Fraser, University of Glasgow, provided in relation to the gene expression experiment. In particular the encouragement and kind words in relation to publication were enormously welcome.

I am also very grateful to the staff at the Biological Procedures Unit for all their help and advice with regards to the *in vivo* model.

I would also like to thank the EPSRC for helping fund my PhD. I am indebted to DePuy International, Leeds, UK for the additional financial support provided to the project. Special thanks to Dr. Allan Ritchie and Professor Graham Isaac, Dr. Cath Hardaker and Dr. Ken Brummit of DePuy International for their constant support and suggestions throughout the course of this project. I would specifically like to thank Dr. Cath Hardaker for arranging the production of the ASR wear debris.

I am also extremely thankful to all my friends whose presence, and the odd 'spontaneous', has made me enjoy my time in the Bioengineering Unit. Finally, I cannot thank my family enough for their endless support through a period that has been the happiest and saddest of our lives.

## Abstract

Recent reports have increased awareness of metal ions and particulate wear debris released from metal-on-metal (MoM) hip implants. These ions and wear debris disseminate into distant organs via the circulation and can induce adverse immunological effects.

In order to assess the toxicity of metal ions ( $\text{Cr}^{6+}$  and  $\text{Co}^{2+}$ ) released from MoM implants, U937 cells and primary human lymphocytes were exposed to these ions at clinically relevant concentrations *in vitro*. In addition, artificially produced CoCr wear debris was implanted into mice to assess the dissemination of metal into the circulation and organs as well as to examine local and systemic immunological effects. Finally, two clinical trials were undertaken to determine whether MoM hip arthroplasty led to a reduction in the number of circulating white blood cells (WBCs) in patients, and whether this was due to an increase in the levels of blood metal ions.

The *in vitro* data demonstrated that exposure to  $\geq 0.1 \mu\text{M Cr}^{6+}$  and  $\geq 1 \mu\text{M Co}^{2+}$  led to decreased U937 cell viability after 24 hr. Flow cytometric analysis showed that reduced viability was due to metal ions inducing apoptosis.

In addition, resting and anti-CD3 activated primary human lymphocytes exposed to 10 and 100  $\mu\text{M Cr}^{6+}$  showed significantly decreased cell viability and increased apoptosis, *in vitro*. The exposure of resting lymphocytes to 100  $\mu\text{M Co}^{2+}$  resulted in significant decreases in cell viability accompanied by a significant increase in apoptosis. Activated lymphocytes also showed this response after exposure to 100  $\mu\text{M Co}^{2+}$ ; in fact, activated cells were significantly more sensitive to  $\text{Co}^{2+}$  toxicity. Exposure to 10  $\mu\text{M Co}^{2+}$  led to significant decreases in cell proliferation and cytokine release, but no significant increase in apoptosis, in activated cells. It was observed that apoptosis induced in lymphocytes by metal ion exposure was primarily a result of mitochondrial damage.

The *in vivo* study used a rodent air-pouch model to demonstrate that CoCr debris induced a specific inflammatory process mediated via monocytes/macrophages that was different to the inflammation following LPS treatment (positive control). Histological analysis also showed that CoCr debris accumulated in the pouch wall and this was accompanied by a vast cellular infiltration and fibrosis around the debris. Inflammatory gene transcripts from air-pouch tissue showed that CoCr wear debris increased expression of cytokines involved in promoting inflammation and fibrosis (IL-1 $\beta$ , TGF- $\beta$ ), and chemokines which promote recruitment of neutrophils and monocytes/macrophages (CXCL2, CCL2). By excision of the draining lymph nodes, it was demonstrated that a single dose of CoCr wear debris had little systemic immune effects. However, metal ion analysis did show that Cr and, to a greater extent Co, accumulated within whole blood and organs such as the kidney and spleen.

The clinical data demonstrated that MoM hip resurfacing led to a significant increase in levels of Cr and Co ions and significant decrease in the number of circulating total WBC and B-lymphocyte number within whole blood of patients 2 years post surgery. However, no correlation between the two parameters was found. No significant alterations in whole blood metal ion levels or WBC numbers was measured following ceramic-on-metal or MoM total hip replacement.

The findings from this thesis suggest that metal ions and wear debris released from CoCr hip implants can induce inflammatory and toxic effects. The clinical data indicate that correctly implanted hip articulations may not produce the high levels of metal ions or debris that can lead to adverse effects. However, continuous monitoring of patients following hip arthroplasty is recommended.

## List of abbreviations

7-AAD	7-Aminoactinomycin D
ALVAL	Aseptic lymphocytic vasculitis-associated lesions
ANOVA	Analysis of variance
AO	Acridine orange
APC	Antigen presenting cells
ARMD	Adverse reactions to metal debris
ASC	Apoptosis-associated speck-like protein containing a CARD
ASR	Articular surface replacement
ASTM	American Society for Testing and Materials
BCL-X <sub>L</sub>	B-cell lymphoma-extra large
BrdU	Bromodeoxyuridine
CARD	Caspase recruitment domain
cDNA	Complementary DNA
CoC	Ceramic-on-Ceramic
CoP	Ceramic-on-Polyethylene
CPTi	Commercially pure titanium
Ct	Threshold cycle
DC	Dendritic cell
DMSO	Dimethyl Sulfoxide
DNA	Deoxyribonucleic acid
EDS	Energy Dispersive Spectroscopy
EDTA	Ethylenediaminetetraacetic acid
ELISA	Enzyme-linked immunosorbent assay
FACS	Fluorescence-activated cell sorting
FCS	Foetal Calf Serum
FITC	Fluorescein isothiocyanate
GM-CSF	Granulocyte-macrophage colony-stimulating factor
H & E	Haematoxylin and eosin
HEPES	4-(2-hydroxyethyl)-1-piperazineethanesulfonic acid
HRP	Horseradish peroxidase
IFN $\gamma$	Interferon gamma
IL-2	Interleukin-2
LPS	Lipopolysaccharide
MHC	Major histocompatibility complex
MHRA	Medicines and Healthcare Regulatory Agency
MoM	Metal-on-Metal
MOMP	Mitochondrial outer membrane permeabilisation
MoP	Metal-on-Polyethylene
mRNA	Messenger RNA

MTT	3-(4,5-Dimethylthiazol-2-yl)-2,5-diphenyltetrazolium bromide
NFAT	Nuclear factor of activated T-cells
NICE	National Institute for Health and Clinical Excellence
NLRP3	NOD-like receptor family, pyrin domain containing 3
NR	Neutral red
PBMC	Peripheral blood mononuclear cell
PBS	Phosphate buffered saline
PE	Phycoerythrin
PGE2	Prostaglandin E2
PHA	Phytohaemagglutinin
PI	Propidium Iodide
PS	Phospholipid phosphatidylserine
RBC	Red blood cell
RNA	Ribonucleic acid
ROS	Reactive oxygen species
RQ	Relative quantitative
RT-PCR	Reverse transcription polymerase chain reaction
SEM	Standard error of mean
TCR	T-cell receptor
Th	Helper T-lymphocyte
TGF	Transforming growth factor
THR	Total hip replacement
TLDA	TaqMan low density array
TMB	3,3',5,5'-Tetramethylbenzidine
TNF $\alpha$	Tumor necrosis factor alpha
UHMWPE	Ultra-high-molecular-weight polyethylene
UV	Ultraviolet
WBC	White blood cell



## List of tables

Table 1.1 Elemental composition (% weight) of cobalt-chromium based metal alloys used in orthopaedic implants.....	7
Table 1.2 Elemental compositions (% weight) of metal alloys used in orthopaedic implants.	8
Table 1.3 Mechanical properties of metal alloys used for orthopaedic prostheses.....	9
Table 1.4 Metal ion levels measured in blood of patients following MoM hip arthroplasty.	15
Table 1.5 Metal ion levels measured in blood of workers following occupational exposure	16
Table 1.6 Selected constituents of innate and adaptive immunity.....	18
Table 1.7 Selected recognition markers for lymphocytes.....	19
Table 2.1 Monoclonal antibodies and isotype controls used to assess dendritic cell activation.....	45
Table 2.2 Preparation of solubilisation matrix solution.....	47
Table 2.3 Monoclonal antibodies and isotype controls used to identify cells in pouch exudate.....	48
Table 2.4 Monoclonal antibodies and isotype controls used to identify cells from mouse lymph nodes.....	53
Table 2.5 Monoclonal antibodies and isotype controls used to identify cells in peripheral human blood.....	55
Table 3.1 Cell viability of U937 cells following 24 and 48 hours exposure to varying concentrations of Cr <sup>6+</sup> and Co <sup>2+</sup> ions, as measured by MTT assay.....	61
Table 3.2 Cell viability of U937 cells following 24 and 48 hours exposure to varying concentrations of Cr <sup>6+</sup> and Co <sup>2+</sup> ions, as measured by NR assay.....	61
Table 3.3 Number of U937 cells displaying apoptotic and necrotic morphology following 48 hours exposure to varying concentrations of Cr <sup>6+</sup> and Co <sup>2+</sup> ions, as recorded by Confocal Laser Scanning Microscopy following staining with Acridine Orange and Propidium Iodide.....	64
Table 3.4 Percentage (±S.E.M) of U937 cells in various stages of cell cycle following exposure to various concentrations of Cr <sup>6+</sup> and Co <sup>2+</sup> ions for 24 and 48 hours.....	67
Table 4.1 Cell viability of resting lymphocytes following 24 and 48 hr exposure to varying concentrations of Cr <sup>6+</sup> and Co <sup>2+</sup> ions, as measured by MTT assay.....	84
Table 4.2 Cell viability of resting lymphocytes following 24 and 48 hr exposure to varying concentrations of Cr <sup>6+</sup> and Co <sup>2+</sup> ions, as measured by NR assay.....	84
Table 4.3 Cell viability of anti-CD3 activated lymphocytes following 24 and 48 hr exposure to varying concentrations of Cr <sup>6+</sup> and Co <sup>2+</sup> ions, as measured by MTT assay.....	85

Table 4.4 Cell viability of anti-CD3 activated lymphocytes following 24 and 48 hr exposure to varying concentrations of Cr <sup>6+</sup> and Co <sup>2+</sup> ions, as measured by NR assay.....	85
Table 4.5 Percentage of resting human lymphocytes (± caspase-3 inhibitor pre-treatment) with healthy mitochondria following exposure to Cr <sup>6+</sup> and Co <sup>2+</sup> for 24 hours, as imaged by Confocal Laser Scanning Microscopy following incubation with DePsipher reagent .....	100
Table 4.6 Percentage of anti-CD3 activated human lymphocytes (± caspase-3 inhibitor pre-treatment) with healthy mitochondria following exposure to Cr <sup>6+</sup> and Co <sup>2+</sup> for 24 hours, as imaged by Confocal Laser Scanning Microscopy following incubation with DePsipher reagent .....	103
Table 5.1 Number of cells within inflammatory exudate following 24hr treatment of air-pouches with different doses of CoCr wear debris .....	119
Table 5.2 Blood metal levels (µg/l) (mean ± S.E.M) in mice (n = 3) at different time points (4 hours, 24 hours, 48 hours, 72 hours, 7 days and 28 days) after injection of CoCr wear particles or sterile PBS.....	123
Table 5.3 Inflammatory factor transcripts in air-pouch tissue at 24h post-injection .....	139
Table 6.1 Number of patients within each subject group.....	159
Table 6.2 Percentage of patients with laboratory defined lymphopenia following MoM hip resurfacing.....	163

## List of figures

Figure 1.1 Illustration of a normal and arthritic hip joint .....	3
Figure 1.2 Hip resurfacing and total hip replacement arthroplasty.....	5
Figure 1.3 Sequence of events involved in the inflammatory and wound-healing response following biomaterial implantation.....	21
Figure 1.4 Schematic diagram of metal exposure induced cytokine release associated with activation of Th1 lymphocytes resulting in inhibitory effects on bone function .....	25
Figure 1.5 Production of reactive intermediates produced by Cr <sup>6+</sup> after entering the cell.....	27
Figure 1.6 Pathways by which Cr <sup>6+</sup> and Co <sup>2+</sup> induce cell death .....	28
Figure 1.7 Summary of effects of metal wear debris and ion release from MoM hip implants that may lead to prosthesis failure.....	30
Figure 2.1 Isolation of peripheral mononuclear cells from buffy coat.....	35
Figure 3.1 Cell viability of U937 cells following 24 hours exposure to varying concentrations of Cr <sup>6+</sup> and Co <sup>2+</sup> ions, as measured by MTT (A) and NR (B) assays ....	60
Figure 3.2 Cell viability of U937 cells following 48 hours exposure to varying concentrations of Cr <sup>6+</sup> and Co <sup>2+</sup> ions, as measured by MTT (A) and NR (B) assays ....	60
Figure 3.3 Confocal Laser Scanning Microscope Images of U937 cells stained with Acridine Orange and Propidium Iodide following 48 hours exposure to Cr <sup>6+</sup> or Co <sup>2+</sup> ions. (A) Control, (B) 1 μM Cr <sup>6+</sup> , (C) 10μM Co <sup>2+</sup> , (D) 1 μM Cr <sup>6+</sup> + 1 μM Co <sup>2+</sup> , (E) 0.1 μM Cr <sup>6+</sup> + 10 μM Co <sup>2+</sup> , (F) 1 μM Cr <sup>6+</sup> + 10 μM Co <sup>2+</sup> .....	63
Figure 3.4 Percentage of U937 cells at various stages of the cell cycle 24 and 48 hour of exposure to Cr <sup>6+</sup> .....	65
Figure 3.5 Percentage of U937 cells at various stages of the cell cycle 24 and 48 hour of exposure to Co <sup>2+</sup> .....	66
Figure 3.6 U937 cells stained with Annexin V and 7-AAD following exposure to 10 μM Cr <sup>6+</sup> and 10 μM Co <sup>2+</sup> for 24 and 48 hours .....	68
Figure 3.7 Total apoptosis in U937 cells following (A) 24 hour or (B) 48 hours of exposure to Cr <sup>6+</sup> and Co <sup>2+</sup> .....	69
Figure 3.8 Necrosis in U937 cells following (A) 24 or (B) 48 hours exposure to Cr <sup>6+</sup> or Co <sup>2+</sup> .....	69
Figure 4.1 Cell viability of primary human lymphocytes following 24 or 48 hours exposure to varying concentrations of soluble anti-CD3, as measured by MTT (A) and NR (B) assays .....	78

Figure 4.2 Cell viability of lymphocytes following 24 (upper) and 48 (lower) hr of exposure to varying concentrations of Cr <sup>6+</sup> and Co <sup>2+</sup> ions, as measured by MTT assay.....	82
Figure 4.3 Cell viability of lymphocytes following 24 (upper) and 48 (lower) hr of exposure to varying concentrations of Cr <sup>6+</sup> and Co <sup>2+</sup> ions, as measured by NR assay.....	83
Figure 4.4 T-lymphocyte activation following 24 hr exposure to Cr <sup>6+</sup> or Co <sup>2+</sup> . (A) anti-CD3-activated and (B) anti-CD3 + anti-CD28 activated lymphocytes.....	86
Figure 4.5 Lymphocyte proliferation following 48 hr exposure to varying concentrations of Cr <sup>6+</sup> and Co <sup>2+</sup> ions.....	88
Figure 4.6 IL-2 production from anti-CD3 ± anti-CD28 activated lymphocytes exposed to varying concentrations of Cr <sup>6+</sup> and Co <sup>2+</sup> ions for 48 hr. ....	89
Figure 4.7 IFN-γ release from anti-CD3 ± anti-CD28 activated lymphocytes exposed to varying concentrations of Cr <sup>6+</sup> and Co <sup>2+</sup> ions for 48 hr .....	90
Figure 4.8 TNFα release from anti-CD3 ± anti-CD28 activated lymphocytes exposed to varying concentrations of Cr <sup>6+</sup> and Co <sup>2+</sup> ions for 48 hr .....	90
Figure 4.9 Percentage of anti-CD3 activated lymphocytes at various stages of the cell cycle following 48 hour of exposure to 100 μM Cr <sup>6+</sup> or Co <sup>2+</sup> .....	91
Figure 4.10 Anti-CD3-activated lymphocytes at different stages of cell cycle following 24 (upper) and 48 (lower) hr of exposure to Cr <sup>6+</sup> (A&C) and Co <sup>2+</sup> (B&D).....	92
Figure 4.11 Resting and anti-CD3 activated lymphocytes stained with Annexin V and 7-AAD following exposure to 100 μM Cr <sup>6+</sup> and 100 μM Co <sup>2+</sup> for 24 hr. Viable cells were Annexin V <sup>-</sup> and 7-AAD <sup>-</sup> .....	94
Figure 4.12 Total apoptosis in lymphocytes following 24 (upper) and 48 (lower) hr of exposure to Cr <sup>6+</sup> and Co <sup>2+</sup> . (A & C) Resting and (B & D) anti-CD3-activated lymphocytes .....	95
Figure 4.13 Total apoptosis in lymphocytes exposed to Cr <sup>6+</sup> or Co <sup>2+</sup> treated with or without a caspase-3 inhibitor .....	96
Figure 4.14 Confocal laser scanning microscope images of resting human lymphocytes (± caspase-3 inhibitor pre-treatment) exposed to Cr <sup>6+</sup> and Co <sup>2+</sup> for 24 hours and then incubated with DePsipher reagent.....	99
Figure 4.15 Confocal laser scanning microscope images of anti-CD3 activated human lymphocytes (± caspase-3 inhibitor pre-treatment) exposed to Cr <sup>6+</sup> and Co <sup>2+</sup> for 24 hours and then incubated with DePsipher reagent .....	102
Figure 4.16 Proliferation of anti-CD3-activated lymphocytes following 48 hr exposure to varying concentrations of Cr <sup>6+</sup> and Co <sup>2+</sup> ions with or without caspase-3 inhibitor treatment .....	104

Figure 4.17 Proliferation of anti-CD3-activated lymphocytes ( $\pm$ 50U/ml IL-2) following 48 hr exposure to varying concentrations of $\text{Cr}^{6+}$ and $\text{Co}^{2+}$ ions.....	105
Figure 4.18 Expression of T-lymphocyte inhibitory markers following 48 hr exposure of anti-CD3 + anti-CD28 activated lymphocytes to $\text{Cr}^{6+}$ and $\text{Co}^{2+}$ .....	106
Figure 4.19 Pathways by which $\text{Cr}^{6+}$ induced mitochondrial damage can lead to apoptosis, with or without the involvement of caspase activation.....	108
Figure 5.1 Scanning Electron Microscopy images of wear debris from an ASR hip implant .....	120
Figure 5.2 Energy Dispersive X-ray Spectroscopy of wear debris from an ASR hip implant .....	121
Figure 5.3 Composition of CoCr wear debris from ASR implant, analysed by EDS .....	121
Figure 5.4 Activation of $\text{CD11c}^+$ dendritic cells (DCs) .....	122
Figure 5.5 Blood metal (Co, Cr and Mo) levels ( $\mu\text{g/l}$ ) in mice after injection of CoCr or sterile PBS at different time points .....	123
Figure 5.6 Chromium levels (ng/g tissue) in the organs of mice following injection of PBS or CoCr debris into the air-pouch.....	125
Figure 5.7 Cobalt levels (ng/g tissue) in the organs of mice following injection of PBS or CoCr debris into the air-pouch.....	126
Figure 5.8 Molybdenum levels (ng/g tissue) in the organs of mice following injection of PBS or CoCr debris into the air-pouch .....	127
Figure 5.9 Total number of cells present in the inflammatory exudates at different time points.....	129
Figure 5.10 Flow cytometric analysis of the inflammatory cells recovered 4 hours post implantation .....	129
Figure 5.11 Number of (A) neutrophils, (B) monocytes/macrophages , (C) T-lymphocytes and, (D) B-lymphocytes present in the inflammatory exudates at different time points .....	130
Figure 5.12. The histological appearance of negative (PBS) and positive (LPS) control and CoCr treated air-pouch membranes, 24 hours post injection.....	131
Figure 5.13 The histological appearance of CoCr treated air- pouch membranes, 24 hours post injection.....	131
Figure 5.14 The histological appearance of negative (PBS) and positive (LPS) control and CoCr treated air-pouch membranes, 72 hours post injection.....	132
Figure 5.15 The histological appearance of CoCr treated air-pouch membranes, 72 hours post injection.....	132

Figure 5.16 The histological appearance of negative (PBS) and positive (LPS) control and CoCr treated air-pouch membranes, 7 days post injection .....	133
Figure 5.17 The histological appearance of CoCr treated air-pouch membranes, 7 days post injection.....	133
Figure 5.18 The histological appearance of negative (PBS) and positive (LPS) control and CoCr treated air-pouch membranes, 28 days post injection .....	134
Figure 5.19 The histological appearance of CoCr treated air-pouch membranes, 28 days post injection.....	135
Figure 5.20 Membrane thickness of air-pouch tissue following treatment with PBS, CoCr debris and, LPS .....	136
Figure 5.21 Number of cells in air-pouch tissue following treatment with PBS, CoCr debris and, LPS.....	136
Figure 5.22 Detection of mRNA isolated from 24 hour air-pouch tissue on agarose gel. The gel has a size marker in first lane, followed by samples which show degraded “smeared” RNA .....	137
Figure 5.23 RT-PCR using primers specific for $\beta_2$ microglobulin and mRNA from 24 hour air-pouch tissue .....	138
Figure 5.24 Changes in cell number in draining lymph nodes after the injection of PBS, CoCr debris or LPS into the air-pouch.....	140
Figure 5.25 Changes in the proportion of lymphocytes in draining lymph nodes after the injection of PBS, CoCr debris or LPS into the air-pouch .....	141
Figure 5.26 Viability of lymphocytes in draining lymph nodes after the injection of PBS, CoCr debris or LPS into the air-pouch.....	142
Figure 5.27 Proportion of apoptotic lymphocytes in draining lymph nodes after the injection of PBS, CoCr debris or LPS into the air-pouch .....	143
Figure 5.28 Viability of lymphocytes activated with anti-CD3 ( $\pm$ anti-CD28) for 24 hours .....	145
Figure 5.29 Proportion of apoptotic lymphocytes following 24 hour activation with anti-CD3 ( $\pm$ anti-CD28).....	147
Figure 6.1 Change in number of circulating white blood cells and different lymphocyte subsets following MoM hip resurfacing arthroplasty surgery using the ASR and Durom implants.....	162
Figure 6.2 Change in whole blood chromium and cobalt levels following MoM hip resurfacing arthroplasty surgery using the ASR and Durom implants.....	164

Figure 6.3 Correlation between changes in whole blood metal ion levels (Cr + Co) and changes in WBCs and lymphocyte populations at 1 and 2 years post MoM arthroplasty using either ASR or Durom implants.....	166
Figure 6.4 Change in number of circulating white blood cells and different lymphocyte subsets following CoM or MoM THR.....	167
Figure 6.5 Change in whole blood chromium and cobalt levels following CoM or MoM THR .....	168

# Materials

<b>Product</b>	<b>Source</b>
<b>7-AAD</b>	BD Bioscience, UK
<b>1-Butanol</b>	Fisher Scientific, UK
<b>Acridine Orange</b>	Sigma-Aldrich, UK
<b>Agarose</b>	Sigma-Aldrich, UK
<b>Ammonium hydroxide</b>	Fisher Scientific, UK
<b>Annexin V-PE</b>	BD Bioscience, UK
<b>Anti-human CD28 (CD28.2)</b>	eBioscience, UK
<b>Anti-human CD3 (HIT3a)</b>	eBioscience, UK
<b>Anti-Mouse CD28 (37.51)</b>	eBioscience, UK
<b>Anti-Mouse CD3 (145- 2C11)</b>	eBioscience, UK
<b>Blue/Orange loading dye</b>	Promega, UK
<b>CaCl<sub>2</sub></b>	Sigma-Aldrich, UK
<b>Chromium Oxide</b>	Alfa Aesar, UK
<b>Cobalt Chloride</b>	Alfa Aesar, UK
<b>CoCr debris</b>	DePuy International, UK
<b>DMSO</b>	Sigma-Aldrich, UK
<b>DNA Ladder</b>	Promega, UK
<b>EDTA</b>	Sigma-Aldrich, UK
<b>Ethidium Bromide</b>	Sigma-Aldrich, UK
<b>FACS Flow</b>	BD Bioscience, UK
<b>FCS</b>	Invitrogen, UK
<b>Formalin (4%)</b>	Sigma-Aldrich, UK
<b>Glacial acetic acid</b>	Sigma-Aldrich, UK



---

<b>GM-CSF</b>	Donated by Dr Owain Millington; University of Strathclyde, Glasgow, UK
<b>HEPES</b>	Sigma-Aldrich, UK
<b>Histopaque-1077</b>	Sigma-Aldrich, UK
<b>Hydrogen peroxide</b>	Sigma-Aldrich, UK
<b>L-Glutamine</b>	Invitrogen, UK
<b>MTT</b>	Sigma-Aldrich, UK
<b>NaCl</b>	Sigma-Aldrich, UK
<b>Nitric acid</b>	Fisher Scientific, UK
<b>NR</b>	Sigma-Aldrich, UK
<b>PBS</b>	Sigma-Aldrich, UK
<b>PBS (Sterile)</b>	Invitrogen, UK
<b>Penicillin</b>	Invitrogen, UK
<b>Propidium Iodide</b>	Sigma-Aldrich, UK
<b>RBC Lysing Buffer</b>	BD Bioscience, UK
<b>Recombinant human IL-2</b>	eBioscience, UK
<b>RPMI-1640</b>	Lonza, UK
<b>Sodium Azide</b>	Sigma-Aldrich, UK
<b>Streptomycin</b>	Invitrogen, UK
<b>Tris base</b>	Sigma-Aldrich, UK
<b>Triton X-100</b>	Sigma-Aldrich, UK
<b>Trypan Blue</b>	Sigma-Aldrich, UK
<b>Tween-20</b>	Sigma-Aldrich, UK
<b>Z-DEVD-FMK</b>	R&D Systems, UK
<b>β<sub>2</sub> microglobulin primer mixture</b>	Applied Biosystems, UK

---

<b>Kit</b>	<b>Source</b>
<b>Ready-SET-Go! ELISA</b>	eBioscience, UK
<b>AffinityScript™ Multiple Temperature cDNA synthesis kit</b>	Agilent Technologies, UK
<b>BrdU Proliferation Assay</b>	Merck, UK
<b>DePsipher Kit</b>	R & D Systems, UK
<b>RNeasy Mini Kit</b>	Qiagen, UK
<b>TaqMan Low Density Arrays</b>	Applied Biosystems, UK

<b>Anti-mouse antibody or Isotype Control</b>	<b>Source</b>
<b>Armenian Hamster IgG-PE</b>	eBioscience, UK
<b>B220-APC (RA3-6B2)</b>	eBioscience, UK
<b>CD11b-PE (M1/70)</b>	eBioscience, UK
<b>CD11c-PE (N418)</b>	eBioscience, UK
<b>CD3e-PerCP (500A2)</b>	eBioscience, UK
<b>CD40-APC (1C10)</b>	eBioscience, UK
<b>CD4-FITC (RM-45)</b>	eBioscience, UK
<b>CD86-FITC (GL-1)</b>	eBioscience, UK
<b>CD8-APC CY7.7 (53-6.7)</b>	eBioscience, UK
<b>Hamster IgG (PerCP)</b>	eBioscience, UK
<b>Ly6G-FITC (RB6-8C5)</b>	eBioscience, UK
<b>MHC Class II-FITC (NIMR-4)</b>	eBioscience, UK
<b>Rat IgG2a-APC</b>	eBioscience, UK
<b>Rat IgG2a-FITC</b>	eBioscience, UK
<b>Rat IgG2b-FITC</b>	eBioscience, UK
<b>Rat IgG2b-PE</b>	eBioscience, UK

<b>Anti-human antibody or Isotype Control</b>	<b>Source</b>
<b>PD-1 APC (clone MIH4)</b>	eBioscience, UK
<b>CTLA-4 PE (clone 14D3)</b>	eBioscience, UK
<b>CD69-APC (clone FN50)</b>	eBioscience, UK
<b>CD20-FITC (2H7)</b>	eBioscience, UK
<b>CD3-FITC (OKT3)</b>	eBioscience, UK
<b>CD4-PE (OKT4)</b>	eBioscience, UK
<b>CD56-PE (MEM-188)</b>	eBioscience, UK
<b>CD8-APC (OKT8)</b>	eBioscience, UK
<b>Mouse IgG2a-APC</b>	eBioscience, UK
<b>Mouse IgG2a-FITC</b>	eBioscience, UK
<b>Mouse IgG2a-PE</b>	eBioscience, UK
<b>Mouse IgG2b-FITC</b>	eBioscience, UK
<b>Mouse IgG2b-PE</b>	eBioscience, UK
<b>Mouse IgG1<math>\kappa</math> -APC</b>	eBioscience, UK

# Table of contents

<b>ACKNOWLEDGEMENTS.....</b>	<b>II</b>
<b>ABSTRACT.....</b>	<b>IV</b>
<b>LIST OF ABBREVIATIONS .....</b>	<b>VI</b>
<b>LIST OF TABLES .....</b>	<b>VIII</b>
<b>LIST OF FIGURES .....</b>	<b>X</b>
<b>MATERIALS .....</b>	<b>XV</b>
<b>TABLE OF CONTENTS.....</b>	<b>XIX</b>
<b>CHAPTER 1 .....</b>	<b>1</b>
<b>1. INTRODUCTION.....</b>	<b>2</b>
<b>1.1 The hip joint .....</b>	<b>2</b>
<b>1.2 Hip replacement .....</b>	<b>3</b>
<b>1.3 Materials used for hip replacement implants.....</b>	<b>6</b>
<b>1.4 Metal-on-Metal arthroplasty .....</b>	<b>10</b>
1.4.1 The case for metal-on-metal.....	10
1.4.2 Metal ion levels following hip arthroplasty.....	12
1.4.3 Adverse effects of metal wear debris and ions.....	17
1.4.3.1 The immune system and biomaterials .....	17
1.4.3.2 Soft tissue masses developing following arthroplasty.....	21
1.4.3.3 Aseptic lymphocytic vasculitis-associated lesions following arthroplasty .....	22
1.4.3.4 Hypersensitivity following arthroplasty .....	23
1.4.3.5 Toxicity of metal ions.....	25
1.4.3.6 Alterations in circulating lymphocyte numbers in patients following arthroplasty .....	29
<b>1.5 Aims of present study .....</b>	<b>31</b>

<b>CHAPTER 2 .....</b>	<b>32</b>
<b>2. MATERIALS AND METHODS: GENERAL .....</b>	<b>33</b>
<b>2.1 Cells .....</b>	<b>33</b>
2.1.1 Cells used .....	33
2.1.1.1 Culturing of U937 cells.....	33
2.1.1.2 Isolation of primary human lymphocytes .....	34
2.1.1.3 Preparation of dendritic cells .....	35
2.1.1.4 Hybridoma 2.4G2 cells .....	35
2.1.2 Preparation of metal ion solutions.....	36
2.1.3 Cell analysis .....	36
2.1.3.1 MTT assay for cell viability.....	36
2.1.3.2 Neutral red assay for cell viability.....	37
2.1.3.3 Flow cytometry analysis of cell cycle.....	38
2.1.3.4 Flow cytometry analysis of apoptosis.....	39
2.1.3.5 Analysis of cell morphology and viability via microscopy .....	40
2.1.3.6 Surface antigen staining of cells for flow cytometry .....	40
2.1.3.7 Cell proliferation assay .....	41
2.1.3.8 ELISA .....	42
2.1.3.9 Assessment of mitochondrial damage .....	43
<b>2.2 <i>In vivo</i> response to metal wear debris .....</b>	<b>43</b>
2.2.1 Preparation of metal wear debris .....	44
2.2.2 Assessing sterility of treated wear debris .....	44
2.2.3 Characterisation of wear particles .....	45
2.2.4 Establishing the air-pouch .....	45
2.2.5 Analysis of metal ions in peripheral blood.....	46
2.2.6 Analysis of metal ions in organs .....	47
2.2.7 Pouch exudate.....	47
2.2.8 Histological evaluation of air-pouch .....	48
2.2.9 Inflammatory gene activation in air-pouch tissue .....	49
2.2.9.1 RNA Extraction .....	49
2.2.9.2 Agarose gel electrophoresis of RNA .....	50
2.2.9.3 cDNA synthesis .....	50
2.2.9.4 Control RT-PCR .....	51
2.2.9.5 Inflammatory gene expression assay .....	51
2.2.10 Evaluation of the effects on draining lymph nodes .....	52
<b>2.3 Determining metal ion concentrations and white blood cell levels in peripheral blood .....</b>	<b>54</b>
2.3.1 Metal ion analysis in peripheral blood .....	54
2.3.3 Surface antigen staining to phenotype cells using flow cytometry .....	54

<b>CHAPTER 3 .....</b>	<b>56</b>
<b>3. EFFECTS OF CHROMIUM AND COBALT ON U937 CELLS <i>IN VITRO</i> .....</b>	<b>57</b>
<b>3.1 Introduction .....</b>	<b>57</b>
<b>3.2 Aims .....</b>	<b>58</b>
<b>3.3 Methods .....</b>	<b>58</b>
3.3.1 Exposure of U937 cells to metal ions .....	58
3.3.2 Analysis of metal ion exposure on U937 Cells .....	58
<b>3.4 Results .....</b>	<b>59</b>
3.4.1 Effects of metal ions on cell viability .....	59
3.4.2 Effects of metal ions on cellular morphology .....	62
3.4.3 Effect of metal ions on the cell cycle .....	64
3.4.4 Effect of metal ion exposure on cellular apoptosis/necrosis .....	67
<b>3.5 Discussion .....</b>	<b>70</b>
<b>CHAPTER 4 .....</b>	<b>74</b>
<b>4. EFFECTS OF CHROMIUM AND COBALT ON HUMAN LYMPHOCYTES <i>IN VITRO</i> .....</b>	<b>75</b>
<b>4.1 Introduction .....</b>	<b>75</b>
<b>4.2 Aims .....</b>	<b>76</b>
<b>4.3 Methods .....</b>	<b>77</b>
4.3.1 Lymphocyte activation protocol .....	77
4.3.2 Exposure of lymphocytes to metal ions .....	78
4.3.3 Caspase inhibition .....	79
4.3.4 Recombinant IL-2 supplementation .....	79
4.3.5 Analysis of the effects of metal ion exposure to primary human lymphocytes .....	79
<b>4.4 Results .....</b>	<b>81</b>
4.4.1 Effects of metal ions on cell viability .....	81
4.4.2 Effect of metal ions on T-lymphocyte activation .....	86
4.4.3 Effects of metal ions on lymphocyte proliferation .....	87
4.4.4 Effects of metal ions on cytokine release .....	88
4.4.5 Effects of metal ions on the cell cycle .....	91
4.4.6 Flow cytometric analysis of apoptosis following metal ion exposure .....	92

4.4.7 Caspase-3 inhibition of lymphocytes .....	95
4.4.7.1 Effect of caspase inhibition on metal ion induced apoptosis.....	95
4.4.7.2 Effects of metal ions on mitochondrial outer membrane permeability ..	97
4.4.7.3 Effects of metal ions on lymphocyte proliferation following caspase-3 inhibitor pre-treatment .....	103
4.4.8 IL-2 supplementation of metal ion exposed lymphocytes.....	104
4.4.9 Effect of metal ion exposure on inhibitory receptors of T- lymphocytes ...	105
<b>4.5 Discussion.....</b>	<b>106</b>
 <b>CHAPTER 5 .....</b>	 <b>114</b>
 <b>5. IN VIVO RESPONSES TO COCR IMPLANT WEAR DEBRIS IN MICE</b>	 <b>115</b>
 <b>5.1 Introduction.....</b>	 <b>115</b>
5.1.1 Wear debris.....	115
5.1.2 Rodent air-pouch .....	115
 <b>5.2 Aims.....</b>	 <b>116</b>
 <b>5.3 Methods.....</b>	 <b>117</b>
5.3.1 Characterisation of wear debris .....	117
5.3.2 Assessment of sterility of wear debris.....	117
5.3.3 Development of model .....	117
5.3.3.1 Volume of air-pouch.....	117
5.3.3.2 Needles used to lavage air-pouch .....	118
5.3.3.3 Mass of debris used.....	118
5.3.4 Exposure of mice to wear debris .....	119
5.3.5 Assessment of the effects on CoCr implantation on mice.....	119
 <b>5.4 Results .....</b>	 <b>120</b>
5.4.1 Characterisation of CoCr wear debris .....	120
5.4.2 Sterility of CoCr debris .....	121
5.4.3 Ion Distribution .....	122
5.4.4 Local inflammatory response .....	128
5.4.4.1 Inflammatory exudate .....	128
5.4.4.2 Tissue response .....	130
5.4.4.3 Inflammatory gene expression.....	137
5.4.5 Systemic immune effects.....	139
5.4.5.1 Lymphocyte numbers within draining lymph nodes .....	139
5.4.5.2 Effects of <i>in vitro</i> activation on lymphocytes from draining lymph nodes .....	143

<b>5.5 Discussion.....</b>	<b>148</b>
<b>CHAPTER 6 .....</b>	<b>156</b>
<b>6. EFFECTS OF METAL-ON-METAL ARTHROPLASTY ON LYMPHOCYTES <i>IN VIVO</i>: CORRELATION WITH BLOOD METAL ION LEVELS.....</b>	<b>157</b>
<b>6.1 Introduction.....</b>	<b>157</b>
<b>6.2 Aims.....</b>	<b>158</b>
<b>6.3 Methods.....</b>	<b>158</b>
6.3.1 Implants .....	158
6.3.2 Patients .....	159
6.3.3 Blood sample collection .....	159
6.3.4 Analysis of peripheral blood .....	160
<b>6.4 Results .....</b>	<b>160</b>
6.4.1 Effects of MoM resurfacing on lymphocyte numbers.....	160
6.4.2 Effect of blood metal ion concentrations on lymphocyte numbers following MoM arthroplasty.....	163
6.4.3 Effects of THR on lymphocyte numbers.....	166
6.4.4 Correlation between blood metal ion concentrations and lymphocyte number .....	168
<b>6.5 Discussion.....</b>	<b>168</b>
<b>CHAPTER 7 .....</b>	<b>174</b>
<b>7. SUMMARY AND FUTURE WORK .....</b>	<b>175</b>
<b>7.1 Summary of the thesis findings.....</b>	<b>175</b>
7.1.1 Effects of chromium and cobalt on U937 cells <i>in vitro</i> .....	175
7.1.2 Effects of chromium and cobalt on primary human lymphocytes <i>in vitro</i> ..	176
7.1.3 <i>In vivo</i> response to CoCr implant wear debris .....	178
7.1.4 Effects of Metal-on-Metal arthroplasty on lymphocytes <i>in vivo</i> in patients	180
7.1.5 Major findings of thesis.....	181
<b>7.2 Limitations of studies.....</b>	<b>182</b>
<b>7.3 Future work .....</b>	<b>184</b>
7.3.1 Mechanism of CoCr debris induced inflammation .....	184



7.3.2 Chronic <i>in vivo</i> experiment .....	185
7.3.3 Specificity of wear debris effects .....	185
<b>7.4 Implications for the safety and future development of hip implants .....</b>	<b>186</b>
<b>APPENDIX .....</b>	<b>188</b>
<b>Appendix 1. List of TLDA gene targets .....</b>	<b>188</b>
<b>Appendix 2. Correlation between changes in Cr or Co ion blood metal levels and changes in WBCs and lymphocyte following MoM hip resurfacing.....</b>	<b>189</b>
<b>Appendix 3. List of publications .....</b>	<b>189</b>
<b>REFERENCES.....</b>	<b>191</b>

# Chapter 1

# **1. Introduction**

## **1.1 The hip joint**

The hip joint is a strong synovial ball-and-socket joint which allows flexion and extension, adduction and abduction, circumduction, and rotation. The joint is formed by the head of the femur inserting into a deep fossa within the pelvis, the acetabulum (Figure 1.1). The head of the femur fits into the acetabulum, where it is held firmly by a thick capsule, which is formed by the iliofemoral, pubofemoral, and ischiofemoral ligaments. The femoral head articulates within the acetabulum and both surfaces have a smooth durable lining of articular cartilage enabling them to articulate freely (Tortora and Grabowski, 2010).

One of the most common reasons for hip pain and disability is arthritis (Sanders et al., 2004). Although there are different types of arthritis, all lead to damage and/or erosion of the articulating cartilage (Figure 1.1). Within the hip, this causes contact between the bone surfaces of the femoral head and acetabulum resulting in pain and stiffness. During the early stages of arthritis, pharmaceutical interventions may alleviate pain, however, in many cases this is not sufficient and hip replacement surgery is the only effective form of treatment for patients (Groeneveld et al., 2008).

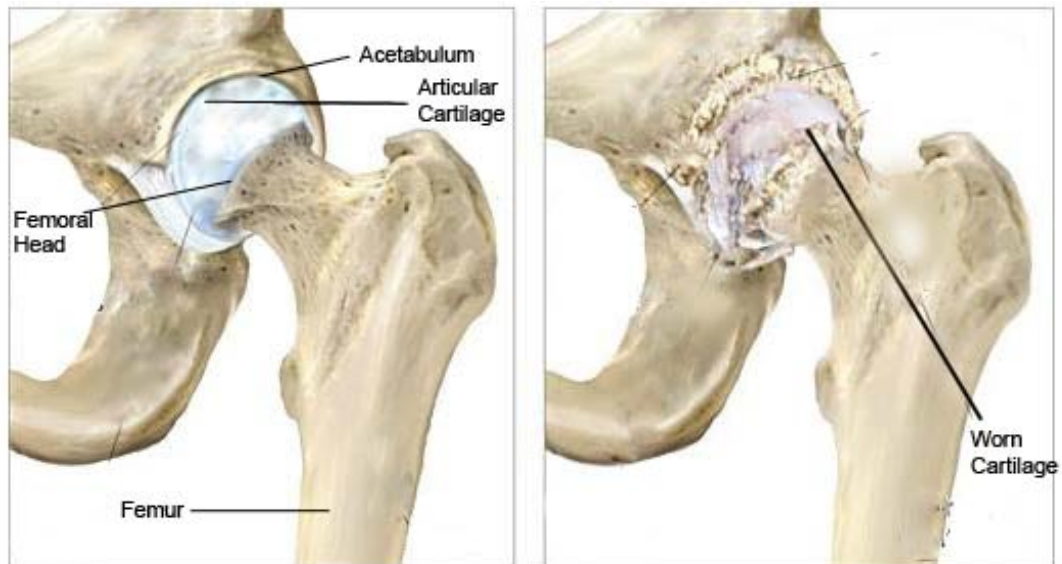


**Figure 1.1 Illustration of a normal and arthritic hip joint.** (adapted from <http://www.hipresurfacing.info/4.html>)

## **1.2 Hip replacement**

One of the earliest hip replacement joints to be described was in 1891 when Professor Themistocles Glück, from Berlin, produced a ball and socket joint made from ivory that was fixed to the bone with nickel-plated screws (Gomez and Morcuende, 2005). Since this, hip replacement prostheses have evolved extensively and as a result hip replacement surgery, or arthroplasty, has become an increasingly common and efficacious orthopaedic reconstructive procedure. This surgical technique has relieved the pain and increased the mobility of millions of arthritis sufferers worldwide. According to statistics from the annual reports produced by the national joint registry for England and Wales and the Scottish arthroplasty project (2010), there were over 80,000 hip replacement surgeries in the UK alone in 2009. There is also an ever increasing number of hip replacement surgeries carried out within the United States and it was estimated that 300,000 would be completed in 2010 (Kurtz et al., 2009).

Hip arthroplasty is a surgical procedure in which a dysfunctional and painful joint is replaced with a prosthetic joint. Hip arthroplasty involves replacing the articulating surfaces of both the 'ball' and 'socket' of the hip joint. Generally, there are two types of hip replacement; total hip replacement (THR) and hip resurfacing (Figure 1.2). THR involves removing some bone from the femur and inserting the replacement stem into the femur. This femoral component has a ball attached at the top. The design of this component can vary, it may be a singular body or the ball and stem may be separate parts. The artificial socket component, or acetabular cup, replaces the natural acetabulum. Bone and cartilage may be removed from the acetabulum to place the acetabular cup. Additionally, a liner may be placed into the replacement acetabular cup to act as the bearing surface with the femoral head. Both the acetabular cup and femoral head may be fixed into place using bone cement such as polymethyl methacrylate (PMMA). Alternatively, the acetabular cup may be screwed into place. An alternative to THR is metal-on-metal (MoM) hip resurfacing. This procedure involves removing less bone as shown in Figure 1.2 and is generally described as re-lining the joint. A metal femoral component is placed over the femoral head and a cup, as in THR, is placed in the acetabulum (Learmonth et al., 2007).

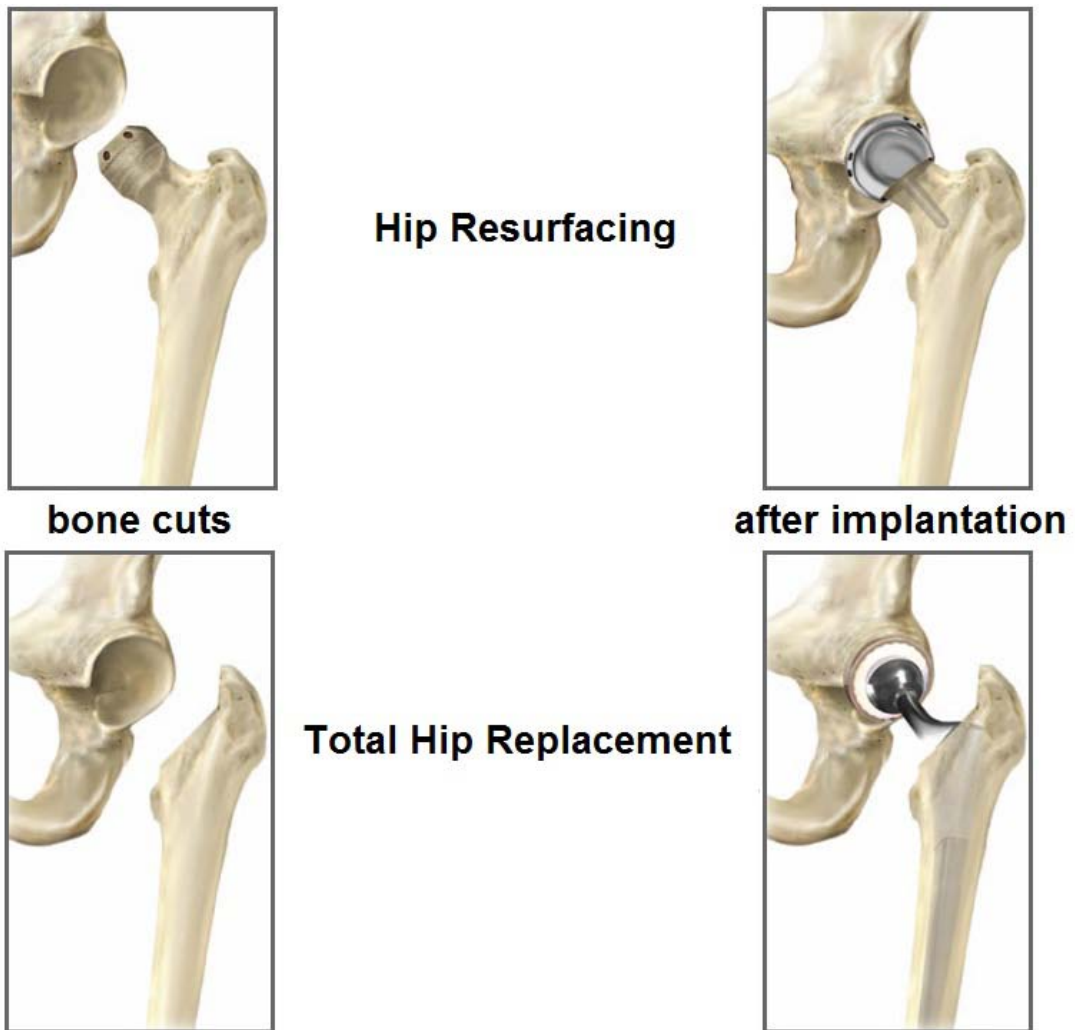


**Figure 1.2 Hip resurfacing and total hip replacement arthroplasty.** Images on the left demonstrate the removal of bone required for each type of hip arthroplasty, images on right illustrate the hip joint following arthroplasty. (adapted from <http://activejointsortho.com/procedure.htm>)

Some component designs which do not use cement are coated with hydroxyapatite or have another porous surface material coating to encourage bone growth into the artificial joint and aid fixation. Whether the components are cemented, screwed or have a coating depends on the type of material used. Irrespective of the type of hip

arthroplasty, the materials used in the prosthesis must have mechanical properties similar to the natural joint and should not be bio-active (Baratz et al., 1999).

### **1.3 Materials used for hip replacement implants**

There are a number of different materials used in the bearing surface of modern hip implants, these include ceramics, metals and, plastic. Alumina and Zirconia are commonly used ceramics in bearing surfaces of hip prostheses and the plastic used is ultra-high-molecular-weight-polyethylene (UHMWPE). A number of different types of metals are used as bearing surfaces in hip implants including; cobalt-chromium (CoCr) alloys, stainless steel and titanium alloy. The bearing surfaces used in hip joint replacement may both be composed of the same material as in metal-on-metal (MoM) and ceramic-on-ceramic (CoC) implants or may be a combination of different materials such ceramic-on-metal (CoM), metal-on-polyethylene (MoP) and ceramic-on-polyethylene (CoP). Although a variety of materials are used as bearing components in hip replacement implants, metal is the most abundantly used as this is not only used as a bearing component but also used as the femoral stem and acetabular cup. The compositions of metal alloys used in hip replacement implants are shown in Tables 1.1 and 1.2.

<b>Alloy</b>	<b>Co</b>	<b>Cr</b>	<b>Mo</b>	<b>Ni</b>	<b>Fe</b>	<b>Si</b>	<b>W</b>	<b>Ti</b>	<b>Al</b>	<b>Mn</b>	<b>Cu</b>	<b>C</b>	<b>V</b>	<b>N</b>
<b>Co-Cr-Mo</b>	61.0-	27.0-	4.5-	< 2.0	<0.75	<1.0	<0.05	<0.05	<0.05	<1.5	<0.05	<0.35	<0.05	<0.05
<b>F75</b>	66.0	30	7.0											
<b>Co-Cr-Mo</b>	46.0-	19.0-	<0.05	9.0-	3.0	<1.0	14.0-	<0.05	<0.05	<2.5	<0.05	<0.15	<0.05	<0.05
<b>F90</b>	51.0	20.0		11.0			16.0							
<b>Co-Cr-Mo</b>	58.0-	26.0-	5.0-	<1.0	<0.75	<1.0	<0.05	<0.05	<0.05	<1.0	<1.0	<0.35	<0.05	<0.25
<b>F799</b>	59.0	30.0	7.0											
<b>Co-Ni-Mo</b>	58.0-	26.0-	5.0-	<1.0	<0.75	<1.0	<0.05	<0.05	<0.05	<1.0	<1.0	<0.35	<0.05	<0.25
<b>F1537</b>	59.0	30.0	7.0											
<b>Co-Ni-Cr</b>	29.0-	19.0-	9.0-	33.0-	<1.0	<0.15	<0.05	<1.0	<0.05	<0.15	<0.05	0.025	<0.05	<0.05
<b>F562</b>	38.8	21.0	10.5	37.0										

**Table 1.1 Elemental composition (% weight) of cobalt-chromium based metal alloys used in orthopaedic implants.** Alloy compositions are standardised by the American Society for Testing and Materials (ASTM). (Co: cobalt, Cr: chromium, Mo: molybdenum, Ni: nickel, Fe: iron, Si: silicon, W: tungsten, Ti: titanium, Al: aluminium, Cu: copper, C: carbon, V: vanadium, N: nitrogen) (Dearnley, 1999, Keegan et al., 2007).



<b>Alloy</b>	<b>Co</b>	<b>Cr</b>	<b>Mo</b>	<b>Ni</b>	<b>Fe</b>	<b>Si</b>	<b>W</b>	<b>Ti</b>	<b>Al</b>	<b>Mn</b>	<b>Cu</b>	<b>C</b>	<b>V</b>	<b>N</b>
<b>Stainless</b>	<0.05	17.0-	2.0-	10.0-	61.0-	<1.0	<2.0	<0.05	<0.05	<0.05	<0.5	<0.06	<0.05	<0.5
<b>Steel F138</b>		19.0	4.0	15.5	68.0									
<b>CPTi</b>	<0.05	<0.05	<0.05	<0.05	0.2-	<0.05	<0.05	99.0	<0.05	<0.05	<0.05	<0.1	<0.05	<0.05
<b>F67</b>					0.5									
<b>Ti-6Al-4V</b>	<0.05	<0.05	<0.05	<0.05	<0.25	<0.05	<0.05	89.0-	5.5-	<0.05	<0.05	<0.08	3.5-4.5	<0.05
<b>F136</b>								91.0	6.5					
<b>Ti-6Al-4V</b>	<0.05	<0.05	<0.05	<0.05	<0.35	<0.05	<0.05	89.0-	5.5-	<0.05	<0.05	<0.08	3.5-4.5	<0.05
<b>F1108</b>								91.0	6.5					

**Table 1.2 Elemental compositions (% weight) of metal alloys used in orthopaedic implants.** Alloy compositions are standardised by the American Society for Testing and Materials (ASTM). (CPTi: commercially pure titanium, Ti: titanium, Al: aluminium, V: vanadium, Co: cobalt, Cr: chromium, Mo: molybdenum, Ni: nickel, Fe: iron, Si: silicon, W: tungsten, Cu: copper, C: carbon, N: nitrogen) (Dearnley, 1999, Keegan et al., 2007).

Although there are different types of metal alloy used in hip replacement implants, the majority of implants have at least one bearing component composed of metal alloy. The majority of these have a CoCr based alloy as modern manufacturing and finishing techniques allow CoCr bearings be super-polished in order to achieve very low surface roughness values (Tipper et al., 2005), hence making it appropriate for articulating surfaces. In addition, the superior fatigue and ultimate tensile strength of CoCr based alloys compared with cortical bone, as shown in Table 1.3, make it suitable for applications that require long serving life without fracture or stress fatigue (Poitout and Kotz, 2004). Although the mechanical properties of CoCr alloy can provide benefits in terms of longevity of the prosthesis, it can also lead a detrimental phenomenon called stress shielding. This is a process in which an implant prevents the bone from being properly loaded. The higher modulus of elasticity of the implant can result in its carrying the majority of the load. Stress shielding may lead to bone resorption in the region where the applied load is lowest (Long, 2008). Therefore, whilst there are mechanical benefits of CoCr alloy there could also be disadvantages.

<b>Material</b>	<b>Yield Strength (MPa)</b>	<b>Ultimate Tensile strength (MPa)</b>	<b>Fatigue Strength (MPa)</b>	<b>Fracture Toughness (MPa)</b>	<b>Elastic modulus (Gpa)</b>
<b>Stainless Steels</b>	170-790	480-1000	180-550	75-85	190-200
<b>CoCr alloys</b>	250-1500	650-1800	300-950	50-60	210-240
<b>Ti alloys</b>	800-1050	900-1100	45-650	50-55	75-115
<b>Cortical bone</b>	80-150	30	2-12	14-22	0-2

**Table 1.3 Mechanical properties of metal alloys used for orthopaedic prostheses.** (Poitout and Kotz, 2004)

## 1.4 Metal-on-Metal arthroplasty

### 1.4.1 The case for metal-on-metal

In 1953 George McKee introduced the use of MoM articulation in hip arthroplasty as a bearing surface for THR (Macpherson and Breusch, 2010). However, limited understanding of the engineering of these bearings as well as poor performance and early failures led to a decline in their use (Clarke et al., 2003). This coincided with the rising popularity of the Charnley cemented MoP THR and by the 1970s the use of these first generation MoM prostheses was virtually abandoned (Macpherson and Breusch, 2010). However, over the last two decades MoM has again become the popular choice in hip arthroplasty. This was primarily driven by the failure of MoP prostheses due to particulate wear debris formations. Wear debris from MoP implants resulted in an inflammatory process leading to osteolysis and aseptic loosening, ultimately resulting in joint failure (Ingham and Fisher, 2000). Due to the actions of the wear debris it became apparent that these types of articulations would not survive beyond 25 years and with increasing numbers of prostheses being implanted into younger more active patients, this led to the increased use of hard-on-hard (i.e. CoC and MoM) bearing components (De Smet et al., 2008). The popularity of MoM implants has also been aided by advancements in engineering and technology which have increased the understanding of the biomechanical and manufacturing requirements for successful MoM bearings (Back et al., 2005). It is estimated that the volumetric wear produced from MoP implants is 40-100 times higher than that of MoM articulations (Amstutz and Grigoris, 1996). Modern MoM prostheses have shown extremely low wear rates in *in vitro* simulation, with values as low as  $0.1\text{mm}^3/10^6$  cycles being recorded (Firkins et al., 2001), compared with wear of  $40.8\text{mm}^3/10^6$  cycles from MoP implants (Smith et al., 1999). This has been emphasised by a number of studies which have consistently shown that bearing surfaces of MoP prostheses produce more wear compared with hard-on-hard bearing surfaces such as CoC or MoM (Boehler et al., 1994, Semlitsch and Willert, 1997, Goldsmith et al., 2000).

Further to the above, it has also been reported that the long-term survival of the early McKee-Farrar MoM prostheses was actually quite high. It has been reported that survivorship of McKee-Farrar MoM THR was 84% and 74% at 20 and 28 years respectively, post arthroplasty (Brown et al., 2002). In addition, the survivorship of McKee-Farrar MOM THR (77%) was higher than the Charnley MoP (73%) after 20 years (Jacobsson et al., 1996). This gave weight to the idea that hard-on-hard bearings, i.e CoC or MoM, are required for long-term survival of prostheses. Although ceramic is a hard and durable material it is also brittle. Implants, where at least one component is composed of ceramic have led to catastrophic failures of the joint despite the assumed toughness of this material (Hummer et al., 1995, Park et al., 2006). In addition, it has been reported that an audible squeaking noise can be heard from CoC implants whilst moving (Keurentjes et al., 2008, Jarrett et al., 2009). For these reasons the case for MoM bearing surfaces in hip arthroplasty was further strengthened.

In addition to the superior wear characteristics relative to MoP, the use of MoM has further been increased by the hip resurfacing arthroplasty (Macpherson and Breusch, 2010). As mentioned previously, this method of hip joint replacement essentially re-lines the articulating surfaces. This type of arthroplasty has primarily been designed for younger more active patients. It was reported that 46% of all primary hip replacement procedures performed in England and Wales during 2007 were MoM hip resurfacing arthroplasty according to data from the National Joint Registry of England and Wales (2008). MoM hip resurfacing arthroplasty is an attractive alternative to THR as it preserves the femoral head and neck and provides a more accurate biomechanical restoration. Further benefits include; lower rates of dislocation, normal femoral loading and reduced stress shielding, as well as an improved range of movement (Shimmin et al., 2008). In addition, this procedure is believed to increase the ease of revision to THR (Sieber et al., 1999, Macpherson and Breusch, 2010). Therefore, this procedure appears ideal for younger patients where a prosthesis is required for a long duration.

Despite the benefits of MoM coupling in hip arthroplasty, there is concern regarding the release of metal, either as wear debris or soluble ions, from these types of implants (Savarino et al., 1999). Although the wear rate of articular surfaces with MoM prostheses is lower than MoP, MoM implants tend to produce a larger number of smaller wear particles. These range from the nanometer scale, with the majority of particles between 15-25 nm, to aggregates of particles with diameters as large as 400  $\mu\text{m}$ . It is estimated that up to  $2.4 \times 10^{14}$  metal particles are produced per year from a single MoM hip implant compared with  $5 \times 10^{11}$  particles from a MoP implant (Ingham and Fisher, 2000). Metal ions may be released from MoM implants via wear debris or as a result of direct corrosion of the implants *in situ* (Keegan et al., 2008). The release of metal ions in conjunction with wear debris production from MoM implants is an area of great concern as these metals can cause a number of adverse effects.

#### **1.4.2 Metal ion levels following hip arthroplasty**

Although orthopaedic implants are composed of various metals, as shown in Tables 1.1 and 1.2, chromium (Cr) and cobalt (Co) are the most abundantly used metals within the alloys used for bearing components of hip implants. Cr and Co are essential trace elements for human health and are absorbed from the diet. Cr is important in the metabolism of carbohydrates and fats (Anderson, 1997), whereas Co is a constituent of vitamin B12 which is involved in the production of red blood cells (RBCs) (Brink et al., 1950). However, excess levels of the ions within the body are toxic and have many adverse effects (Anderson, 1989, Keegan et al., 2008). The release of these ions from orthopaedic implants has been of great interest for some time. These ions have been measured within the circulation following hip arthroplasty and have been proposed as an indicator for the performance of metal bearings *in situ* (MacDonald et al., 2004, De Smet et al., 2008).

Numerous studies have shown that patients who receive a MoM hip prosthesis have higher levels of Cr and Co within blood, serum or urine compared with MoP patients (Savarino et al., 2002, MacDonald et al., 2003, Rasquinha et al., 2006, Maezawa et

al., 2009). The current author estimates that there are over 50 publications in the last 25 years which have measured metal ion levels in blood following hip arthroplasty surgery. The metal ion levels as measured from a small number of recent studies which show the wide range of metal ions measured within blood are summarised in Table 1.4. Although many studies have shown that Cr and Co levels within the circulation following MoM hip replacement are generally below  $1\mu\text{M}$  (Table 1.4), there are some reports of blood metal ion levels above this value (De Haan et al., 2008, De Smet et al., 2008, Langton et al., 2009). As observed from the peak ion values in Table 1.4, there are also individual subjects within each study who have exceptionally high ion levels compared with the population mean/median. In addition to this, extremely high levels of metal ions ( $>100\ \mu\text{M}$ ) have also been measured in joint fluid around the prostheses of patients with a failed MoM hip resurfacing implant (De Smet et al., 2008, Langton et al., 2010). Furthermore, post-mortem studies have also measured high levels of metals in the liver, lymph nodes, and spleen following traditional hip arthroplasty where at least one bearing component was composed of metal alloy (Langkamer et al., 1992, Case et al., 1994). The high levels of metal ions measured in blood and tissues following MoM hip arthroplasty has been attributed to the wear of these implants due to design, positioning or size of prosthesis (Clarke et al., 2003, Back et al., 2005, Daniel et al., 2006, De Haan et al., 2008, Langton et al., 2010).

To the current author's knowledge, other than the above mentioned post-mortem studies, there are limited data on the disposition of Cr and Co ions following their release from metal implants. However, there have been a number of animal studies which demonstrate that chromium and cobalt may accumulate in certain organs following exposure. Jakobsen and colleagues (2007) demonstrated that chromium, but not cobalt, accumulates within the liver following intramuscular implantation of CoCr alloy wire. In addition, studies which have injected soluble chromium (Tsapakos et al., 1983, Sipowicz et al., 1997) or cobalt (Gregus and Klaassen, 1986, Jansen et al., 1996) into rats have shown significantly higher levels within the kidneys and liver compared with untreated controls. Whilst there are also reports of appreciable levels of Cr and Co in the heart, lungs and spleen of rodents following

acute inhalation or oral exposure to these metals (Wehner and Craig, 1972, Brune et al., 1980, Glaser et al., 1986, Ayala-Fierro et al., 1999).

Author	Type	Follow Up	Cr ( $\mu\text{M}$ )	Co ( $\mu\text{M}$ )	Peak Cr ( $\mu\text{M}$ )	Peak Co ( $\mu\text{M}$ )
<b>Savarino et al., 2002</b>	THR	26 months	0.03*	0.02*	0.12	0.09
<b>Clarke et al., 2003</b>	THR	20 months	0.19*	0.22*	0.58	0.87
	Resurfacing	16 months	0.53*	0.38*	1.65	1.44
<b>Hart et al., 2006</b>	Resurfacing	21 months	0.03	0.07	-	-
<b>Iavicoli et al., 2006</b>	Resurfacing	15.3 months	0.06	0.23	0.09	0.73
<b>Witzleb et al., 2006</b>	Resurfacing	24 months	0.10*	0.07*	-	-
	THR	24 months	0.02*	0.03*	-	-
<b>Daniel et al., 2007</b>	Resurfacing	1 year	0.05	0.02	0.07	0.06
	Resurfacing	4 years	0.02	0.02	0.05	0.04
<b>De Smet et al., 2008</b>	Resurfacing	2.9 years	0.25*	0.10*	1.79	1.60
<b>Moroni et al., 2008</b>	Resurfacing	24 months	0.04	0.02	0.14	0.15
	THR	26.3 months	0.03	0.02	0.13	0.09
<b>Langton et al., 2009</b>	Resurfacing	26 months	0.07*	0.04	1.34	4.60
<b>Hailer et al., 2011</b>	Resurfacing	47 months	0.08	0.02	0.77	2.49
	THR	6 years	0.02	0.01	-	-

**Table 1.4 Metal ion levels measured in blood of patients following MoM hip arthroplasty.** Ion concentrations are means except those denoted by \* which are median values. Peak values indicate highest individual levels recorded in study, if available.



Metal ion exposure is not limited to arthroplasty patients alone; there are a number of occupational exposure hazards also. Metals such as Cr and Co are used in a wide range of industries, from metal refineries and metal finishing (i.e. chrome plating) to leather tanning (Cr). These metals are also used as pigments for industrial painting processes as well as in glass and porcelain manufacture. Occupational biomonitoring of physiological solutions such as blood has been used as a biomarker to evaluate exposure. There have been numerous studies (as summarised in Table 1.5) which have shown higher levels of blood Cr or Co following occupational exposure (Ichikawa et al., 1985, Raffn et al., 1988, Katiyar et al., 2008, Zhang et al., 2011). Workplace exposure limits in the United Kingdom for Cr are 17 µg/l (0.33 µM) and 5 µg/l (0.08 µM) for Co, in blood (2005). However, up until April 2010 there were no safety limits set for hip arthroplasty. Following concerns regarding the toxicity of metal ions from orthopaedic implants, the Medicines and Healthcare products Regulatory Agency (MHRA) stated that blood metal ion levels should be observed in patients following MoM arthroplasty and set a safety level of 7 µg/l for Cr and Co (Cr: 0.13 µM, Co: 0.12 µM) (MDA/2010/033, 2010). However, as mentioned above many patients have blood levels higher than these values and the effects of this exposure are yet to be determined.

<b>Occupation</b>	<b>Author</b>	<b>Cr (µM)</b>	<b>Co (µM)</b>
Chromeplaters	Zhang et al., 2011	0.15	-
Industrial Paint Processing	Katiyar et al., 2008	1.30	-
Leather Tanning	Katiyar et al., 2008	18.58	-
Hard Metal Workers	Raffn et al., 1988	-	0.13
Porcelain Paint Workers	Ichikawa et al., 1985	-	0.04

**Table 1.5 Metal ion levels measured in blood of workers following occupational exposure.** Ion concentrations are means except those denoted by \* which are median values

Although excess environmental and occupational exposure to Cr and Co has been shown to have toxic effects such as; cardiomyopathy, gastrointestinal bleeding, kidney tubular dysfunction and allergic contact dermatitis (Lauwerys and Lison, 1994, Miksche and Lewalter, 1997), the potential chronic effects of elevated levels of metal debris and ion levels following hip arthroplasty remain poorly defined. At present, with the increasing popularity of MoM hip replacement implants there is growing concern that elevated levels of metal debris and ions may lead to a number of adverse immunological and cellular responses.

### **1.4.3 Adverse effects of metal wear debris and ions**

#### **1.4.3.1 The immune system and biomaterials**

In order to appreciate the biomaterial-tissue reactions following metal debris and ion release post hip arthroplasty, it is essential to introduce the concepts and organisation of the immune system. The immune system is an extensive topic, encompassing the complexities of innate and adaptive immunity, and therefore this section will only provide a broad overview of the immune system and the responses to biomaterials. However, particular details will be given on processes which may be involved in hip prosthesis failure.

In general, the immune system is a network of cells, tissues, and proteins and organs that work together to defend the host against attacks and injury by ‘foreign’ invaders such as bacteria and viruses (Ratner et al., 2004 ). Some of the constituents of the innate and adaptive immune systems are shown in Table 1.6. The immune system primarily accomplishes its protective role by distinguishing ‘self’ and ‘non-self’ molecules and initiating a response to remove or isolate the invading body. In most cases, the immune response is so specific and well-regulated that host tissues are not significantly affected. However, severe infections, persistent injury, or autoimmunity (inappropriate immune response to self molecules) may lead to tissue injury caused by the host immune system. Once the immune system identifies an incursion of foreign bodies an immune response is triggered (Todd and Spikett,

2010). The innate immune system provides early rapid response and is composed of cells and proteins which defend the host in a non-specific manner (Murphy et al., 2007). The components of the innate immune system distinguish non-self structures and sites of injury resulting in the activation and recruitment of white blood cells (WBCs) as well as other elements of the immune system (Todd and Spikett, 2010). The primary responding cell types in the early stages are phagocytes such as neutrophils and macrophages. Phagocytes are capable of ingesting and destroying foreign bodies. The primary responding phagocytes are neutrophils which are short-lived cells that, along with phagocytosis, are capable of releasing proteins that aid in the defence of the host. Macrophages, which are mature monocytes, are long-lived phagocytes that are recruited secondary to neutrophils (Murphy et al., 2007). WBCs are activated and recruited to infected and injured sites through a number of chemotactic signals such as increased release of proteins (e.g chemokines and cytokines) or increased expression of adhesion molecules on damaged tissue.

	<b>Innate</b>	<b>Adaptive</b>
<b>Physical/chemical barriers</b>	Skin, mucosal epithelium, antimicrobial proteins	Lymphocytes in epithelia, antibodies
<b>Blood proteins</b>	Complement	Antibodies
<b>Cells</b>	Phagocytes (dendritic cells, macrophages, neutrophils) natural killer cells	Lymphocytes

**Table 1.6 Selected constituents of innate and adaptive immunity.**

Unlike innate immunity which responds in a stereotypical manner to foreign bodies, the adaptive response is highly specific. Cells of the adaptive immune system can only recognise and respond to a specific antigenic determinant. The large number of cells enables the immune system to respond to a wide diversity of foreign bodies. The adaptive component of the immune system is primarily composed of a set of

specialised WBCs called lymphocytes. These cells are mainly divided into two types; B-lymphocytes and T-lymphocytes and additionally, there are also subsets of T-lymphocytes (Todd and Spikett, 2010). Lymphocytes can be distinguished by expression of proteins on the surface of these cells and the most common of these are shown below (Table 1.7).

<b>Lymphocyte</b>	<b>Surface Proteins</b>
B-lymphocyte	CD19, CD20, CD21
Helper T-lymphocyte	CD3, CD4
Cytotoxic T-Lymphocyte	CD3, CD8

**Table 1.7 Selected recognition markers for lymphocytes.**

Adaptive immunity is commonly split into humoral and cell-mediated responses (Murphy et al., 2007). The humoral response is mediated by B-lymphocytes, which bind to a cognate antigen and become activated leading to cell division. Once these cells differentiate into activated plasma cells they produce antibodies that can bind to the foreign matter and aid in its destruction, targeting it for phagocytosis by other WBCs (Ratner et al., 2004 ).

Whilst B-cells are able to recognise antigens T-lymphocytes are not. In order for T-lymphocytes to respond they must be presented with the ‘processed’ cognate antigen by antigen presenting cells (APCs). APCs can be B-lymphocytes, or phagocytic cells such as macrophages and dendritic cells (DCs). Once an APC processes the cognate antigen it expresses specific peptides which interact with T-cell receptors (TCR) on the surface of T-lymphocytes (the TCR is a group of molecules called the CD3 complex and this is known as Signal 1) (Murphy et al., 2007). A second signal (Signal 2) is also required to fully activate T-lymphocytes. Signal 2 is the result of proteins expressed by APCs that interact with co-stimulatory receptors such as CD28 (Jenkins, 1994). Although Signal 1 stimulation alone can lead to T-lymphocyte activation (Andris et al., 2004), in many cases the lack of co-stimulation results in anergy (non-responsive T-lymphocytes) (Murphy et al., 2007). Activation of T-

lymphocytes results in release of cytokines such as interleukin-2 (IL-2) which positively aids T-lymphocyte activation. Activated T-lymphocytes are then able to proliferate and respond (Malek, 2008).

Helper (Th) and cytotoxic T-lymphocytes respond in different ways. CD4<sup>+</sup> helper T-lymphocytes regulate and assist in active immune responses (by assisting B-lymphocyte activation as well as recruitment and activation of cells of the innate system) via direct cell-cell interactions or secretion of cytokines such as IL-2, interferon- $\gamma$  (IFN $\gamma$ ) and tumour necrosis factor- $\alpha$  (TNF $\alpha$ ). CD8<sup>+</sup> cytotoxic T-lymphocytes release cytotoxins such as perforin, granzymes and granulysin that enter infected or damaged cells by creating pores on the surface membrane of these cells. This leads to apoptosis of the damaged or infected cell. In addition, once T-lymphocytes are activated, they also differentiate into memory cells so that future exposure to their cognate antigen leads to a more rapid expansion. This is also the case in B-lymphocyte responses and this is a key characteristic of the adaptive immune system. In addition, there is also a further subset of T-lymphocytes called regulatory T-cells which are able to suppress the immune system such that it does not react to self molecules (Zheng and Rudensky, 2007).

Although different in their recognition and effector processes, the innate and adaptive responses are not exclusive but are integrated components of the overall host defence system in which all cells and proteins function cooperatively. As described above, the innate system can stimulate the adaptive component and influence the adaptive response. In addition, adaptive immunity can direct and utilise the effector mechanisms of innate immunity to clear foreign agents.

The placement of a biomaterial *in vivo* initiates a response by the host defence system (Figure 1.3). The initial response, lasting hours or days, is an inflammatory process characterised by exudation of fluid and plasma proteins and the migration of WBCs. WBC (mainly neutrophil) recruitment to the implant site is, in part, regulated by chemotactic agents and molecules on cell surfaces. The main purpose of this cell migration is phagocytosis, however, this is not always possible due to the

size and properties of the biomaterial. The early stages of inflammation are dominated by neutrophils, however, longer durations (days) lead to the presence of mononuclear cells such as macrophages, lymphocytes and plasma cells. These cells are able to mediate the healing process of granulation tissue formation as well as fibrosis and/or tissue regeneration (Ratner et al., 2004 ).

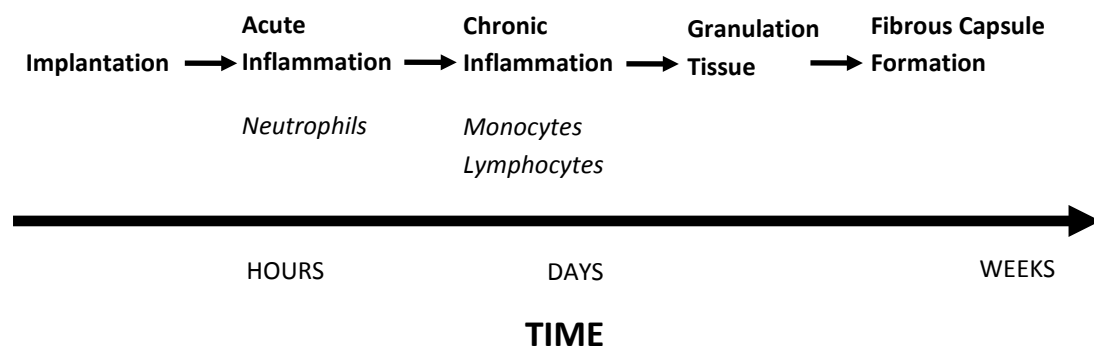


**Figure 1.3 Sequence of events involved in the inflammatory and wound-healing response following biomaterial implantation.**

#### **1.4.3.2 Soft tissue masses developing following arthroplasty**

There are a number of reports of peri-prosthetic soft-tissue masses in patients with MoM hip resurfacing or THR arthroplasty. Madan and colleagues (2000), describe an intra-pelvic cyst, filled with cement and metallic debris, in a female patient 14 years post implantation of a MoM THR. These authors report that the cause was most likely due to the debris. There have also been isolated case reports of peri-prosthetic soft tissue masses, or pseudotumours, in female patients following MoM hip resurfacing arthroplasty (Boardman et al., 2006, Counsell et al., 2008). In both of these cases there was evidence of necrotic tissue within the synovium as well as lymphocyte infiltration. Boardman et al. (2006) also described infiltrations of foreign-body giant cells (fusion of giant macrophages in an attempt to phagocytose large material) and histiocytes, areas of fibrous tissue and the presence of metal

debris. Additionally, these authors recorded high concentrations of Cr (122 µg/g; 2.35 µM/g) and Co (277 µg/g; 4.70 µM/g) in the excised mass.

Initially it was thought that these pseudotumours were confined to female patients, however, recently there have been reports of the presence of symptomatic soft-tissue masses in male patients, following MoM hip resurfacing or THR arthroplasty (Pandit et al., 2008, Toms et al., 2008). In a series of 20 MoM resurfaced joints (3 male), patients presented symptoms varying from dislocation, pain, the presence of a lump and rash (Pandit et al., 2008). The pseudotumours, which were predominantly composed of necrotic connective tissue accompanied by granulomatosis, were locally very destructive and 13 of the patients required revision surgery. In several cases, the authors also noted the presence of lymphocyte and macrophage infiltrations as well as metal particles.

A similar soft-tissue response was described in a review of 19 patients (8 male) reporting early post-operative pain following MoM THR (Toms et al., 2008). At the time of revision, a soft tissue thickening and/or fluid filled cavity were observed. In addition, tissue necrosis and lymphocytic infiltration were described. In this study and those described above, microbiological data did not reveal any evidence of infection. These data show that this inflammatory process is not mediated by a microorganism rather it is sterile inflammation. It has also been suggested that these masses may be part of an allergic response to a moderate release of metal wear particles or the result of toxicity from a large concentration of metal wear debris or ions (Pandit et al., 2008).

#### **1.4.3.3 Aseptic lymphocytic vasculitis-associated lesions following arthroplasty**

Prior to the discovery of pseudotumours there had been reports of a T-lymphocyte associated immune response following MoM hip arthroplasty. Dense lymphocyte infiltrations, described as aseptic lymphocytic vasculitis-associated lesions (ALVAL), were observed following MoM THR (Davies et al., 2005, Willert et al., 2005, Witzleb et al., 2006). In a series of 19 MoM implants, which were revised due

to pain and swelling, histological examination of the periprosthetic tissue demonstrated intense perivascular lymphocytic cuffing (Davies et al., 2005). These authors suggested that a delayed T-lymphocyte mediated hypersensitivity reaction had occurred as a result of particulate metal wear debris. Similar lymphocyte infiltrations, which may be accompanied by pseudotumours as described above, have been also observed in periprosthetic tissues following MoM hip resurfacing arthroplasty (Counsell et al., 2008, Pandit et al., 2008, Toms et al., 2008). In comparison with periprosthetic tissues from MoP patients, periprosthetic tissues from MoM implants contain more lymphocytes and plasma cells and less macrophages. The dense lymphocytic infiltration is thought to be a distinct histological characteristic of tissue reactions to MoM bearing surfaces and, is said to be part of an inflammatory process which leads to periprosthetic osteolysis and ultimately joint failure (Davies et al., 2005, Willert et al., 2005, Witzleb et al., 2006).

#### **1.4.3.4 Hypersensitivity following arthroplasty**

It has been documented that polyethylene particles from MoP hip implants elicit a non-specific foreign body immune response consisting mainly of macrophages and fibroblasts (Al-Saffar et al., 1994, Campbell et al., 1996). This involves foreign-body giant cells and fibrosis surrounding the biomaterial and isolating it, and a foreign-body reaction from the local tissue environment. In contrast, it has been suggested that metal released from MoM implants may lead to an adaptive or antigen-specific immune response. This cell-mediated hypersensitivity is the response to a previously encountered antigen that results in helper T-lymphocyte activation and in some cases granuloma formations. It is reported that metal ions bind to serum proteins to form metal-protein complexes (Yang and Black, 1994, Merritt and Rodrigo, 1996) and these complexes may be antigens that induce hypersensitivity responses (Hallab et al., 2008). Whilst these metal-protein complexes are immunologically active and can induce activation and proliferation of lymphocytes *in vitro* (Hallab et al., 2001), the mechanism by which these complexes elicit lymphocyte activation is currently unclear. It has been suggested that metal-protein complexes lead to non-specific activation of T-lymphocytes by cross-linking



receptors similar to superantigens. Alternatively, antigen-independent pathways which could cause cross-linking of the thiols of cell-surface proteins activating a tyrosine kinase that is involved in the activation of T-lymphocytes. Despite these reports, the limited evidence below indicates that antigen-dependent stimulation via a delayed-type IV cell mediated hypersensitivity is the dominant mechanism associated with implant-related hypersensitivity responses.

Immunohistochemical analysis of periprosthetic tissues from failed metal implants showed the presence of metal wear debris and of extensive numbers of T-lymphocytes which expressed CD25 (the IL-2 receptor which is a marker of T-lymphocyte activation) (Lalor and Revell, 1993). Further studies showed that macrophages within periprosthetic tissue expressed co-stimulatory molecules which would enhance T-lymphocyte activation (Doorn et al., 1996, Davies et al., 2005, Witzleb et al., 2006). Recent *in vitro* studies have also shown that CoCr alloy particles and individual metal ions can lead to monocyte upregulation of T-lymphocyte co-stimulatory molecules (Caicedo et al., 2010). In particular this study showed that metal ions induce a stronger response than metal particles. This could indicate that metal-protein complexes have antigenic properties which may lead to T-lymphocyte activation following antigen presentation by monocytes.

Metal allergy or dermal hypersensitivity following implantation of a metal orthopaedic prosthesis has only rarely been reported (Goodman, 2007). However, this may be because no reliable standard tests for metal allergy or hypersensitivity exist at present (Shimmin et al., 2008). None-the-less there are a number of reports which show that lymphocytes from MoM arthroplasty patients may be activated in the presence of metal ions *in vitro*. It has been shown that T-lymphocytes from patients with a loose metal prosthesis are more activated following *in vitro* exposure to Cr or Co extract than lymphocytes from control subjects with no metal prosthesis (Granchi et al., 2000). Additionally, primary lymphocytes from patients with well-functioning MoM total hip implants showed a stronger proliferative response to Cr and Co when cultured *in vitro* compared with lymphocytes of healthy control subjects (Hallab et al., 2008). Further to this, this study also demonstrated a

differential secretion of T-lymphocyte associated cytokines following THR, indicating a Th1 cell type response following MoM THR. These authors went on to propose a mechanism by which T-lymphocyte mediated metal reactivity, involving cytokine and prostaglandin E2 (PGE2) release, may contribute to osteolysis following metal debris or ion production (Figure 1.4). However, a recent study which also used this *in vitro* culture method was unable to distinguish alterations in lymphocyte response between patients with a pseudotumour and those currently unaffected (Kwon et al., 2009a).

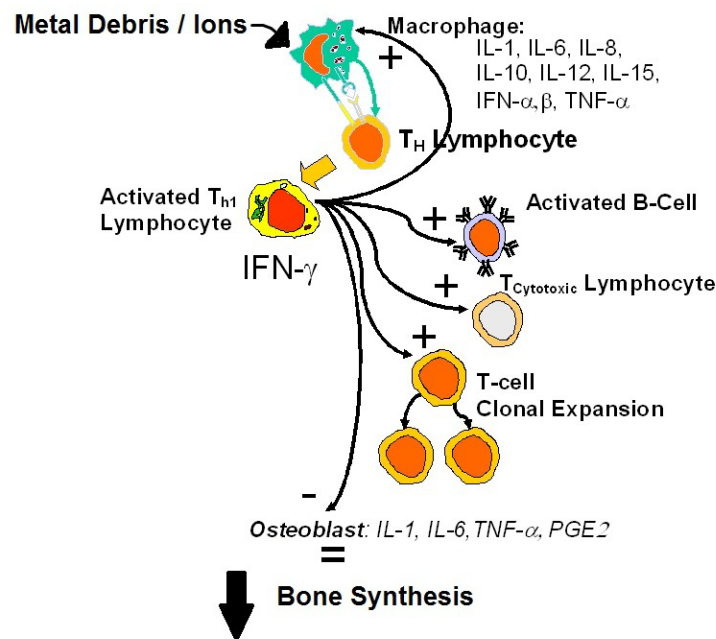


**Figure 1.4 Schematic diagram of metal exposure induced cytokine release associated with activation of Th1 lymphocytes resulting in inhibitory effects on bone function.** (adapted from Hallab et al., 2008).

#### 1.4.3.5 Toxicity of metal ions

Although metal particles and ions may induce stimulatory effects on cells of the immune system, the majority of *in vitro* data suggest that metal, particles or individual ions, will also have toxic effects. Chromium ions, particularly in the form of Cr<sup>6+</sup>, are cytotoxic. It is currently unclear whether the hexavalent form (Cr<sup>6+</sup>) or

the trivalent form ( $\text{Cr}^{3+}$ ) of chromium is released from MoM implants. However,  $\text{Cr}^{3+}$  is unable to cross the cell membrane whereas  $\text{Cr}^{6+}$  can readily enter the cell through non-specific anionic channels (Carter, 1995). Merritt and Brown (1995) demonstrated that only  $\text{Cr}^{6+}$  entered red blood cells (RBCs), in addition they also demonstrated that the intracellular  $\text{Cr}^{6+}$  collected in RBCs was rapidly reduced to  $\text{Cr}^{3+}$  following corrosion of stainless steel and CoCr implants *in vivo*. Therefore, it is believed that  $\text{Cr}^{6+}$  is released from CoCr implants before it enters cells (Merritt and Brown, 1995, Shettlemore and Bundy, 1999).  $\text{Cr}^{6+}$  exposure has been demonstrated to cause cytotoxicity, genotoxicity, and carcinogenicity (Sargeant and Goswami, 2007). Once  $\text{Cr}^{6+}$  enters the cell it is reduced to  $\text{Cr}^{3+}$  (Figure 1.5). The intermediate species formed are highly reactive and lead to the generation of reactive oxygen species (ROS). This can result in activation of caspases, promotion of death signals, inhibition of survival factors as well as intracellular damage as shown in Figure 1.6 (Pulido and Parrish, 2003).  $\text{Co}^{2+}$  can also enter cells, possibly through transporters involved in the uptake of divalent cations (Mabilleau et al., 2008). In addition,  $\text{Co}^{2+}$  ions are capable of forming free radicals via a Fenton-like reaction [ $\text{Co}^{2+} + \text{H}_2\text{O}_2 \rightarrow \text{Co}^{3+} + \cdot\text{OH} + \text{OH}^-$ ] (Leonard et al., 1998) resulting in cellular apoptosis, as displayed in Figure 1.6.

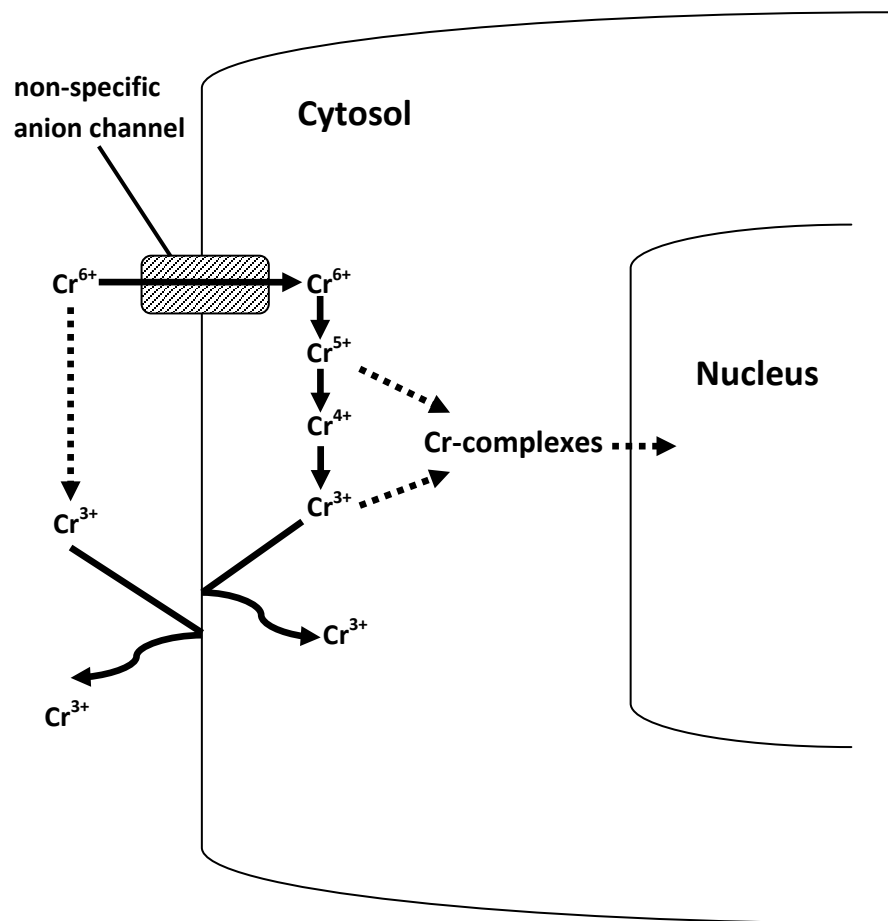


**Figure 1.5 Production of reactive intermediates produced by  $\text{Cr}^{6+}$  after entering the cell.**

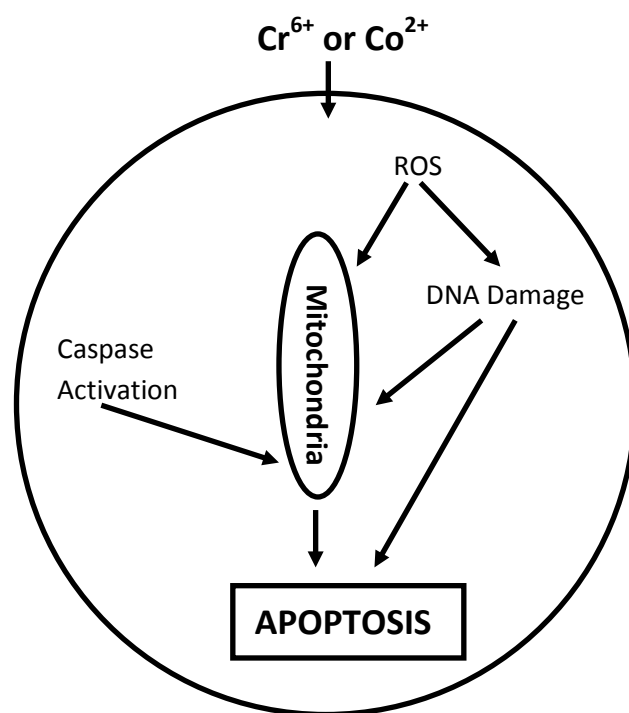


**Figure 1.6 Pathways by which Cr<sup>6+</sup> and Co<sup>2+</sup> induce cell death. Metal ion exposure can result in caspase activation as well as ROS formation leading to mitochondrial and DNA damage causing cell death.** (adapted from Pulido and Parrish, 2003).

Both Cr and Co ions as well as CoCr alloy particles have been shown to induce death of lymphocytes, macrophages and monocytes following *in vitro* exposure (Granchi et al., 1998a, Vasant et al., 2003, Huk et al., 2004, Hallab et al., 2008, Kwon et al., 2009b, Caicedo et al., 2010), however, the concentrations at which cell death occurs is debatable. Several authors have shown cytotoxicity at concentrations below 50  $\mu$ M (Bagchi et al., 2000, Vasant et al., 2003, Lalaouni et al., 2007, Raghunathan et al., 2009), whereas others have reported cytotoxicity to occur only at 100  $\mu$ M and above (Hallab et al., 2008, Kwon et al., 2010). Additionally, metal ions have been shown to modulate release of cytokines involved in activation and proliferation of these cells following exposure to micromolar concentrations of metal ions (Wang et al., 1996a, Wang et al., 1996b, Granchi et al., 1998b, Gavin et al., 2007).

Further to the above cytotoxic effects, Cr ions can also lead to DNA damage within the cell. This can occur due to oxidative damage resulting from the intracellular reduction of Cr<sup>6+</sup> or by the binding of Cr<sup>3+</sup> to DNA (Sargeant and Goswami, 2007). In addition to this, both Cr<sup>6+</sup> and Co<sup>2+</sup> can also inhibit DNA repair mechanisms (Witkiewicz-Kucharczyk and Bal, 2006). Worryingly, clinical data also show increased levels of chromosomal translocations and aneuploidy in peripheral lymphocytes from patients following MoM hip arthroplasty (Ladon et al., 2004, Dunstan et al., 2008).

#### **1.4.3.6 Alterations in circulating lymphocyte numbers in patients following arthroplasty**

It has been reported that the cytotoxicity of metal ions may lead to decreased numbers of circulating lymphocytes *in vivo* in patients following MoM hip replacement. An association between metal ion levels and the number of circulating lymphocytes has been reported (Hart et al., 2006, Hart et al., 2009). It was shown that lymphocyte counts were reduced, particularly CD8<sup>+</sup> cytotoxic T-lymphocytes, following MoM hip replacement. These authors also put forward a threshold value of combined levels of blood Cr and Co in excess of 5 µg/l (~0.09 µM) which would result in decreased numbers of lymphocytes. It is also proposed that metal ions could reduce circulating lymphocyte numbers by diverting them from the circulation to the hip joint or by modulating the process of antigen presentation to and expansion of lymphocytes. Savarino and colleagues (1999) also observed significant reductions in the number of helper T-lymphocytes, B-lymphocytes and natural killer cells in patients with failed hip implants. It was suggested that metal ions released from these implants may have mediated their toxic effects on lymph nodes resulting in the decreased numbers of circulating cells.

With the increasing numbers of hip prostheses being implanted, particularly in younger more active patients, there is growing concern about the long-term exposure to metal debris and ions. Although a number of first generation MoM THR

prostheses remain *in situ* ( $\geq 30$  years) with limited reports of any fatal responses (Sauve et al., 2007), considering the adverse effects following short-term implantation described above (and summarised in Figure 1.7) there is a clear requirement to investigate the potential toxic effects of metal debris and ion release.

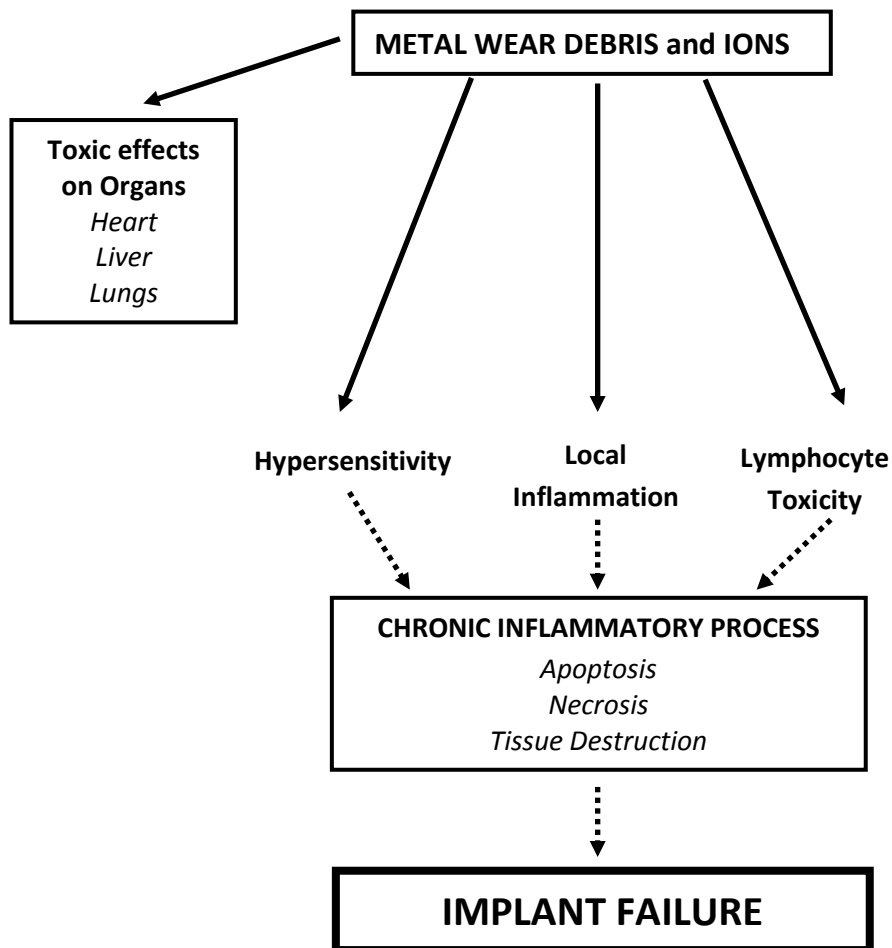


**Figure 1.7 Summary of effects of metal wear debris and ion release from MoM hip implants that may lead to prosthesis failure.**

## 1.5 Aims of present study

This discussion has illustrated that the release of metal wear debris or ions from MoM hip implants is a cause for concern for both clinicians and patients. As described, metal release from these implants can lead to detrimental effects on the immune system as well as on other body systems. It is essential to determine the potential effects of long-term exposure to metal ions or debris, as well as identifying the mechanism(s) involved in any adverse effects. To this end this thesis has been focussed on an investigation into the interactions of Cr and Co ions, and particulate debris, with the immune system. The aims of the studies described in the thesis are:

1. To determine the toxicity of Cr<sup>6+</sup> and Co<sup>2+</sup> to U937 monocytes at clinically relevant concentrations, *in vitro*. Also, to identify whether there is any synergy in the toxic effects of these two ions when used in combination.
2. To assess the toxicity of Cr<sup>6+</sup> and Co<sup>2+</sup> to primary human lymphocytes at clinically relevant concentrations, *in vitro*.
3. To investigate possible mechanisms for toxicity or effects that may modulate the function of primary human lymphocytes. Also, to identify whether there is any synergy in the effects of these two ions when used in combination.
4. To develop and implement an *in vivo* model which can be used to assess the inflammatory processes involved following metal debris release. Also, to determine the distribution of metal ions released from hip implants wear debris *in vivo* into distant organs.
5. To identify alterations in circulating WBC numbers in patients following MoM hip arthroplasty, and to determine whether any changes observed in WBC numbers is related to whole blood metal ion levels.



# Chapter 2

## **2. MATERIALS AND METHODS: GENERAL**

This chapter outlines the general materials, methods and equipment used for the duration of the current research. Methods which were adapted at specific stages of the research are described in the appropriate later chapters.

### **2.1 Cells**

This section details the cells used in this research, how they were prepared, maintained and treated and the analysis methods employed.

#### **2.1.1 Cells used**

The following cell types were used throughout the research;

- U937 cells, a human leukemic pre-monocyte lymphoma cell line (European Collection of Cell Cultures; Wiltshire, UK)
- Primary human lymphocytes, isolated from Buffy Coat (Scottish Blood Transfusion Service; Glasgow, UK)
- Dendritic cells (DCs), derived from mouse bone marrow (Lutz et al., 1999)
- 2.4G2 Hybridoma cells were used to produce 2.4G2 antibody which binds to Fc $\gamma$  II/III receptors

##### **2.1.1.1 Culturing of U937 cells**

U937 cells were cultured in 10ml complete RPMI-1640 in 25cm<sup>2</sup> culture flasks (Iwaki; Iwaki City, Japan) at 37°C, 5% CO<sub>2</sub>. Complete RPMI-1640 consisted of RPMI-1640 (Lonza, Slough, UK) medium supplemented with 10% (v/v) foetal calf serum (FCS), L-glutamine (2 mM), penicillin (100 µg/ml), streptomycin (100 µg/ml) (all from Invitrogen; Paisley, UK). These cells were routinely split every three days

at a ratio of 1:10. This was achieved by centrifuging 10ml of cell suspension at 50xg for 5 minutes. The supernatant was aspirated and the cells resuspended in 2ml of fresh complete RPMI-1640. 200 $\mu$ l of this cell suspension was then added to a fresh 25cm<sup>2</sup> culture flask containing 9.8ml of fresh complete RPMI-1640.

#### **2.1.1.2 Isolation of primary human lymphocytes**

Peripheral blood mononuclear cells (PBMCs) were isolated by density gradient centrifugation using Histopaque-1077 (Sigma-Aldrich; Dorset, UK) from approximately 60ml of Buffy Coat under sterile conditions. In order to achieve this, 60ml of buffy coat was added to 60ml of RPMI-1640. 30ml of diluted buffy coat was then gently layered onto 15ml of Histopaque-1077 in a 50ml centrifuge tube. This was then centrifuged at 600xg for 25 minutes, with the brake set to 'off'. This allowed four distinct layers to be formed in the tube (Figure 2.1). Once the top layer was aspirated off, the cellular layer was removed and resuspended in 45ml of RPMI-1640. This was then centrifuged at 250xg for 10 minutes and the supernatant aspirated. This step was repeated twice more. Following this, lymphocyte enrichment was achieved as previously described (Martín-Romero et al., 2000). Briefly, PBMCs ( $2.5 \times 10^6$  cells/ml) were incubated in a 75cm<sup>2</sup> culture flask (Iwaki; Iwaki City, Japan) with complete RPMI-1640 for 1 hour at 37°C, 5% CO<sub>2</sub>. The medium with the non-adherent cell suspension was then transferred to another culture flask and incubated for a further hour to further deplete the monocyte population and yield an enriched lymphocyte population in suspension.

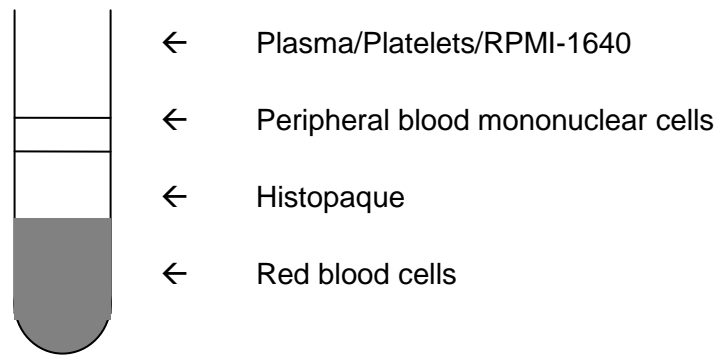


**Figure 2.1 Isolation of peripheral mononuclear cells from buffy coat.**

### **2.1.1.3 Preparation of dendritic cells**

Bone marrow DCs were prepared from mouse bone marrow obtained from femurs and tibias excised from female BALB/c mice. Under sterile conditions, the epiphyses of the bones were cut off, and the bone marrow within the shaft flushed through with RPMI-1640 and a 23 gauge needle (BD Bioscience; Oxford, UK). Following this, the bone marrow cell concentration was adjusted to  $5 \times 10^5$  cells/ml and cultured in six-well plates (Nunc A/S; Roskilde, Denmark) in complete RPMI-1640 containing 10% of culture supernatant from X63 myeloma cells transfected with mouse GM-CSF cDNA (kindly supplied by Dr Owain Millington; Centre for Biophotonics, University of Strathclyde, Glasgow, UK). Fresh complete medium was added to the cell cultures every 3 days.

### **2.1.1.4 Hybridoma 2.4G2 cells**

Hybridoma 2.4G2 cells (kindly supplied by the Centre for Biophotonics, University of Strathclyde; Glasgow, UK) were cultured in complete RPMI-1640 in  $25\text{cm}^2$  culture flasks. Two days after these cells became confluent, the cells were centrifuged and supernatant removed. The supernatant, which contained the 2.4G2

antibody, was stored at 4°C. This antibody blocks non-antigen-specific binding of immunoglobulins to the FcγIII and FcγII, and possibly FcγI, receptors.

## **2.1.2 Preparation of metal ion solutions**

Freshly weighed chromium oxide (Cr<sub>2</sub>O<sub>3</sub>) and cobalt chloride (CoCl<sub>2</sub>) (both from Alfa Aesar; Lancashire, UK) were dissolved in sterile distilled water and filter-sterilized, using a 0.2µm filter, to give 100 mM stock solutions of Cr<sup>6+</sup> and Co<sup>2+</sup>, respectively. These were then used to prepare the required concentrations of Cr<sup>6+</sup> and Co<sup>2+</sup> in complete RPMI-1640. These solutions were all made freshly on the day of the experiment.

## **2.1.3 Cell analysis**

### **2.1.3.1 MTT assay for cell viability**

The MTT assay is a colorimetric assay system which measures the reduction of the yellow tetrazolium salt MTT (3-(4,5-Dimethylthiazol-2-yl)-2,5-diphenyltetrazolium bromide), which is readily taken up by cells, into an intense blue formazan product by the reductase enzymes in the cytosol and mitochondria of viable cells. The water-insoluble formazan accumulates within viable cells and is measured spectrophotometrically. Any increase in formazan production is proportional to the number of viable cells that are able to generate it by the dehydrogenases within the cells (Mosmann, 1983).

In order to make a 10mM solution of MTT, 414.3mg of MTT (Sigma-Aldrich; Dorset, UK) was dissolved in 100ml of Phosphate-Buffered Saline (PBS; Sigma-Aldrich; Dorset, UK) which had been adjusted to pH 6.75 by the addition of HCl. This solution was sterile filtered with a 0.2µm filter and stored at 4°C until required.

At each culture end-point cells were collected via centrifugation (350xg for 5 minutes). Where cells were cultured in 24 well flat-bottomed plates, cell suspensions were transferred into 1.5ml eppendorff tubes before centrifugation, and, where 96 well round-bottomed plates were used, cells were centrifuged in these. Once collected, the supernatant was removed and cells were resuspended in MTT solution (250µl for 24 well cultures and 50µl for 96 well cultures). Following an incubation period of 4 hours at 37°C, the cells were centrifuged (350g for 5 minutes) and supernatant removed. The cells were then suspended in dimethyl sulfoxide (DMSO; Sigma-Aldrich; Dorset, UK) to dissolve the formazan product (1ml for 24 well cultures and 200µl for 96 well cultures). The absorbance of light was measured at 540nm immediately using a Bio-Rad Model 450 microplate reader and the data were recorded. For 24 well cultures, the dissolved product was transferred into a 96 well plate before measuring absorbance.

### **2.1.3.2 Neutral red assay for cell viability**

The Neutral Red (NR) assay is based on the ability of viable cells to incorporate the NR dye. NR is a weak cationic dye which readily penetrates through membranes of cells by non-ionic diffusion and accumulates intracellularly within lysosomes of only viable cells. Damaged or dead cells lose the ability to retain the dye. This retention of NR leads to the lysosomes appearing bright red. The NR destain solution is used to extract the dye from the viable cells and the absorbance of solubilised dye is then determined spectrophotometrically. Quantification of the extracted NR by spectrophotometry has been correlated with cell numbers by equating the intensity of the red colour with the number of cells (Repetto et al., 2008).

5mg of NR powder (Sigma-Aldrich; Dorset, UK) were dissolved in 100ml of PBS. The solution was incubated overnight at 37°C and undissolved crystals were filtered out with a 0.2µm filter. The filtered solution was stored at 4°C. The NR destain was made by mixing together 50ml ethanol, 1ml glacial acetic acid and 49ml distilled water and was then stored in a flammable solvent cupboard.

At each culture end-point, cells were collected via centrifugation (350xg for 5 minutes). The cells cultured in different culture plates were centrifuged in the manner described in section 2.1.3.1. Once centrifuged, the supernatant was removed and cells were resuspended in NR solution (500µl for 24 well cultures and 100µl for 96 well cultures) and incubated for 3 hours at 37°C. The cells were then centrifuged (350g for 5 minutes) and supernatant removed. At this point the cells were resuspended in PBS (1ml for 24 well cultures and 200µl for 96 well cultures). Following this the cells were centrifuged and supernatant discarded. NR destain solution was then added (500µl for 24 well cultures and 100µl for 96 well cultures). A homogeneous colour was obtained by placing the culture plate on an orbital shaker for at least 30 minutes or by vortexing the eppendorff tubes for 30 seconds. The absorbance of light was measured at 540nm using a Bio-Rad Model 450 microplate reader and the data were recorded. For 24 well cultures, the solubilised product was transferred into a 96 well plate before measuring absorbance.

### **2.1.3.3 Flow cytometry analysis of cell cycle**

Cell suspensions were transferred into 12x75mm BD Falcon FACS tubes (BD Biosciences; Oxford, UK). These were centrifuged (350xg for 5minutes) and supernatant aspirated. The cells were then resuspended in FACS buffer, which consisted of 10% (v/v) FCS and 0.02% (w/v) sodium azide (Sigma-Aldrich; Dorset, UK) dissolved in PBS, and then centrifuged for 5 minutes (350xg) and the supernatant removed. Following this wash step, the cells were suspended in 1ml of 70% (v/v) ethanol and placed on ice for 15 minutes. After this period, the cells were washed twice with FACS buffer and resuspended in 100µl propidium iodide (PI) solution comprising of 50µg/ml PI, 50µg/ml RNase A (both Sigma Aldrich; Dorset, UK), and FACS buffer. The cells were then incubated at 4°C for 30 minutes. At the end of this period, 200µl of FACS buffer were added and the samples were analysed using a Becton Dickinson FACS Canto flow cytometer with FACSDiva (BD Biosciences; Oxford, UK) software programme. The percentages of cells within the G<sub>0</sub>/G<sub>1</sub>, S, and G<sub>2</sub>/M phases of the cell cycle were determined using FlowJo software (Tree Star; Oregon, USA). This was achieved since PI binds with DNA and as the

DNA content of cells duplicates during the S phase of the cell cycle the fluorescence of cells in the G<sub>2</sub>/M phase is twice as high as cells in G<sub>0</sub>/G<sub>1</sub> phase (Krishan, 1975).

#### **2.1.3.4 Flow cytometry analysis of apoptosis**

Cell suspensions were transferred into FACS tubes and were centrifuged for 5 minutes (350xg). The supernatant was aspirated and the cells resuspended in FACS buffer. Following this, the cells were centrifuged for 5 minutes (350xg) and supernatant discarded. The cells were then resuspended in 100ul Annexin binding buffer, which consists of 0.01M HEPES, 0.14M NaCl and 2.5mM CaCl<sub>2</sub> (all Sigma Aldrich; Dorset, UK) in distilled water (pH 7.4). 5µl of Annexin V-phycoerythrin (PE) and 7-Aminoactinomycin D (7-AAD) (both BD Bioscience; Oxford, UK) were then added to each tube. The tubes were vortexed and incubated at room temperature for 15 minutes in the dark. Following this incubation period, 200µl of Annexin binding buffer and FACS Flow (BD Bioscience; Oxford, UK) were added to each tube. The data were recorded using a FACSCanto flow cytometer and using FACSDiva software. It was possible to distinguish cells which were viable, in early stages of apoptosis, in late stages of apoptosis and necrotic. This was possible as Annexin V binds to the negatively charged phospholipid phosphatidylserine (PS) which is redistributed from the inner to outer layer of the cell membrane during apoptosis. This is an early event whilst the cell is still viable and therefore not permeable to chemicals such as 7-AAD (which binds to DNA in the nuclei) (Vermees et al., 1995). Cells in early stages of apoptosis are not permeable to 7-AAD but bind to Annexin V. Cells which bind to Annexin V, and are permeant to 7-AAD are in the later stage of apoptosis as the cell membrane is compromised. Cells which have 7-AAD bound to DNA, but are not Annexin V positive are said to be necrotic, as they are non-viable but not through apoptotic mechanisms.



### **2.1.3.5 Analysis of cell morphology and viability via microscopy**

In order to assess the effects on cell morphology and viability, cells were stained with Acridine Orange (AO) (Sigma-Aldrich; Dorset, UK) and PI. PI ingresses into cells with damaged cell membranes staining and interacting with DNA to stain red. AO is cell permeable and enters intact cell membranes to produce a fluorescent green product.

60mm<sup>2</sup> Petri dishes (BD Bioscience; Oxford, UK) were coated with 2ml 0.01% (v/v) poly-L-lysine (Sigma-Aldrich; Dorset, UK). After 10 minutes the poly-L-lysine was aspirated and Petri dishes allowed to dry at room temperature overnight. Cells suspended in 4 ml of complete RPMI-1640 were then seeded onto the coated dish and 1µmol of PI and AO each was added. This was then incubated at 37°C for 30 minutes. Following this incubation period, the medium was aspirated and cells were gently washed twice with PBS. The cells were then viewed using a Carl Zeiss Axio Imager microscope under a 40x water immersion lens (NA 0.80). Fluorescence was excited using a mercury lamp and emission was recorded using a fluorescein isothiocyanate (FITC)/Rhodamine filter block (485/515-530nm; 546/580-563nm) for AO and PI. Digital images were captured and analysed using AxioVision 4.6. The number and percentage of cells displaying characteristics of apoptosis and necrosis was determined from 5 independent images from random areas on the petri dish. Typically, an area of 0.2 mm<sup>2</sup> was examined.

### **2.1.3.6 Surface antigen staining of cells for flow cytometry**

Cells in suspension were added to FACS tubes, centrifuged for 5 minutes (350xg) and the supernatant aspirated. The cells were then washed twice with FACS Buffer. Once washed the cells were resuspended in FACS buffer containing Fc block (2.4G2 hybridoma supernatant) together with the appropriate combinations of fluorochrome-conjugated monoclonal antibody. Sample cells were also added to a separate tube containing Fc block and the relevant isotype control(s) to identify any non-specific binding. The tubes were then vortexed gently and incubated for 15 minutes in the dark at room temperature. After this incubation period the tubes were centrifuged at

350x g for 5 minutes and the supernatant removed. 2 ml of FACS buffer were added to each tube and they were then centrifuged at 350x g for 5 minutes. The supernatant was aspirated and this step was repeated. Following this, the cells were suspended in 400 $\mu$ L FACS flow and mixed thoroughly. The samples were analyzed on a FACS Canto flow cytometer using FACSDiva software.

### **2.1.3.7 Cell proliferation assay**

Cell proliferation was determined by a non-isotopic BrdU Cell Proliferation Immunoassay kit (Merck Chemicals; Nottingham, UK). This immunoassay quantifies cell proliferation by incorporating BrdU into the newly synthesized DNA strands of actively proliferating cells. The kit provided all the agents and solutions required.

Briefly, 10 $\mu$ l of BrdU label was added to each well of a 96 well culture plate during the final 4 hours of culture. The plate was then centrifuged (300x g for 10 minutes) and the supernatant aspirated. The cells were then fixed, permeabilized and DNA denatured by adding 200 $\mu$ l of the supplied fixative/denaturing solution to each well. The plate was then covered and incubated at room temperature for 30 minutes. Following this period, the fixative/denaturing solution was aspirated from each well. 100 $\mu$ l/well of detector anti-BrdU monoclonal antibody was then added and allowed to incubate for 1 hour. The wells were then washed with wash buffer and 100 $\mu$ l/well horseradish peroxidase (HRP) conjugated goat anti-mouse antibody added. Following 30 minutes incubation the wells were washed with wash buffer and 100 $\mu$ l tetra-methylbenzidine (TMB) added and incubated for 15 minutes in the dark at room temperature. Following this, 100 $\mu$ l stop solution (2.5N sulfuric acid) was added and absorbance measured in each well using a Thermo Scientific Multiskan Ascent spectrophotometer plate reader at dual wavelengths of 450-590 nm.

### 2.1.3.8 ELISA

Cytokine levels were determined by collecting supernatants from appropriate cell cultures. These were then assayed using Ready-SET-Go! enzyme-linked immunosorbent assay (ELISA) kits (eBioscience; Hatfield, UK). The kit provided all components required except wash buffer, which consisted of 0.05% Tween-20 (Sigma-Aldrich; Dorset, UK) dissolved in PBS, and 2M H<sub>2</sub>SO<sub>4</sub> (Fisher Scientific; UK).

Prior to collecting supernatant, each well of the ELISA plate was coated with 100 µl capture antibody dissolved in coating buffer, which was PBS, pH 7.4. The plate was sealed and incubated overnight at 4°C. Following this incubation the samples were aspirated and washed 5 times with 250 µl/well of wash buffer. The samples were then blocked with 200 µl/well of assay diluent and incubated at room temperature for 1 hour. Once this period had elapsed, the liquid was aspirated and samples washed as above. The standards were prepared in assay diluent, as noted on the Certificate of Analysis and 2-fold serial dilutions of the top standards were performed to make the standard curve (range of standards; 500, 250, 125, 62.5, 31.25, 0 pg/ml) . 100 µl/well of each standard or collected supernatant was added to the appropriate wells (where required the collected supernatant was diluted in complete RPMI-1640 before addition to the well). The plate was sealed and incubated at room temperature for 2 hours. Following this incubation period, the wells were washed as above. 100 µl of detection antibody diluted in assay diluent was added to each well and the plate sealed and incubated at room temperature for 1 hour. This was followed by a wash step as described above and then 100 µl/well of Avidin-HRP diluted in assay diluent was added. The plate was sealed and incubated at room temperature for 30 minutes. The samples were then aspirated, and washed as above. 100 µl of substrate (TMB) solution was added to each well and then the plate was incubated at room temperature for 15 minutes. Following this period 50 µl of 2M H<sub>2</sub>SO<sub>4</sub> was added to each well. At this point the absorbance was measured in each well using a Thermo Scientific Multiskan Ascent spectrophotometer plate reader at dual wavelengths of 450-570 nm.

### **2.1.3.9 Assessment of mitochondrial damage**

The DePsipher kit (R & D Systems; Abindon, UK) is an assay which analyses the extent of mitochondrial membrane potential disruption. This disruption leads to mitochondrial outer membrane permeabilisation (MOMP) which results in apoptosis. The DePsipher kit contains a cationic dye (5,5',6,6'-tetrachloro-1,1',3,3'-tetraethylbenzimidazolylcarbocyanine iodide) that readily enters cells and fluoresces brightly red in its multimeric form within healthy mitochondria. In apoptotic cells, the mitochondrial membrane potential collapses, and the reagent cannot accumulate within the mitochondria, therefore remaining in the cytoplasm in its green fluorescent monomeric form. All buffers and solutions were provide in the kit.

At the appropriate culture end-point, cells ( $\sim 1 \times 10^6$ ) were transferred into 1.5ml eppendorff tubes. These were then centrifuged at 500x g for 5 minutes and the medium aspirated off. The cells were then resuspended in 1 ml of reaction buffer plus 1  $\mu$ l of DePsipher solution. The reaction buffer was diluted with distilled water from 10x concentrate plus 20  $\mu$ l of stabiliser solution; both these reagents were supplied in the kit. The resuspended cells were then incubated at 37 °C in a 5% CO<sub>2</sub> for 15-20 minutes. Following this, the cells were centrifuged and aspirated as above. The cells were resuspended in 100  $\mu$ l of reaction buffer. 50  $\mu$ l of cell suspension was immediately poured onto a glass slide and a coverslip placed over the cells. The cells were then imaged using a Carl Zeiss Axio Imager microscope with dry lens 20 x and 40x. Fluorescence was excited using a mercury lamp and emission was recorded using a FITC/Rhodamine filter block (485/515-530nm; 546/580-590nm). The number of cells displaying damaged mitochondria was determined from 5 independent digital images. Typically an area of 0.73 mm<sup>2</sup> was examined.

## **2.2 *In vivo* response to metal wear debris**

This section details the methods employed in creating an *in vivo* model to assess the response to metal wear debris from a MoM hip implant. It also describes the techniques used to determine the effects of the wear debris.

### **2.2.1 Preparation of metal wear debris**

CoCr wear debris was kindly donated by DePuy International (Leeds, UK). The wear debris was produced over 250,000 cycles from a size 39mm DePuy Articular Surface Replacement (ASR) joint on a multistation hip joint simulator.

Once produced the wear debris, which was suspended in distilled water, was centrifuged at 3500xg for 10 minutes. The majority of the water was aspirated. The remaining suspension was heat treated (180°C for 5 hr, 60kPa) in a vacuum oven to eliminate the remaining water and destroy any endotoxin. The dry debris was then suspended in sterile PBS (Invitrogen; Paisley, UK).

### **2.2.2 Assessing sterility of treated wear debris**

In order to assess the presence of microbial contamination of the treated wear debris, DCs were exposed to it for 24 hours and their activation status assessed. In order to achieve this, DCs which had been cultured for 6 days were washed with 2ml of RPMI-1640 and then harvested. DCs were then seeded  $1 \times 10^6$ /well in a 6-well culture plate with complete RPMI-1640 and incubated overnight at 37°C, 5%CO<sub>2</sub>. Following this, the medium in each well was aspirated and DCs washed with 2ml of RPMI-1640. The DCs were then either incubated with 2.5mg wear debris suspension or 1µg/ml lipopolysaccharide (LPS; Sigma-Aldrich; Dorset, UK) in complete RPMI-1640. Negative controls of complete RPMI-1640 and the carrier, sterile PBS, were also set up. After incubation, activation status of CD11c<sup>+</sup> DCs was characterized on a FACS Canto using monoclonal antibodies and relevant isotype controls (eBioscience; Hatfield, UK) listed in Table 2.1, and following the protocol described in section 2.1.3.6.

Antibody (clone)	Isotype control	Purpose
CD11c-PE (N418)	Armenian Hamster IgG-PE	Expressed on DCs
CD86-FITC (GL-1)	Rat IgG2a-FITC	Expressed on activated cells
CD40-APC (1C10)	Rat IgG2a-APC	Expressed on activated cells
MHC Class II-FITC (NIMR-4)	Rat IgG2b-FITC	Expressed on activated cells

**Table 2.1 Monoclonal antibodies and isotype controls used to assess dendritic cell activation.**

### 2.2.3 Characterisation of wear particles

A sample of wear debris suspended in distilled water was dispersed onto double sided carbon tape. This was left for 2 days to allow the water to evaporate. Following this period the debris was transferred to a Hitachi TM-1000 scanning electron microscope. Images were taken at magnifications of 100-1000x and digital images obtained. Energy Dispersive X-ray Spectroscopy (EDS) was used for quantitative analysis of elemental composition. Hitachi TM-1000 and EDSwift-TM software was used to obtain the images and chemical spectra of the wear debris.

### 2.2.4 Establishing the air-pouch

Air-pouches were generated according to a modified method of that described by (Sedgwick et al., 1983). In order to form the air pouch, the lower dorsal skin of an 8-10 week old male BALB/c mouse was cleaned with alcohol and shaved. A subcutaneous injection of 1ml of sterile air was injected at a single site in this area with a 25-gauge needle and 1ml syringe (both BD Bioscience; Oxford, UK). Three days later air pouches were injected with 0.5ml of sterile air to maintain the pouch.

Three days following the second injection, the pouches were injected with either 2.5mg of sterile wear debris or 1µg LPS each of which was dissolved in 500µl of sterile PBS. Negative control animals were injected with 500µl of sterile PBS alone. A 23.5 gauge needle (BD Bioscience; Oxford, UK) was used to carry out these injections. In order to avoid pain the mice were briefly anesthetized with isoflurane for the above procedures.

### **2.2.5 Analysis of metal ions in peripheral blood**

At the end of each time point, mice were anaesthetised by receiving a single intraperitoneal injection of Hypnovel (0.25 mg midazolam; Roche; West Sussex, UK) + Hypnorm (0.5 mg fluanisone, 0.016 mg fentanyl citrate; VetaPharma; Leeds, UK). Once anaesthetised, a small incision was made in the skin around the carotid artery and a small cavity created with the skin. The carotid artery was then cut and peripheral blood collected into a Vacuette tube (Greiner; Stonehouse, UK) using a plastic pasteur pipette.

The metal ion concentration within peripheral blood was kindly measured by the author's colleague, Dr Grace Afolaranmi. All samples, standards and quality controls were diluted 10-fold using the solubilisation matrix solution (Table 2.2). The standards were prepared at a concentration of 10x higher than the final concentration required. 40µg/l of rhodamine internal standard (I.S) was prepared in the solubilisation matrix solution. 500µl of the blood sample or standard was added to 2.5ml of the I.S dilution matrix in a plastic vial. 2ml of deionized water was then added into each vial. A final solution of 5ml was attained giving a 10X dilution of the samples and standards and each sample was then sonicated. The samples were then analysed using an Agilent 7500ce octopole reaction system ICP-MS (Agilent Technologies; Wokingham, UK) in helium gas mode.

Reagent	% in solution (w/v)	Quantity for 1 l solution
1-Butanol	1.5%	15 ml
EDTA	0.01mM	2.9224mg
Triton X-100	0.07%	0.7ml
Ammonium hydroxide	0.7mM	26.92ml
Water	Make up to vol.	Make up to 1l

**Table 2.2 Preparation of solubilisation matrix solution.**

### 2.2.6 Analysis of metal ions in organs

At the end of each time point, the following organs were excised for metal ion concentration analysis; brain, heart, kidney, liver, spleen and testes. The metal ion concentration within these organs was measured by the author's colleague, Dr Grace Afolaranmi. In order to do this each organ was weighed and then suspended in 0.25 ml nitric acid (65% v/v) in a 15ml polypropylene tube. The tubes were heated using a hot block (Techne driblock DB-2D; Techne Incorporated, USA) at 103<sup>0</sup>C for 20 minutes. Then 0.5ml of 30% hydrogen peroxide (Sigma-Aldrich; Dorset, UK) was added and the digestion continued for 20 minutes. After cooling, 1.25 ml of 40 µg/l of rhodamine standard (internal standard) in water was added and the volume made up to 2.5ml with deionised water to yield a final sample dilution of 1 in 5. The solution was then centrifuged at 2000 rpm for 5 min and filtered using a using a 0.2µm filter before metal ion analysis using the ICPMS system mentioned in section 2.2.5.

### 2.2.7 Pouch exudate

At the end of each time point, the pouches were lavaged with 500µl of sterile PBS using a 21 gauge needle (BD Bioscience; Oxford, UK). The cells were then counted using Trypan Blue (Sigma-Aldrich; Dorset, UK) and a haemocytometer. Once counted, the cells were transferred into FACS tubes and were stained for surface



antigens as described in section 2.1.3.6. The monoclonal antibodies and relevant isotype controls (eBioscience, Hatfield, UK) listed in Table 2.3 were used to identify the phenotype of the cells within the pouch exudate. The method to do this is as described in section 2.1.3.6.

<b>Antibody (clone)</b>	<b>Isotype control</b>	<b>Identifies</b>
<b>CD3e-PerCP (500A2)</b>	Hamster IgG (PerCP)	T-lymphocytes
<b>B220-APC (RA3-6B2)</b>	Rat IgG2a-APC	B-lymphocytes
<b>Ly6G-FITC (RB6-8C5)</b>	Rat IgG2b-FITC	Granulocytes
<b>CD11b-PE (M1/70)</b>	Rat IgG2b-PE	Monocytes/Macrophages

**Table 2.3 Monoclonal antibodies and isotype controls used to identify cells in pouch exudate.**

### **2.2.8 Histological evaluation of air-pouch**

At the end of each time point, the pouch was dissected and one-half fixed in 4% formalin (Sigma-Aldrich; Dorset, UK) for histological evaluation. Once tissue samples were fixed they were processed and stained with haematoxylin and eosin (H&E) by Veterinary Diagnostic Services, University of Glasgow (Glasgow, UK). This was carried out by dehydrating and embedding the tissue in paraffin blocks. Sections were then cut and samples mounted onto glass microscope slides. These were then stained and slides permanently bonded with coverslips.

In order to analyse the tissue samples, the slides were viewed under a Carl Zeiss Axio Imager microscope using 10-100x dry lens. Digital images were taken and analysed using AxioVision 4.6. Pouch membrane thickness was determined at six points on each section, with an even distribution of measurements. Total number of cells (based upon nucleus count) was determined as cells per mm<sup>2</sup>, and cells identified based upon nuclear morphology.

## **2.2.9 Inflammatory gene activation in air-pouch tissue**

At the end of each time point, the pouch was dissected free from surrounding tissue and one-half immersed in ice-cold RNAlater (Qiagen; Crawley, UK).

### **2.2.9.1 RNA Extraction**

RNA was isolated using an RNeasy Mini Kit (Qiagen; Crawley, UK) and following the manufacturer's instructions. This kit provided all the required agents and tubes for the process. Briefly, the tissue was then disrupted and homogenised by initially snipping it using scissors, followed by sonication in 300  $\mu$ l of RLT buffer. This was then centrifuged at 15000x g for 3 minutes in a microcentrifuge. The supernatant was then transferred to a new microcentrifuge tube which contained an equal volume of 70% (v/v) ethanol. This was mixed by pipetting and then 700  $\mu$ l of this mixture was transferred into an RNeasy spin column placed in a 2 ml collection tube. This was then centrifuged for 15 s at 8000x g. The flow-through in the collection tube was discarded and 350  $\mu$ l Buffer RW1 added to the RNeasy spin column. This was then centrifuged for 15 s at 8000 x g and flow-through in the collection tube discarded. 80  $\mu$ l of DNase I incubation mix was then directly added to the RNeasy spin column membrane, and place on the benchtop for 15 minutes. Following this period 350  $\mu$ l Buffer RW1 was added to the RNeasy spin column and then centrifuged for 15 s at 8000x g. The follow-through was discarded and 700  $\mu$ l of Buffer RW1 was added to the RNeasy spin column. This was then centrifuged at 8000xg for 15s and the flow-through discarded. Following this, 500  $\mu$ l of Buffer RPE was added to the RNeasy spin column. This was then centrifuged for 15 s at 8000 x g and the flow-through discarded. 500  $\mu$ l of Buffer RPE was again added to the RNeasy spin column and the tube centrifuged for 2 minutes at 8000x g. The RNeasy Spin column was then placed in a new collection tube and 50  $\mu$ l of RPE buffer was added directly to the spin column membrane. This was then centrifuged at 8000x g for 1 minute to elute the mRNA into the collection tube. The mRNA was then quantified using a Nanodrop™ 1000 Spectrophotometer and Nanodrop 1000 V3.7 software (Thermo Scientific; Wilmington, USA). This measured absorbance at wavelengths of 260 and 280 nm from a 1  $\mu$ l sample of RNA.

### **2.2.9.2 Agarose gel electrophoresis of RNA**

The overall quality of isolated the RNA preparation was assessed by electrophoresis on an agarose gel. A 1% (w/v) agarose gel was cast by adding 2.5g of agarose (Sigma-Aldrich; Dorset, UK) to 250ml of Tris-acetate-EDTA (TAE) buffer. TAE buffer consisted of 4.84 g Tris base, 1.14 ml glacial acetic acid and 2 ml of 0.5M Ethylenediamine tetraacetic acid (EDTA) solution (all Sigma-Aldrich; Dorset, UK) dissolved in deionized water to make up a total volume of 1l. Once the agarose was added to TAE buffer, the solution was heated in a microwave for 1 minute in order for the agarose to dissolve. Once heated the solution was swirled and left to cool slightly. Following this, 1 µl of Ethidium Bromide was added to the gel solution and then it was poured into the gel tank. The gel solution was left at room temperature until it set.

Whilst the gel set, the samples were prepared for loading. 2 µg of RNA from each sample were mixed Blue/Orange loading dye (Promega; Southampton, UK) to make a total volume of 10 µl for each sample. Once the gel had set, TAE buffer was poured into the tank to submerge the cast gel. Then 10 µl of sample solution was loaded into each well of the gel. The last well was loaded with 5 µl of 1kb DNA Ladder (Promega; Southampton, UK) as a size marker. Electrodes were attached to the tank and the gel run at 5V/cm until the marker had migrated as far as  $\frac{3}{4}$  length of the gel. The gel was removed carefully from the tank and visualised under a UV transilluminator. Intact RNA will have sharp bands at 1.9kb and 4.7kb whereas degraded RNA will have a smeared appearance lacking these sharp bands.

### **2.2.9.3 cDNA synthesis**

Following its extraction, cDNA was synthesized from RNA. This was achieved using an AffinityScript™ Multiple Temperature cDNA synthesis kit (Agilent Technologies; Stockport, UK). The kit provided all reagents required for cDNA synthesis and the process was completed by following the manufacturer's instructions. Briefly, 2 ng of mRNA were combined with 2 µl of random primers in a microcentrifuge tube. This was made up to a volume of 15.7 µl with RNase-free

water and incubated at 65°C for 5 minutes. The reaction was then allowed to cool for 10 minutes before adding 2.0 µl of 10 x AffinityScript RT Buffer, 0.8 µl of dNTP mix, 0.5 µl of RNase Block Ribonuclease Inhibitor (40 U/µl), and 1 µl of AffinityScript Multiple Temperature RT in that order. This was then incubated initially at 25°C for 10 minutes before incubating for 60 minutes in a temperature-controlled thermal block at 42–55°C. The reaction was then terminated by incubating at 70°C for 15 minutes. The cDNA was then stored at -20°C until required.

#### **2.2.9.4 Control RT-PCR**

In order to assess whether the transcripts were detectable, a typical reverse transcription polymerase chain reaction (RT-PCR) using primers specific for  $\beta_2$  microglobulin was undertaken. PCR amplification of  $\beta_2$  microglobulin was achieved by adding 0.4 µl of  $\beta_2$  microglobulin primer mixture (Applied Biosystems; Warrington, UK) to 19.6 µl of transcribed cDNA. This reaction was completed by incubating at 94°C for 10 seconds, then at 60°C for 20 seconds and then at 72°C for 45 seconds for 40 cycles in a temperature-controlled thermal block. The amplified samples were then loaded onto a 1% agarose gel and visualised as in section 2.2.9.3.

#### **2.2.9.5 Inflammatory gene expression assay**

TaqMan Low Density Arrays (TLDA) are 384-well microfluidic cards that can perform 384 RT-PCR reactions simultaneously. The card allows several samples to be run in parallel against a range of gene targets that are pre-loaded into each of the wells on the card. A custom plate was designed with a 32-gene format (appendix 1), allowing analysis of four different isolates per plate, each tested for 32 different target genes in triplicate.

The plates contained primer pairs for a broad range of chemokines and cytokines that could be involved in WBC recruitment and inflammatory processes following implantation of CoCr wear debris. In addition the plates contained a mandatory

internal control against 18S ribosomal gene and a second TATA-binding protein control. The complete list of gene targets and primer sequences is included in Appendix 1. All products and reagents in this section were from Applied Biosystems (Warrington, UK).

In order to assess the expression of the gene targets, stored cDNA was thawed and then gently vortexed. Following this, 1 µg of cDNA was placed in a 1.5 ml eppendorff tube and RNase-free water was then added to make the volume up to 50 µl. 50 µl of TaqMan PCR Mastermix (no AMPErase) was then added, and the solution was thoroughly mixed the solution by vortexing. 100 µl of the PCR mix was then loaded into a reservoir of the TLDA plate. This was done for each individual sample. The array plates were then twice centrifuged at 330 x g for 1 minute to distribute the cDNA samples in the reaction wells. The array plate was then sealed using the TaqMan sealer in order to isolate the wells of the array. Once sealed the reservoirs of the array were cut away using scissors and the array was run on a 7900HT TaqMan reader using a standard sequence detection software (SDS) programme. The data was quantified using the comparative method from the cycle threshold (Ct) values obtained.  $\Delta$ Ct values were generated by normalizing to 18S for each treatment and  $\Delta\Delta$ Ct values by normalizing to the mean  $\Delta$ Ct from the PBS treated air-pouch control. The Relative Quantitation value (RQ) was then calculated as  $2^{-\Delta\Delta Ct}$ .

Results were expressed as fold change over the untreated control. Data are shown in the appropriate results section are means plus standard error of the mean (S.E.M) from three independent samples.

### **2.2.10 Evaluation of the effects on draining lymph nodes**

At the required time points; the auxiliary, brachial, and inguinal lymph nodes were excised and suspended in 2ml of complete RPMI-1640. The lymph nodes were mechanically disrupted using a sterile 40µm nylon mesh cell strainer (BD

Biosciences; Oxford, UK) under sterile conditions. The cells from the lymph nodes were counted using Trypan Blue and a haemocytometer.

An aliquot of  $1 \times 10^6$  cells were removed from each sample and placed in the FACS tubes for surface antigen staining and apoptosis analysis. These cells were stained with the monoclonal antibodies or isotype controls (eBioscience; Hatfield, UK) listed below. These were also stained with Annexin V-PE and 7-AAD.

Antibody(clone)	Isotype control	Identifies
CD4-FITC (RM-45)	Rat IgG2a-FITC	T-Helper cells
CD8-APC CY7.7 (53-6.7)	Rat IgG2a-Apc CY7.7	Cytotoxic-T Cells
B220-APC (RA3-6B2)	Rat IgG2a-APC	B-Lymphocytes

**Table 2.4 Monoclonal antibodies and isotype controls used to identify cells from mouse lymph nodes.**

Following collection into FACS tubes, the cells were stained with the above antibodies or isotype controls as per section 2.1.3.6. However, following the final wash step the cells were resuspended in 100  $\mu$ l Annexin binding buffer, and 5  $\mu$ l of PE Annexin V and 7-AAD were added to each tube. The tubes were then incubated in the dark at room temperature for 15 minutes and the remainder of the method described in section 2.1.3.4 was completed.

100  $\mu$ l from the remaining cells from the mouse lymph nodes were seeded ( $1 \times 10^6$  cells/ml) in round bottom 96-well plates precoated with anti-CD3 (clone 145-2C11; 1  $\mu$ g/ml)  $\pm$  soluble anti-CD28 (clone 37.51; 0.1  $\mu$ g/ml) (both eBioscience; Hatfield, UK) in complete RPMI-1640. The cells were then incubated for 24 hours at 37°C, 5% CO<sub>2</sub>. Following this period the cells were transferred into FACS tubes and stained with Annexin V-PE, 7-AAD, the above monoclonal antibodies or isotype controls (Table 2.4) as described.

## **2.3 Determining metal ion concentrations and white blood cell levels in peripheral blood**

This section details the methods utilised in determining the white blood cells level and metal ion concentrations in peripheral blood of patients undergoing hip resurfacing in the Glasgow Southern General Hospital, UK.

### **2.3.1 Metal ion analysis in peripheral blood**

Once collected, metal ion concentration within peripheral blood was kindly measured by the author's colleague, Dr Grace Afolaranmi as described in section 2.2.5.

### **2.3.2 White Blood Cell Count**

White blood cells were counted by adding 100 $\mu$ L of whole blood to 1.9ml of RBC Lysing Buffer (BD Bioscience; Oxford, UK) in a bijoux. This was then mixed thoroughly and incubated for 15 minutes at room temp. The cells were then counted on a haemocytometer.

### **2.3.3 Surface antigen staining to phenotype cells using flow cytometry**

100 $\mu$ l of peripheral blood was added to FACS tubes containing Fc block and appropriate combinations of fluorochrome-conjugated monoclonal antibody or relevant isotype control (eBioscience; Hatfield, UK) listed in Table 2.5. The tube was then vortexed gently and incubated for 15 minutes in the dark at room temperature. After this incubation period, 2ml of RBC lysis buffer was added to each tube and samples incubated for 15 minutes in the dark at room temperature. Following this, the tubes were centrifuged at 350 x g for 5 minutes, the supernatant discarded and 2 ml of FACS buffer were added to each tube. These were then centrifuged at 350 g for 5 minutes and the supernatant aspirated. Once this step was repeated, the cells

were suspended in 400 $\mu$ L FACS flow and mixed thoroughly, using a vortex. The samples were analyzed on a FACS Canto flow cytometer.

<b>Antibody(clone)</b>	<b>Isotype control</b>	<b>Identifies</b>
<b>CD3-FITC (OKT3)</b>	Mouse IgG2a-FITC	T-Lymphocytes
<b>CD4-PE (OKT4)</b>	Mouse IgG2b-PE	T-Helper Cells
<b>CD8-APC (OKT8)</b>	Mouse IgG2a-APC	Cytotoxic-T Cells
<b>CD20-FITC (2H7)</b>	Mouse IgG2b-FITC	B-Lymphocytes
<b>CD56-PE (MEM-188)</b>	Mouse IgG2a-PE	Natural Killer Cells

**Table 2.5 Monoclonal antibodies and isotype controls used to identify cells in peripheral human blood.**



# Chapter 3

## **3. Effects of chromium and cobalt on U937 cells *in vitro***

### **3.1 Introduction**

Over the past decade more than 300,000 CoCr alloy based MoM articulations have been implanted in patients with end-stage arthritis of the hip (Learmonth and Case, 2007). Despite increasing the mobility and quality of life of these patients, there are increasing concerns that MoM hip implants release high levels of metal ions and wear debris. As described in section 1.4.2, elevated levels of metal (Cr and Co) ions have been measured in blood and organs of patients following MoM hip arthroplasty. In addition, extremely high levels of metal ions have also been measured around the implant. This has caused increasing alarm that metal ions released from CoCr alloy hip implants lead to toxic effects which may contribute to the adverse effects described in section 1.4.3.

It has previously been demonstrated that *in vitro* exposure Cr or Co ions can result in toxic effects (section 1.4.3.5). Studies have shown that these ions lead to a decrease in of viability lymphocytes, macrophages and monocytes (Granchi et al., 1998a, Hallab et al., 2008, Kwon et al., 2009b). In addition, *in vitro* exposure can also result in the cells becoming apoptotic or necrotic following metal ion exposure (Granchi et al., 1998a, Huk et al., 2004). Further to this, there are reports of DNA damage in WBCs isolated from MoM hip arthroplasty patients (Ladon et al., 2004, Dunstan et al., 2008). It has also been shown that metal ions, particularly Cr ions, can induce DNA damage within cells following *in vitro* exposure resulting in cell cycle arrest and apoptosis (Ye and Shi, 2001, O'Brien et al., 2002b). The above mentioned data signify the importance of assessing the toxic nature of metal ions that are released from MoM hip implants.

## 3.2 Aims

The aim of this chapter is to assess the toxicity of clinically recorded concentrations of chromium and cobalt ions on an immortalised human cell line, *in vitro*. Further to this, the presence of any synergistic toxic effects when the ions were combined was also investigated.

## 3.3 Methods

### 3.3.1 Exposure of U937 cells to metal ions

Cultured U937 cells (as described in section 2.1.1) were seeded at  $0.5 \times 10^6$  cells per ml in 24-well culture plates (1ml per well) and incubated in the absence or presence of  $\text{Cr}^{6+}$  and  $\text{Co}^{2+}$  in complete RPMI-1640 at  $37^\circ\text{C}$ , 5%  $\text{CO}_2$  for 24 and 48 hours. U937 cells were exposed to 0.1, 1 and  $10\mu\text{M}$   $\text{Cr}^{6+}$  or  $\text{Co}^{2+}$  individually. Cells were also exposed to the following combined concentrations of metal ions;  $0.1\mu\text{M}$   $\text{Cr}^{6+}$  +  $1\mu\text{M}$   $\text{Co}^{2+}$ ,  $0.1\mu\text{M}$   $\text{Cr}^{6+}$  +  $10\mu\text{M}$   $\text{Co}^{2+}$ ,  $1\mu\text{M}$   $\text{Cr}^{6+}$  +  $1\mu\text{M}$   $\text{Co}^{2+}$  and,  $1\mu\text{M}$   $\text{Cr}^{6+}$  +  $10\mu\text{M}$   $\text{Co}^{2+}$ .

### 3.3.2 Analysis of metal ion exposure on U937 Cells

In order to assess the effects of metal ion exposure on U937 cells, the following methods were implemented at each end-point;

- MTT and Neutral Red Assays were used to measure **cell viability** (method described in sections 2.1.3.1 and 2.1.3.2),
- **Cellular morphology and viability** were visualised using CLSM, following staining with AO and PI which would allow the discrimination of live and dead cells (section 2.1.3.5)
- Alterations in **cell cycle** were determined by flow cytometry analysis of DNA content (section 2.1.3.3),

- Level of **cellular apoptosis and necrosis** were investigated by flow cytometry following cellular staining with Annexin V and 7-AAD which would distinguish cells in various stages of apoptosis and necrotic cells (section 2.1.3.4)

## 3.4 Results

### 3.4.1 Effects of metal ions on cell viability

The viability of U937 cells following exposure to  $\text{Cr}^{6+}$  or  $\text{Co}^{2+}$  for 24 and 48 hr is displayed in Figures 3.1 and 3.2. The results demonstrated that all of the concentrations of  $\text{Cr}^{6+}$  employed caused a significant ( $p < 0.05$ ) decrease in the viability of U937 cells at 24 and 48 hours. As seen in Figures 3.1 and 3.2,  $\text{Cr}^{6+}$  appeared to decrease cell viability in a dose-dependent manner. The maximum decrease in cell viability was measured by the MTT assay following 48 hr exposure of 10  $\mu\text{M}$   $\text{Cr}^{6+}$ , viability was reduced to 10.38 ( $\pm 1.57$ ) % (mean  $\pm$  SEM,  $n = 12$ ). Exposure of U937 cells to  $\text{Co}^{2+}$  for 24 hours induced a significant decrease in cell viability at concentrations of 1 and 10  $\mu\text{M}$ ; this effect was recorded by both MTT and NR assays (Figures 3.1 and 3.2). The NR assay showed that viability was reduced to 81.82 ( $\pm 4.20$ ) % and 70.40 ( $\pm 4.30$ ) % (mean  $\pm$  SEM,  $n = 12$ ), respectively at these concentrations. Figures 3.1 and 3.2 also indicate that at 1 and 10  $\mu\text{M}$   $\text{Cr}^{6+}$  caused a significantly greater decrease in cell viability than the equivalent concentrations of  $\text{Co}^{2+}$ .

Tables 3.1 and 3.2 show the effect of exposing U937 cells to  $\text{Cr}^{6+}$  and  $\text{Co}^{2+}$  in combination on cell viability. Exposing cells to 1  $\mu\text{M}$   $\text{Cr}^{6+}$  + 10  $\mu\text{M}$   $\text{Co}^{2+}$  for 24 hours led to a significant decrease in cell viability when compared with the respective effects of both individual ions. No other combined exposure conditions showed any significant difference in cell viability when compared with the respective individual effects.

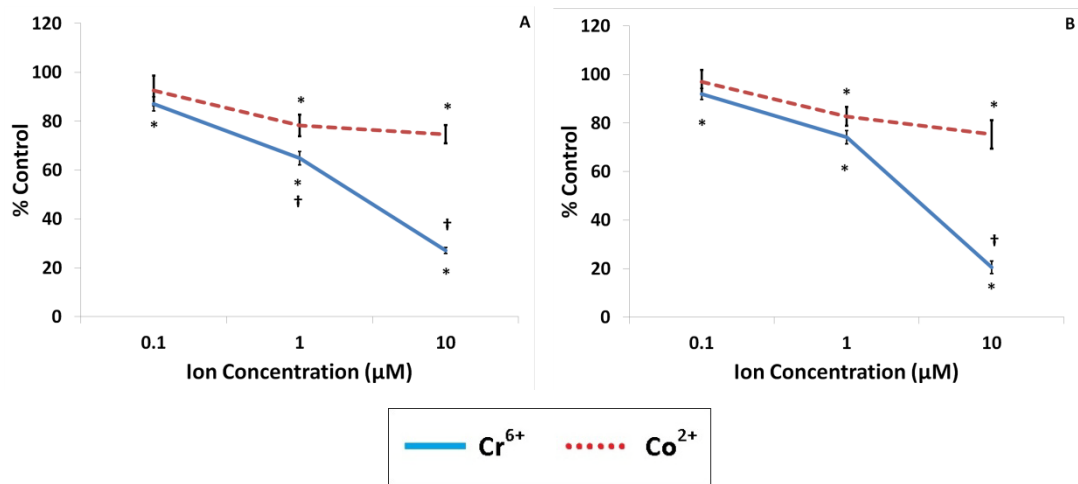


**Figure 3.1** Cell viability of U937 cells following 24 hours exposure to varying concentrations of Cr<sup>6+</sup> and Co<sup>2+</sup> ions, as measured by MTT (A) and NR (B) assays. 100% indicates unexposed control cells; results are means ± SEM, n=12; \* indicates significant difference from control values, P<0.05, by one-way ANOVA followed by Dunnett's multiple comparison test, † indicates significant difference from Co<sup>2+</sup> values, P<0.05, by 2-sample t-test.

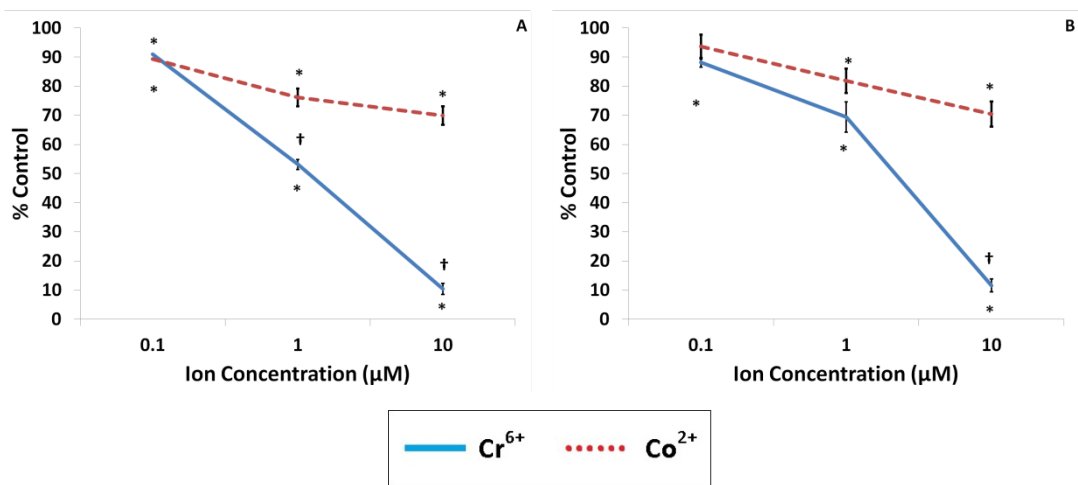


**Figure 3.2** Cell viability of U937 cells following 48 hours exposure to varying concentrations of Cr<sup>6+</sup> and Co<sup>2+</sup> ions, as measured by MTT (A) and NR (B) assays. 100% indicates unexposed control cells; results are means ± SEM, n=12; \* indicates significant difference from control values, P<0.05, by one-way ANOVA followed by Dunnett's multiple comparison test, † indicates significant difference from Co<sup>2+</sup> values, P<0.05, by 2-sample t-test.

Exposure	24h	48h
0.1µM Cr <sup>6+</sup>	87.06±2.87	91.01±1.76
1µM Cr <sup>6+</sup>	64.86±2.71	53.11±1.91
1µM Co <sup>2+</sup>	78.26±4.46	76.12±3.22
10µM Co <sup>2+</sup>	74.64±3.74	69.90±4.05
0.1µM Cr <sup>6+</sup> + 1µM Co <sup>2+</sup>	88.91±1.69	100.45±1.93
0.1µM Cr <sup>6+</sup> + 10µM Co <sup>2+</sup>	91.00±2.59	86.38±1.79
1µM Cr <sup>6+</sup> + 1µM Co <sup>2+</sup>	83.26±1.76	77.76±1.65
1µM Cr <sup>6+</sup> + 10µM Co <sup>2+</sup>	51.88±3.24*	65.20±1.27

**Table 3.1 Cell viability of U937 cells following 24 and 48 hours exposure to varying concentrations of Cr<sup>6+</sup> and Co<sup>2+</sup> ions, as measured by MTT assay.** Results are expressed as % Control (± SEM, n6) where 100% indicates unexposed control values; \* indicates significant difference from both individual concentrations, P<0.05, by 2-sample t-test.

Exposure	24h	48h
0.1µM Cr <sup>6+</sup>	91.96±2.29	88.18±1.65
1µM Cr <sup>6+</sup>	74.16±2.75	69.45±5.21
1µM Co <sup>2+</sup>	82.70±3.89	81.82±4.20
10µM Co <sup>2+</sup>	75.29±5.93	70.40±4.30
0.1µM Cr <sup>6+</sup> + 1µM Co <sup>2+</sup>	85.19±0.71	97.08±1.86
0.1µM Cr <sup>6+</sup> + 10µM Co <sup>2+</sup>	90.74±1.08	83.48±1.73
1µM Cr <sup>6+</sup> + 1µM Co <sup>2+</sup>	82.30±2.49	75.15±1.59
1µM Cr <sup>6+</sup> + 10µM Co <sup>2+</sup>	46.91±1.46*	63.01±1.23

**Table 3.2 Cell viability of U937 cells following 24 and 48 hours exposure to varying concentrations of Cr<sup>6+</sup> and Co<sup>2+</sup> ions, as measured by NR assay.** Results are expressed as % Control (± SEM, n6) where 100% indicates unexposed control values; \* indicates significant difference from both individual concentrations, P<0.05, by 2-sample t-test.

### 3.4.2 Effects of metal ions on cellular morphology

Figure 3.3 and Table 3.3 show the effects of metal ion exposure on cellular morphology following staining with AO and PI. As can be seen from Figure 3.3A control cells were mainly circular and fluoresced green indicating that they were generally healthy following 48 hours culture. There was a scattering of apoptotic cells which had a damaged membrane (indicated by the red colour) and a shrunken morphology. In contrast, exposure to 1  $\mu\text{M}$   $\text{Cr}^{6+}$  led to fewer cells, also there was only a limited number of cells that displayed healthy characteristics (Figure 3.3B). The majority of cells appeared apoptotic; there was clear cell blebbing, shrinkage and loss of membrane integrity. As displayed in Figure 3.3C there was still a large number of healthy cells following exposure to 10  $\mu\text{M}$   $\text{Co}^{2+}$  for 48 hours, this is also reflected in Table 3.3. There were a number of cells which displayed apoptotic characteristics. However, there were also a number of cells which appeared to be necrotic; these cells were larger (likely to be due to cell swelling) and seemed to be leaking cytoplasmic detail. These cell also displayed red fluorescence within the nuclei, which showed that PI had entered the nucleus as the cell membrane had been compromised. The effects of exposing U937 cells to both ions simultaneously are displayed in Figures 3.3(D,E,F) and Table. 3.3. The addition of 1  $\mu\text{M}$   $\text{Co}^{2+}$  to 1  $\mu\text{M}$   $\text{Cr}^{6+}$  did not appear to provide any additive effects. Figure 3.3D shows a number of shrunken cells displaying apoptotic characteristics, similar to figure 3.3B. Although there appeared to be fewer cells in culture following exposure to 0.1  $\mu\text{M}$   $\text{Cr}^{6+}$  + 10  $\mu\text{M}$   $\text{Co}^{2+}$ , the cells are generally healthy with a similar percentage displaying apoptotic and necrotic characteristic as seen following 10  $\mu\text{M}$   $\text{Co}^{2+}$  exposure alone (Figures 3.3C and 3.3E, Table 3.3). Exposing U937 cells to 1  $\mu\text{M}$   $\text{Cr}^{6+}$  and 10  $\mu\text{M}$   $\text{Co}^{2+}$  simultaneously, led to cells presenting primarily as apoptotic (Figures 3.3F). The morphology of most of the cells was very similar to cells which had been exposed to 1  $\mu\text{M}$   $\text{Cr}^{6+}$  only, although there were even fewer viable cells.

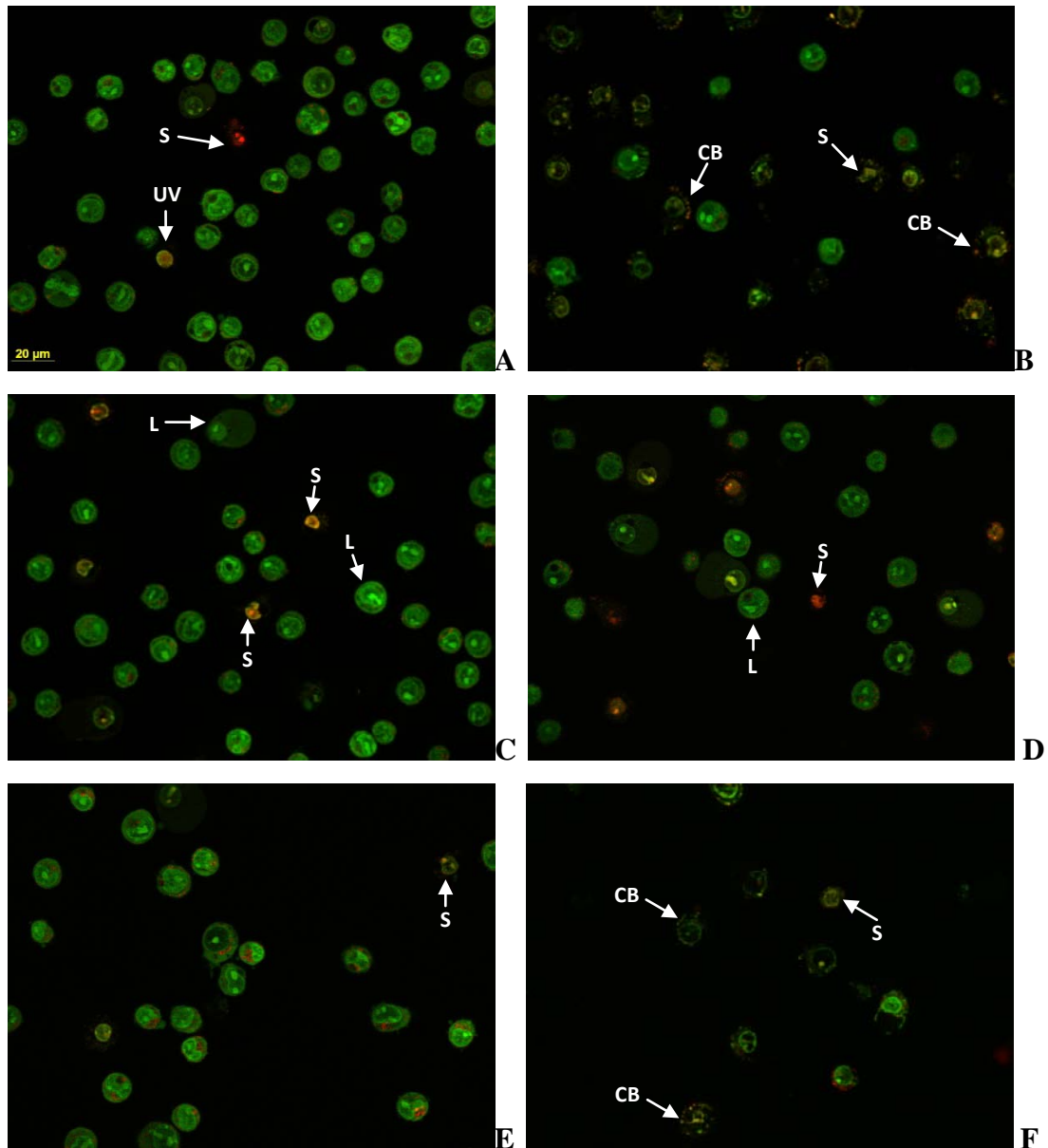


**Figure 3.3 Confocal Laser Scanning Microscope Images of U937 cells stained with Acridine Orange and Propidium Iodide following 48 hours exposure to  $\text{Cr}^{6+}$  or  $\text{Co}^{2+}$  ions. (A) Control, (B)  $1 \mu\text{M Cr}^{6+}$ , (C)  $10\mu\text{M Co}^{2+}$ , (D)  $1 \mu\text{M Cr}^{6+} + 1 \mu\text{M Co}^{2+}$ , (E)  $0.1 \mu\text{M Cr}^{6+} + 10 \mu\text{M Co}^{2+}$ , (F)  $1 \mu\text{M Cr}^{6+} + 10 \mu\text{M Co}^{2+}$ . Acridine orange stained green and indicates live cells, propidium iodide stained nuclei red, indicating damaged cells. 'CB' indicates cell blebbing, 'L' indicates leaking cytoplasmic detail, 'S' indicates shrunken morphology, 'UV' indicates unviable cell.**



	<b>Total Cells</b>	<b>No. of Apoptotic</b>	<b>% Apoptotic</b>	<b>No. of Necrotic</b>	<b>% Necrotic</b>
<b>Control</b>	227	7	<i>3.08</i>	3	<i>1.32</i>
<b>1µM Cr<sup>6+</sup></b>	87	50	<i>57.47</i>	5	<i>5.75</i>
<b>10µM Co<sup>2+</sup></b>	180	25	<i>13.89</i>	12	<i>6.67</i>
<b>1µM Cr<sup>6+</sup> + 1µM Co<sup>2+</sup></b>	76	14	<i>18.42</i>	5	<i>6.58</i>
<b>0.1µM Cr<sup>6+</sup> + 10µM Co<sup>2+</sup></b>	146	30	<i>20.54</i>	19	<i>13.01</i>
<b>1µM Cr<sup>6+</sup> + 10µM Co<sup>2+</sup></b>	39	24	<i>61.54</i>	5	<i>12.82</i>

**Table 3.3 Number of U937 cells displaying apoptotic and necrotic morphology following 48 hours exposure to varying concentrations of Cr<sup>6+</sup> and Co<sup>2+</sup> ions, as recorded by Confocal Laser Scanning Microscopy following staining with Acridine Orange and Propidium Iodide. Results are data recorded from 5 independent images from each sample.**

### **3.4.3 Effect of metal ions on the cell cycle**

Exposure to 1µM Cr<sup>6+</sup> for 24 hours resulted in a significant increase in the percentage of U937 cells at S phase of the cell cycle (Figure 3.4 and Table 3.4). There was also a significant decrease in the percentage of cells at G<sub>0</sub>/G<sub>1</sub> phase of the cell cycle. However, following 48 hours exposure at this concentration there was a significant increase in the percentage of apoptotic cells and those in G<sub>2</sub>/M phase, this coincided with a decrease in the percentage of cells at the other phases of the cell cycle. Table 3.4 also indicates that exposure to 10 µM Cr<sup>6+</sup> led to an increased percentage of cells becoming apoptotic.

Exposure to 0.1 or 1  $\mu\text{M}$   $\text{Co}^{2+}$  led to no significant changes in the percentage of cells at various phases of the cell cycle. However, exposure to 10 $\mu\text{M}$   $\text{Co}^{2+}$  led to a small but significant increase in the percentage of cells at S phase of cell cycle, this corresponded with a decrease at  $\text{G}_0/\text{G}_1$  at 24 hours (Figure 3.5 and Table 3.4).

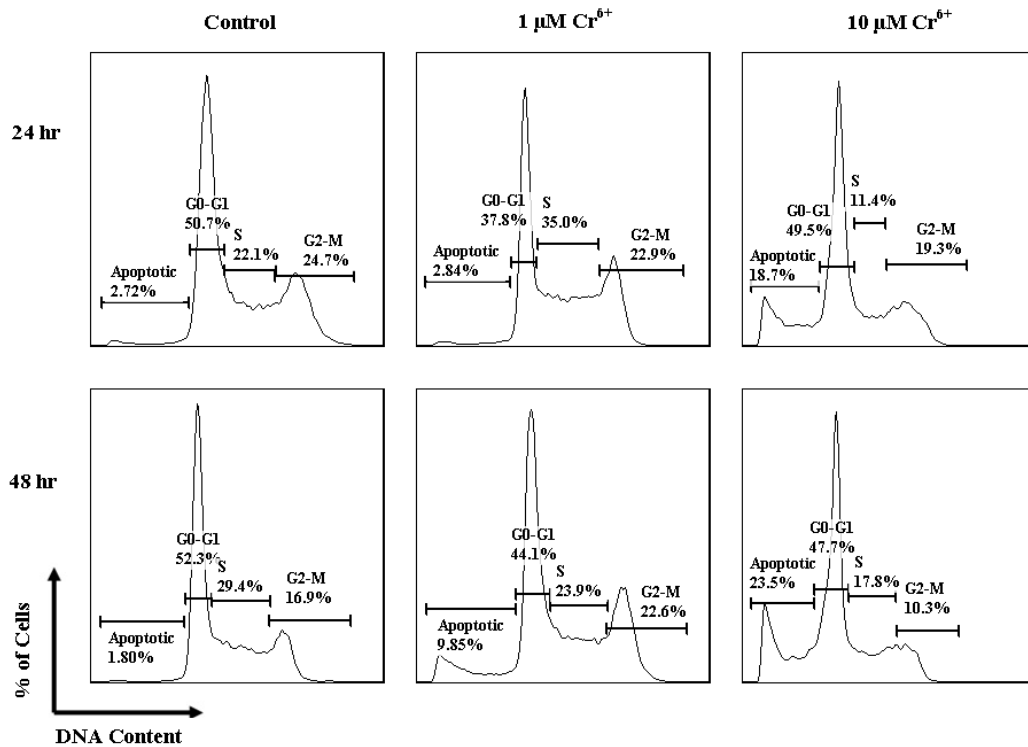


**Figure 3.4 Percentage of U937 cells at various stages of the cell cycle 24 and 48 hour of exposure to  $\text{Cr}^{6+}$ .**

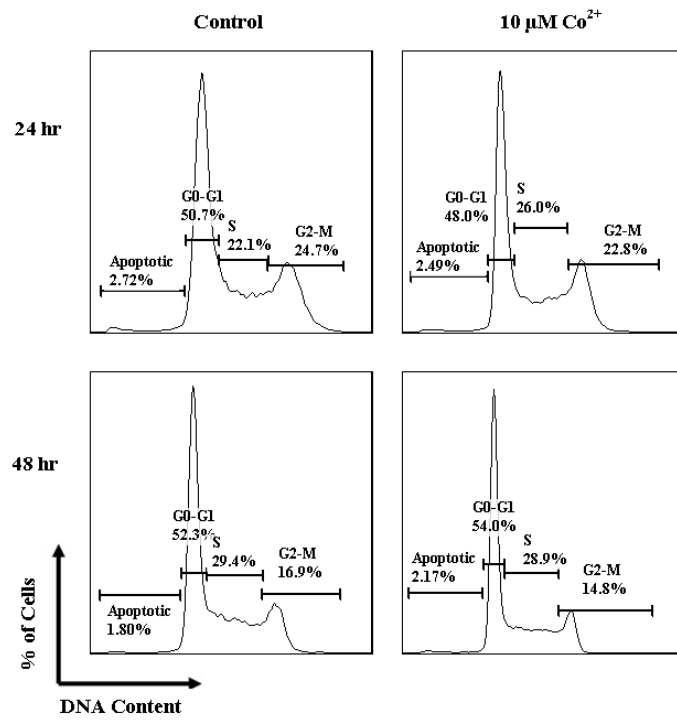


**Figure 3.5 Percentage of U937 cells at various stages of the cell cycle 24 and 48 hour of exposure to Co<sup>2+</sup>.**

	24h				48h			
	G <sub>0</sub> /G <sub>1</sub>	S	G <sub>2</sub> /M	Apop	G <sub>0</sub> /G <sub>1</sub>	S	G <sub>2</sub> /M	Apop
<b>Control</b>	51.07 ±0.07	21.80 ±0.61	22.97 ±0.09	2.44 ±0.01	52.87 ±0.57	28.93 ±0.47	16.23 ±0.67	1.83 ±0.03
<b>0.1µM Cr<sup>6+</sup></b>	50.13 ±0.09	22.03 ±0.03	24.40 ±0.21	2.44 ±0.03	53.97 ±0.43	25.73 ±0.37	16.40 ±0.80	3.33 ±0.31
<b>1µM Cr<sup>6+</sup></b>	38.80 ±0.40*	30.80 ±3.43*	22.97 ±0.58	2.82 ±0.04	44.47 ±0.37*	22.83 ±1.07*	21.07 ±1.53*	11.87 ±2.02*
<b>10µM Cr<sup>6+</sup></b>	48.37 ±0.58*	13.83 ±1.36*	17.67 ±0.82*	18.60 ±0.32*	46.37 ±1.33*	18.13 ±0.33	10.23 ±0.07*	18.13 ±0.33*
<b>0.1µM Co<sup>2+</sup></b>	50.70 ±0.10	25.50 ±0.20	21.40 ±0.30	2.35 ±0.18	52.63 ±0.08	29.23 ±0.04	15.90 ±0.61	1.72 ±0.07
<b>1µM Co<sup>2+</sup></b>	50.87 ±0.27	22.87 ±0.32	23.67 ±0.33	2.41 ±0.03	54.27 ±0.57	28.07 ±0.65	15.43 ±0.29	1.80 ±0.08
<b>10µM Co<sup>2+</sup></b>	48.47 ±0.23*	25.93 ±0.03*	22.13 ±0.33	2.73 ±0.12	54.30 ±0.30	28.15 ±0.75	15.45 ±0.65	2.08 ±0.09

**Table 3.4 Percentage (±S.E.M) of U937 cells in various stages of cell cycle following exposure to various concentrations of Cr<sup>6+</sup> and Co<sup>2+</sup> ions for 24 and 48 hours.** n=3; \* indicates significant difference from control values, P<0.05, by one-way ANOVA followed by Dunnett's multiple comparison test.

### 3.4.4 Effect of metal ion exposure on cellular apoptosis/necrosis

Figures 3.6, 3.7A and 3.7B show that exposure of U937 cells to 1 and 10 µM Cr<sup>6+</sup> led to significant apoptosis. 10µM Co<sup>2+</sup> also appeared to induce cellular apoptosis, however, the extent of this was less than that with chromium exposure. 1µM Co<sup>2+</sup> also increased the level of apoptosis but this increase was not significant. Further to this, the data presented in Figure 3.7B also indicates that 1 and 10 µM Cr<sup>6+</sup> led to a greater level of apoptosis than the equivalent Co<sup>2+</sup> concentrations.

It can be seen from Figure 3.6 and 3.8A that metal ion exposure led to an increase of necrotic cells at 24 hours, however, at this time point the increase was small. At 48 hours both  $\text{Cr}^{6+}$  and  $\text{Co}^{2+}$  exposure led to significant increases in the percentage of necrotic cells at concentrations of 1 and 10  $\mu\text{M}$  (Figures 3.6 and 3.8B). Comparing Figures 3.7B and 3.8B, it is apparent that  $\text{Cr}^{6+}$  exposure caused cells to become predominantly apoptotic whereas  $\text{Co}^{2+}$  exposure induced similar levels of apoptosis and necrosis following 48 hours of exposure.

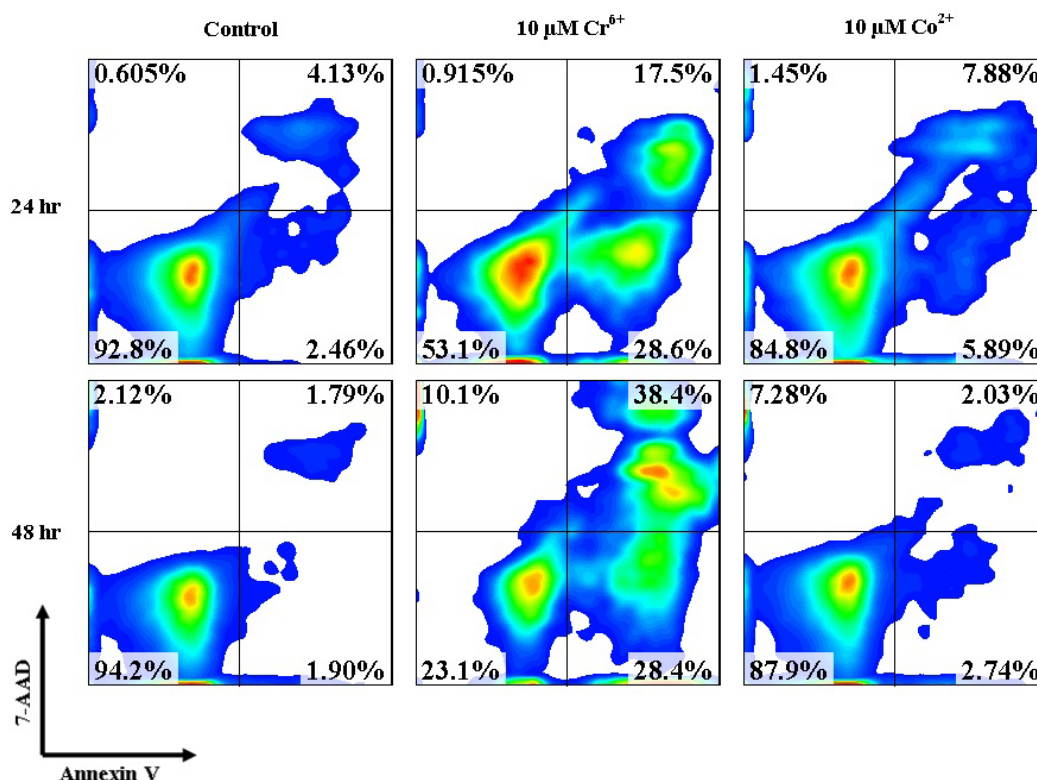


**Figure 3.6** U937 cells stained with Annexin V and 7-AAD following exposure to 10  $\mu\text{M}$   $\text{Cr}^{6+}$  and 10  $\mu\text{M}$   $\text{Co}^{2+}$  for 24 and 48 hours. Viable cells were Annexin V<sup>-</sup> and 7-AAD<sup>-</sup>. Cells in early stages of apoptosis were Annexin V<sup>+</sup> but 7-AAD<sup>-</sup>, whereas cells in late stages of apoptosis were both Annexin V<sup>+</sup> and 7-AAD<sup>+</sup>. Cells that were only 7-AAD<sup>+</sup> were necrotic.

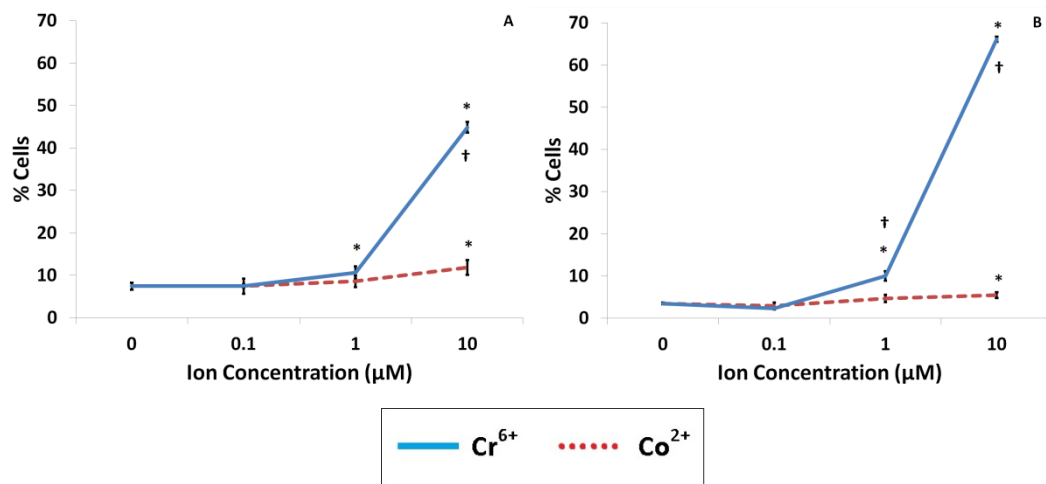


**Figure 3.7 Total apoptosis in U937 cells following (A) 24 hour or (B) 48 hours of exposure to Cr<sup>6+</sup> and Co<sup>2+</sup>.** Results are mean ( $\pm$  SEM, n=3) percentage of cells expressing Annexin V; \* indicates significant difference from control values, P<0.05, by one-way ANOVA followed by Dunnett's multiple comparison test, † indicates significant difference from Co<sup>2+</sup> values, P<0.05, by 2-sample t-test.

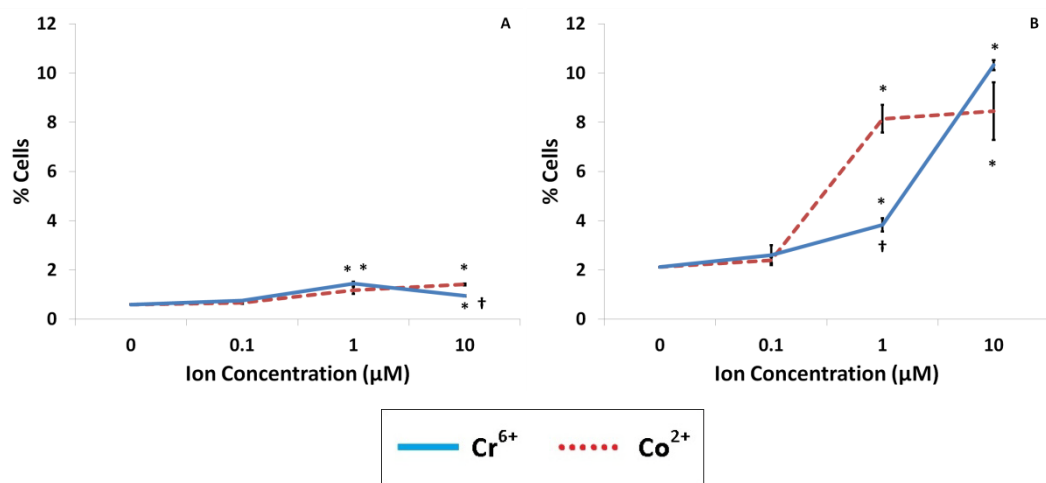


**Figure 3.8 Necrosis in U937 cells following (A) 24 or (B) 48 hours exposure to Cr<sup>6+</sup> or Co<sup>2+</sup>.** Results are mean ( $\pm$  SEM, n=3) percentage of cells permeable to 7-AAD and not expressing Annexin V; \* indicates significant difference from control values, P<0.05, by one-way ANOVA followed by Dunnett's multiple comparison test, † indicates significant difference from Co<sup>2+</sup> values, P<0.05, by 2-sample t-test.

### 3.5 Discussion

There are numerous reports which have recorded excess levels of metal ions, in particular Cr and Co, in peripheral blood of MoM resurfacing patients. A number of studies have shown that high levels of these metal ions have a cytotoxic effect on a variety of cells, *in vitro* (Allen et al., 1997, Fleury et al., 2006, Petit et al., 2006). However, where previous studies have implemented higher concentrations of metal ions, the current study has only used exposure concentrations which have been recorded in peripheral blood of MoM resurfacing patients (De Smet et al., 2008). This chapter has demonstrated that exposing human U937 cells to Cr<sup>6+</sup> and Co<sup>2+</sup>, at clinically recorded concentrations, resulted in a significant decrease in cell viability. These findings showed Cr<sup>6+</sup> exposure, at a concentration of 0.1 µM and above, led to a significant reduction in cell viability. Concentrations of 0.1 µM Cr<sup>6+</sup> and above have been measured in MoM resurfacing patients (summarised in section 1.4.2). Although small, the decrease in viability of cells exposed to this concentration of chromium was significant. It is clear that higher concentration of Cr<sup>6+</sup> decreased cell viability even further. In addition, the data indicated that this decrease was due to Cr<sup>6+</sup> initiating apoptosis. These results are consistent with past publications which have shown *in vitro* exposure to Cr<sup>6+</sup> causes apoptosis in cells via numerous mechanisms (Granchi et al., 1998a, Blasiak and Kowalik, 2000, Huk et al., 2004). Cr<sup>6+</sup> is a ROS promoting agent and within the cell is reduced to Cr<sup>3+</sup>. During this process reactive intermediates are formed which also initiate apoptotic events (Vasant et al., 2001, Vasant et al., 2003). Cr<sup>6+</sup> exposure to fibroblasts, human PBMCs, lung epithelial cells and U937 cells has also been shown to result in caspase activation, mitochondrial instability and formation of DNA-Cr adducts (Ye et al., 1999, Pritchard et al., 2000, Quievryn et al., 2003, Vasant et al., 2003, Hayashi et al., 2004). O'Brien and co-workers (2002b) reported that Cr<sup>6+</sup> induced DNA damage in *Saccharomyces cerevisiae* can result in G<sub>2</sub>/M phase cell cycle arrest. Additionally, it has also been shown that U937 cells exposed to 20 µM Cr<sup>6+</sup> for 24 hr undergo G<sub>2</sub>/M phase cell cycle arrest (Hayashi et al., 2004). It was reported that this arrest was due to ROS formation and mitochondrial damage and that the end result was apoptosis. Similarly, in the current study exposure to 1 µM Cr<sup>6+</sup> produced an apparent S-phase

delay at 24 hr and G<sub>2</sub>/M phase delay at 48 hr. At 24 hr it is possible that cells that contain damaged DNA are attempting DNA repair, however, prolonged exposure leads to excessive damage and cell cycle arrest at 48 hr leading to apoptosis (Pritchard et al., 2001, O'Brien et al., 2002a). At the higher concentration of Cr<sup>6+</sup>, only a small effect on cell cycle was observed. This indicates that at this concentration apoptosis may occur via the other mechanisms described above, e.g. ROS formation or mitochondrial damage, as well as DNA damage.

Although data from the flow cytometric analysis of cell cycle also identified apoptotic cells, these values are lower than those measured following Annexin V staining. As described in section 2.1.3.4, Annexin V binds to the membrane PS, which is translocated to the outer leaflet of the plasma membrane during the early stages of apoptosis. On the other hand PI staining of fixed cells only identifies apoptotic cells through their lower DNA content. Therefore, it is likely that the cells identified as apoptotic within the cell cycle analysis are in the latter stages of apoptosis, whereas Annexin V staining can identify apoptotic cells from an early stage through to cell death. Hence, the author has primarily referenced results following Annexin V staining when describing the apoptotic effects of metal ions.

Although Cr<sup>6+</sup> mainly induces apoptosis there is also an increase in necrosis. This increase is observed at 48 hours post exposure. This is due to prolonged exposure to toxic concentrations and is secondary to apoptosis (Granchi et al., 1998a, Huk et al., 2004).

Cobalt is also toxic to U937 cells, however, cytotoxic effects were only observed following exposure to 1 and 10 µM Co<sup>2+</sup>. Whilst there is some evidence of cell cycle delay at S-phase, the present data primarily indicated that the loss of cell viability following exposure Co<sup>2+</sup> is due to small increases in apoptosis at 24 hours followed by necrotic cell death following prolonged exposure. These results are in concordance with previous studies indicating that the mode of cytotoxicity is time dependent as well as concentration dependent (Granchi et al., 1998a, Huk et al., 2004, Catelas et al., 2005). As with Cr<sup>6+</sup>, the exact mechanism of Co<sup>2+</sup> toxicity has



not been elucidated. Existing data have demonstrated that  $\text{Co}^{2+}$  exposure *in vitro* can lead to excessive ROS formation as well as an inhibition of intracellular anti-oxidation enzymes. At present it is unknown whether  $\text{Co}^{2+}$  exposure can lead to DNA damage, however, several studies have shown that it can lead to inhibition of DNA repair (Kawanishi et al., 2002). This may be the cause for the small increase in the proportion of cells at S-phase of the cell cycle following 24 hour exposure to 10  $\mu\text{M}$   $\text{Co}^{2+}$ .

Interestingly, the current study demonstrated that  $\text{Co}^{2+}$  is less potent than  $\text{Cr}^{6+}$ . However, many previous publications have stated that cobalt ions are more toxic than chromium ions, *in vitro* (Catelas et al., 2005, Fleury et al., 2006, Kwon et al., 2009a). However, these researchers have primarily used the trivalent form of chromium rather than the hexavalent form, as it is more stable but less toxic (Schaffer et al., 1999, Blasiak and Kowalik, 2000). As described in Chapter 1, only the hexavalent form can enter a cell, once inside it is reduced to the trivalent form (Schaffer et al., 1999). At the present time it is unclear what valency of chromium ion is released from implants. However, following measurements of chromium within erythrocytes of MoM arthroplasty patients it is believed that chromium ions are released as the hexavalent form before entering cells and being reduced to the trivalent form (Merritt and Brown, 1995).  $\text{Co}^{2+}$  is not reduced within the cell unlike the  $\text{Cr}^{6+}$  ions which produce reactive intermediates. Therefore, the current author postulates that  $\text{Cr}^{6+}$  ions may be more potent than  $\text{Co}^{2+}$  because they are reduced within the cell and each of the ion intermediates formed exert further intracellular damage (see Figure 1.5).

In addition, the present study also investigated the possible synergistic effects of Co and Cr in inducing cytotoxicity. While it has been suggested that there may be synergistic toxicity between cobalt and chromium ions (Hart et al., 2006), to the current author's knowledge there have been no previous data describing this. There are, however, reports of synergistic toxic effects of other transition metal ions to other cell systems (Roesems et al., 2000, Merolla and Richards, 2005, Poyner et al., 1993). The data presented here suggests there may be a little synergy between cobalt

and chromium. Exposure to 1  $\mu\text{M}$   $\text{Cr}^{6+}$  and 10  $\mu\text{M}$   $\text{Co}^{2+}$  together for 24 hours showed a greater effect on cell viability than both of the individual exposures. This would appear to be more of an additive effect rather than any synergy. No other exposure conditions led to any synergistic effects. It is possible that these two ions can have synergistic effect since  $\text{Cr}^{6+}$  can cause DNA damage and  $\text{Co}^{2+}$  inhibits DNA repair. Due to the extreme cytotoxic nature of these ions, especially  $\text{Cr}^{6+}$ , it may be difficult to identify any synergy at high concentrations or at the longer durations of exposure.

In summary, the author has found that  $\text{Cr}^{6+}$  and  $\text{Co}^{2+}$  are toxic to a human leukemic monocytic cell line, U937, in vitro. It appears that  $\text{Cr}^{6+}$  is more toxic than  $\text{Co}^{2+}$ . These ions show a cytotoxic effect at concentrations measured in the peripheral blood of patients who have undergone MoM hip resurfacing. At these concentrations, metal ions can induce cellular apoptosis as well as necrosis following longer exposure periods. It is important to mention that these concentrations are ten fold lower than those recorded around the hip following MoM hip resurfacing (De Smet et al., 2008). Further to this, these ions may exhibit synergetic toxic effects when released in combination. Therefore, adverse effects following MoM hip resurfacing may be partly due to the cytotoxic effects of metal ions released.

# Chapter 4

## 4. Effects of chromium and cobalt on human lymphocytes *in vitro*

### 4.1 Introduction

As mentioned in chapter 1, high levels of metal ions measured in MOM resurfacing patients has led to concerns about the long term effects of metal ion exposure, particularly the immunological effects specific to MoM arthroplasty (Macpherson and Breusch, 2010). It is postulated that this immunologically mediated reaction is a result of high levels of metal ions and/or metallic wear debris which leads to local toxicity or delayed type IV hypersensitivity (Willert et al., 2005, Counsell et al., 2008, Pandit et al., 2008, Kwon et al., 2009a). The current evidence suggests that the adverse effects are an adaptive immune response to metal debris and/or ions in which T-lymphocytes are a central component.

As mentioned in section 1.4.3.1, T-lymphocytes are normally in a resting state and require activation in order to proliferate and initiate a response. It has been suggested that metal ions released following MoM hip arthroplasty may be toxic to T-lymphocytes thus altering their functionality (Hart et al., 2006). Previous *in vitro* studies have shown that metal ion exposure can lead to toxic and immunomodulatory effects, as described in section 1.4.3.5. It was shown by Vasant et al. (2003) that exposure of T-lymphocytes to  $\text{Cr}^{6+}$  *in vitro* can lead to apoptosis. It was further shown that inhibition of the end effector caspase, caspase-3, could reverse the  $\text{Cr}^{6+}$  induced apoptosis. *In vitro* data has also demonstrated that Cr or Co ion exposure can lead to an inhibition of T-lymphocyte activation (Bravo et al., 1990) and proliferation (Wang et al., 1996a). Wang et al. (1996a) also reported that the lower proliferative response following metal ion exposure was reversible following IL-2 supplementation in the culture medium. In addition, there are numerous reports that show that the production of cytokines, that are essential in T-lymphocytes responses (i.e. IL-2, IFN- $\gamma$  and TNF $\alpha$ ), are modulated following metal ion exposure (Wang et al., 1996b, Granchi et al., 1998b, Gavin et al., 2007). Further to this, it has also been suggested these cytokines may have a key role in the osteolytic processes following

metal ion exposure (Hallab et al., 2008). Although many studies have focussed on the role of T-lymphocyte stimulatory signals following metal ion exposure, there has been a recent advance in the understanding of the role that inhibitory signal from proteins such as CTLA-4 and PD-1 in the regulation of T-lymphocyte responses. These two proteins, which are expressed on the surface of T-lymphocytes, negatively regulate the T-lymphocyte responses (Blank and Mackensen, 2007). These proteins lead to a reduction in IL-2 and IFN- $\gamma$  production, reduce T-lymphocyte proliferation and initiate apoptosis all which are key phases in termination of normal T-lymphocyte responses (McCoy and Le Gros, 1999, Freeman et al., 2000). It is possible that metal ion exposure may lead to the increased expression of these proteins, thus inhibiting T-lymphocyte responses. The above data suggests that metal ions that are released from hip implants could lead to toxicity before T-lymphocytes are activated or inhibit the activation and proliferation processes as well as affecting the functionality of these cells following activation. Therefore, it is important to identify the processes which may be affected following metal ion exposure.

## **4.2 Aims**

The presence of lymphocytes in the various clinical and histological manifestations of the adverse effects following MoM hip arthroplasty suggests that the immunotoxicity of Cr<sup>6+</sup> and Co<sup>2+</sup> released from MoM implants may be mediated via or involve lymphocytes, especially T-lymphocytes. Therefore, the aim of this study was to investigate the effects of clinically recorded concentrations of Cr and Co ions on human peripheral blood lymphocytes. In addition, some preliminary investigations were undertaken to identify the presence of any synergistic toxic effects when the ions are combined. This chapter aims to identify the effects of Cr and Co ions on key T-lymphocyte parameters such as; viability, activation, proliferation and cytokine release.

## 4.3 Methods

### 4.3.1 Lymphocyte activation protocol

In order to fully assess the effect of metal ion exposure on primary human lymphocytes it was necessary to expose them in a resting and activated state. A protocol was therefore devised to initiate T-lymphocyte activation. Lymphocytes (isolated as described in section 2.1.1.2) were cultured ( $0.1 \times 10^6$  cells/well) in 96-well round-bottom plates (100  $\mu$ l/well) in complete RPMI-1640 that was supplemented with varying concentrations of soluble anti-CD3 (clone HIT3a; eBioscience; Hatfield, UK) for 24 and 48 hour at 37°C under 5% CO<sub>2</sub>/air. Soluble anti-CD3 was used to crosslink with the TCR complex to initiate an intracellular biochemical pathway resulting in cellular activation. The following concentrations of soluble anti-CD3 were used to produce a dose-response curve; 1, 10 and, 100 ng/ml. At each-point MTT and NR assays were carried out as described in sections 2.1.3.1 and 2.1.3.2, respectively.

As indicated by Figure 4.1, both 10 and 100 ng/ml anti-CD3 induce positive effects on lymphocytes following 24 and 48 hours exposure. Although neither of these assays directly measures cell activation or proliferation, they do indicate an increase in the number of viable cells (NR) as well as greater cell respiration (MTT). It was decided that 100 ng/ml anti-CD3 would be sufficient to activate T-lymphocytes, *in vitro*. In the current study soluble anti-CD3 was primarily used to activate T-lymphocytes, however, in some investigations soluble anti-CD28 (clone CD28.2; 0.1  $\mu$ g/ml; eBioscience; Hatfield, UK) was introduced in addition with soluble anti-CD3 to provide co-stimulatory signals to the lymphocytes *in vitro*. The primary aim of this was to identify whether co-stimulation would enable recovery of any inhibitory effects of metal ion exposure on T-lymphocyte activation or proliferation.

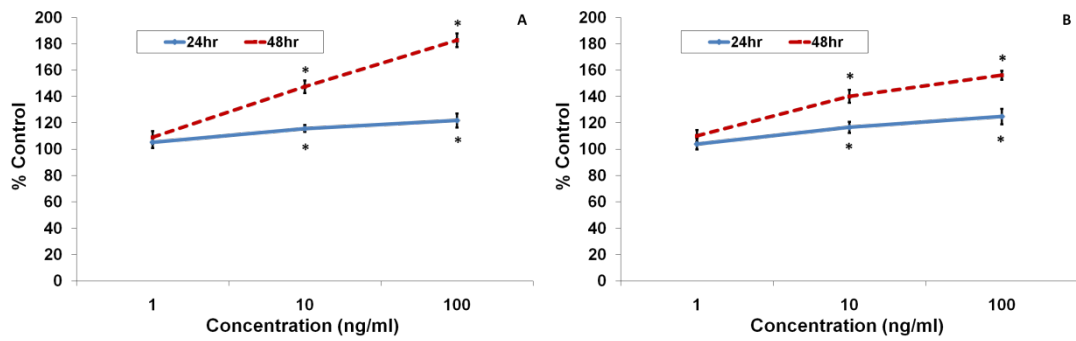


**Figure 4.1 Cell viability of primary human lymphocytes following 24 or 48 hours exposure to varying concentrations of soluble anti-CD3, as measured by MTT (A) and NR (B) assays.** 100% indicates unexposed control cells; results are means  $\pm$  SEM, n=8; \* indicates significant difference from control values,  $P < 0.05$ , by one-way ANOVA followed by Dunnett's multiple comparison test.

### 4.3.2 Exposure of lymphocytes to metal ions

Isolated peripheral human lymphocytes (prepared as described in section 2.1.1.2) were exposed to  $\text{Cr}^{6+}$  and  $\text{Co}^{2+}$  in resting and activated states. For the analyses using resting lymphocytes, the lymphocytes were cultured ( $0.1 \times 10^6$  cells/well) in 96-well round-bottom plates (100  $\mu\text{l}$ /well) with 0.1, 1, 10 and 100  $\mu\text{M}$  of  $\text{Cr}^{6+}$  or  $\text{Co}^{2+}$  in complete RPMI-1640 for 24 and 48 hr at  $37^\circ\text{C}$  under 5%  $\text{CO}_2$ /air. For analyses using anti-CD3-activated cells, lymphocytes were cultured ( $0.1 \times 10^6$  cells/well) in 96-well round-bottom plates (100  $\mu\text{l}$ /well), and incubated with 0.1, 1, 10, or 100  $\mu\text{M}$  of  $\text{Cr}^{6+}$  or  $\text{Co}^{2+}$  for 24 and 48 hr in complete RPMI-1640 that was supplemented with soluble anti-CD3 ( $\pm$  soluble anti-CD28) at  $37^\circ\text{C}$  under 5%  $\text{CO}_2$ /air.

In addition, both resting and anti-CD3 activated lymphocytes were treated in the same manner with the following combinations of  $\text{Cr}^{6+}$  or  $\text{Co}^{2+}$  ions;  $1\mu\text{M Cr}^{6+} + 1\mu\text{M Co}^{2+}$ ,  $1\mu\text{M Cr}^{6+} + 10\mu\text{M Co}^{2+}$ ,  $10\mu\text{M Cr}^{6+} + 1\mu\text{M Co}^{2+}$  and,  $10\mu\text{M Cr}^{6+} + 10\mu\text{M Co}^{2+}$ .

### 4.3.3 Caspase inhibition

To evaluate any potential role that caspase(s) might have in any observed effects of  $\text{Cr}^{6+}$  or  $\text{Co}^{2+}$  on the lymphocytes, both resting and anti-CD3 activated lymphocytes were pre-treated with 50  $\mu\text{M}$  of the global caspase inhibitor Z-Asp (OCH<sub>3</sub>)-Glu (OCH<sub>3</sub>)-Val-Asp (OCH<sub>3</sub>)-FMK (Z-DEVD-FMK) (R&D Systems, Abingdon, UK) for 24 hr (Vasant et al., 2003) prior to their exposure to  $\text{Cr}^{6+}$  or  $\text{Co}^{2+}$  as described above.

### 4.3.4 Recombinant IL-2 supplementation

To evaluate the potential role of IL-2 treatment in recovering from any adverse effects of  $\text{Cr}^{6+}$  or  $\text{Co}^{2+}$  on cell proliferation, lymphocytes were cultured in complete media supplemented with soluble anti-CD3  $\pm$  50U/ml recombinant human IL-2 during their exposure to  $\text{Cr}^{6+}$  or  $\text{Co}^{2+}$  as described above.

### 4.3.5 Analysis of the effects of metal ion exposure to primary human lymphocytes

In order to assess the effects of metal ion exposure on lymphocytes the following methods were implemented at each end-point;

- MTT and NR Assays were used to measure **cell viability** (sections 2.1.3.1 and 2.1.3.2) of both resting and anti-CD3 activated lymphocytes following 24 and 48 hour exposure
- **T-Lymphocyte activation** was assessed following 24 hour exposure to metal ions. This parameter was measured via flow cytometry following surface staining (section 2.1.3.6) with anti-human CD3-FITC (clone: OKT-3) which would phenotype T-lymphocytes, anti-human CD69-APC (clone FN50) a protein that is expressed on activated T-lymphocytes, Mouse IgG1k Isotype-APC and, Mouse IgG2ak Isotype-FITC (all eBioscience; Hatfield UK) which both distinguish non-specific binding.



- Measurement of anti-CD3 ( $\pm$  anti-CD28) activated **lymphocyte proliferation** was determined following 48 hours metal ion exposure via BrDU assay (section 2.1.3.7)
- **Cytokine (IL-2, IFN- $\gamma$ , TNF- $\alpha$ ) release** into culture medium from anti-CD3 ( $\pm$  anti-CD28) activated lymphocytes, following 48 hour metal ion exposure, was measured via ELISA (section 2.1.3.8).
- Alterations in **cell cycle** of anti-CD3 activated lymphocytes were determined by flow cytometry (section 2.1.3.3) at 24 and 48 hour post exposure
- Level of **cellular apoptosis and necrosis** were investigated by flow cytometry following Annexin V and 7-AAD staining (section 2.1.3.4) of resting and anti-CD3 activated lymphocytes ( $\pm$ caspase inhibitor pre-treatment) at 24 and 48 hour post exposure
- **Mitochondrial outer membrane permeability (MOMP)**, which is an indicator of the onset of apoptosis, was determined following 24 hour exposure of resting and anti-CD3 activated lymphocytes ( $\pm$ caspase inhibitor pre-treatment). Cells were stained using a DePsipher kit and imaged under a CLSM (section 2.1.3.9).
- The effects of metal ion exposure on the expression of inhibitory surface receptors that negatively regulate T-lymphocyte response was assessed via flow cytometry. The **expression of inhibitory T-lymphocyte regulators** on anti-CD3 + anti-CD28 activated lymphocytes was assessed following 48 hours of metal ions treatment. Lymphocytes were stained with anti-human CD3-FITC (clone OKT3) which would phenotype T-lymphocytes, anti-human PD-1APC (clone MIH4) and anti-human CTLA-4 PE (clone 14D3) which would identify the inhibitory surface proteins PD-1 and CTLA-4. The following isotype controls were also used to distinguish non-specific binding; Mouse IgG2 $\kappa$  Isotype FITC, Mouse IgG1 $\kappa$  Isotype APC and, Mouse IgG2 $\alpha$  Isotype-PE, (all eBioscience, Hatfield, UK).

## 4.4 Results

### 4.4.1 Effects of metal ions on cell viability

The viability of resting and anti-CD3-activated lymphocytes following exposure to  $\text{Cr}^{6+}$  or  $\text{Co}^{2+}$  for 24 and 48 hours is shown Figures 4.2 and 4.3. The results show that 1, 10, and 100  $\mu\text{M}$   $\text{Cr}^{6+}$  caused a significant ( $p < 0.05$ ) decrease in the viability of resting and anti-CD3-activated lymphocytes at both time points. No effect on cell viability was observed following exposure to 0.1  $\mu\text{M}$   $\text{Cr}^{6+}$ . Exposure of resting lymphocytes to  $\text{Co}^{2+}$  ions induced a significant decrease in cell viability only at a concentration of 100  $\mu\text{M}$ ; this effect was seen at 24 and 48 hr where cell viability was reduced to 85.10 ( $\pm 4.26$ ) % and 85.28 ( $\pm 4.86$ ) % (mean  $\pm$  SEM,  $n = 18$ ), respectively, as measured by NR assay (Figure 4.3). However, viability of activated lymphocytes at 24 hr was decreased significantly after exposure to 10 and 100  $\mu\text{M}$   $\text{Co}^{2+}$  (Figures 4.2B and 4.3B), whereas at 48 hr it was reduced after exposure to all of the concentrations of  $\text{Co}^{2+}$ , as measured by NR assay (Figure 4.3D). These results also show that  $\text{Cr}^{6+}$  caused a greater decrease in cell viability than  $\text{Co}^{2+}$ .

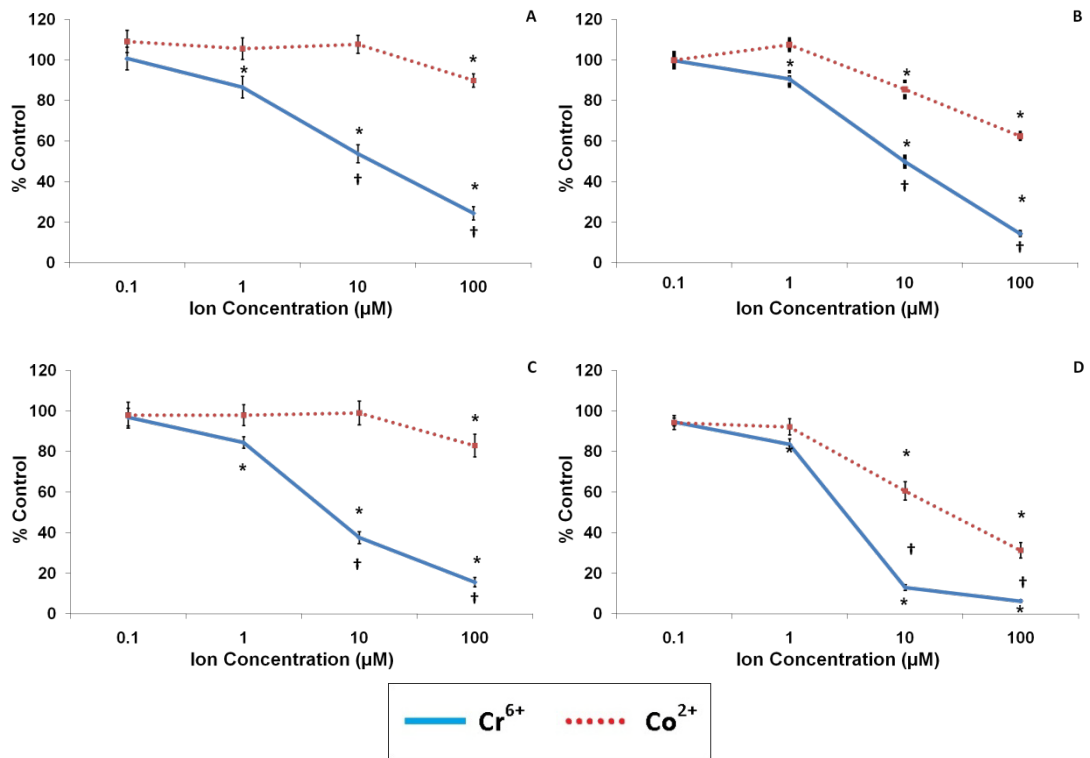


**Figure 4.2 Cell viability of lymphocytes following 24 (upper) and 48 (lower) hr of exposure to varying concentrations of Cr<sup>6+</sup> and Co<sup>2+</sup> ions, as measured by MTT assay. (A & C) Resting and (B & D) anti-CD3-activated lymphocytes. A value of 100% indicates unexposed control cells; results are means ± SEM (n = 18). \*Significantly different from control values (at p < 0.05) by one-way ANOVA followed by Dunnett's multiple comparison test. †Significantly different from Co<sup>2+</sup> values (at p < 0.05) by 2-sample t-test.**

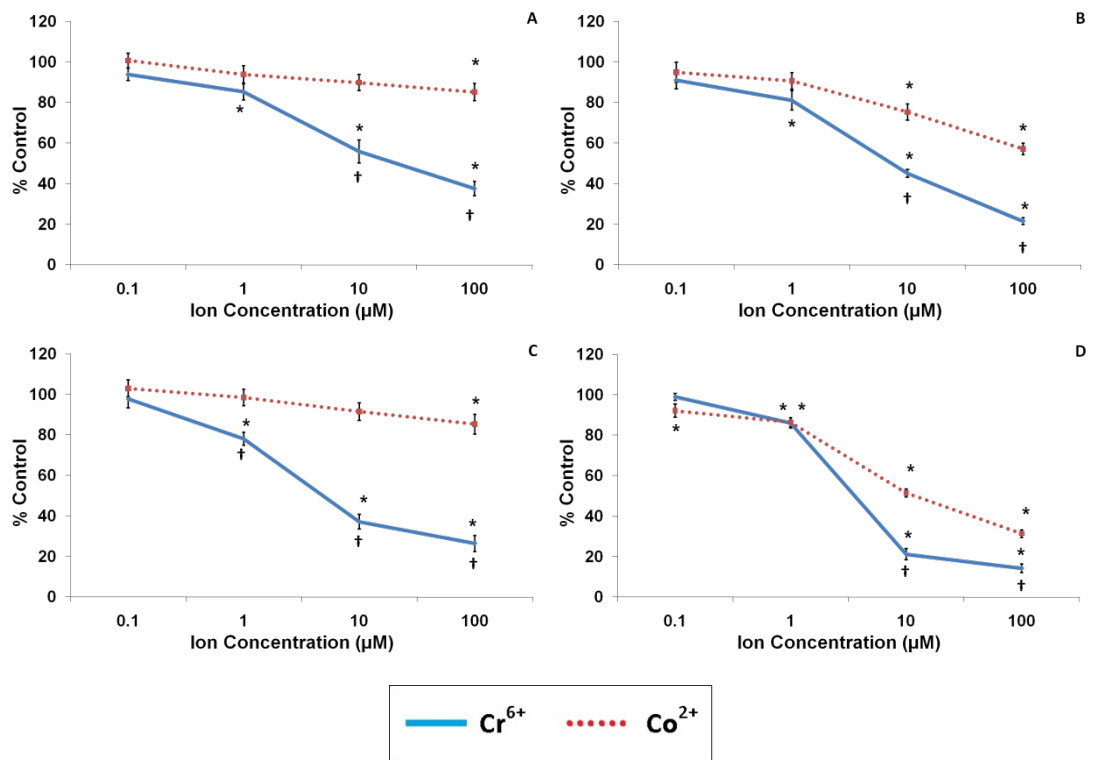


**Figure 4.3 Cell viability of lymphocytes following 24 (upper) and 48 (lower) hr of exposure to varying concentrations of Cr<sup>6+</sup> and Co<sup>2+</sup> ions, as measured by NR assay. (A & C) Resting and (B & D) anti-CD3-activated lymphocytes. A value of 100% indicates unexposed control cells; results are means  $\pm$  SEM (n = 18). \*Significantly different from control values (at p < 0.05) by one-way ANOVA followed by Dunnett's multiple comparison test. †Significantly different from Co<sup>2+</sup> values (at p < 0.05) by 2-sample t-test.**

Tables 4.1, 4.2, 4.3 and 4.4 shows the effect of exposing resting and anti-CD3 activated lymphocytes to Cr<sup>6+</sup> and Co<sup>2+</sup> in combination on cell viability. These data demonstrate that no combined exposure conditions show any significant difference in cell viability when compared with the respective individual effects. This is the case for resting and anti-CD3 activated lymphocytes.

Exposure	24hr	48hr
1 $\mu$ M Cr <sup>6+</sup>	86.50 $\pm$ 5.29	84.38 $\pm$ 2.85
10 $\mu$ M Cr <sup>6+</sup>	53.60 $\pm$ 4.45	37.53 $\pm$ 2.91
1 $\mu$ M Co <sup>2+</sup>	105.57 $\pm$ 5.09	97.89 $\pm$ 5.18
10 $\mu$ M Co <sup>2+</sup>	107.73 $\pm$ 5.53	98.93 $\pm$ 5.89
1 $\mu$ M Cr <sup>6+</sup> + 1 $\mu$ M Co <sup>2+</sup>	95.07 $\pm$ 3.26	91.63 $\pm$ 4.56
1 $\mu$ M Cr <sup>6+</sup> + 10 $\mu$ M Co <sup>2+</sup>	96.03 $\pm$ 2.50	89.72 $\pm$ 4.19
10 $\mu$ M Cr <sup>6+</sup> + 1 $\mu$ M Co <sup>2+</sup>	49.42 $\pm$ 1.38	40.50 $\pm$ 1.53
10 $\mu$ M Cr <sup>6+</sup> + 10 $\mu$ M Co <sup>2+</sup>	45.53 $\pm$ 1.90	31.87 $\pm$ 2.26

**Table 4.1 Cell viability of resting lymphocytes following 24 and 48 hr exposure to varying concentrations of Cr<sup>6+</sup> and Co<sup>2+</sup> ions, as measured by MTT assay.** Results are expressed as % Control ( $\pm$  SEM,  $n \geq 18$ ) where 100% indicates unexposed control values; no significant difference of combined ion exposure from both individual concentrations was found,  $P < 0.05$ , by 2-sample t-test.

Exposure	24hr	48hr
1 $\mu$ M Cr <sup>6+</sup>	85.28 $\pm$ 4.00	78.08 $\pm$ 3.20
10 $\mu$ M Cr <sup>6+</sup>	55.98 $\pm$ 5.67	37.14 $\pm$ 3.71
1 $\mu$ M Co <sup>2+</sup>	93.84 $\pm$ 4.22	98.49 $\pm$ 18.15
10 $\mu$ M Co <sup>2+</sup>	89.14 $\pm$ 3.94	91.48 $\pm$ 4.30
1 $\mu$ M Cr <sup>6+</sup> + 1 $\mu$ M Co <sup>2+</sup>	77.86 $\pm$ 1.96	77.00 $\pm$ 1.91
1 $\mu$ M Cr <sup>6+</sup> + 10 $\mu$ M Co <sup>2+</sup>	76.20 $\pm$ 1.78	71.00 $\pm$ 2.48
10 $\mu$ M Cr <sup>6+</sup> + 1 $\mu$ M Co <sup>2+</sup>	53.84 $\pm$ 1.40	30.04 $\pm$ 2.64
10 $\mu$ M Cr <sup>6+</sup> + 10 $\mu$ M Co <sup>2+</sup>	51.16 $\pm$ 1.16	34.64 $\pm$ 1.13

**Table 4.2 Cell viability of resting lymphocytes following 24 and 48 hr exposure to varying concentrations of Cr<sup>6+</sup> and Co<sup>2+</sup> ions, as measured by NR assay.** Results are expressed as % Control ( $\pm$  SEM,  $n \geq 18$ ) where 100% indicates unexposed control values; no significant difference of combined ion exposure from both individual concentrations was found,  $P < 0.05$ , by 2-sample t-test.

Exposure	24hr	48hr
1µM Cr <sup>6+</sup>	90.63±3.54	83.52±10.99
10µM Cr <sup>6+</sup>	49.89±2.68	13.02±6.07
1µM Co <sup>2+</sup>	107.47±2.82	92.11±16.91
10µM Co <sup>2+</sup>	85.40±4.02	60.54±19.34
1µM Cr <sup>6+</sup> + 1µM Co <sup>2+</sup>	81.96±1.48	75.05±2.20
1µM Cr <sup>6+</sup> + 10µM Co <sup>2+</sup>	84.73±2.05	58.23±1.33
10µM Cr <sup>6+</sup> + 1µM Co <sup>2+</sup>	40.06±0.65	9.46±1.66
10µM Cr <sup>6+</sup> + 10µM Co <sup>2+</sup>	42.55±1.34	8.10±0.099

**Table 4.3 Cell viability of anti-CD3 activated lymphocytes following 24 and 48 hr exposure to varying concentrations of Cr<sup>6+</sup> and Co<sup>2+</sup> ions, as measured by MTT assay.** Results are expressed as % Control (± SEM, n 18) where 100% indicates unexposed control values; no significant difference of combined ion exposure from both individual concentrations was found, P<0.05, by 2-sample t-test.

Exposure	24hr	48hr
1µM Cr <sup>6+</sup>	81.07±4.76	86.10±2.63
10µM Cr <sup>6+</sup>	45.09±1.96	21.17±2.74
1µM Co <sup>2+</sup>	90.63±4.01	86.40±2.20
10µM Co <sup>2+</sup>	75.304±4.05	51.47±2.00
1µM Cr <sup>6+</sup> + 1µM Co <sup>2+</sup>	83.18±3.32	74.48±1.93
1µM Cr <sup>6+</sup> + 10µM Co <sup>2+</sup>	71.73±1.53	52.61±1.64
10µM Cr <sup>6+</sup> + 1µM Co <sup>2+</sup>	43.15±1.02	22.45±0.84
10µM Cr <sup>6+</sup> + 10µM Co <sup>2+</sup>	43.03±2.99	22.11±1.11

**Table 4.4 Cell viability of anti-CD3 activated lymphocytes following 24 and 48 hr exposure to varying concentrations of Cr<sup>6+</sup> and Co<sup>2+</sup> ions, as measured by NR assay.** (Results are expressed as % Control (± SEM, n 18) where 100% indicates unexposed control values; no significant difference of combined ion exposure from both individual concentrations was found, P<0.05, by 2-sample t-test)

#### 4.4.2 Effect of metal ions on T-lymphocyte activation

The presence of 10 and 100  $\mu\text{M}$   $\text{Cr}^{6+}$  significantly inhibited anti-CD3 and anti-CD3 + anti-CD28 induced activation (Figure 4.4). Exposure to these concentrations reduced the expression of CD69 on the surface of  $\text{CD3}^+$  lymphocytes to below 50% of control values.

Figure 4.4 also shows that only exposure to 100  $\mu\text{M}$   $\text{Co}^{2+}$  significantly reduced Signal 1 and Signals 1 and 2 induced T-Lymphocyte activation. This concentration reduced surface expression of CD69 to 84.05 ( $\pm 7.19$ ) % and 74.98 ( $\pm 11.93$ ) % ( $n=3$ ) of control values. No other concentration of  $\text{Co}^{2+}$  significantly inhibited Signal 1- or Signals 1 and 2-stimulated cell activation. The results shown in Figure 4.4 indicate that metal ion exposure has a similar effect on the early activation of Signal 1- and Signals 1 and 2-activated lymphocytes. No significant differences were observed between Signal 1- and Signals 1 and 2-activated lymphocytes when comparing the effects of metal ions on activation.

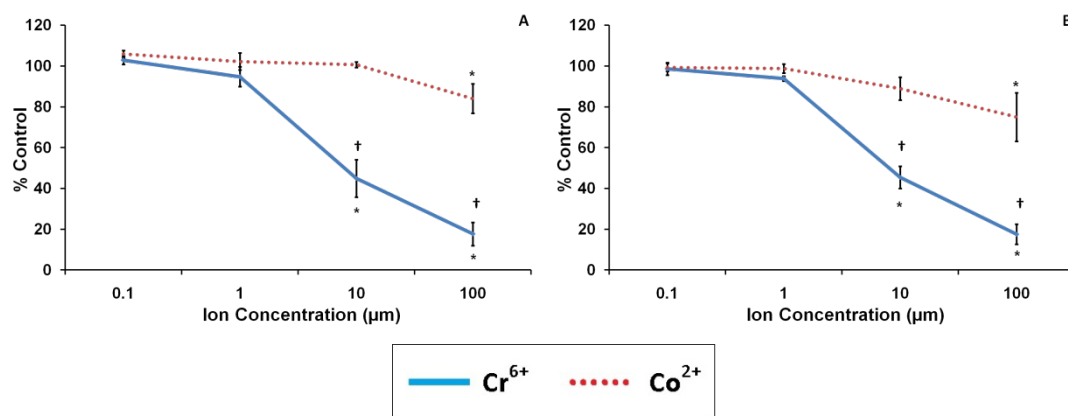


**Figure 4.4 T-lymphocyte activation following 24 hr exposure to  $\text{Cr}^{6+}$  or  $\text{Co}^{2+}$ . (A) anti-CD3-activated and (B) anti-CD3 + anti-CD28 activated lymphocytes.** Results are mean ( $\pm$  SEM;  $n = 3$ ) proportion of  $\text{CD3}^+$  lymphocytes expressing CD69. A value of 100% indicates baseline CD69 expression in unexposed control cells. \*Significantly different from control values (at  $p < 0.05$ ) by one-way ANOVA followed by Dunnett's multiple comparison test. †Significantly different from  $\text{Co}^{2+}$  values (at  $p < 0.05$ ) by 2-sample t-test.

#### **4.4.3 Effects of metal ions on lymphocyte proliferation**

The presence of  $\text{Cr}^{6+}$  ions significantly reduced anti-CD3-induced proliferation at all concentrations (Figure 4.5). This reduction was substantial in lymphocytes exposed to 10 and 100  $\mu\text{M}$   $\text{Cr}^{6+}$  where the proliferation was below 20% of control values. In the presence of both Signal 1 and 2 (anti-CD3 + anti-CD28) stimuli, a substantial and significant decrease in proliferation was observed at concentrations of 10 and 100  $\mu\text{M}$   $\text{Cr}^{6+}$ .

Exposure to 100  $\mu\text{M}$   $\text{Co}^{2+}$  significantly reduced Signal 1- and Signals 1 and 2-stimulated cell proliferation. Signals 1 and 2-induced proliferation was also slightly but significantly reduced to 88.56 ( $\pm$  3.87) % ( $n = 12$ ) following exposure to 10  $\mu\text{M}$   $\text{Co}^{2+}$ . No other concentration of  $\text{Co}^{2+}$  significantly inhibited Signal 1-stimulated cell proliferation, but that Signals 1 and 2 stimulated cell proliferation was slightly but significantly inhibited by 10  $\mu\text{M}$   $\text{Co}^{2+}$ . The results shown in Figure 4.5 indicate that metal ion exposure has a similar effect on proliferation of Signal 1- and Signals 1 and 2-activated lymphocytes. No significant differences were measured between Signal 1- and Signals 1 and 2-activated lymphocytes when comparing the effects of metal ions on proliferation.



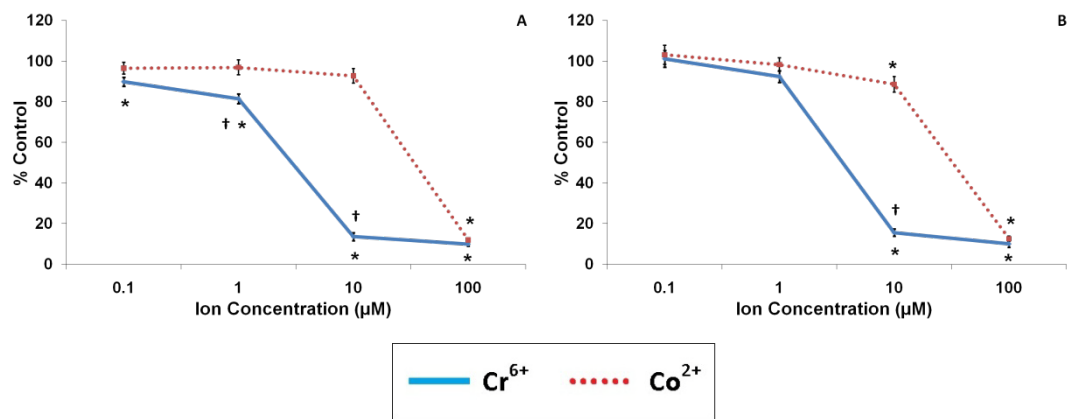


**Figure 4.5 Lymphocyte proliferation following 48 hr exposure to varying concentrations of Cr<sup>6+</sup> and Co<sup>2+</sup> ions.** (A) anti-CD3-activated and (B) anti-CD3 + anti-CD28 activated lymphocytes. A value of 100% indicates unexposed control cells; results are means  $\pm$  SEM (n = 12). \*Significantly different from control values (at p < 0.05) by one-way ANOVA followed by Dunnett's multiple comparison test. †Significantly different from Co<sup>2+</sup> values (at p < 0.05) by 2-sample t-test.

#### 4.4.4 Effects of metal ions on cytokine release

As shown in Figure 4.6, metal ions significantly decreased IL-2 release from stimulated lymphocytes. Both Cr<sup>6+</sup> and Co<sup>2+</sup> ion exposure significantly inhibited IL-2 production, even following exposure to the lowest concentrations of each. Figure 4.6 also indicates that in Signal 1 and 2-stimulated lymphocytes, production of IL-2 was more susceptible to inhibition by the metal ions than was Signal 1-stimulated production, when compared to the respective untreated control values.

IFN- $\gamma$  production by Signal 1- and Signals 1 and 2-stimulated lymphocytes was significantly inhibited following exposure to 10 and 100  $\mu$ M Cr<sup>6+</sup> (Figure 4.7). Exposure to 10 and 100  $\mu$ M Co<sup>2+</sup> also inhibited IFN- $\gamma$  release by Signal 1- and Signals 1 and 2-stimulated lymphocytes.

Exposure to 10 and 100  $\mu$ M Cr<sup>6+</sup> resulted in a significant decrease in TNF $\alpha$  production by Signal 1- and Signals 1 and 2-stimulated lymphocytes. There was also a significant decrease in TNF $\alpha$  measured from of Signal 1-stimulated lymphocytes

exposed to 1  $\mu\text{M}$   $\text{Cr}^{6+}$ .  $\text{Co}^{2+}$  ions also inhibited  $\text{TNF}\alpha$  release by Signal 1- and Signals 1 and 2-stimulated lymphocytes. Significant inhibition was observed following exposure to 100  $\mu\text{M}$ .  $\text{Co}^{2+}$  exposure did not significantly inhibit  $\text{TNF}\alpha$  release from Signal 1- or Signals 1 and 2-stimulated lymphocytes at concentrations of below 100  $\mu\text{M}$ .

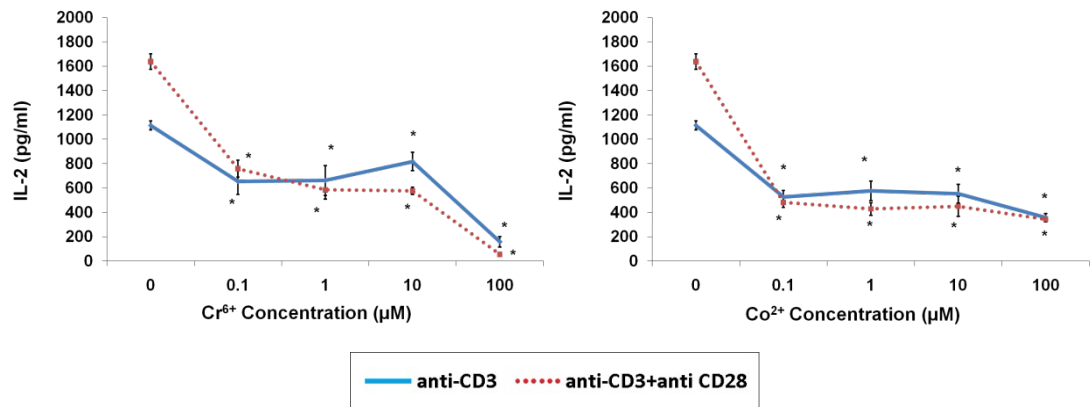


**Figure 4.6 IL-2 production from anti-CD3  $\pm$  anti-CD28 activated lymphocytes exposed to varying concentrations of  $\text{Cr}^{6+}$  and  $\text{Co}^{2+}$  ions for 48 hr. Results are means  $\pm$  SEM (n = 3). \*Significantly different from control values (at  $p < 0.05$ ) by one-way ANOVA followed by Dunnett's multiple comparison test.**

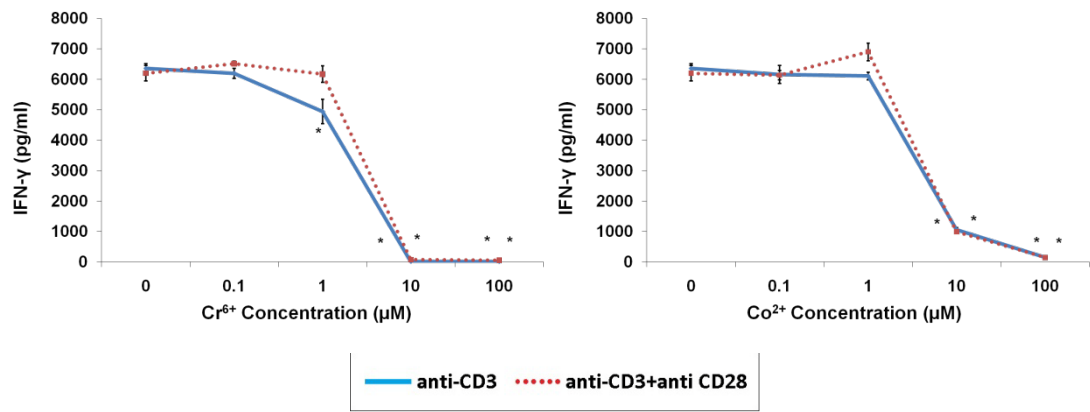


**Figure 4.7** IFN- $\gamma$  release from anti-CD3  $\pm$  anti-CD28 activated lymphocytes exposed to varying concentrations of Cr<sup>6+</sup> and Co<sup>2+</sup> ions for 48 hr. Results are means  $\pm$  SEM (n = 3). \*Significantly different from control values (at p < 0.05) by one-way ANOVA followed by Dunnett's multiple comparison test.

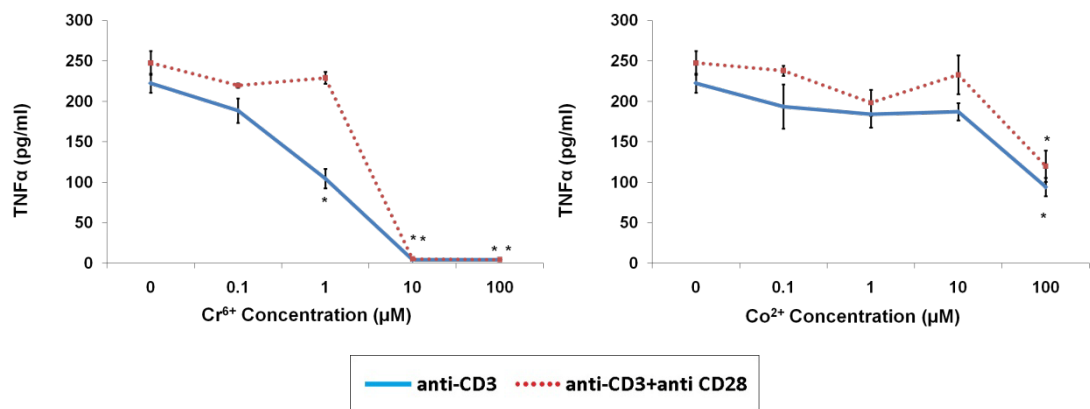


**Figure 4.8** TNF $\alpha$  release from anti-CD3  $\pm$  anti-CD28 activated lymphocytes exposed to varying concentrations of Cr<sup>6+</sup> and Co<sup>2+</sup> ions for 48 hr. Results are means  $\pm$  SEM (n = 3). \*Significantly different from control values (at p < 0.05) by one-way ANOVA followed by Dunnett's multiple comparison test.

#### 4.4.5 Effects of metal ions on the cell cycle

Exposure to 10 and 100  $\mu\text{M}$   $\text{Cr}^{6+}$  for 24 hours resulted in a significant increase ( $p < 0.05$ ) in the proportion of apoptotic anti-CD3 activated lymphocytes compared with unexposed control cells (Figure 4.10A). This is accompanied by a significant decrease of cells at  $G_0/G_1$  and  $G_2/M$ -phases of the cell cycle. Following 48 hours exposure to 10 and 100  $\mu\text{M}$   $\text{Cr}^{6+}$  there was also a significant increase in cells at S-phase of the cell cycle (Figures 4.9 and 4.10C).

Exposure to 0.1 or 1  $\mu\text{M}$   $\text{Co}^{2+}$  lead to no significant changes in the proportion of cells at various phases of the cell cycle (Figure 4.10B and 4.10D). However, exposure to 10  $\mu\text{M}$   $\text{Co}^{2+}$  resulted in a significant decrease in  $G_0/G_1$  phases of the cell cycle at 24 hours. There was a significant decrease in the proportion of anti-CD3 activated lymphocytes at cells at  $G_0/G_1$  and  $G_2/M$ -phases of the cell cycle following exposure to 100  $\mu\text{M}$   $\text{Co}^{2+}$  (Figures 4.9, 4.10B and 4.10D). This coincided with a significant increases in the proportion of cells measured as being apoptotic.

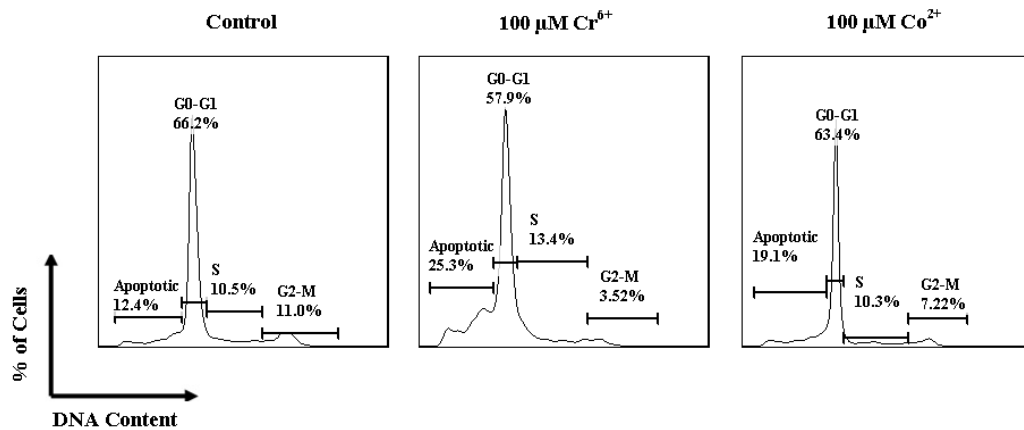
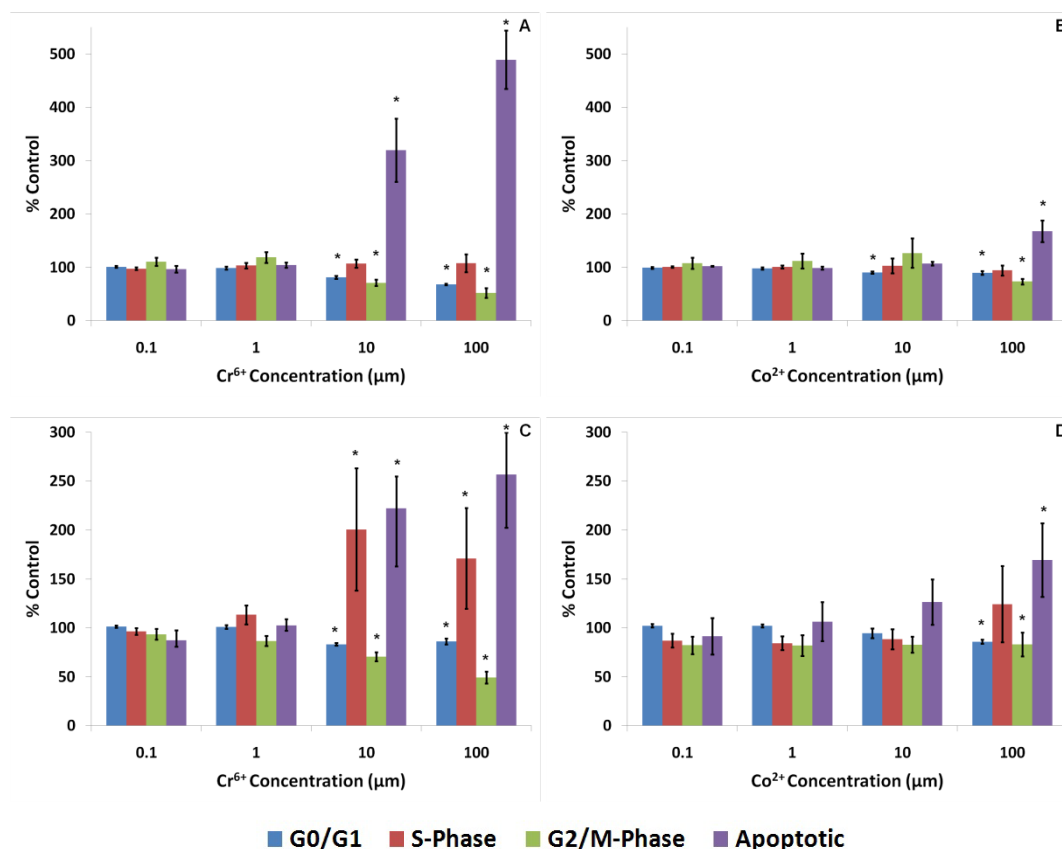


Figure 4.9 Percentage of anti-CD3 activated lymphocytes at various stages of the cell cycle following 48 hour of exposure to 100  $\mu\text{M}$   $\text{Cr}^{6+}$  or  $\text{Co}^{2+}$ .



**Figure 4.10** Anti-CD3-activated lymphocytes at different stages of cell cycle following 24 (upper) and 48 (lower) hr of exposure to Cr<sup>6+</sup> (A&C) and Co<sup>2+</sup> (B&D). Results are mean ( $\pm$  SEM; n = 3) proportion of lymphocytes at different phases of cell cycle. A value of 100% indicates values of unexposed control cells. \*Significantly different from control values (at  $p < 0.05$ ) by one-way ANOVA followed by Dunnett's multiple comparison test.

#### 4.4.6 Flow cytometric analysis of apoptosis following metal ion exposure

Since it was demonstrated that Cr<sup>6+</sup> and Co<sup>2+</sup> exposure leads to a decrease in cell viability and proliferation of anti-CD3 activated lymphocytes, the cell cycle of these cells was analysed following ion exposure to identify a possible mechanism. Exposure of resting lymphocytes to Cr<sup>6+</sup> led to a significant increase of total

apoptosis (early plus late) at 10 and 100  $\mu\text{M}$  (Figures 4.11 and 4.12). Resting lymphocytes exposed to 100  $\mu\text{M}$   $\text{Co}^{2+}$  show a significant increase in apoptosis at 24 and 48 hr.  $\text{Co}^{2+}$  concentrations that were  $< 100 \mu\text{M}$  did not cause an increase in apoptosis compared to control values. In addition, anti-CD3 activated lymphocytes exposed to 10 or 100  $\mu\text{M}$   $\text{Cr}^{6+}$  for 24 and 48 hr underwent significantly more apoptosis than respective unexposed control cells (Figure 4.11, 4.12B and 4.12D). Treatment of anti-CD3 activated lymphocytes with 100  $\mu\text{M}$   $\text{Co}^{2+}$  led to an increase of apoptosis to 145.42 ( $\pm 18.45$ ) % at 24 hr and 143.57 ( $\pm 7.08$ ) % at 48 hr. As with resting lymphocytes, exposure to lower concentrations of  $\text{Co}^{2+}$  ions did not lead to any significant increase in the proportion of apoptotic cells. Furthermore, the extent of necrotic cell death was small, even at the highest test concentration (as shown in top left quadrants of Figure 4.11). Figure 4.12 also illustrates  $\text{Cr}^{6+}$  exposure led to increased levels of apoptosis (compared to those due to  $\text{Co}^{2+}$ ) in both resting and anti-CD3 activated lymphocytes.

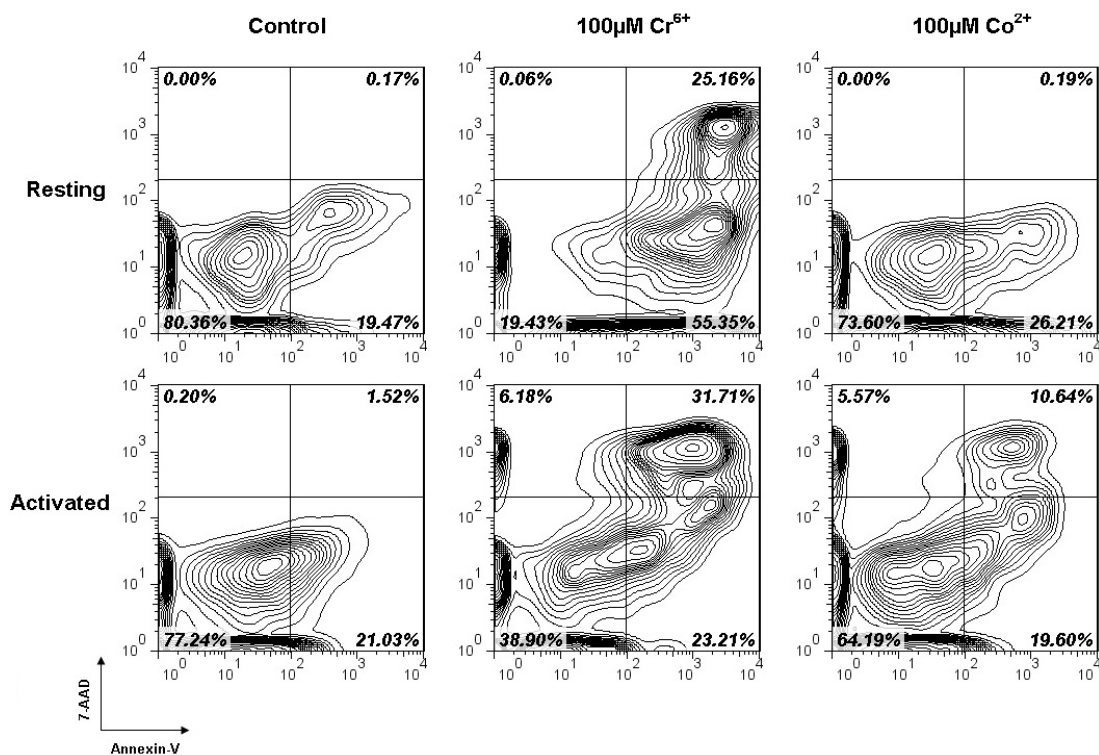


**Figure 4.11** Resting and anti-CD3 activated lymphocytes stained with Annexin V and 7-AAD following exposure to 100 µM Cr<sup>6+</sup> and 100 µM Co<sup>2+</sup> for 24 hr. Viable cells were Annexin V<sup>-</sup> and 7-AAD<sup>-</sup>. Cells in early stages of apoptosis were Annexin V<sup>+</sup> but 7-AAD<sup>-</sup>, whereas cells in late stages of apoptosis were both Annexin V<sup>+</sup> and 7-AAD<sup>+</sup>.

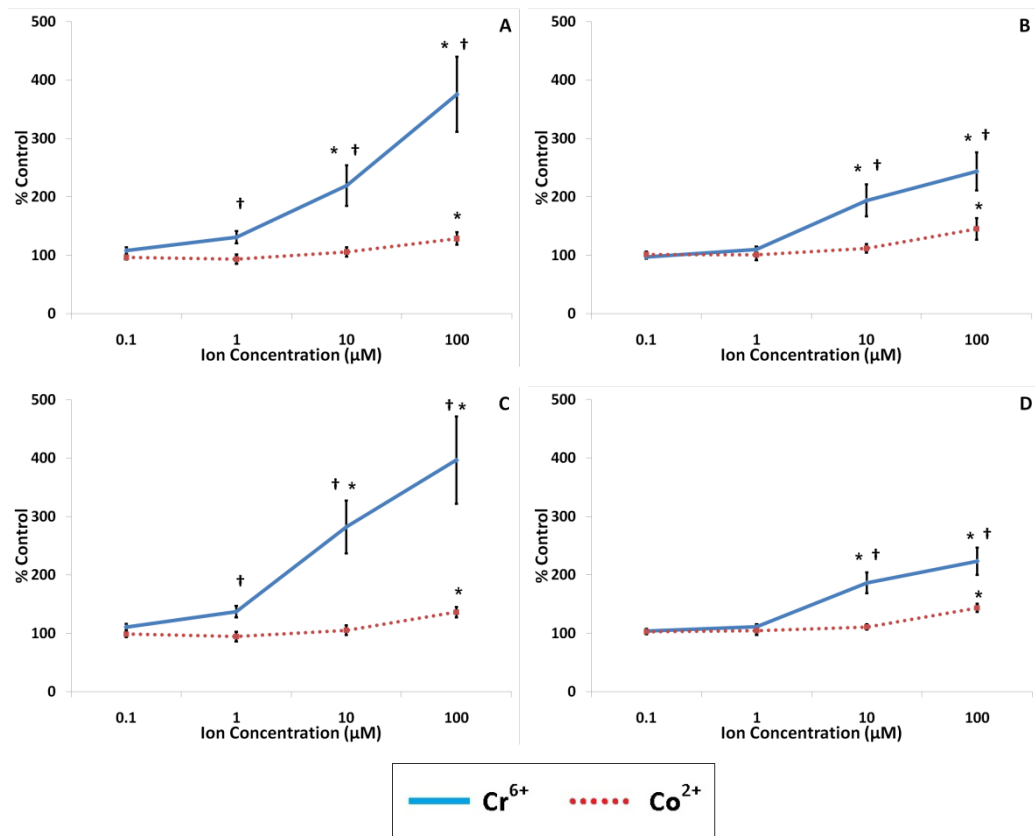


**Figure 4.12. Total apoptosis in lymphocytes following 24 (upper) and 48 (lower) hr of exposure to Cr<sup>6+</sup> and Co<sup>2+</sup>.** (A & C) Resting and (B & D) anti-CD3-activated lymphocytes. Results are mean ( $\pm$  SEM; n = 6) proportion of lymphocytes expressing Annexin V. A value of 100% indicates baseline apoptosis in unexposed control cells. \*Significantly different from control values (at p < 0.05) by one-way ANOVA followed by Dunnett's multiple comparison test. †Significantly different from Co<sup>2+</sup> values (at p < 0.05) by 2-sample t-test.

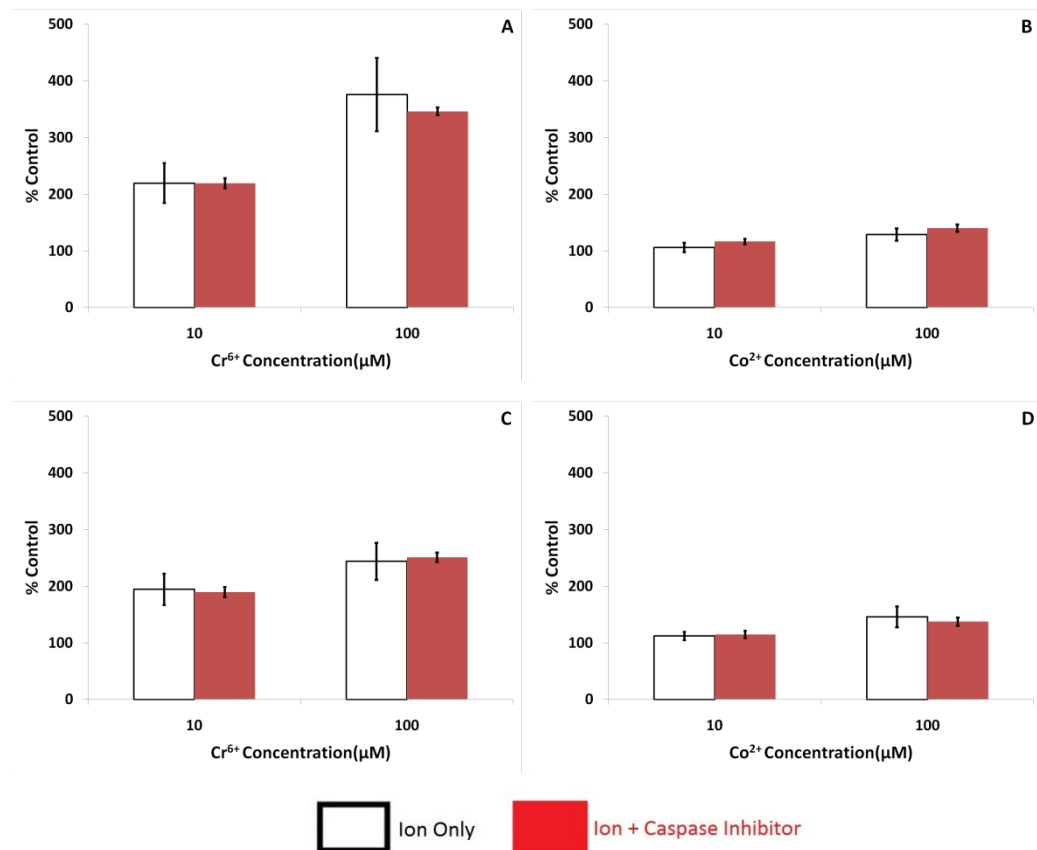
## 4.4.7 Caspase-3 inhibition of lymphocytes

### 4.4.7.1 Effect of caspase inhibition on metal ion induced apoptosis

Figures 4.13 indicates that caspase inhibition did not reduce the level of apoptosis following 24 hour of exposure to 10 and 100  $\mu$ M of Cr<sup>6+</sup> or Co<sup>2+</sup>. Following treatment of resting or anti-CD3 activated lymphocytes with the caspase-3 inhibitor



Z.Devd.FMK, there was no significant difference in the level of metal ion-induced apoptosis when compared with cells that were not treated.

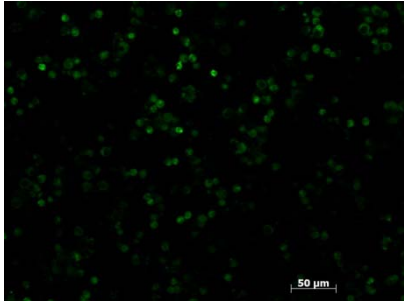
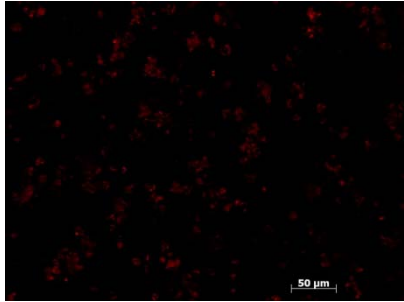
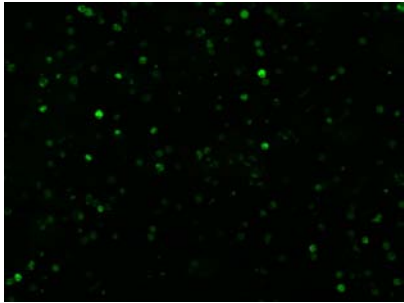
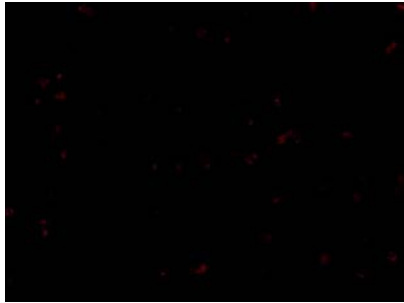
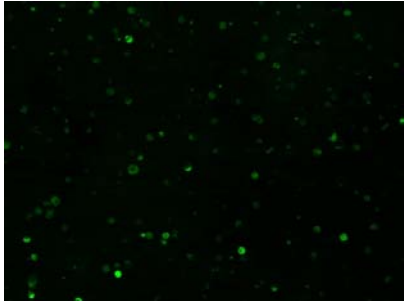
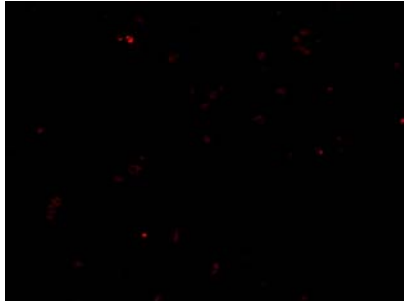
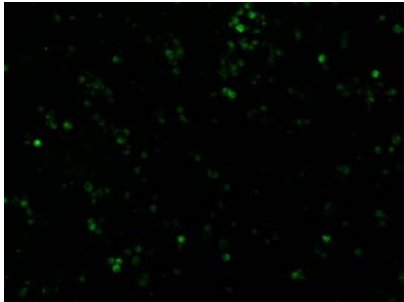
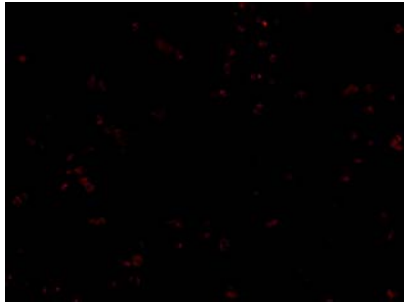
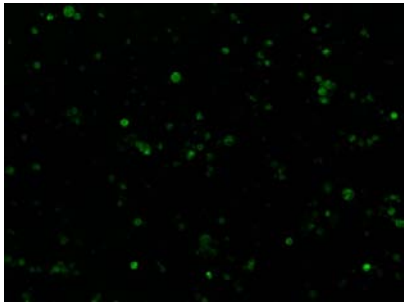
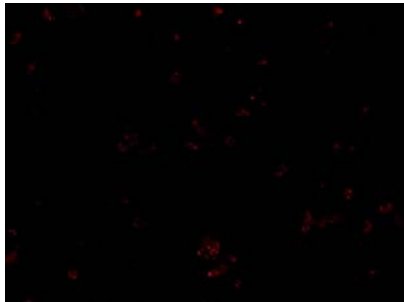


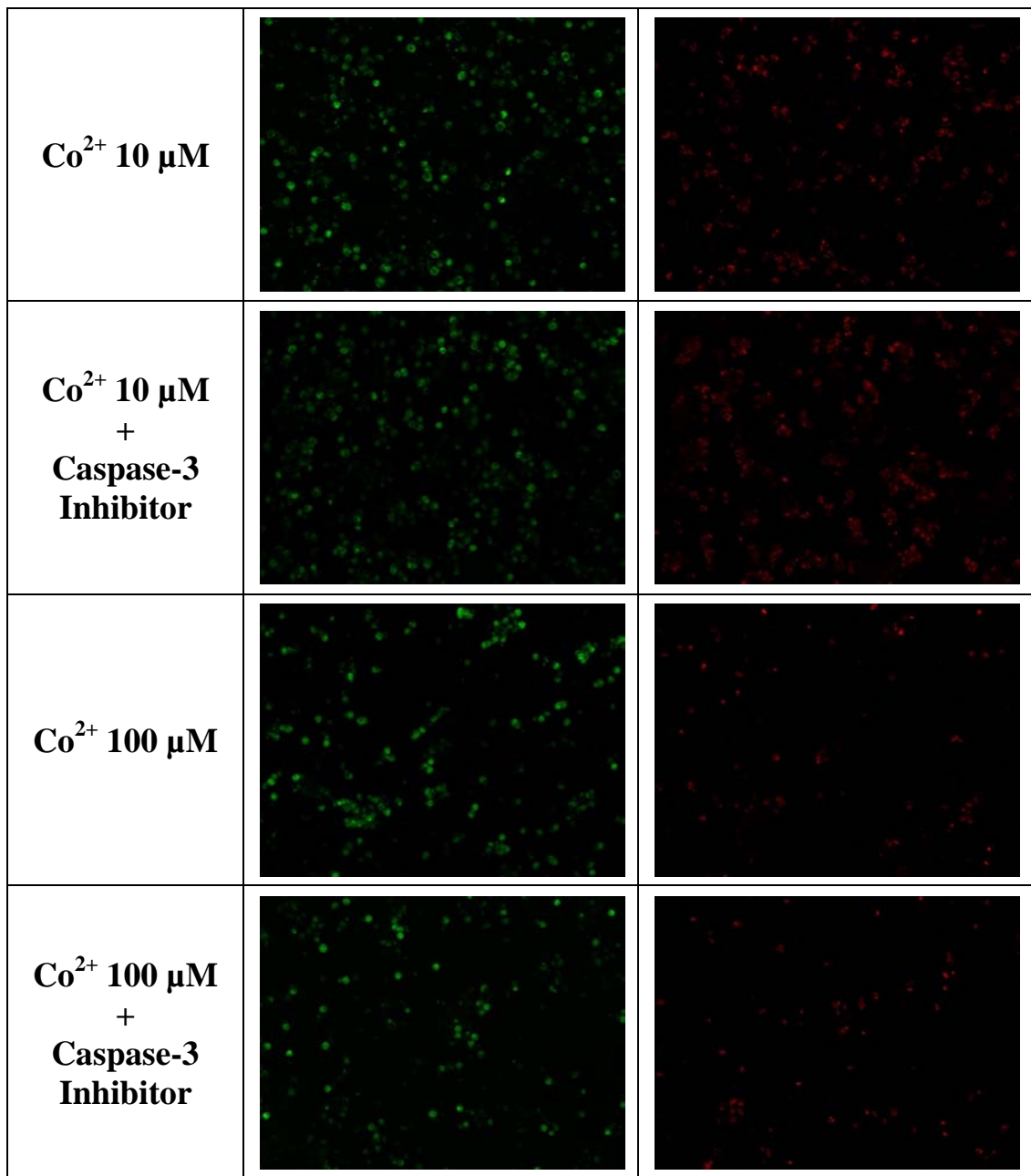
**Figure 4.13 Total apoptosis in lymphocytes exposed to Cr<sup>6+</sup> or Co<sup>2+</sup> treated with or without a caspase-3 inhibitor.** Resting (upper) and anti-CD3-activated (lower) lymphocytes. Lymphocytes were pre-treated for 24 hr with/without caspase-3 inhibitor [50μM Z.Devd.FMK] and then exposed to Cr<sup>6+</sup> (A & C) or Co<sup>2+</sup> (B&D) in the presence or absence of the caspase-3 inhibitor. Apoptosis was measured via flow cytometry following Annexin V and 7-AAD staining. Total apoptosis was defined as the cells which were Annexin V<sup>+</sup> irrespective of 7-AAD status. Results are mean (± SEM; n ≥ 3) proportion of lymphocytes expressing Annexin V. A value of 100% indicates baseline apoptosis in unexposed control cells not pre-treated with the inhibitor.

#### **4.4.7.2 Effects of metal ions on mitochondrial outer membrane permeability**

Figure 4.14 and 4.15 show lymphocytes stained with DePsipher reagent. Cells are able to uptake this reagent which aggregates in healthy mitochondria within the cell to form a red fluorescent compound. However, in apoptotic cells, where MOMP is disrupted, the DePsipher reagent remains in its monomeric form within the cytoplasm and fluoresces green.

Images from Figure 4.14 indicate that exposure of 10 and 100  $\mu\text{M}$   $\text{Cr}^{6+}$  to resting lymphocytes caused a disruption of MOMP. This is indicated by the decrease in the number of cells which displayed healthy mitochondria. These images also show that pre-treatment of lymphocytes with caspase-3 inhibitor does not lead to any beneficial effect; this is also indicated from the results in Table 4.4. There appears to be similar levels of healthy mitochondria in control lymphocytes and those exposed to 10  $\mu\text{M}$   $\text{Co}^{2+}$ . However, exposure of 100  $\mu\text{M}$   $\text{Co}^{2+}$  results in a reduced number of cells with healthy mitochondria. Again, caspase-3 inhibitor treatment does not appear to have any effect on mitochondrial health following metal ion exposure.

	Fluorescein	Rhodamine
<b>Control</b>		
<b>Cr<sup>6+</sup> 10 μM</b>		
<b>Cr<sup>6+</sup> 10 μM + Caspase-3 Inhibitor</b>		
<b>Cr<sup>6+</sup> 100 μM</b>		
<b>Cr<sup>6+</sup> 100 μM + Caspase-3 Inhibitor</b>		

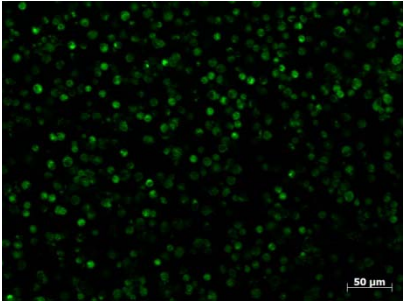
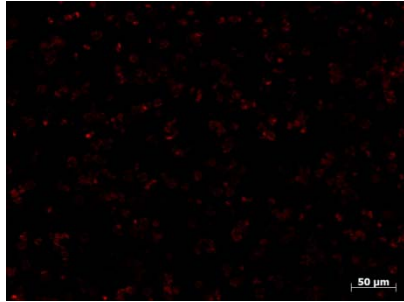
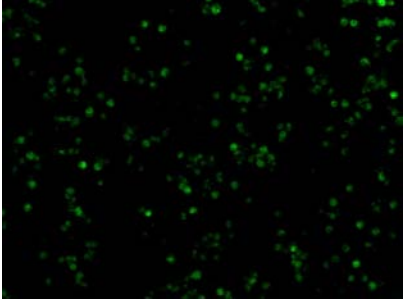
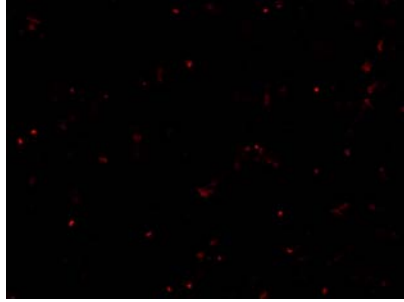
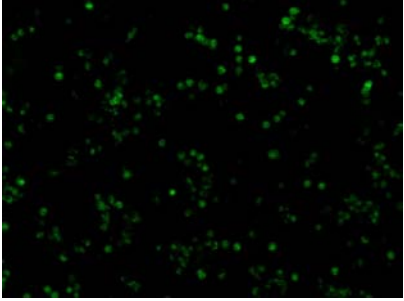
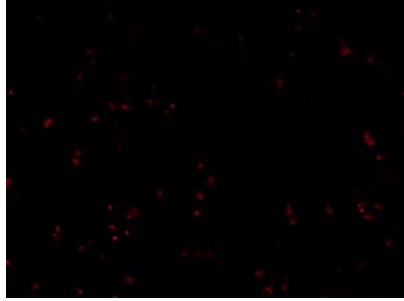
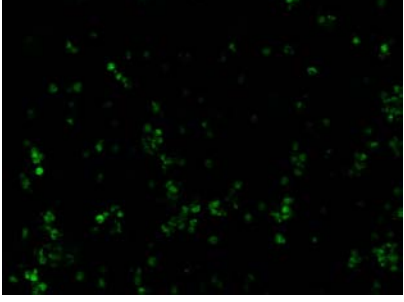
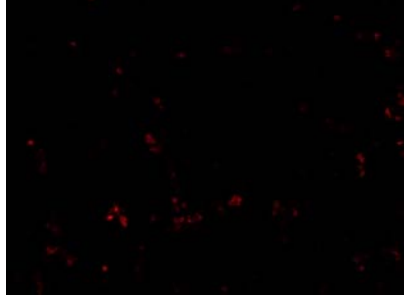
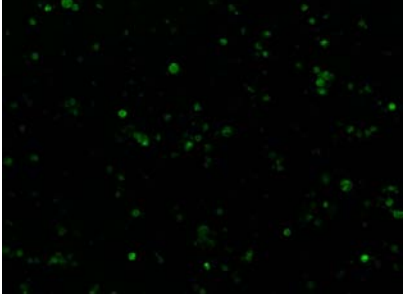
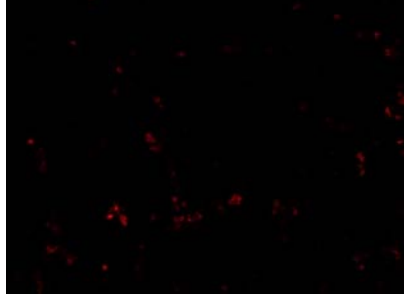


**Figure 4.14** Confocal laser scanning microscope images of resting human lymphocytes ( $\pm$  caspase-3 inhibitor pre-treatment) exposed to  $\text{Cr}^{6+}$  and  $\text{Co}^{2+}$  for 24 hours and then incubated with DePsipher reagent. The fluorescein filter imaged cells which uptake the reagent and fluoresce green. The rhodamine filter allowed imaging of the multimeric form of the dye within healthy mitochondria (red).

	% Healthy Mitochondria	
	- Inhibitor	+ Inhibitor
<b>Control</b>	89.7	-
<b>Cr<sup>6+</sup> 10 μM</b>	21.4	18.2
<b>Cr<sup>6+</sup> 100 μM</b>	22.9	24.1
<b>Co<sup>2+</sup> 100 μM</b>	76.3	81.7
<b>Co<sup>2+</sup> 100 μM</b>	34.7	38.9

**Table 4.5 Percentage of resting human lymphocytes ( $\pm$  caspase-3 inhibitor pre-treatment) with healthy mitochondria following exposure to Cr<sup>6+</sup> and Co<sup>2+</sup> for 24 hours, as imaged by Confocal Laser Scanning Microscopy following incubation with DePsipher reagent.** Results are data recorded from 5 independent images from each exposure concentration. Typically an area of 0.73 mm<sup>2</sup> was examined.

Figure 4.15 and Table 4.6 indicate that exposure of 10 and 100 μM Cr<sup>6+</sup> to anti-CD3 activated lymphocytes led to mitochondrial damage. In the anti-CD3 activated cells exposure of 10 and 100 μM Co<sup>2+</sup> also results in a reduced number of cells which have healthy mitochondria; a greater effect being observed following 100 μM exposure. It is also evident that pre-treatment of anti-CD3 activated lymphocytes with caspase-3 inhibitor does not alter the effect of either metal ion exposure.

	Fluorescein	Rhodamine
<b>Control</b>		
<b>Cr<sup>6+</sup> 10 μM</b>		
<b>Cr<sup>6+</sup> 10 μM + Caspase-3 Inhibitor</b>		
<b>Cr<sup>6+</sup> 100 μM</b>		
<b>Cr<sup>6+</sup> 100 μM + Caspase-3 Inhibitor</b>		

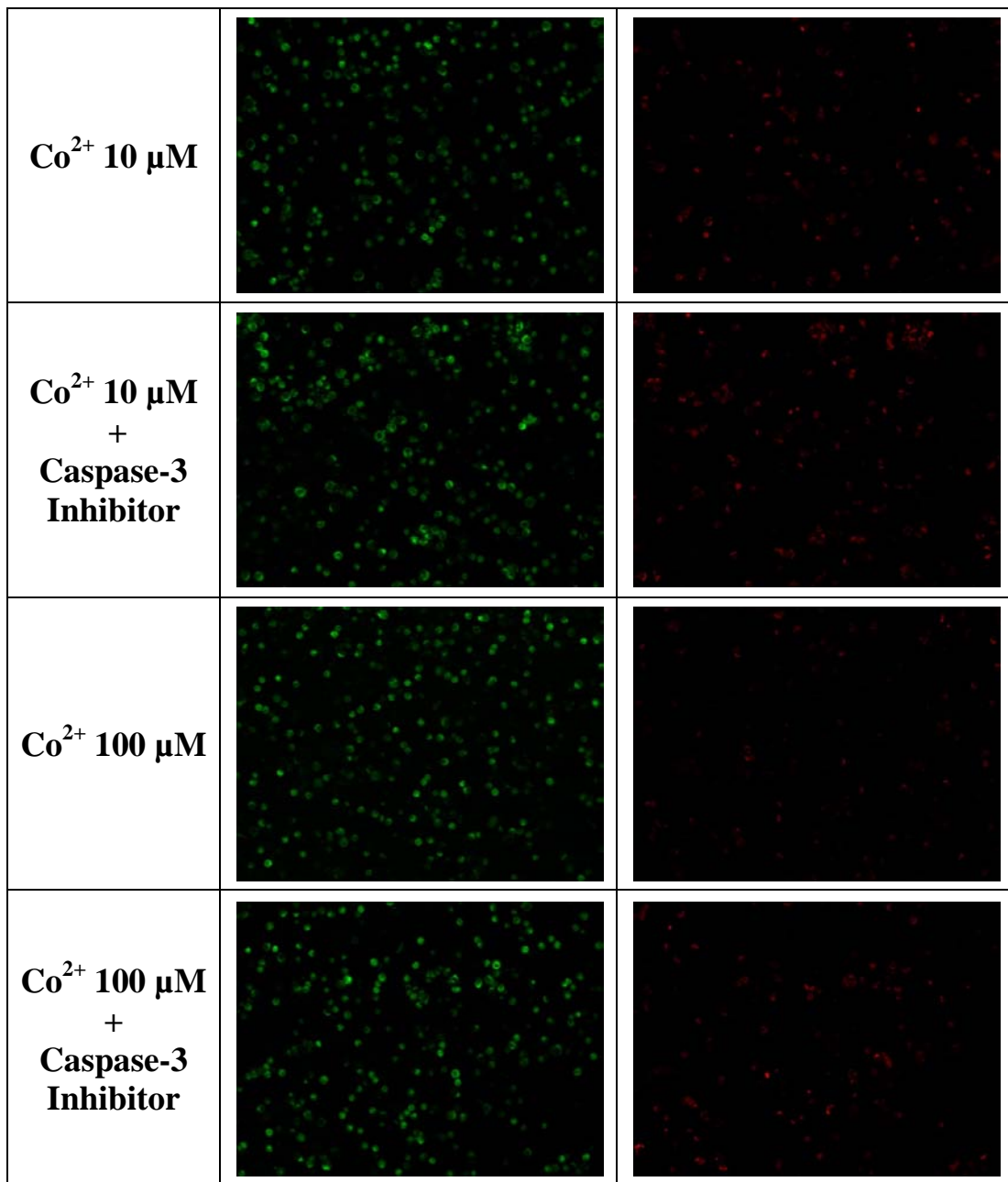


**Figure 4.15** Confocal laser scanning microscope images of anti-CD3 activated human lymphocytes ( $\pm$  caspase-3 inhibitor pre-treatment) exposed to  $\text{Cr}^{6+}$  and  $\text{Co}^{2+}$  for 24 hours and then incubated with DePsipher reagent. The fluorescein filter imaged cells which uptake the reagent and fluoresce green. The rhodamine filter allowed imaging of the multimeric form of the dye within healthy mitochondria (red).

	% Healthy Mitochondria	
	- Inhibitor	+ Inhibitor
<b>Control</b>	86.2	-
<b>Cr<sup>6+</sup> 10 μM</b>	18.3	15.1
<b>Cr<sup>6+</sup> 100 μM</b>	21.5	26.6
<b>Co<sup>2+</sup> 10 μM</b>	52.1	60.4
<b>Co<sup>2+</sup> 100 μM</b>	34.6	41.5

**Table 4.6 Percentage of anti-CD3 activated human lymphocytes ( $\pm$  caspase-3 inhibitor pre-treatment) with healthy mitochondria following exposure to Cr<sup>6+</sup> and Co<sup>2+</sup> for 24 hours, as imaged by Confocal Laser Scanning Microscopy following incubation with DePsipher reagent.** Results are data recorded from 5 independent images from each exposure concentration. Typically an area of 0.73 mm<sup>2</sup> was examined.

#### **4.4.7.3 Effects of metal ions on lymphocyte proliferation following caspase-3 inhibitor pre-treatment**

Caspase-3 inhibitor pre-treatment of anti-CD3 activated lymphocytes had no significant effects on the proliferation of metal ion exposed cells (Figure 4.16). This was the case for both Cr<sup>6+</sup> and Co<sup>2+</sup>.



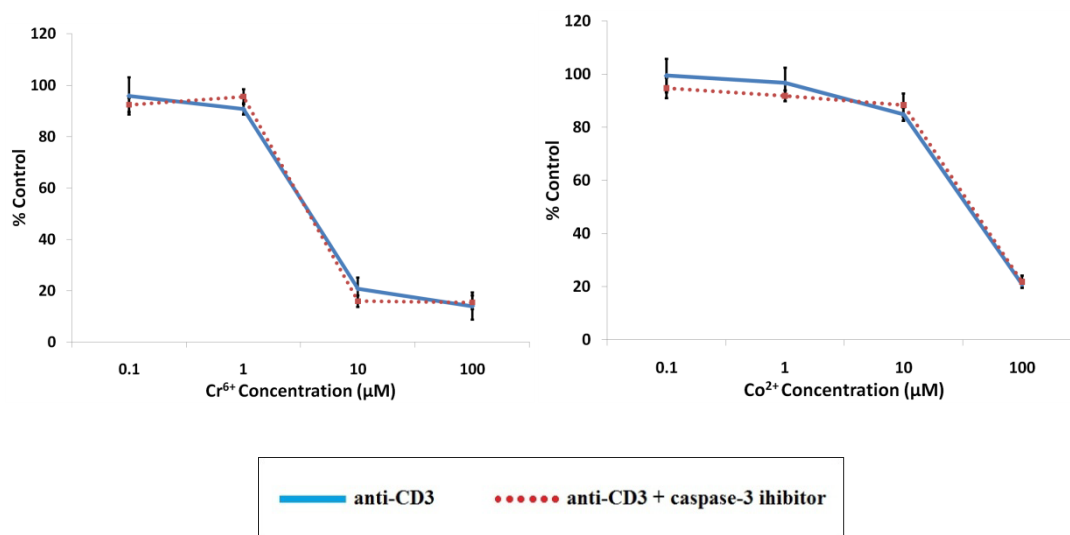


**Figure 4.16 Proliferation of anti-CD3-activated lymphocytes following 48 hr exposure to varying concentrations of Cr<sup>6+</sup> and Co<sup>2+</sup> ions with or without caspase-3 inhibitor treatment.** Cells were pre-treated for 24 hr with/without caspase-3 inhibitor [50μM Z.Devd.FMK] and then exposed to metal ions in the presence or absence of the caspase-2 inhibitor. A value of 100% indicates unexposed control cells; results are means ± SEM (n = 3).

#### 4.4.8 IL-2 supplementation of metal ion exposed lymphocytes

Figure 4.17 indicates that supplementing culture media with IL-2 did not lead to any significant alteration in anti-CD3 activated lymphocyte proliferation following metal ion exposure at concentrations that had previously inhibited proliferation (10 and 100 μM).

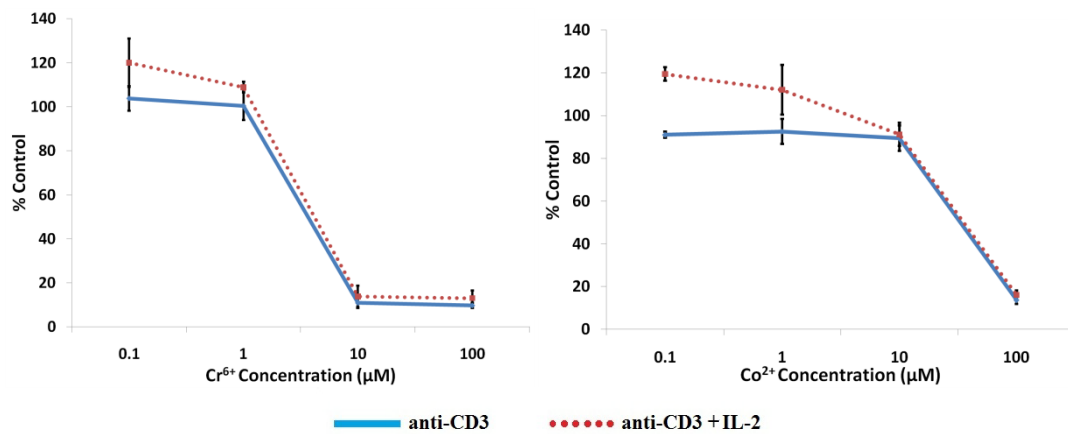


**Figure 4.17 Proliferation of anti-CD3-activated lymphocytes ( $\pm$  50U/ml IL-2) following 48 hr exposure to varying concentrations of Cr<sup>6+</sup> and Co<sup>2+</sup> ions. A value of 100% indicates unexposed anti-CD3 activated cells; results are means  $\pm$  SEM (n = 3).**

#### **4.4.9 Effect of metal ion exposure on inhibitory receptors of T-lymphocytes**

Following exposure to 10 and 100  $\mu$ M Cr<sup>6+</sup> for 48 hours, there was a significant decrease in the proportion of CD3<sup>+</sup> cells expressing PD-1. These concentrations of Cr<sup>6+</sup> reduced surface expression of PD-1 to 29.25 ( $\pm$ 5.68) % and 14.06 ( $\pm$ 1.66) % of control values, respectively. Exposure to 100  $\mu$ M Co<sup>2+</sup> for 48 hours also significantly reduced the expression of PD-1 to 38.98 ( $\pm$ 7.92) % of control values (Figure 4.18A). However, metal ion exposure did not lead to any significant changes in the proportion of cells expressing CTLA-4 (Figure 4.18B).

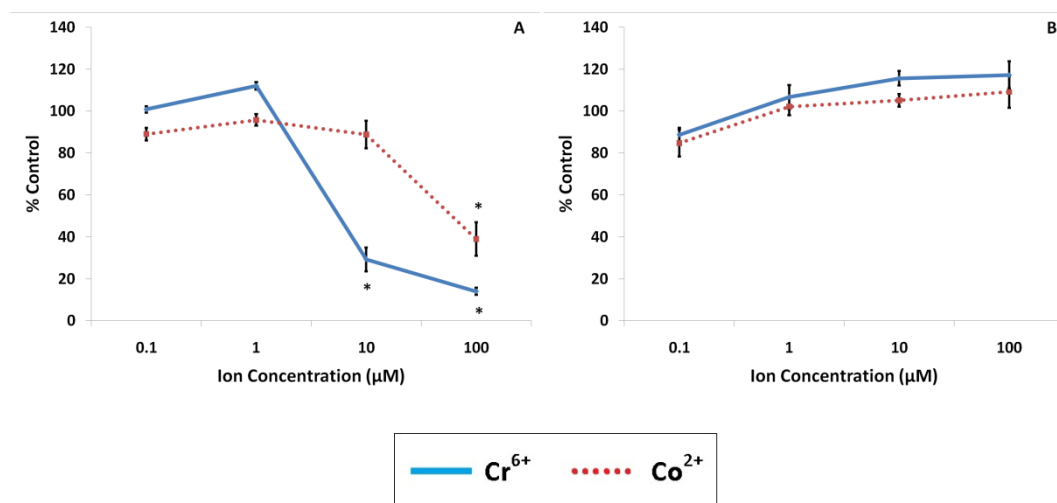


**Figure 4.18** Expression of T-lymphocyte inhibitory markers following 48 hr exposure of anti-CD3 + anti-CD28 activated lymphocytes to Cr<sup>6+</sup> and Co<sup>2+</sup>. (A) PD-1 and (B) CTLA-4 expression on activated lymphocytes. Results are mean (± SEM; n = 3) proportion of CD3<sup>+</sup> lymphocytes expressing PD-1 or CTLA-4. A value of 100% indicates baseline expression in unexposed control cells. \*Significantly different from control values (at p < 0.05) by one-way ANOVA followed by Dunnett's multiple comparison test.

## 4.5 Discussion

This chapter has shown that metal ion exposure decreases the viability of peripheral human lymphocytes. Cr<sup>6+</sup> significantly decreased cell viability at concentrations of 1 and 10 μM. These results also indicate that Cr<sup>6+</sup> reduces cell viability in resting and CD3-activated lymphocytes to a similar degree, when compared with the respective unexposed controls. The data also showed that Cr<sup>6+</sup> exposure inhibited T-lymphocyte proliferation, especially at higher concentrations. However, the results show a significant increase in apoptosis at Cr<sup>6+</sup> concentrations that also led to a significant decrease in cell proliferation and viability. There is also evidence that Cr<sup>6+</sup> can disrupt the cell cycle of activated cells indicated by the increasing proportion of cells at S-phase; this may be representative of cells that have DNA

damage. Therefore, it is likely that the cells are becoming apoptotic and unable to divide further rather than any direct impedance of cell activation and proliferation. Cr<sup>6+</sup> ions have been shown to induce apoptosis in lung epithelial cells (Russo et al., 2005) and fibroblasts (Carlisle et al., 2000) as well as in lymphocytes (Vasant et al., 2003) and macrophages (Kwon et al., 2009b). Cr<sup>6+</sup> is known to stimulate extrinsic and intrinsic apoptotic pathways (Sargeant and Goswami, 2007). Extrinsic pathways usually involve external signals which lead to the activation of caspases that are cytoplasmic pro-enzymes that initiate and amplify death signals or degrade cellular components (Pulido and Parrish, 2003). Intrinsic apoptosis can be initiated following excess reactive oxygen species (ROS) formation during intracellular reduction of Cr<sup>6+</sup> (hexavalent chromium) to Cr<sup>3+</sup> (trivalent chromium). The excess ROS disrupts the mitochondrial membrane initiating events which induce apoptosis (Ye et al., 1999, Vasant et al., 2003, Sargeant and Goswami, 2007). The current study has shown that the treatment of lymphocytes with a caspase-3 inhibitor does not inhibit the apoptosis induced following metal ion exposure.

Although there are previous reports that indicated caspase inhibition could lead to a reduction in the level of apoptosis and recovery of cell proliferation following PBMC exposure to Cr<sup>6+</sup> ions (Vasant et al., 2003), data from the current study indicate that metal ion exposure led to MOMP irrespective of caspase inhibition. Since effects on MOMP occur upstream of caspase activation, and attempts to reverse the observed apoptosis by inhibiting caspase activity are therefore unlikely to work (Figure 4.19). These inhibitors are incapable of preventing MOMP, a process that leads to release of mitochondrial proteins culminating in cell death (Kroemer and Martin, 2005). Therefore, metal ion exposure can lead to cellular apoptosis irrespective of caspase inhibition (Pritchard et al., 2000).

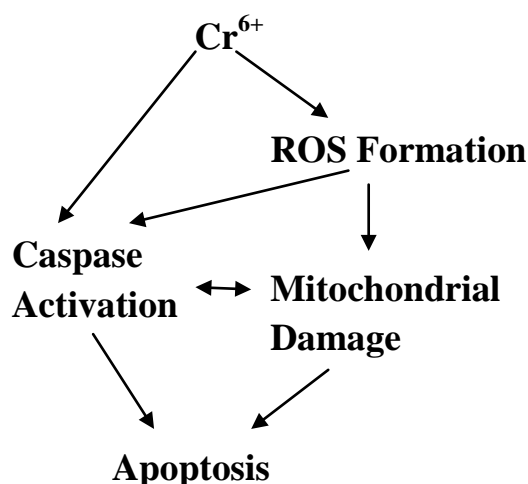


**Figure 4.19 Pathways by which Cr<sup>6+</sup> induced mitochondrial damage can lead to apoptosis, with or without the involvement of caspase activation.**

The data from the present study also indicate that Co<sup>2+</sup> exposure may be more toxic to activated T-lymphocytes than to resting lymphocytes. The viability of proliferating lymphocytes is reduced to a greater extent than resting lymphocytes when compared with their respective unexposed control values. These results also indicate that the reduction in cell viability is likely to be due to an increase in apoptosis and/or reduced cell activation and proliferation. Although significant increases in apoptosis are only seen at the highest concentration, there is also a small increase following exposure to 10 μM. It is likely that the highest concentrations of cobalt ion exposure induce apoptosis (Huk et al., 2004), thus inhibiting further T-lymphocyte proliferation. Like Cr<sup>6+</sup>, Co<sup>2+</sup> ions have also been shown to cause apoptosis by initiating intrinsic and extrinsic pathways. In the current study, apoptosis following exposure to high concentrations of cobalt ions is likely to be a result of MOMP caused by excessive ROS formation.

The greater decrease in viability of activated lymphocytes (at 10μM Co<sup>2+</sup>) possibly indicates that Co<sup>2+</sup> may be acting through additional mechanisms, which also reduce cell proliferation, rather than simply initiating apoptosis. Co<sup>2+</sup> is a known calcium channel antagonist (Reuter, 1983) and the present author hypothesises that it may compete with calcium for binding sites at both calcium channels and intracellular

calcium-binding proteins. Intracellular  $\text{Ca}^{2+}$  flux is essential in T-lymphocyte activation (Wulfing et al., 1997). For example, elevated  $\text{Ca}^{2+}$  levels result in calcineurin activation which leads to increased dephosphorylation of NFAT (nuclear factor of activation of T-cells) which is a key process in T-lymphocyte activation and proliferation. It may be that  $\text{Co}^{2+}$  exposure can result in decreased T-lymphocyte proliferation similar to other  $\text{Ca}^{2+}$  channel antagonists (Birx et al., 1984, Marx et al., 1990). The author hypothesises that this may explain the reduced viability and proliferation measured without the accompanying significant increase in apoptosis following exposure of activated lymphocytes to  $10 \mu\text{M Co}^{2+}$ . This possibly explains the greater potency of  $\text{Co}^{2+}$  to cause loss of viability in activated T-lymphocytes compared with resting lymphocytes. Although  $\text{Co}^{2+}$  exposure has been reported to cause cell cycle dysregulation (Glahn et al., 2008), using flow cytometric cell cycle analysis of CD3-activated lymphocytes exposed to  $\text{Co}^{2+}$  no evidence of this was observed in the present study. Therefore,  $\text{Co}^{2+}$  concentrations that are not directly cytotoxic to lymphocytes may affect events at a molecular level impeding lymphocyte activation and proliferation.

Interestingly, both metal ions inhibited T-lymphocyte proliferation in both Signal 1- and Signals 1 and 2-stimulated cells to a similar degree, when compared to their respective un-exposed controls. T-Lymphocyte activation initiated via Signal 1 and Signal 2 augments T-lymphocyte proliferation and survival. Co-stimulation leads to enhanced T-lymphocyte generation and survival by a number of mechanisms, including increased IL-2 production. IL-2 has previously been shown to be the primary T-lymphocyte growth factor and its production is key to their survival (Jenkins, 1994, Rüdiger et al., 2006). Reduced IL-2 release and availability can lead T-lymphocytes to become unresponsive and apoptotic (Boise et al., 1995a). Although the data show that metal ion exposure leads to decreased IL-2 release, the reduction in release began at concentrations that have a limited effect on lymphocyte viability and proliferation. As a result, it appears that this is not the mechanism by which these metal ions affect cell proliferation or induce apoptosis in lymphocytes. Interestingly, Wang and colleagues (1996a) previously showed that metal ion exposure of phytohemagglutinin (PHA)-activated lymphocytes led to an IL-2-

dependent decrease in cell proliferation. However, the data from Figures 4.5 and 4.6 here suggest that IL-2 release was not the prime mechanism through which the Cr and Co ions reduced anti-CD3 ( $\pm$  CD28)-induced lymphocyte proliferation since IL-2 production was significantly decreased at ion concentrations which had little effect on lymphocyte proliferation. Further, when the lymphocyte cultures (exposed to metal ions) were supplemented with 50 U recombinant IL-2/ml, no recovery in cell proliferation was observed. As a result, the present author does not believe that inhibition of IL-2 release was directly involved in the mechanism by which these two metal ions affected proliferation or induced apoptosis in lymphocytes.

As well as enhanced IL-2 release, co-stimulation also up-regulates expression of anti-apoptotic molecules and resists pro-apoptotic signalling. Previous research has demonstrated lymphocytes to have enhanced expression of the survival gene BCL-X<sub>L</sub> (long form of B-cell lymphoma X) following co-stimulation (Boise et al., 1995a, Boise et al., 1995b, Noel et al., 1996). This up-regulation correlates with protection from CD95-mediated apoptosis (Lenschow et al., 1996, Kerstan et al., 2006). The results of the current study indicate that the anti-apoptotic benefits of co-stimulation provide little protection against the cytotoxic effects of these metal ions on lymphocytes. However, activation of T-lymphocytes also sensitizes cells to apoptosis by increasing expression of pro-apoptotic molecules (Brenner et al., 2008). For example, Co<sup>2+</sup> exposure *in vitro* can lead to a down-regulation of BCL-X<sub>L</sub> (Pulido and Parrish, 2003). The current author speculates that exposure to these metal ions may affect the equilibrium between anti- and pro-apoptotic protein expression, possibly explaining the lack of apoptotic protection observed following co-stimulation.

IFN $\gamma$  release from activated lymphocytes was also inhibited following the metal ion exposures. However, unlike for IL-2, only exposure to 10 and 100  $\mu$ M of Cr<sup>6+</sup> or Co<sup>2+</sup> led to a reduction in IFN $\gamma$  release. These are the same concentrations that substantially inhibited cell proliferation, reduced cell viability, and led to an increase in apoptosis. Therefore, it is likely that these ion concentrations induce activated

lymphocytes to become apoptotic and non-viable such that the cells are unable to produce this key cytokine.

There was a similar effect on TNF $\alpha$  release from activated lymphocytes. Following metal ion exposure inhibitory effects were only observed at concentrations which had previously been shown to have a cytotoxic effect on activated lymphocytes. Therefore, as with IFN $\gamma$  release, it is likely that metal ion exposed cells which are non-viable are unable to generate this key cytokine. Interestingly, previous authors have shown an increase in TNF $\alpha$  release from macrophages and monocytes following metal ion treatment. This release has been correlated with metal ion induced apoptosis in these cells. In the present study, lymphocytes were exposed rather than macrophages or monocytes, and the opposite effect was observed. This further implies that extrinsic apoptotic pathways, which involve the TNF receptor family as well as caspase activation, have less influence than intrinsic pathways within the current *in vitro* model.

The present study has observed that release of three key cytokines of the immune system; IL-2, IFN $\gamma$  and TNF $\alpha$  are significantly inhibited following activated lymphocyte exposure to metal ions. These observations are in keeping with past research which has also shown cytokine release from mitogen stimulated PBMCs to be inhibited following metal ion exposure. As mentioned previously, this is likely to be an effect of metal ion induced apoptosis rather than a mechanism by which apoptosis is caused (Granchi et al., 1998b, Gavin et al., 2007).

There was also no evidence of a negative regulatory mechanism causing the effects seen following metal ion exposure. Neither PD-1 nor CTLA-4 was upregulated on the surface of activated lymphocytes following metal ion exposure. These two cell surface molecules negatively regulate T-lymphocyte responses following co-stimulation (Smith-Garvin et al., 2009). The presence of these negative co-stimulatory molecules provides a mechanism of control for the immune system. Increased signalling through these two receptors leads to reduced T-lymphocyte activation and expansion as well as attenuated release of IL-2 and IFN- $\gamma$ . Further to



this, signalling through PD-1 can also lead to apoptosis (Fife and Bluestone, 2008). Although exposure of lymphocytes to high concentrations of metal ions leads to reduced activation, proliferation and cytokine release accompanied by increased apoptosis, there is no evidence that this is mediated through regulatory molecules. As mentioned previously, these effects are likely to be due to direct toxicity of the metal ion on lymphocytes.

Although high concentrations of both metal ions are cytotoxic, the data indicate that  $\text{Cr}^{6+}$  is more toxic than  $\text{Co}^{2+}$ .  $\text{Cr}^{6+}$  reduced cell viability and increased apoptosis to a greater degree than  $\text{Co}^{2+}$  when compared to unexposed control. This is likely to be due to the difference in mode of toxicity between the ions. Specifically,  $\text{Cr}^{6+}$  enters cells and yields reactive intermediates as it is reduced to  $\text{Cr}^{3+}$ . These individual intermediates are extremely toxic and, in combination with oxidative stress and damage, lead to a cascade of cellular events that activate the p53 apoptosis regulatory gene, causing the genotoxicity/carcinogenicity associated with  $\text{Cr}^{6+}$  (Sargeant and Goswami, 2007). Although  $\text{Co}^{2+}$  can inhibit DNA repair as well as induce mitochondrial permeability (Pulido and Parrish, 2003), it does not produce reactive intermediates; thus may explain its inferior cytotoxicity potency.

Even though *in vitro* exposure of  $\text{Cr}^{6+}$  or  $\text{Co}^{2+}$  is cytotoxic to lymphocytes, the present data demonstrates that there is little synergistic toxic effect on lymphocyte viability when these ions are combined. This was the case for both resting and anti-CD3 activated lymphocytes. As mentioned in chapter 3, it is possible that these two ions can have synergistic effects, however, due to the extreme cytotoxic nature of these ions, especially  $\text{Cr}^{6+}$ , it may be difficult to identify any synergy at high concentrations. Therefore, it may be informative to expose lymphocyte to combinations of ions at concentrations that are slightly lower than toxic levels when used individually.

The present study has shown that the metal ions,  $\text{Cr}^{6+}$  and  $\text{Co}^{2+}$ , can induce apoptosis and thus inhibit T-lymphocyte expansion following Signal 1 and Signals 1 and 2 types of activation. This inhibition is seen at concentrations that have been

measured in hip aspirate and local lymph nodes in patients with a MOM implant.  $\text{Co}^{2+}$  is less potent than  $\text{Cr}^{6+}$  and at lower levels does not induce apoptosis, but may still inhibit lymphocyte function. Whilst the precise mechanism of chromium or cobalt toxicity to lymphocytes was not elucidated, it is clear that it is likely to be multifactorial and that a singular intervention (i.e. caspase inhibition) may not be sufficient to reverse the toxic effects of these metal ions.

Also, the current findings show IL-2 release to be inhibited following exposure to these metal ions, even at the lowest concentrations. Although this does not appear to have an effect on T-lymphocyte proliferation *in vitro*, it still could result in disturbed immune regulation. It may be at these lower, less toxic concentrations that more chronic adverse reactions occur *in vivo*. Although T-lymphocytes undergo apoptosis following metal ion exposure, this may occur *in vivo* as a protective effect. Following activation, T-lymphocytes are ultimately destined to undergo apoptosis in order to end the immune response and maintain homeostasis of the immune system. Metal ion induced apoptosis following ion exposure may occur in order to avoid adverse effects and maintain a control of the adaptive immune system. However, chronic exposure to these lower concentrations may not result in cell death but in a modulated response. This may contribute to the adverse effects, such as inflammatory masses, presented following MoM arthroplasty. A number of further experiments must be conducted in order to fully explain the mechanism of chronic metal ion toxicity

In conclusion, it has been shown that *in vitro* exposure of lymphocytes to the metal ions  $\text{Cr}^{6+}$  or  $\text{Co}^{2+}$ , at concentrations that have previously been measured in patients with a MoM hip implant, have a significant negative effect on the adaptive immune system.

# Chapter 5

## **5. *In Vivo* responses to CoCr implant wear debris in mice**

### **5.1 Introduction**

#### **5.1.1 Wear debris**

Metal-on-Metal (MoM) hip resurfacing is reported to account for 6-8% of all hip arthroplasties. Unfortunately hip resurfacing also has one of the highest rates of revisions of all primary hip replacement procedures, in particular certain MoM hip resurfacings prostheses show extremely high revision levels (>10%) 5 years post surgery (7<sup>th</sup> Annual Report, National Joint Registry for England and Wales, 2010). One of the major reasons for this failure is thought to be a peri-prosthetic soft-tissue reaction to wear debris released from the implant, termed adverse reactions to metal debris (ARMD) (Macpherson and Breusch, 2010). ARMD is an umbrella term that manifests in a range of clinical and histological effects. These include a rash, pain in the hip region and/or the presence of a soft tissue mass (pseudotumour) surrounded by extensive necrosis and granuloma formation (Counsell et al., 2008). It is postulated that ARMD is an inflammatory process in response to excessive particulate metal wear debris and ions (Willert et al., 2005, Counsell et al., 2008, Hallab et al., 2008).

It is accepted that most biomaterials induce an acute inflammatory response following implantation. However, it is clearly important to understand the longer-term host-material interactions that occur in response to implant debris in order to understand the etiology of inflammation and tissue destruction around the prostheses.

#### **5.1.2 Rodent air-pouch**

Clearly an *in vivo* model would make a considerable contribution to fully understanding the processes that initiate and drive the inflammatory response to MoM wear debris. The limitations of *in vitro* models and the limited access to

human joint tissue add further weight to the requirement for an accurate *in vivo* animal model. There have been a number of animal prosthetic implant models reported, however, many of these are extremely complex, time-consuming and expensive. A number of researchers have previously employed the rodent air-pouch model to investigate the inflammatory response to biomaterials including orthopaedic materials (Wooley et al., 2002, Barbosa et al., 2004). This model described by (Sedgwick et al., 1983) was developed as a facsimile synovium for the study of inflammatory processes. It allows the quantification and analysis of cellular infiltration and mediators within the pouch cavity and surrounding tissue. This model involves creating a cavity by repeated subcutaneous injections of sterile air. This cavity can be injected with a biomaterial and then lavaged at a later stage to assess the cellular infiltrate. This tissue can also be excised and allow for the examination of cytokines and chemokine expression that may drive biomaterial induce inflammation. Therefore, we have employed this simple *in vivo* model to assess the inflammatory processes induced by metal wear debris.

## **5.2 Aims**

The aim of this section was to develop a simple *in vivo* model where the inflammatory response to MoM implant wear debris can be assessed. Once developed, the acute and chronic immunological effects of implanting MoM wear debris were examined, as well as the distribution of metal ions within peripheral blood and organs.

## **5.3 Methods**

### **5.3.1 Characterisation of wear debris**

CoCr wear debris was kindly donated by DePuy International (Leeds, UK). Images were produced and the elemental composition of the CoCr wear debris analysed as described in section 2.2.3.

### **5.3.2 Assessment of sterility of wear debris**

Following heat treatment of CoCr debris (section 2.2.1) the presence of microbial contamination was assessed by exposing DCs to the debris for 24 hours. This was followed by surface staining of activation markers and analysis by flow cytometry (section 2.2.2).

### **5.3.3 Development of model**

It was decided that air pouches would be raised in 8-10 week old male BALB/c mice. The basic rodent air-pouch model involves repeated subcutaneous injections of sterile air over a period of 6 days to establish the cavity. To comply with the current Home Office project license, only two injections of sterile air were administered to each animal. Therefore, the model needed to be adapted to successfully create and analyse the responses within the air-pouch. The volume of air injected in creating the air pouch had to be optimised to create a cavity which could be lavaged easily. Also, a method to successfully lavage the air-pouch following cellular infiltration and to determine a relevant level of metal debris to be introduced into the air-pouch was required.

#### **5.3.3.1 Volume of air-pouch**

Air-pouches were raised on the lower dorsal region of isoflurane anaesthetised male BALB/c mice aged 8-10 weeks. Large and small volume pouches were created to optimise this model. All injections were carried out on isoflurane anaesthetised mice

with a 25 gauge needle. Small discrete pouches were created by injecting 1ml of sterile air subcutaneously followed up by a second injection of 0.5 ml sterile air into the cavity 3 days later. Larger pouches were created with an initial injection of 2.5 ml sterile air, followed by a second injection of 2 ml sterile air into the cavity three days later. Three days after the second injection, 1 $\mu$ g of LPS dissolved in 500  $\mu$ l sterile PBS was injected into each of the cavities to induce inflammation. Four hours following the LPS injection, attempts were made to lavage the air-pouch with 500  $\mu$ l of PBS using a 25 gauge needle. It was observed that only 100  $\mu$ l of fluid was recovered from the larger pouch, whereas 300  $\mu$ l was recovered from the smaller pouch. It was decided that the smaller pouches would be more simple to create and easier to recover any inflammatory exudate from.

### **5.3.3.2 Needles used to lavage air-pouch**

Following the observation that just over 50% of the fluid injected into the cavity was recovered when attempting to lavage the pouch, it was clear that a more successful technique was required to recover the majority of the cellular infiltrate. It was decided to use a larger needle diameter to lavage the pouch in order to increase the recovery. It was found that using a 21 gauge needle to lavage a small discrete air-pouch 4 hours following LPS administration, increased recovery of the fluid to 100%, consistently.

### **5.3.3.3 Mass of debris used**

Due to the nature of the CoCr debris produced it was not possible to quantify the number of particles. Therefore, it was decided to administer the dose in terms of dry weight. Either 2.5 mg or 5 mg (suspended in 500  $\mu$ l sterile PBS) of the CoCr wear debris were injected into a small discrete air-pouch. 24 hours later, each pouch was lavaged with 500  $\mu$ l of sterile PBS using a 21 gauge needle. The cells within the fluid were counted using a haemocytometer. It was observed that 2.5 mg treatment lead to higher levels of cellular infiltrate within the air-pouch than did exposure to 5

mg (Table 5.1). Therefore, it was decided for future experiments to expose mice to the lower level of CoCr wear debris.

<b>Dose (mg)</b>	2.5	5
<b>Cell Count (x10<sup>6</sup>)</b>	0.35	0.04

**Table 5.1 Number of cells within inflammatory exudate following 24hr treatment of air-pouches with different doses of CoCr wear debris.**

### **5.3.4 Exposure of mice to wear debris**

Small discrete air-pouches were raised in the lower dorsal region of isoflurane anaesthetised 8-10 week old male BALB/c mice. Subsequently, the air-pouches were injected with either 500µl sterile PBS, 2.5mg of sterile wear debris or 1µg LPS (both in 500µl sterile PBS). This is described in detail in section 2.2.4. Mice were exposed for 4, 24, 48 and 72 hours and 7, 28 and 56 days, with 3 mice at each timepoint for each exposure condition.

### **5.3.5 Assessment of the effects on CoCr implantation on mice**

In order to assess the effects of CoCr debris exposure the following parameters were analysed at each end-point;

- **Metal ion concentrations in peripheral blood and organs** were measured via ICPMS (sections 2.2.5 and 2.2.6).
- **Local inflammatory responses** were determined by analysing the inflammatory exudate using flow cytometry (section 2.2.7), assessing the histological changes in the pouch tissue following H&E staining (2.2.8) and inflammatory gene activation in the pouch tissue via RT-PCR (2.2.9).
- **Systemic changes in the draining lymph nodes** were determined by flow cytometry. Lymphocyte numbers, viability and apoptosis levels were assessed before and after lymphocyte activation (section 2.2.10)



## 5.4 Results

### 5.4.1 Characterisation of CoCr wear debris

Wear debris produced on a hip simulator from an ASR resurfacing implant are shown in Figure 5.1. The images, taken on a SEM, indicate a wide variety of irregular shaped particles. The debris varies in size, from micrometer to nanometre. The larger irregular particles appear to be agglomerates of smaller particles.

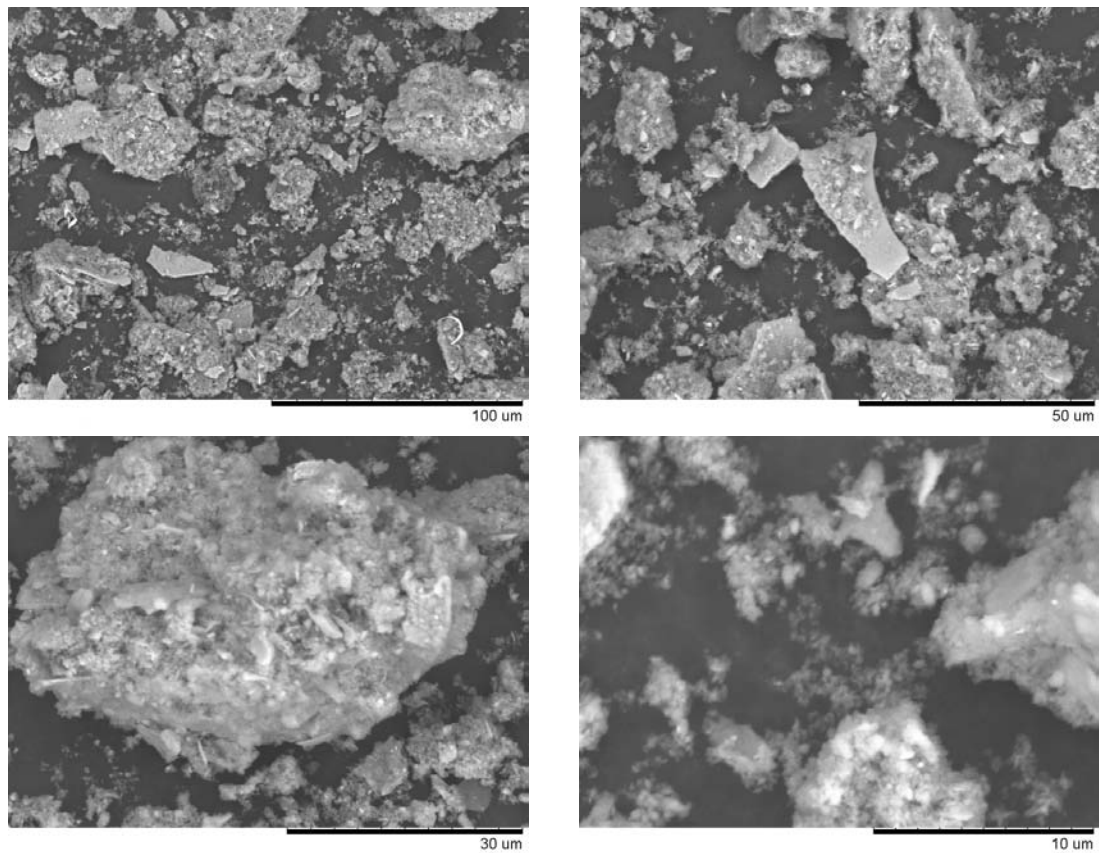


**Figure 5.1 Scanning Electron Microscopy images of wear debris from an ASR hip implant.** Image taken at 800-7000x.

Energy Dispersive X-ray Spectroscopy (EDS) indicated that ASR wear debris is primarily composed of cobalt (Figures 5.2 and 5.3). Analysis of 25 different

particles indicated a mean composition of 54.48% cobalt and 38.43% chromium, with a small percentage of molybdenum present.

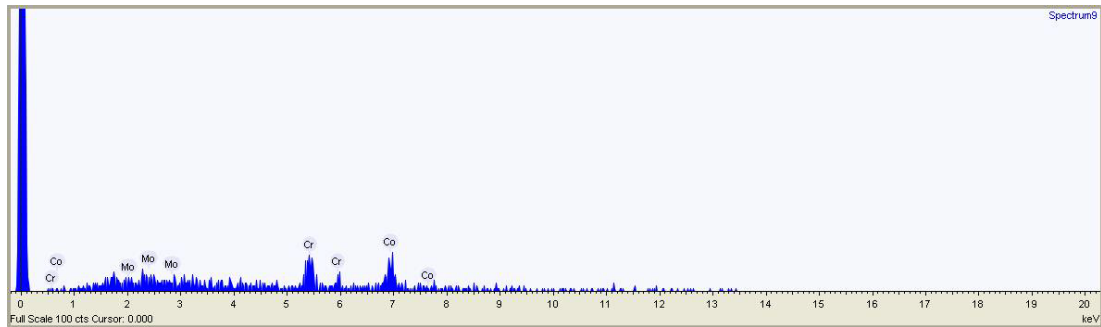


**Figure 5.2 Energy Dispersive X-ray Spectroscopy of wear debris from an ASR hip implant.**

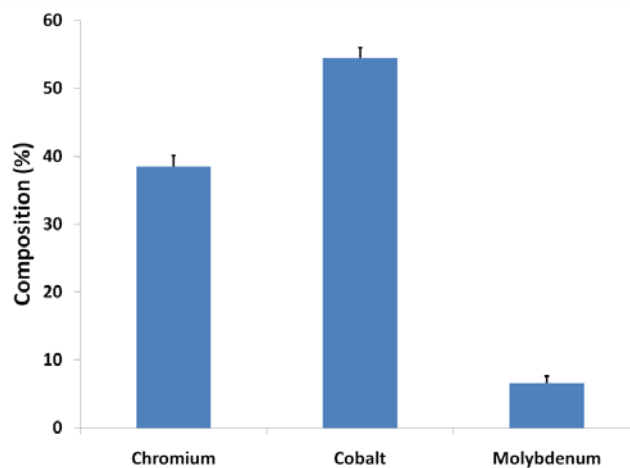


**Figure 5.3 Composition of CoCr wear debris from ASR implant, analysed by EDS. Results are means  $\pm$  SEM, n=25.**

#### **5.4.2 Sterility of CoCr debris**

The results shown in Figure 5.4 indicate that the wear debris did not activate DCs. DCs exposed to heat treated CoCr wear debris *in vitro* did not show an increase in surface expression of stimulatory proteins compared to negative (RPMI) and vehicle (PBS) controls (Figure 5.4). Interestingly, the results show that CoCr wear debris significantly reduced the expression of these surface proteins.

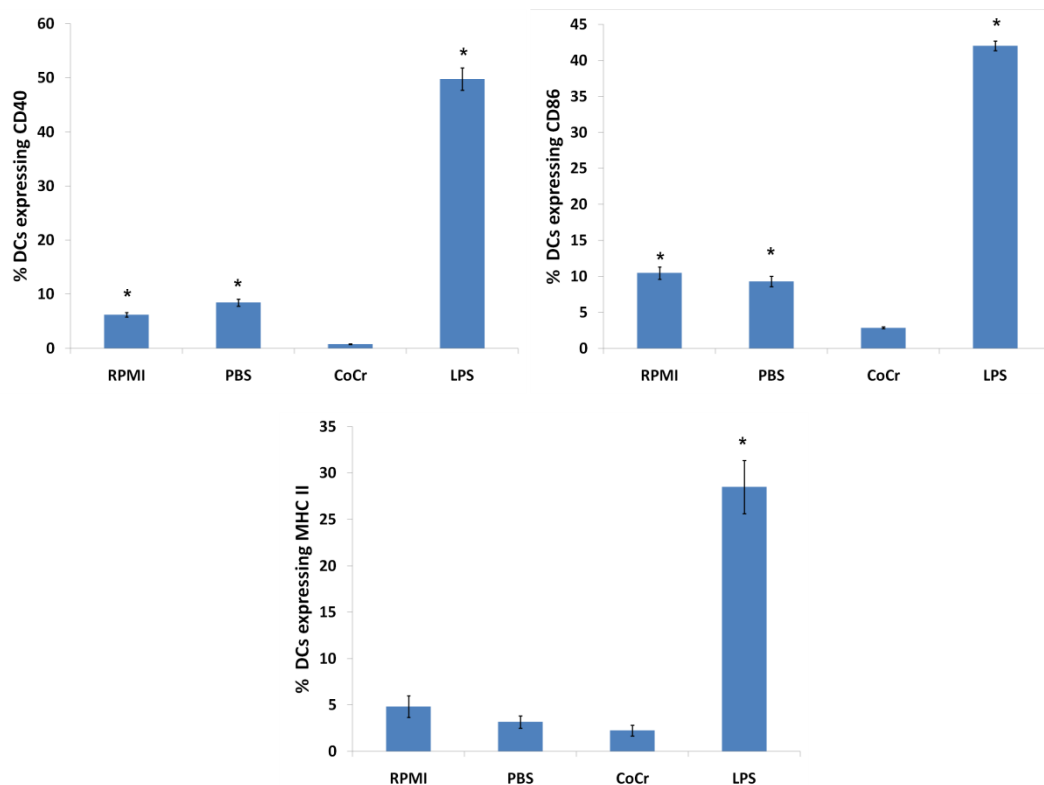


**Figure 5.4 Activation of CD11c<sup>+</sup> dendritic cells (DCs).** Results are mean percentage of DCs expressing stimulatory surface proteins ( $\pm$  SEM, n=3) following 24 hour culture in complete RPMI-1640 alone or supplemented with sterile PBS, 1  $\mu$ g LPS or 2.5 mg CoCr wear debris. \*Significantly different from CoCr values (at  $p < 0.05$ ) by one-way ANOVA followed by Dunnett's multiple comparison test.

### 5.4.3 Ion Distribution

It can be seen from Table 5.2 that metal debris exposure leads to significant increases in blood metal ion levels compared with unexposed controls. It was found that chromium, cobalt and molybdenum levels were significantly higher in mice exposed to wear debris compared with those that received only a saline injection. This difference was observed up to 72 hours post injection for chromium and molybdenum levels, whereas cobalt levels were still significantly elevated 7 days post injection. The elevated metal levels in the peripheral blood peaked at 48 hours for all three elements. Cobalt showed the greatest level of difference between the unexposed and exposed mice (Table 5.2 and Figure 5.5).

	Chromium ( $\pm$ SEM)		Cobalt ( $\pm$ SEM)		Molybdenum ( $\pm$ SEM)	
	PBS	CrCo	PBS	CrCo	PBS	CrCo
<b>4h</b>	9.85 $\pm$ 2.36	21.37 $\pm$ 2.96*	3.53 $\pm$ 1.06	29.24 $\pm$ 6.04*	5.33 $\pm$ 1.51	11.43 $\pm$ 0.92*
<b>24h</b>	16.57 $\pm$ 1.55	26.45 $\pm$ 1.64*	3.55 $\pm$ 0.35	38.84 $\pm$ 2.43*	7.72 $\pm$ 0.80	10.85 $\pm$ 0.43*
<b>48h</b>	20.87 $\pm$ 1.97	35.54 $\pm$ 1.55*	3.16 $\pm$ 0.16	77.02 $\pm$ 19.70*	8.28 $\pm$ 0.78	10.75 $\pm$ 0.14*
<b>72h</b>	17.20 $\pm$ 0.57	24.75 $\pm$ 0.86*	3.85 $\pm$ 0.08	33.22 $\pm$ 8.12*	6.74 $\pm$ 0.08	8.70 $\pm$ 0.24*
<b>7d</b>	11.98 $\pm$ 0.75	15.67 $\pm$ 1.95	3.55 $\pm$ 0.25	17.45 $\pm$ 4.97*	8.97 $\pm$ 0.26	8.39 $\pm$ 1.06
<b>28d</b>	1.72 $\pm$ 0.15	1.92 $\pm$ 0.15	9.63 $\pm$ 3.89	4.16 $\pm$ 0.46	9.11 $\pm$ 0.05	11.80 $\pm$ 0.90

**Table 5.2 Blood metal levels ( $\mu\text{g/l}$ ) (mean  $\pm$  S.E.M) in mice (n = 3) at different time points (4 hours, 24 hours, 48 hours, 72 hours, 7 days and 28 days) after injection of CoCr wear particles or sterile PBS. \* Significantly different from PBS values (at  $p < 0.05$ ) by one-way ANOVA.**

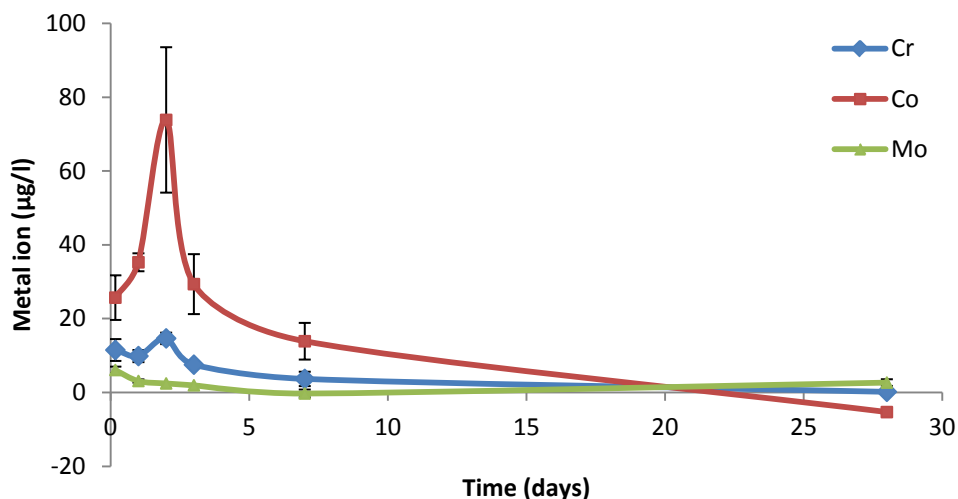
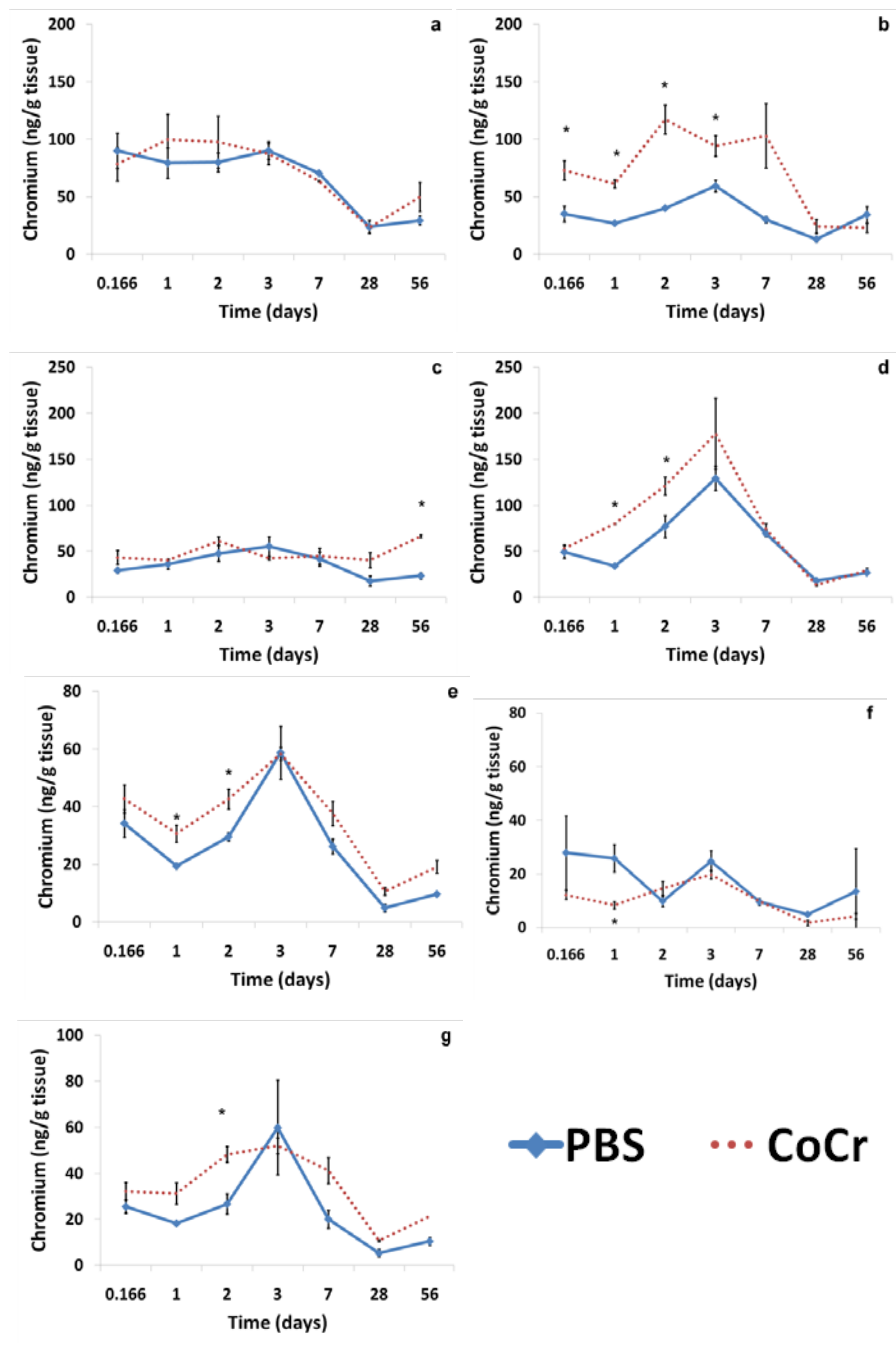


**Figure 5.5 Blood metal (Co, Cr and Mo) levels ( $\mu\text{g/l}$ ) in mice after injection of CoCr or sterile PBS at different time points.** Values shown are mean  $\pm$  S.E.M in mice (n = 3), corrected by deducting metal levels in control (PBS) mice from the levels in metal treated mice at each time point.

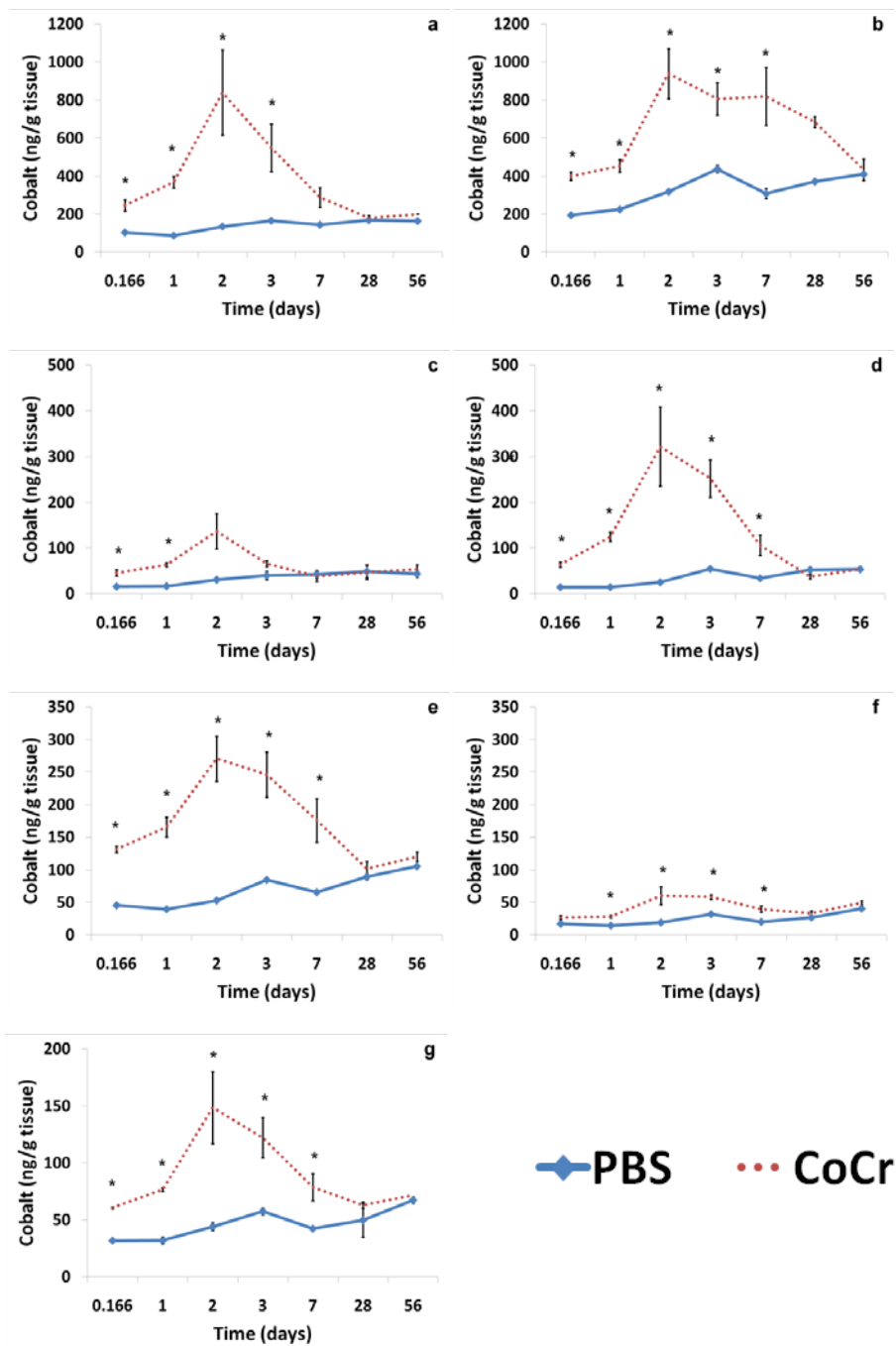
Following implantation of CoCr wear debris into the air-pouch, no significant increase in chromium levels were observed in the liver compared with PBS treated controls (Figure 5.6a). However, chromium levels were significantly elevated in the kidney, lung, heart and testes following implantation of CoCr debris. The levels in these organs returned to control levels 7 days post implantation (Figure 5.6). The spleen is the only organ which shows significantly higher levels of chromium past 7 days, which persist up to 56 days following exposure (Figure 5.6 c). Interestingly, there is a small but significant reduction in chromium levels within the brain 1 day post implantation.

Figure 5.7 indicates that cobalt levels are significantly increased in all excised organs following CoCr debris implantation. In all organs this increase peaks following two days exposure. The liver and the kidney showed the highest levels of cobalt;  $838.94 \pm 223.66$  ng/g and  $938.79 \pm 131.61$  ng/g respectively. The cobalt level in all organs returned to control levels by 28 days post implantation.

The levels of molybdenum following implantation of CoCr debris are shown Figure 5.8. Significant increases in molybdenum levels are observed in the kidney at days 1, 3, 7 and 28 (Figure 5.8b). The liver, lungs and brain all show a significant increase 1 day after implantation. There was also a significant increase in molybdenum levels in the spleen following 56 days of exposure (Figure 5.6c).



**Figure 5.6 Chromium levels (ng/g tissue) in the organs of mice following injection of PBS or CoCr debris into the air-pouch.** (a.) liver, (b.) kidney, (c.) spleen, (d.) lung, (e.) heart, (f.) brain, and (g.) testes of mice after injection of CoCr debris or sterile PBS at different time points. Values shown are mean  $\pm$  S.E.M in mice ((n = 3), except at 56 days where n=2). \* indicates significant difference by 2 sample t-test ( $p \leq 0.05$ ) with respect to PBS



**Figure 5.7 Cobalt levels (ng/g tissue) in the organs of mice following injection of PBS or CoCr debris into the air-pouch.** (a.) liver, (b.) kidney, (c.) spleen, (d.) lung, (e.) heart, (f.) brain, and (g.) testes of mice after injection of metal particles (metal treated) or sterile PBS (control) at different time points. Values shown are mean  $\pm$  S.E.M in mice ((n = 3), except at 56 days where n=2). \* indicates significant difference by 2 sample t-test ( $p \leq 0.05$ ) with respect to PBS.

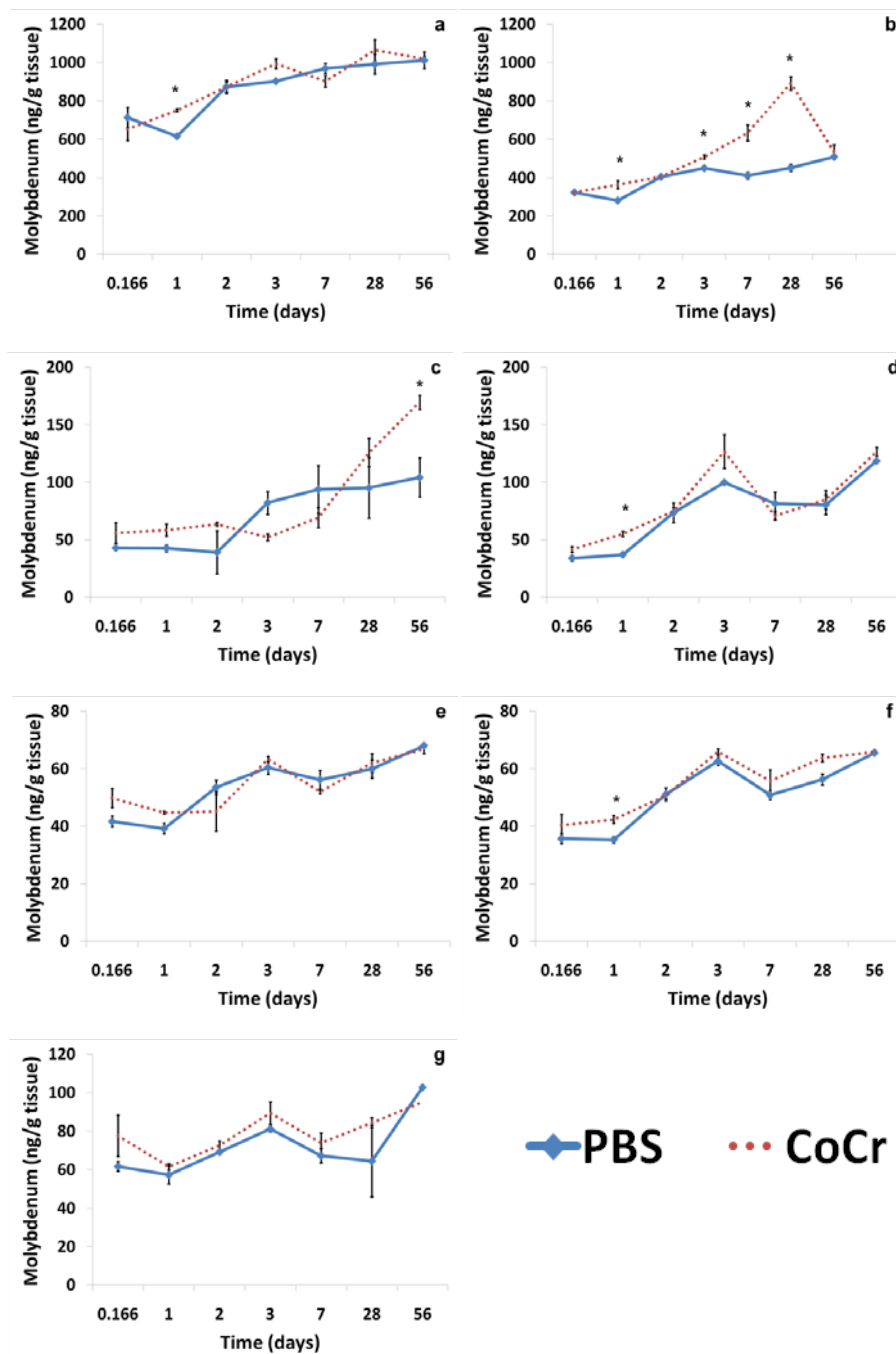


**Figure 5.8 Molybdenum levels (ng/g tissue) in the organs of mice following injection of PBS or CoCr debris into the air-pouch.** (a.) liver, (b.) kidney, (c.) spleen, (d.) lung, (e.) heart, (f.) brain, and (g.) testes of mice after injection of CoCr debris or sterile PBS at different time points. Values shown are mean  $\pm$  S.E.M in mice ((n = 3), except at 56 days where n=2). \* indicates significant difference by 2 sample t-test ( $p \leq 0.05$ ) with respect to PBS.



## **5.4.4 Local inflammatory response**

### **5.4.4.1 Inflammatory exudate**

The cellular kinetics of the acute inflammatory response to CoCr wear debris within the air-pouches are shown in Figures 5.9, 5.10 and 5.11. The air-pouches were injected with either sterile PBS, CoCr debris or, LPS. The data in Figure 5.9 show that there was only a low level of cellular infiltrate in air-pouches injected with PBS. Both CoCr debris and LPS caused a significant increase in the number of cells recovered from the inflammatory cavity at all time points.

Cells within the inflammatory exudate were identified by flow cytometry using antibodies recognising lineage specific markers (Figures 5.10). The data indicate that LPS caused a significant increase in neutrophil infiltration at 4 and 24 hours compared with PBS control values (Figure 5.11A). Although there were higher levels of neutrophils within the inflammatory exudate of CoCr compared with PBS, this increase was not significant ( $p>0.05$ ). Both CoCr and LPS induced a significant increase in monocyte/macrophage infiltration into the pouch cavity 4 and 24 hours post injection (Figure 5.11B). There was also a higher level of these cells present in the inflammatory exudate recovered from LPS treated mice at 72 hours.

In contrast to neutrophils and monocytes/macrophages, both T and B-lymphocytes were present in low numbers. An elevation in T-lymphocytes was only observed 48 hours after CoCr implantation as displayed in Figure 5.11C. Both LPS and CoCr induced a small but significant increase in the number of B-lymphocytes present in the inflammatory exudate at 72 hours, compared with PBS treatment (Figure 5.11D).

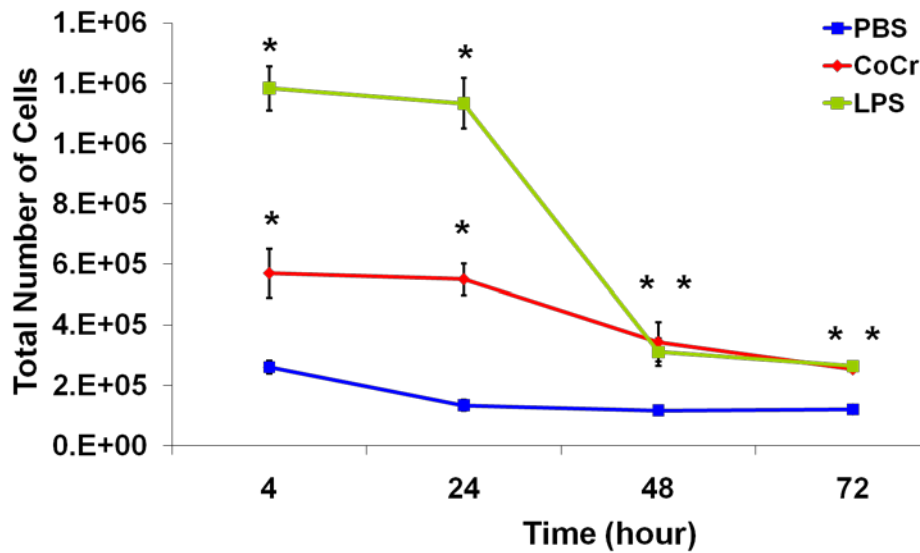


**Figure 5.9** Total number of cells present in the inflammatory exudates at different time points. Cells were collected from the air-pouches following the injection of PBS, CoCr debris or LPS. Results are means  $\pm$  SEM (n = 3). \*Significantly different from PBS (negative control) values (at  $p < 0.05$ ) by one-way ANOVA followed by Dunnett's multiple comparison test.

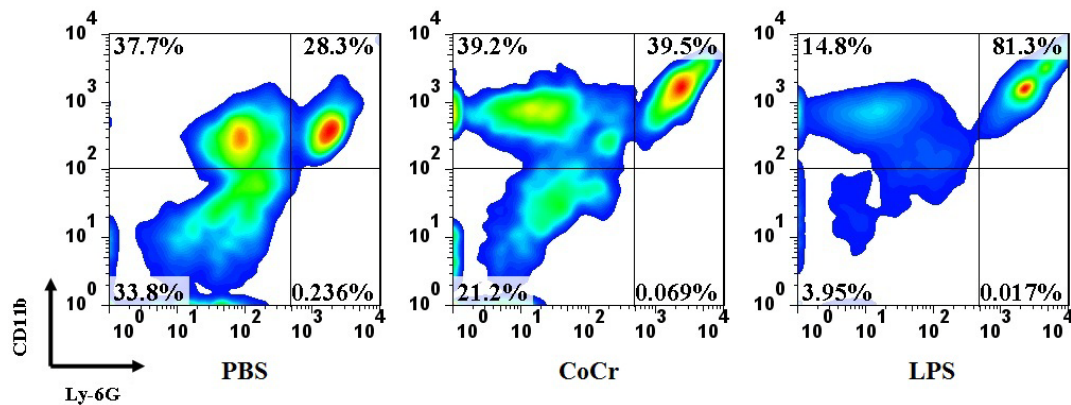


**Figure 5.10\*** Flow cytometric analysis of the inflammatory cells recovered 4 hours post implantation. Cells which were Ly-6G<sup>+</sup> and CD11b<sup>+</sup> were determined to be neutrophils, Ly-6G<sup>-</sup> and CD11b<sup>+</sup> cells were identified as monocytes/macrophages.

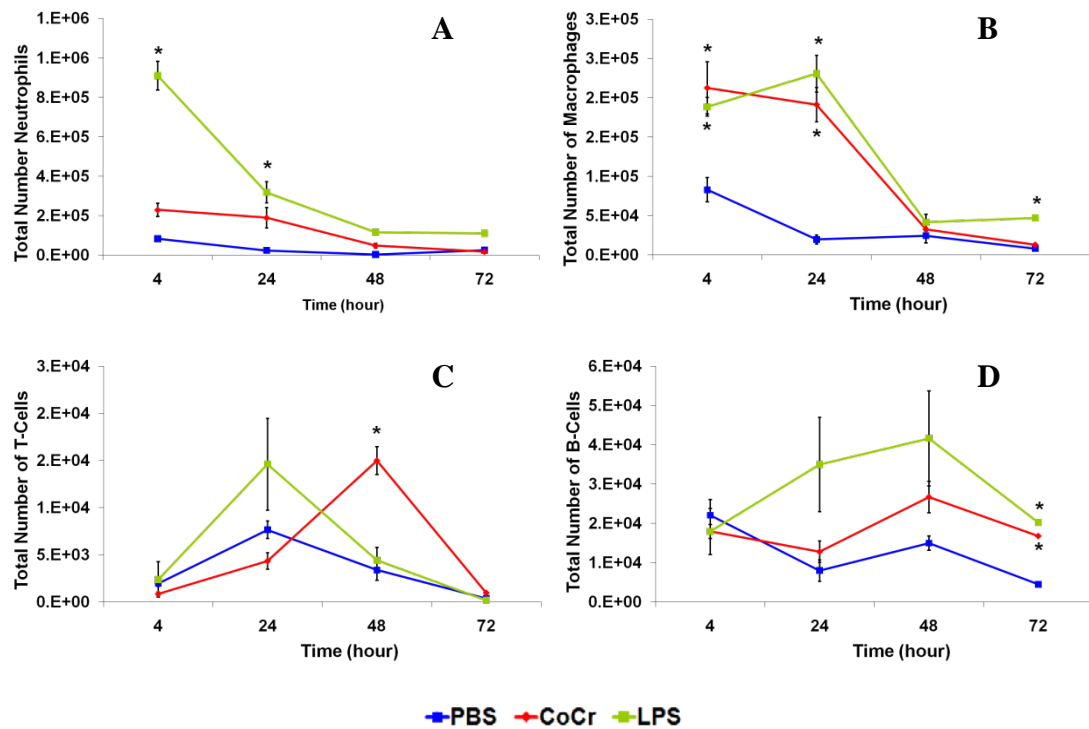


**Figure 5.11** Number of (A) neutrophils, (B) monocytes/macrophages , (C) T-lymphocytes and, (D) B-lymphocytes present in the inflammatory exudates at different time points. Cells were collected from the air pouches after the injection of PBS, CoCr debris or LPS. Results are means  $\pm$  SEM (n = 3). \*Significantly different from PBS (negative control) values (at p < 0.05) by one-way ANOVA followed by Dunnett's multiple comparison test.

#### 5.4.4.2 Tissue response

The histological appearance of the treated air pouches 24 hours after instillation of PBS, LPS or CoCr is displayed in Figure 5.12 and 5.13. All the pouches are typically characterised by an outer fibrous layer and an inner layer mainly consisting of inflammatory cells. At 24 hours, the LPS treated pouches appear more inflamed and with increased cellularity compared with PBS treated pouches. Interestingly, at 24 hour CoCr debris appears to have migrated into the pouch tissue. The CoCr debris appears to be surrounded by inflammatory cells (Figure 5.13).

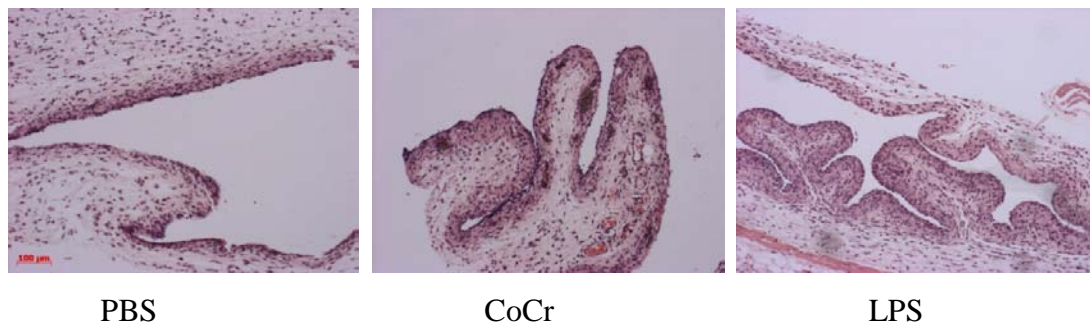


**Figure 5.12** The histological appearance of negative (PBS) and positive (LPS) control and CoCr treated air-pouch membranes, 24 hours post injection. Images taken at 10x magnification following H & E staining.

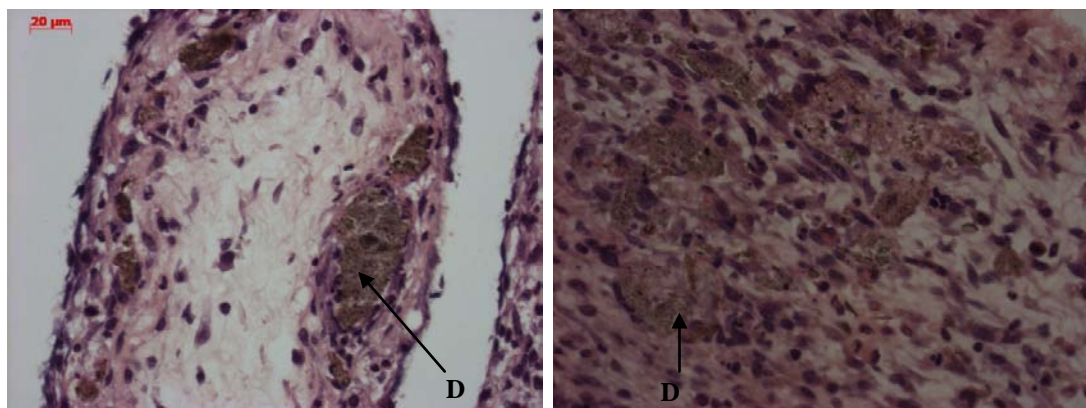


**Figure 5.13** The histological appearance of CoCr treated air- pouch membranes, 24 hours post injection. Images taken at 40x magnification following H & E staining. ‘D’ indicates CoCr debris within the tissue.

At 72 hours the cellularity of the PBS pouches appears to have decreased compared with that at 24 hours (Figures 5.14 and 5.15). The CoCr treated pouches show that the debris is embedded in the inner layer of the pouch. Further examination shows some cell death around the area where the CoCr debris is embedded. There also appears to be areas of cell death around the CoCr debris, area marked ‘A’ in Figure 5.15. This may be indicative of cellular apoptosis as the bodies present are smaller than complete cells and may be apoptotic fragments. In addition, the area marked ‘F’ in Figure 5.15 indicates the formation of fibrous tissue around the debris.

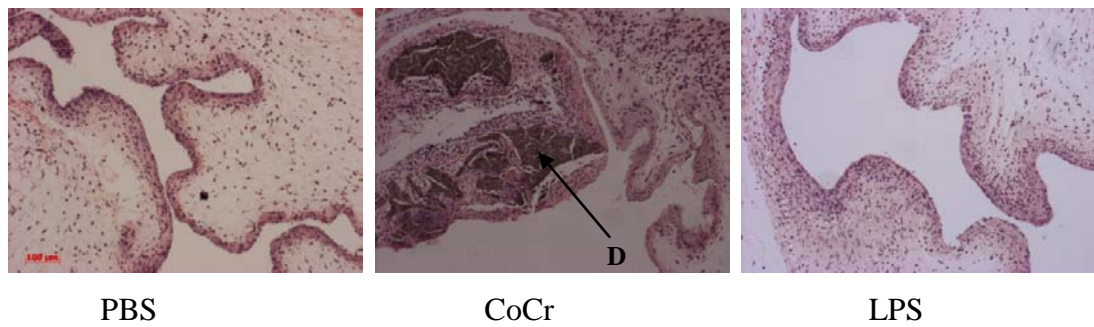


**Figure 5.14** The histological appearance of negative (PBS) and positive (LPS) control and CoCr treated air-pouch membranes, 72 hours post injection. Images taken at 10x magnification following H & E staining. “D” indicates CoCr debris within the tissue.

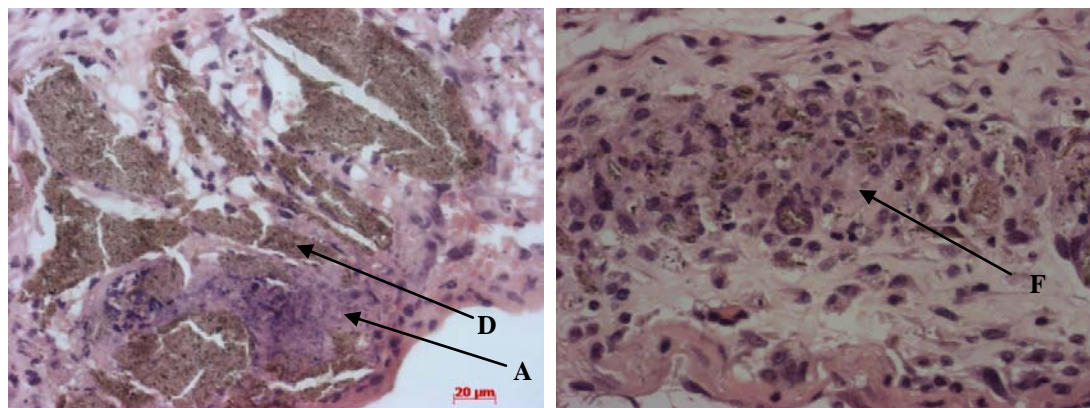


**Figure 5.15** The histological appearance of CoCr treated air-pouch membranes, 72 hours post injection. Images taken at 40x magnification following H & E staining. “D” indicates CoCr debris within the tissue. ‘A’ indicates areas of cell death, ‘F’ indicates fibrotic tissue.

At 7 days post injection, PBS and LPS treated pouches appear to have collapsed (Figure 5.16). The inflammatory layer can be identified but it does not appear as pronounced as at the earlier time points. However, there still appears to be a large cellular infiltrate within the CoCr treated air-pouches. Figure 5.17 indicates that these cellular infiltrates are concentrated in areas where CoCr debris is present. It shows that mononuclear cells encircle the CoCr debris, indicative of granuloma

formation. In addition there are areas of fibrous tissue (marked “F”) and cell death (marked “A”) around the CoCr debris (Figure 5.17)

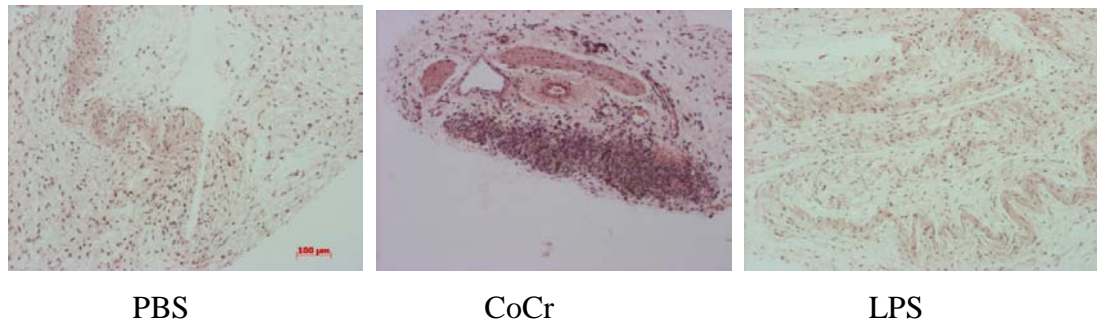


**Figure 5.16 The histological appearance of negative (PBS) and positive (LPS) control and CoCr treated air-pouch membranes, 7 days post injection. Images taken at 10x magnification following H & E staining.**

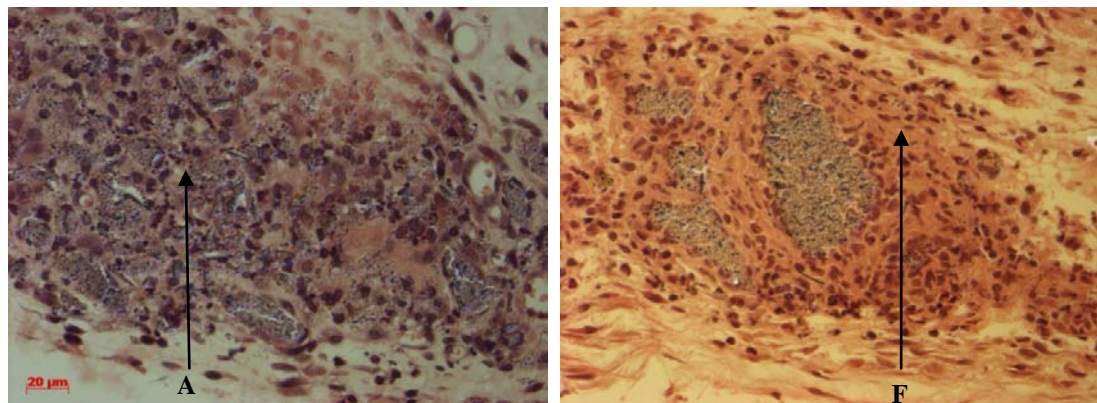


**Figure 5.17 The histological appearance of CoCr treated air-pouch membranes, 7 days post injection. Images taken at 40x magnification following H & E staining. ‘A’ indicates areas of cell death, ‘F’ indicates fibrotic tissue.**

The PBS and LPS treated pouches appear as layers of fibrous tissue 28 days after injection (Figure 5.18). There are still a relatively small number of cells present within the tissue at this time point. Air-pouches treated with CoCr also appear as layers of fibrous tissue. However, as at 7 days there are still areas where a number of mononuclear cells are present. These cells are primarily located in areas where CoCr

debris is present. There also appears to be a number of dead cells as well as large areas of fibrous tissue around the debris (Figure 5.19).

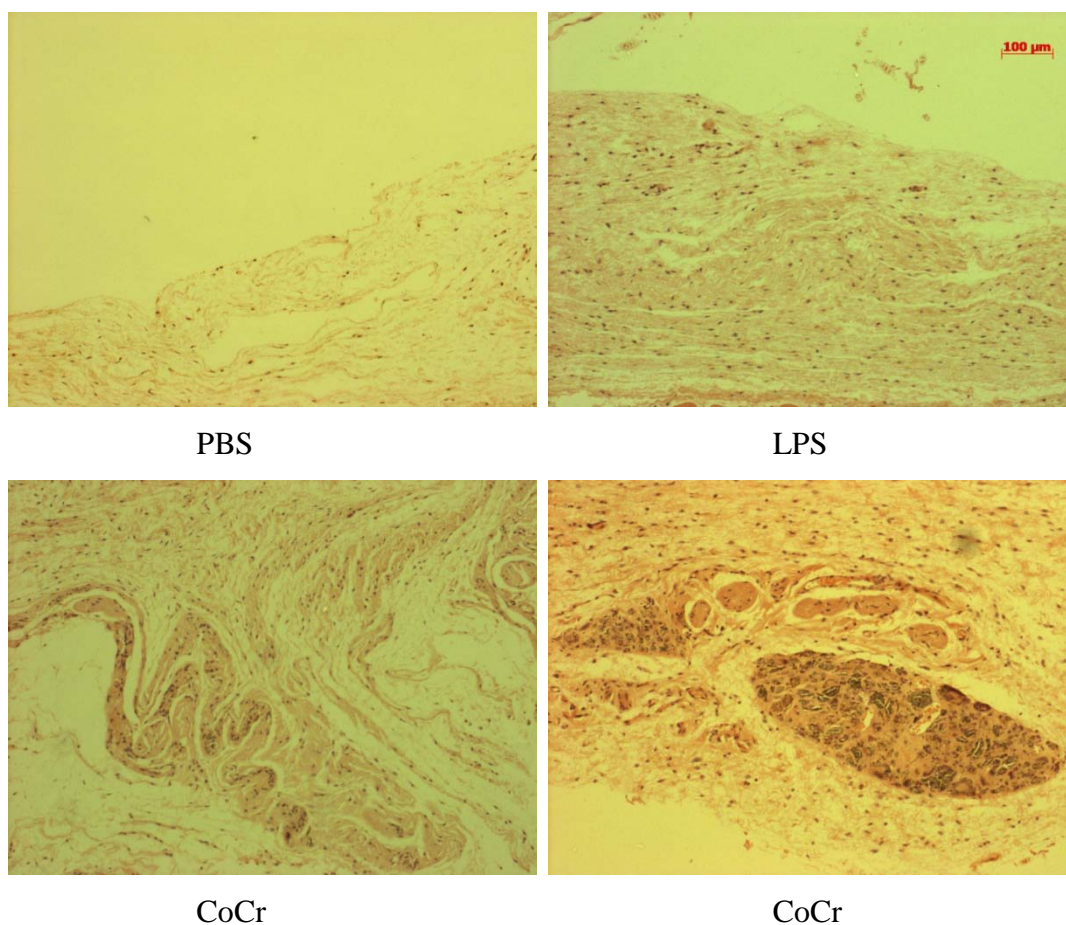


**Figure 5.18** The histological appearance of negative (PBS) and positive (LPS) control and CoCr treated air-pouch membranes, 28 days post injection. Images taken at 10x magnification following H & E staining.

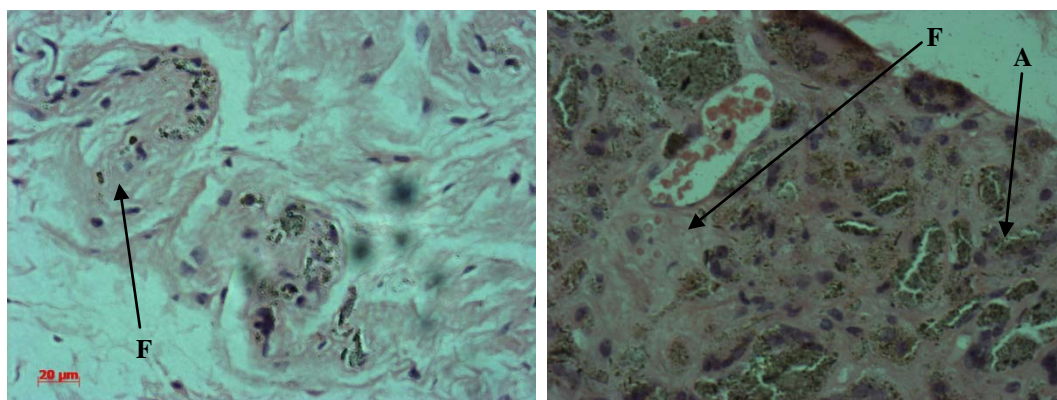


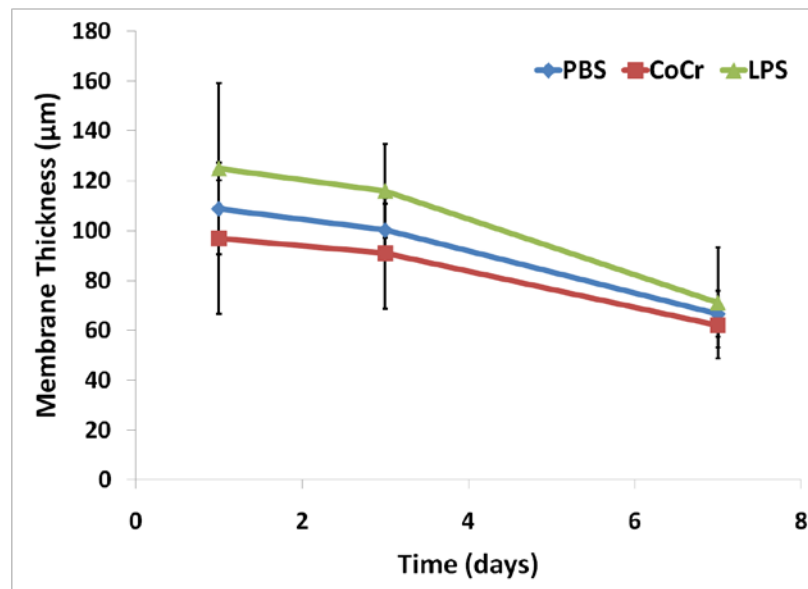
**Figure 5.19** The histological appearance of CoCr treated air-pouch membranes, 28 days post injection. Images taken at 40x magnification following H & E staining. ‘A’ indicates areas of cell death, ‘F’ indicates fibrotic tissue.

The histological parameters, membrane thickness and cellularity, were measured from images taken from all samples (Figure 6.20 and 6.21). Only images up to 7 days were analysed as at 28 days not all the pouches were sectioned successfully, and those that were only had a limited examinable area. No pouches were successfully sectioned at 56 days. This may have been due to the migration of inflammatory cells from the pouch lumen into the tissue and resulted in the collapsed pouch observed above.

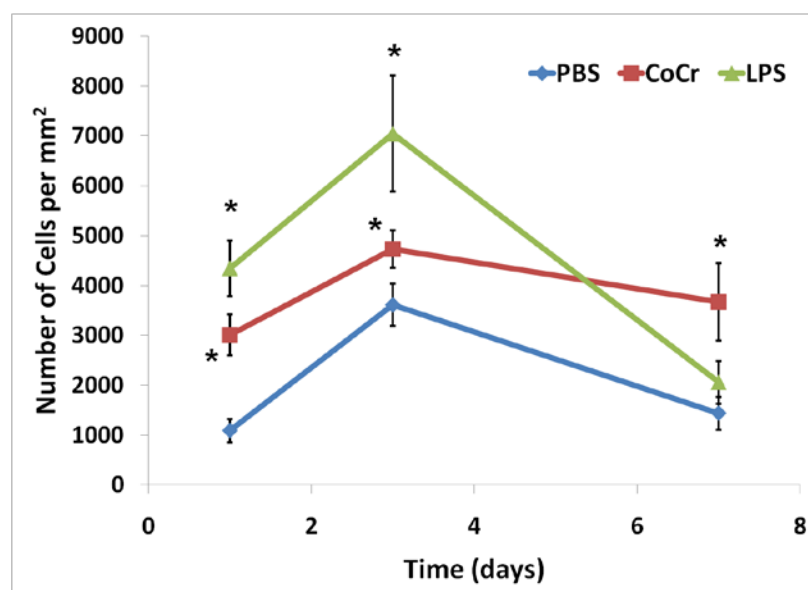
Measurements of pouch membrane thickness as determined from six points on each section showed that LPS and CoCr treated pouches had thicker membranes than PBS treated pouches, however, this difference was not found to be significant (Figure 5.20).

Figure 5.21 indicates that both CoCr and LPS treatment significantly increased the cellularity of the air-pouch at 24 and 72 hours post injection, compared with PBS values. The highest density of cells infiltrating the pouch membrane was observed at 72 hours for all the air pouches. The cellularity at this time point was  $3613 \pm 418$ ,  $4730 \pm 372$  and,  $7048 \pm 1161$  cells/mm<sup>2</sup> in PBS, CoCr and LPS treated pouches, respectively. These data also indicate that CoCr pouches have a significantly higher cellularity than PBS treated pouches 7 days post implantation.





**Figure 5.20 Membrane thickness of air-pouch tissue following treatment with PBS, CoCr debris and, LPS.** Results are means  $\pm$  SEM (n = 3). No significant differences of treated air-pouches from PBS (negative control) values were found ( $p < 0.05$ ) by one-way ANOVA followed by Dunnett's multiple comparison test.



**Figure 5.21 Number of cells in air-pouch tissue following treatment with PBS, CoCr debris and, LPS.** Results are means  $\pm$  SEM (n = 3). \*Significantly different from PBS (negative control) values (at  $p < 0.05$ ) by one-way ANOVA followed by Dunnett's multiple comparison test.

#### 5.4.4.3 Inflammatory gene expression

Sections 5.4.4.1 and 5.4.4.2 have demonstrated that CoCr implantation into the air-pouch results in an inflammatory process which is dominated by the recruitment and migration of mononuclear immune cells, mainly macrophages. In order to give greater insight into the mechanism driving the inflammatory response to CoCr wear debris, mRNA was isolated from control and treated air pouches and the expression of 32 inflammatory gene targets was analysed.

The quality of an mRNA preparation from 24 hour pouch tissue was assessed by agarose gel electrophoresis (Figure 5.22). Although mRNA was detected in all samples, its quality appeared poor by the high level of smearing. The results of a typical RT-PCR using a primer specific for  $\beta_2$  microglobulin are shown in Figure 5.23. This indicates that transcripts were detectable.

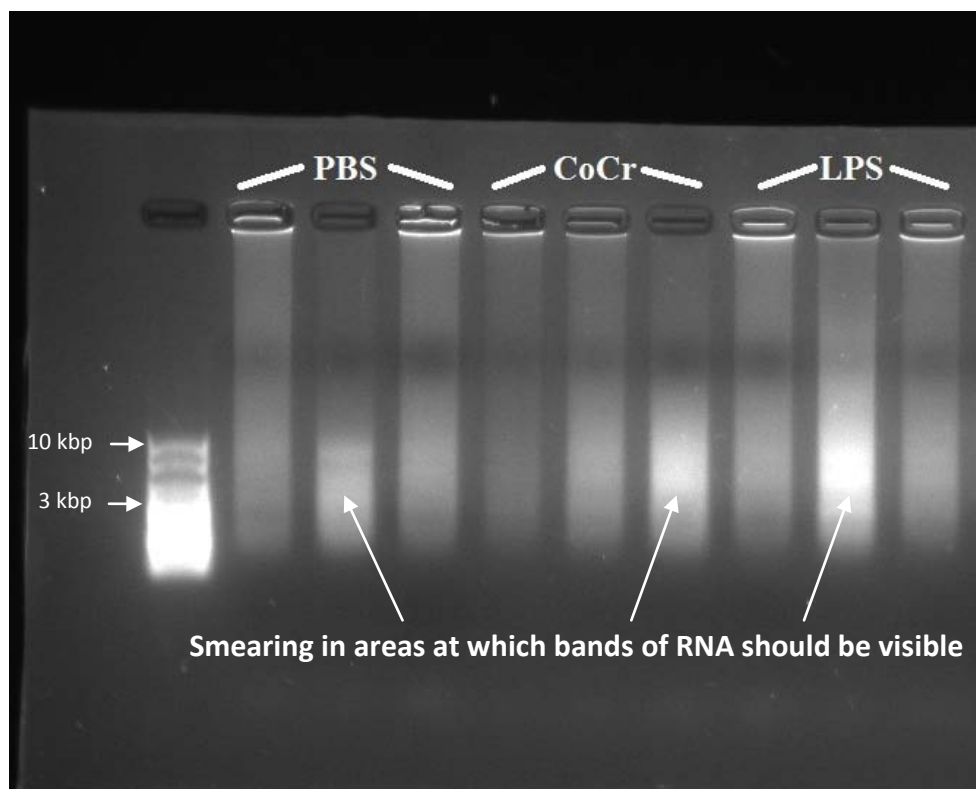


**Figure 5.22 Detection of mRNA isolated from 24 hour air-pouch tissue on agarose gel.** The gel has a size marker in first lane, followed by samples which show degraded “smear” RNA.

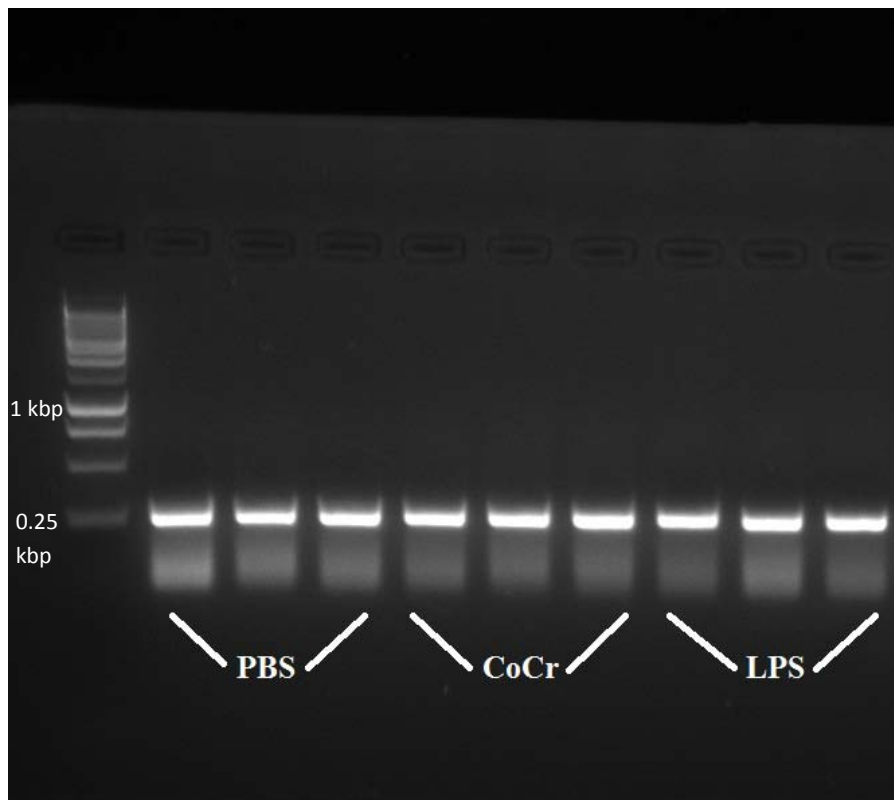


**Figure 5.23 RT-PCR using primers specific for  $\beta_2$  microglobulin and mRNA from 24 hour air-pouch tissue.** The gel has a size marker in first lane followed by samples which show a clear band at ~0.25 kbp indicating successful PCR amplification from the transcripts.

TLDA was used to perform RT-PCR using cDNA transcribed from the mRNA of air-pouches. The custom plates were designed to analyse 32 different target genes (appendix 1). The data generated were expressed as fold change over untreated control (PBS) values. A number of the target genes had low level expression which resulted in amplification which was below robust detection level. Despite extensive signs of inflammation demonstrated in sections 5.4.4.1 and 5.4.4.2 only 6 targets, of the 32 genes on the array card, showed any marked changes, and these are listed in Table 5.3. Although these are all elevated; but only CXCL13 after LPS treatment showed a significant difference compared with PBS treated pouches. None of the changes measured after exposure to CoCr were significantly different from the PBS treated pouches.

<b>Inflammatory Factor</b>	<b>CoCr</b>	<b>LPS</b>
<b>IL-1<math>\beta</math></b>	7.58 $\pm$ 1.95	18.40 $\pm$ 14.17
<b>TGF-<math>\beta</math></b>	2.18 $\pm$ 0.58	1.57 $\pm$ 0.61
<b>CCL2</b>	4.83 $\pm$ 1.64	4.63 $\pm$ 3.21
<b>CCL4</b>	2.38 $\pm$ 0.80	13.00 $\pm$ 10.21
<b>CXCL2</b>	11.33 $\pm$ 4.17	30.01 $\pm$ 25.68
<b>CXCL13</b>	1.94 $\pm$ 0.64	48.05 $\pm$ 9.18*

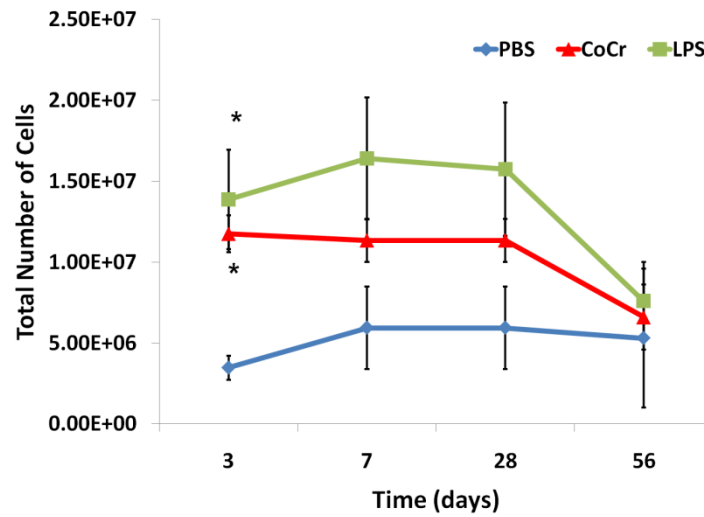
**Table 5.3 Inflammatory factor transcripts in air-pouch tissue at 24h post-injection.** The mRNA from air-pouch tissue from mice treated with LPS or CoCr debris was assessed using TLDA analysis, and expressed as fold change over levels from PBS-injected air-pouches. Results are shown as means  $\pm$  SEM (n = 3). \* indicates significant difference (p < 0.05) measured when compared with PBS values by one-way ANOVA followed by Dunnett's multiple comparison test.

## 5.4.5 Systemic immune effects

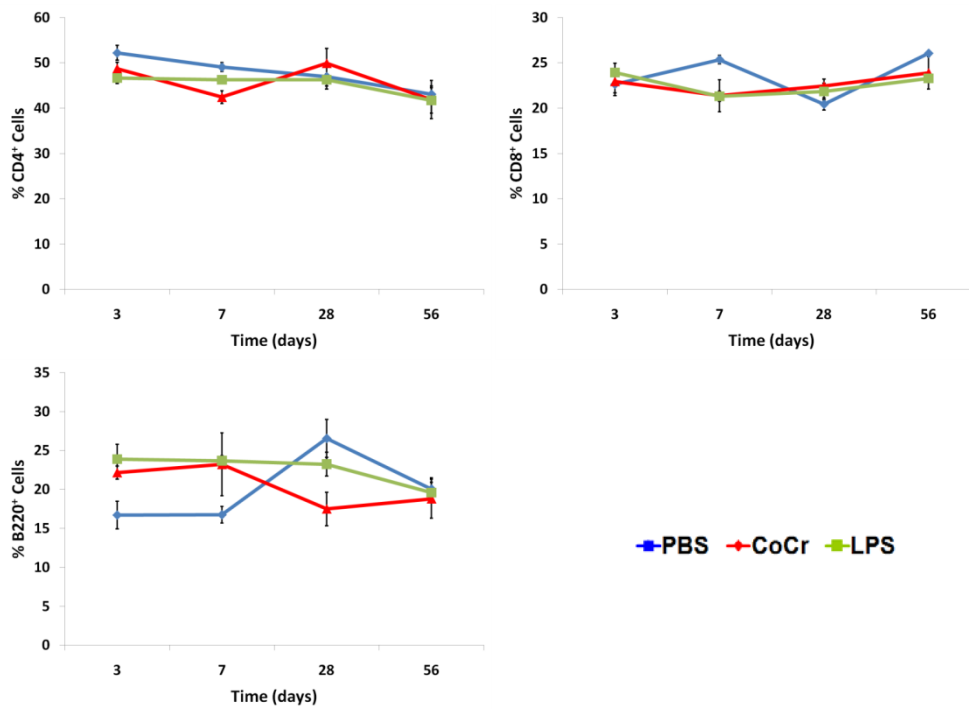
### 5.4.5.1 Lymphocyte numbers within draining lymph nodes

Figure 5.24 shows the number of cells from the draining (axillary, brachial and inguinal) lymph nodes of mice treated with PBS, CoCr debris or LPS. This figure shows that CoCr debris and LPS treated mice have higher numbers of cells in the draining lymph nodes compared with PBS treated mice. However, this was only significant at day 3 post treatment.

Figure 5.25 indicates that the proportion of CD4<sup>+</sup> helper T-cells, CD8<sup>+</sup> cytotoxic T-cells and B220<sup>+</sup> B-lymphocytes within the draining lymph nodes did not differ between the various groups despite the increase in the total number of cells within the draining lymph nodes shown in Figure 5.24.



**Figure 5.24 Changes in cell number in draining lymph nodes after the injection of PBS, CoCr debris or LPS into the air-pouch.** Results are means  $\pm$  SEM (n = 3 except at day 56 where n=2). \*Significantly different from PBS (negative control) values (at  $p < 0.05$ ) by one-way ANOVA followed by Dunnett's multiple comparison test.



**Figure 5.25** Changes in the proportion of lymphocytes in draining lymph nodes after the injection of PBS, CoCr debris or LPS into the air-pouch. Results are means  $\pm$  SEM (n = 3 except at day 56 where n=2).

Figures 5.26 and 5.27 show the viability of, and level of apoptosis, respectively, in lymphocytes isolated from the draining lymph nodes. These figures demonstrate that lymphocytes from all the groups of mice had similar levels of viability and apoptosis throughout the course of the experiment. Viability of the lymphocytes remained relatively constant for the duration of the experiment, even though the isolated lymphocytes were more apoptotic at 28 and 56 days. This was the case for all mice, irrespective of treatment.

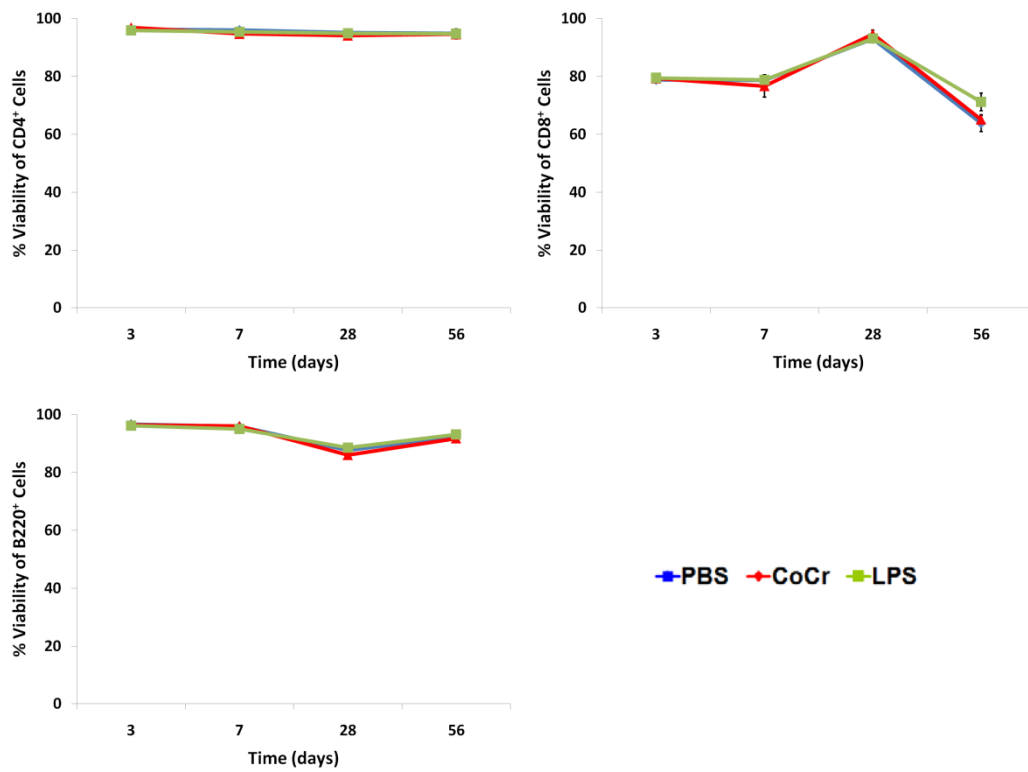


**Figure 5.26 Viability of lymphocytes in draining lymph nodes after the injection of PBS, CoCr debris or LPS into the air-pouch.** Viability was measured via flow cytometry following staining with 7-AAD. Viable cells were 7-AAD<sup>-</sup>. Results are means  $\pm$  SEM (n = 3 except at day 56 where n=2).

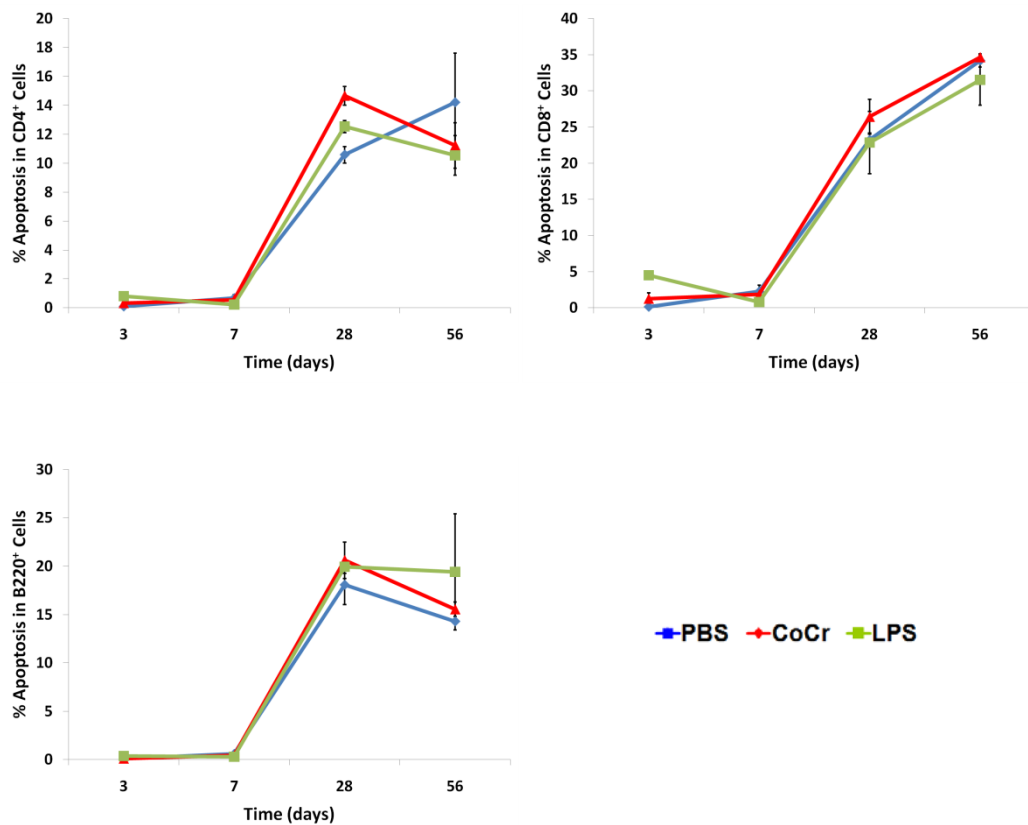


**Figure 5.27 Proportion of apoptotic lymphocytes in draining lymph nodes after the injection of PBS, CoCr debris or LPS into the air-pouch.** Apoptosis was measured via flow cytometry following staining with Annexin V. Apoptotic cells were Annexin V<sup>+</sup>. Results are means  $\pm$  SEM (n = 3 except at day 56 where n=2).

#### 5.4.5.2 Effects of *in vitro* activation on lymphocytes from draining lymph nodes

Data in section 5.4.5.1 demonstrated that the CoCr debris treatment did not affect the viability or level of apoptosis of lymphocytes isolated from the draining lymph nodes. Therefore, in order to assess whether CoCr debris exposure could affect the functioning of lymphocytes; resting lymphocytes from the draining lymph nodes were activated with anti-CD ( $\pm$  anti-CD28) for 24 hours *in vitro*. Figure 5.28 shows the cell viability of anti-CD3 ( $\pm$  anti-CD28) activated lymphocytes after 24 hours culture. The results show that lymphocytes (CD4<sup>+</sup>, CD8<sup>+</sup> and B220<sup>+</sup>) from mice, treated with CoCr debris for 7 days, have a significantly higher viability following anti-CD3 activation than cells from untreated (PBS) mice. No other duration of



CoCr debris exposure showed any significant changes from untreated control values. This was the case for all three types of lymphocyte. It was also observed that CD4<sup>+</sup> cells from mice, treated with LPS for 7 and 28 days, had a significantly higher viability than cells from untreated control mice. In addition, the viability of CD4<sup>+</sup> cells from mice treated with LPS for 28 and 56 days was significantly higher than CD4<sup>+</sup> cells from PBS treated mice following anti-CD3 + anti-CD28 activation. Conversely, B220<sup>+</sup> cells from LPS treated mice (56 days) had significantly lower viability than the equivalent cells from PBS treated mice following anti-CD3 + anti CD28.

Overall, there was little evidence of a consistent response from lymphocytes of CoCr treated mice, compared with cells of untreated control mice, following *in vitro* activation. However, it was noticeable that the viability of activated cells (irrespective of their *in vivo* treatment) was generally at lower levels than that observed of resting cells in section 5.4.5.1. This is particularly evident in CD8<sup>+</sup> cells at 28 and 56 days.

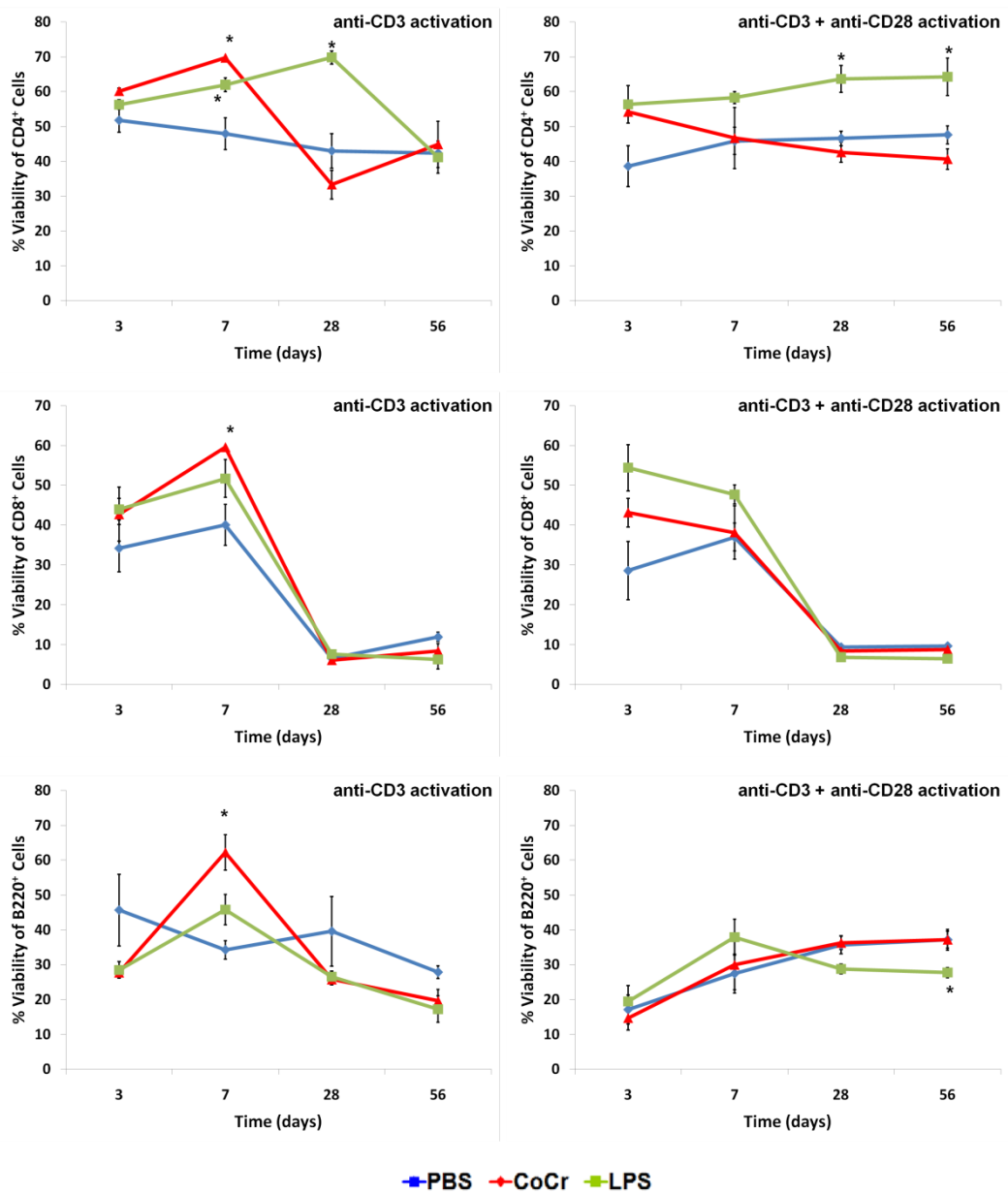


**Figure 5.28 Viability of lymphocytes activated with anti-CD3 ( $\pm$  anti-CD28) for 24 hours.** Lymphocytes were isolated from draining lymph nodes at time points after the injection of PBS, CoCr debris or LPS into air pouch. Viability was measured via flow cytometry following staining with 7-AAD. Viable cells were 7-AAD<sup>-</sup>. Results are means  $\pm$  SEM (n = 3 except at day 56 where n=2). \* Significantly different from PBS (negative control) values (at p < 0.05) by one-way ANOVA followed by Dunnett's multiple comparison test.

In addition to assessing the viability of anti-CD3 ( $\pm$  anti-CD28) activated lymphocytes, the level of apoptosis was also measured. The proportion of apoptotic lymphocytes, from the draining lymph nodes, following 24 hour *in vitro* anti-CD3 ( $\pm$  anti-CD28) activation are shown in Figure 5.29. These data indicate that lymphocytes isolated from 7 day CoCr or LPS exposed mice are significantly less apoptotic compared with lymphocytes from PBS treated mice, following *in vitro* anti-CD3 activation. No other cells isolated from CoCr treated mice led to any significant changes in apoptosis compared to with the equivalent isolated cells from untreated control mice.

CD4<sup>+</sup> and CD8<sup>+</sup> cells isolated from LPS exposed mice (28 days) were significantly less apoptotic than cells from PBS treated control mice (Figure 5.29). These results also show that lymphocytes from mice treated with LPS for 28 or 56 days are less apoptotic compared with lymphocytes from PBS treated mice following anti-CD3  $\pm$  anti-CD28 activation.

Overall, only cells from 7 day CoCr treated mice show any significant difference from cells isolated from the draining lymph nodes of PBS control mice. Similar to the observation made regarding cell viability, it was again observed that the level of apoptosis measured in activated cells is higher than those observed with resting cells (section 5.4.5.1), irrespective of *in vivo* treatment.

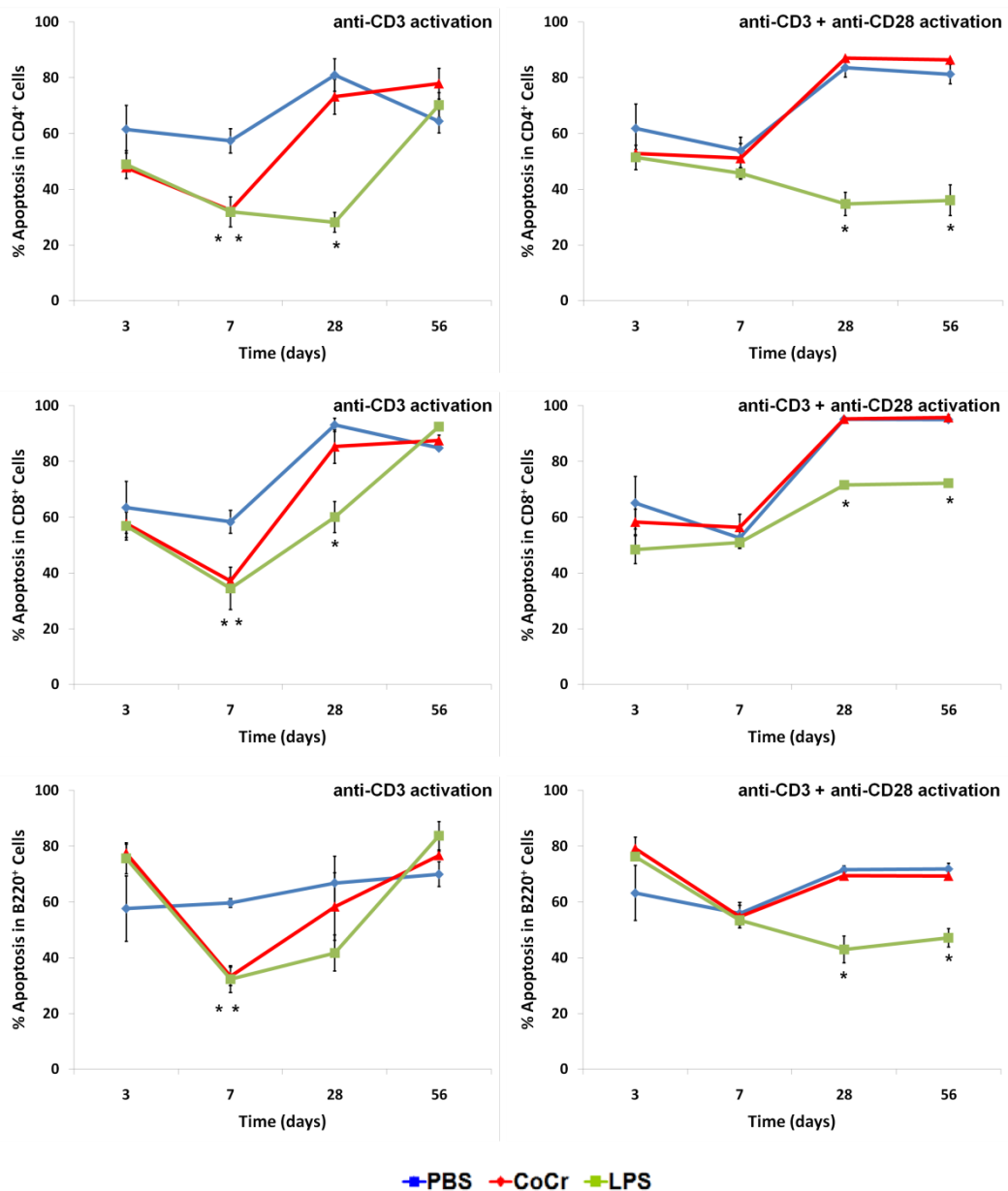


**Figure 5.29 Proportion of apoptotic lymphocytes following 24 hour activation with anti-CD3 ( $\pm$  anti-CD28).** Lymphocytes were isolated from draining lymph nodes at time points after the injection of PBS, CoCr debris or LPS into air pouch. Apoptosis was measured via flow cytometry following staining with Annexin V. Apoptotic cells were Annexin V<sup>+</sup>. Results are means  $\pm$  SEM (n = 3 except at day 56 where n=2). \* Significantly different from PBS (negative control) values (at p < 0.05) by one-way ANOVA followed by Dunnett's multiple comparison test.

## 5.5 Discussion

The current chapter has described the development and implementation of an *in vivo* model to evaluate the biological response to orthopaedic wear debris. CoCr wear debris, from an ASR hip implant, was found to range in size and shape. These irregularly shaped particles ranged from the nanometre scale to micrometre particles; some of the latter were aggregates of the smaller particles. Due to the irregular nature of these particles it was difficult to accurately quantify their number or measure their surface area. Therefore, the dose for implantation studies was quantified as a dry mass which could easily be suspended in PBS and implanted via a simple injection. Previous simulator testing has shown that around 8mm<sup>3</sup> of debris per million cycle was produced under harsh conditions (Leslie et al., 2008, Williams et al., 2008). The density of the CoCr alloy used to produce the wear debris was ~8.32 mg/mm<sup>3</sup>, as a result, 8 mm<sup>3</sup> of wear would equate to 66.56mg of debris per million cycle (Medley et al., 1996). It has been reported that a very active person can walk up to 3.5 million cycles per year (Schmalzried et al., 1998), assuming that the prosthesis is *in situ* for 25 years that would equate to 5824mg of debris produced in the total life-time of the prosthesis. This would be the equivalent to 0.08mg/g in a 75kg human. In the current study the mice were administered with 2.5 mg, this would equate to a dose 0.125mg/g. Therefore, the mice were administered a life-times quantity of wear debris produced in the harshest conditions in a single dose. Hence, the author does concede that 2.5mg per ~20g mouse is a relatively high dose. However, at the time of administration it was hypothesised that the CoCr wear debris would be contained within the air-pouch and that any migration or ion release would occur slowly. This would have allowed the model to mimic the release of wear debris from a MoM hip prosthesis, however, this was later found not to be the case.

These sterile CoCr wear debris particles were injected into a rodent air-pouch allowing the investigation of metal distribution as well as the local and systemic immunological changes that may be induced following release of particles from MoM hip resurfacing arthroplasty. Flow cytometry revealed that CoCr debris induced significant recruitment of inflammatory cells into the pouch cavity;

primarily neutrophils and macrophages/monocytes at 24-48 hours post-injection. However, the CoCr debris appeared to induce quite a different inflammatory pattern compared with the positive control (LPS) in terms of cellular composition and chemokine profile. As expected, LPS induced inflammation was characterised by initially high numbers of neutrophils, followed by increased levels of monocyte/macrophages (Kadl et al., 2009). In contrast, CoCr debris induced a different cellular response to LPS, which induces similar numbers of neutrophils and monocyte/macrophage within the pouch cavity. Thus, CoCr debris induced lower levels of neutrophil infiltrate compared with LPS but had similar levels of monocyte/macrophage infiltrate within the pouch cavity. This correlates well with the inflammatory factor transcript data from the air-pouch tissue, which indicated that LPS stimulation resulted in a mean 30-fold up-regulation of the neutrophil-recruiting chemokine CXCL2 (Wolpe et al., 1989). In contrast, CoCr stimulation resulted in only an 18-fold increase. Both LPS and CoCr showed a similar 3-4 fold increase in CCL2, a potent monocyte and macrophage migration factor (Deshmane et al., 2009), which resulted in similar absolute numbers of macrophages in the tissue and exudate. During the early phase of CoCr debris induced inflammation, neither T nor B-lymphocytes seemed to be significantly attracted to the air-pouch cavity, although there was an increase in B-lymphocytes at 72 hours. This could explain the increased expression of CXCL13, a chemokine that is selectively chemotactic for B-lymphocytes (Legler et al., 1998). The cellular phenotype present in inflammatory responses generally varies with time from induction with phagocytes being predominant during the early phases of inflammation, whereas lymphocytes become more evident in chronic inflammation (Anderson, 1994). It was not possible to lavage the air-pouch after 72 hours, and the point at which lymphocyte migration into the cavity occurred could therefore not be determined.

The histological data further demonstrate that CoCr debris provokes a specific inflammatory response with an appearance distinct from that induced by LPS. LPS stimulation led to pronounced up-regulation of certain chemokines such as CCL4 and CXCL13, which were less pronounced following CoCr stimulation. Additionally, CoCr wear debris led to the development of large inflammatory infiltrates in the air-

pouch tissue. The majority of these cells were localised around the debris which became embedded deep within the tissue. The cells surrounding this debris appeared to be mainly monocytes/macrophages and the pattern strongly resembled peri-prosthetic tissue recovered from revision surgery (Boss et al., 1990). There was also granuloma formation and increased levels of fibrous tissue around the debris, especially at later time points. There was some evidence even at 24 hours that CoCr debris caused an increase in TGF- $\beta$  gene expression (2-fold increase over both PBS and LPS stimulation), which has a role in wound resolution, scarring and fibrosis. Again this is reminiscent of previous histological findings which have been described in ARMD (Pandit et al., 2008, Mahendra et al., 2009).

Although LPS also induces inflammatory processes such as cellular infiltrates, this appears to be spread over the whole area of the pouch, whereas the response to CoCr appears to be localised around the debris. This is particularly evident at the longer time points post implantation. Whilst the number of cells within the tissue of LPS-treated pouches is reduced at 7 days, the level of cellular infiltration in the CoCr debris-treated pouches remains constant. The current study demonstrated that sterile CoCr debris initiates a distinct inflammatory process which can lead to a high level of monocyte/macrophage infiltration. It has previously been shown that *in vitro* exposures of monocytes and macrophages to CoCr wear debris resulted in up-regulation of antigen presentation and pro-inflammatory properties of these cells (Caicedo et al., 2009, Caicedo et al., 2010). These *in vitro* studies have shown that CoCr wear debris leads to increased expression of co-stimulatory surface molecules as well as increased macrophage reactivity. In particular, these studies have demonstrated increased secretion of the pro-inflammatory cytokine IL-1 $\beta$ , in the response to CoCr wear debris, which was confirmed by transcript data from the present study. These *in vitro* results also correlate with *in vivo* responses observed following implantation of CoCr engineered particles into air-pouches of mice for 48 hr (Wooley et al., 2002). The increasing evidence which implies a central role for IL-1 $\beta$  in metal-induced pro-inflammatory effects has led to the suggestion that IL-1 receptor antagonists may be used a therapeutic intervention for implant debris induced inflammation (Caicedo et al., 2009).

The histological data indicate that the implanted CoCr debris becomes encapsulated by fibrous tissue and inflammatory cells by day 7, and this is clearly evident at day 28. Biomaterial implantation has previously been shown to induce fibrosis or fibrous capsule development (Gretzer et al., 2006). This process has been observed in patients following MoM hip resurfacing surgery and in particular, has been defined as the major histological feature from soft tissue around loose implants (McMinn et al., 1996). High levels of macrophages/monocytes around the debris may facilitate this process since activated macrophages are reported to produce pro-fibrotic factors which enhance fibrogenesis by fibroblasts (Song et al., 2000). This fibrotic response, as well as the above mentioned cell infiltrates and cell death, was only observed in the CoCr treated air-pouches. Since these are not observed in the inflammatory response to LPS, it is a fair assumption that this is a processes induced by CoCr wear debris.

In addition, histological data also displayed evidence of cell death around the embedded CoCr debris. Earlier chapters have demonstrated that Cr and Co ion exposure induce apoptosis, *in vitro*. Although the current study did not measure metal ion levels in the air-pouch, circulatory metal ion levels were measured. Within the blood of CoCr treated mice; Cr ions peaked at 35.54  $\mu\text{g/l}$  (0.68  $\mu\text{M}$ ) and Co ions at 77.02  $\mu\text{g/l}$  (1.31  $\mu\text{M}$ ). *In vitro* studies described in chapters 3 and 4 demonstrated that these concentrations are cytotoxic to U937 cells but, not to primary human lymphocytes. However, the levels of these ions have been shown to be higher locally around the joint than in blood of patients following MoM hip resurfacing arthroplasty (Langton et al., 2009). Therefore, it is possible that high, toxic metal ions concentrations exist around the CoCr debris within the pouch that result in the observed cell death. However, cell death in the form of apoptosis is also the natural end process of inflammation and wound healing (Greenhalgh, 1998). Therefore, the cell death observed in the current model may also be part of the inflammatory response associated with CoCr debris.

Although metal debris and/or ions may have induced cell death locally, there is little evidence from the current study that treatment with CoCr debris can lead to any



systemic immune effects. As mentioned, earlier chapters have shown that metal ions are toxic to primary human lymphocytes, *in vitro*. However, despite increased levels of Cr and Co ions within the circulation and organs such as the spleen, there was little effect on the viability or level of apoptosis in lymphocytes isolated from the draining lymph nodes of CoCr treated mice. Although the number of cells isolated from the draining lymph nodes of CoCr treated mice was higher than PBS treated control mice, the proportion of cell type, viability and apoptosis level did not alter. The increase in the number of cells isolated from the lymph nodes is likely to be a result of general lymph node inflammation, as the number of cells isolated from the draining lymph nodes of LPS treated mice was also high.

Further to the above, lymphocytes isolated from the draining lymph nodes of CoCr treated mice also showed limited differences from cells of PBS treated mice following anti-CD3 ( $\pm$  anti-CD28) activation, *in vitro*. The only significant difference was observed following the *in vitro* activation of cells isolated from 7 day exposed mice. Interestingly, cells isolated from mice which were exposed to an inflammatory stimulus *in vivo* had higher levels of viability and reduced apoptosis following anti-CD3 activation *in vitro*. This observation is difficult to explain as one would assume a negative effect of CoCr debris exposure. In addition, the data from the cells isolated at other time-points and/or activated with anti-CD3 + anti-CD28 do not show a similar response. Therefore, as cells isolated from CoCr debris and LPS exposed mice at 7 days produced similar effects, it is postulated that the above response is as a result of *in vivo* inflammation that may have primed the cells for activation, thus the *in vitro* stimulus led to cells which were healthier once activated.

As mentioned above there were generally no systemic immune effects observed following CoCr debris treatment, despite the response of cells isolated from 7 day treated mice. The absence of expression of Th1/Th17 and Th2 related chemokines and cytokines in the pouch from CoCr treated mice may be due to a combination of the tissue site being sufficiently distant from the draining lymph nodes and the early inflammatory response being satisfactory such that chronic inflammation may not occur. However, as there is no antigen specific stimulation within the current *in vivo*

model it is more likely the case that inflammatory process observed following CoCr debris treatment is the result of sterile inflammation. The sterile inflammatory response is a process in which IL-1 $\beta$  and monocytes/macrophages have a prominent role (Chen and Nunez, 2010), similar to observations within the current model. In addition it has been shown that CoCr particles activate the inflammasome danger signalling pathway (Caicedo et al., 2009), a key element in the sterile inflammatory response (Rock et al., 2010, Chen et al., 2011). Thus, any chronic effects may be mediated via monocytes/macrophages rather than through antigen specific pathways. Although no significant systemic immune effects were observed following CoCr treatment, it was clearly evident that metal disseminated through the circulation into various organs. Within the blood and the majority of organs, chromium and cobalt levels peaked two days post treatment. The peak levels measured within the blood were within the range that had previously been observed in blood of patients following MoM hip arthroplasty, as summarised in Table 1.4. Although higher than the lowest recorded ion levels in patients, the levels observed in the current model were not as high as some of the extreme patient cases described. Therefore, despite the possible high dose of CoCr debris administered to the mice, the level of metal ions within the circulation appear to be comparable to those measured in MoM hip arthroplasty patients. Within the current study the author chose to measure metal ions in whole blood despite there being debate as to which of whole blood or serum can provide an accurate measurement of blood metal ion levels (MacDonald et al., 2004). Whole blood metal ion levels were measured as it has been demonstrated that metal ions, in particular Cr, can accumulate within RBCs and WBCs (Coogan et al., 1991, Merritt and Brown, 1995). As such, the author believes that measuring metal ion levels within the serum alone would not provide true measurement of blood metal ions.

Within the organs, the greatest increases for all elements were observed in the kidney. This was expected as the kidney is the likely mode of excretion. Of the three elements analysed, cobalt had the highest levels in all tissues and this is likely to be due to the composition of the debris. Interestingly, no increase in chromium levels was observed in the liver. Along with the kidney, this organ is known to be

involved in the excretion of many metals (Jakobsen et al., 2007). Previous *in vivo* models have documented increases in chromium levels in this excretory organ following intramuscular or intraperitoneal implantation of CoCr alloy (Jakobsen et al., 2007). In addition, mice that were injected subcutaneously with chromium solution (Carmo Pereira et al., 1999) or given a chromium solution orally (Costa, 1997) also showed high levels of chromium within the kidneys and liver. Post-mortem studies from traditional total hip replacement patients have shown extremely high chromium levels within the liver (Langkamer et al., 1992, Case et al., 1994). As described earlier, it has been shown that trivalent chromium is not easily transported into cells unlike the hexavalent form (Merritt and Brown, 1995, Schaffer et al., 1999). The results in this study could possibly indicate that the relatively immobile trivalent form of chromium, rather than the extremely mobile hexavalent form, is primarily released from the debris. However, it is possible that  $\text{Cr}^{6+}$  is released from CoCr debris, but as postulated by previous authors it may form insoluble chromium phosphate complexes locally around the area of implantation (Tkaczyk et al., 2009, Langton et al., 2010). Alternatively, the lower levels of Cr measured may be due to the treatment of the CoCr debris once it was produced. The debris was produced on a simulator in deionised water. The debris was then stored in deionised water until it was treated for any microbial contamination. This was done 3 days before the sterile CoCr debris was administered to the mice. Therefore, the storage and treatment of the debris could have affected the valency of Cr ions.

The metal ion levels within blood and organs return to control levels by day 28; only cobalt and molybdenum level within the spleen are elevated at after this period. These results indicate that although the metal ion concentrations in blood and distant organs increased more than 5-fold, the ions were adequately excreted through the kidney. Brown et al. (1988) also demonstrated that both Cr and Co are excreted rapidly. These authors showed that hamsters that had CoCr alloy (F-75) rods inserted subcutaneously excreted over 40% of Co into urine within 24 hours whereas only ~20% of Cr was excreted within the same period. In MoM resurfacing patients, it is suggested that metal ions do not accumulate progressively because the rate of excretion matches rate of production (Cobb and Schmalzreid, 2006). Therefore,

metal ions released from a single dose of CoCr particles may be adequately excreted, and this does not allow the accumulation of metal ions to toxic level.

It is clear that the current *in vivo* model produces a number of features resembling processes identified in the pathology of ARMD and provides valuable details regarding the inflammatory process due to CoCr wear debris. It is evident that this debris induces a specific inflammatory response mediated by monocytes/macrophages, possibly due to a sterile inflammatory response mediated by the inflammasome. Further to this, it is clear that debris released *in vivo* following MoM hip resurfacing, is likely to lead to high metal ion levels in blood and organs which may lead to additional adverse effects. However, whether the inflammatory response or the high levels of metal ions from wear production induce the systemic and chronic effects remains undetermined. The release of wear debris *in situ* is continuous for the duration of the implant, whereas the current model only provides the equivalent of a single release of wear debris leading to a transient response. The current model accurately mimics a single release from wear debris. A similar model allowing continuous release of debris will lead to accumulation of metal ions within blood and organs, and may mimic more severe local inflammatory responses and chronic adverse effects. In order to fully assess this possibility, repeated doses of CoCr debris should be administered in future studies for complete evaluation of the chronic responses induced following MoM resurfacing arthroplasty.

# Chapter 6

## **6. Effects of metal-on-metal arthroplasty on lymphocytes *in vivo*: Correlation with blood metal ion levels.**

### **6.1 Introduction**

MoM hip arthroplasty, both resurfacing and THR, often involve the use of cobalt chrome alloys. It is believed that this type of material extends the durability of hip replacement and reduces the requirement for revision (Merritt and Brown, 1996). However, MoM articulating surfaces generate metallic nano-particulate wear debris as well as corroding *in vivo* releasing metal ions. The release of soluble and particulate metallic debris from such metal implants has been extensively documented (Case et al., 1994, Lhotka et al., 2003, Vendittoli et al., 2007). Increased levels of metal ions, in particular Cr and Co, have been recorded in peripheral blood of patients following MoM hip resurfacing or THR (Back et al., 2005, Milosev et al., 2006). The MHRA and NICE have expressed concern over the effects of long-term exposure to metal debris/ions, particularly in younger patients and women. In April 2010 the MHRA issued an alert mandating an annual follow up of blood metal ion levels in MoM hip implant patients for the first five years after the surgery.

As mentioned earlier, it is believed that exposure to high levels of circulating metal ions, particularly Cr and Co, leads to detrimental effects causing DNA damage and immune dysfunction (Ladon et al., 2004, Delaunay et al., 2010). Several studies have observed reduced levels of white blood cells (WBCs), in particular lymphocytes, following MoM hip arthroplasty (Savarino et al., 1999, Hart et al., 2006, Hart et al., 2009). Hart and co-workers reported the presence of laboratory defined T-cell lymphopenia (circulation levels of T-lymphocytes  $< 0.8 \times 10^9$  cells/l) in peripheral blood of patients with MoM hips compared with those with MoP hips. This was particularly evident in CD8<sup>+</sup> cytotoxic T-lymphocytes. Specifically they have reported that combined levels of blood Cr and Co in excess of 5 ng/ml will lead

to reduced numbers of lymphocytes. These authors also reported an inverse correlation between the circulating levels of Cr and Co in patients with MoM hips and absolute lymphocyte counts. In addition, it has also been reported that MoM THR leads to reduced numbers of circulating CD4<sup>+</sup> helper T-lymphocytes and CD16<sup>+</sup> natural killer (NK) cells (Savarino et al., 1999). The findings in the earlier chapters of this thesis have also shown that Cr and Co ions have toxic effects on lymphocytes, *in vitro*. Therefore, it is postulated that metal ions released from MoM implants lead to toxic effects which result in reduced levels of circulating lymphocytes.

## **6.2 Aims**

The primary aim of this chapter was to assess whether MoM hip arthroplasty would lead to any alterations in the number of circulating lymphocytes and if these changes correlated with blood metal ion levels. This chapter investigated whether these parameters were affected following MoM hip resurfacing, with different prostheses. It also assessed whether MoM and ceramic-on-metal (CoM) THR lead to similar changes.

## **6.3 Methods**

### **6.3.1 Implants**

The MoM resurfacing implants used in the study were the Durom™ resurfacing system (Zimmer; Winterthur, Switzerland) and ASR (Articular Surface Replacement; DePuy; Leeds, UK). The femoral and acetabular components of both the Durom and ASR implants are made of high carbon ( $\geq 0.2\%$ ) content CoCr alloy (ISO 5832-12).

The components used in THR in the study were supplied by DePuy (Leeds, UK). All subjects received a Pinnacle® acetabular cup and Corail® femoral stem. The

acetabular cup was composed primarily of titanium (Ti) with a CoCr liner (36mm) and the femoral stem was primarily Ti coated with hydroxyapatite. The CoM subjects received a ceramic articulating femoral head whereas patients within the MoM group received a CoCr component (both 36mm).

### 6.3.2 Patients

The number of patients within each subject group is shown in Table 6.1. This table shows the number of patients at each time point, it also displays the number of patients for whom metal ion data was available.

Implant	Time				
	Pre-Op	6 weeks	6 months	1 year	2 year
ASR	12 (12)	12 (9)	8 (6)	9 (8)	7 (7)
DUROM	23 (21)	20 (20)	16 (12)	17 (14)	11 (8)
CoM (THR)	15 (11)	10 (9)	10 (8)	8 (5)	-
MoM (THR)	17 (11)	14 (13)	10 (10)	10 (9)	-

**Table 6.1 Number of patients within each subject group.** Data shows the number of patients at each time point and the figure in brackets indicates the number of patients with blood metal ion concentration data available. Inclination angle was less than 55° in all patients. Renal function in all subjects was within acceptable limits (measured at time of surgery).

### 6.3.3 Blood sample collection

Ethical permission from the local regional ethics committee was obtained to withdraw blood from patients about to undergo primary hip replacement surgery, and postoperatively during follow up visits at 6 weeks, 6 months, 1 year and 2 years.



Blood samples (50 ml) were collected into sodium citrate tubes from each subject by inserting a plastic cannula in the antecubital fossa after discarding the first 5 ml to avoid contamination from the needle. All vessels used for the collection of specimens were verified to be free of metal contamination.

### **6.3.4 Analysis of peripheral blood**

Following collection, the WBC and lymphocyte numbers were quantified via flow cytometry as described in section 2.3.2. An aliquot of the blood sample was stored in the freezer at a temperature of  $-70^{\circ}\text{C}$  until analysed for trace metal ions as described in section 2.3.3. Both WBC numbers and metal ion levels were compared with each individual patients own pre-operative levels and expressed as a change from these values.

## **6.4 Results**

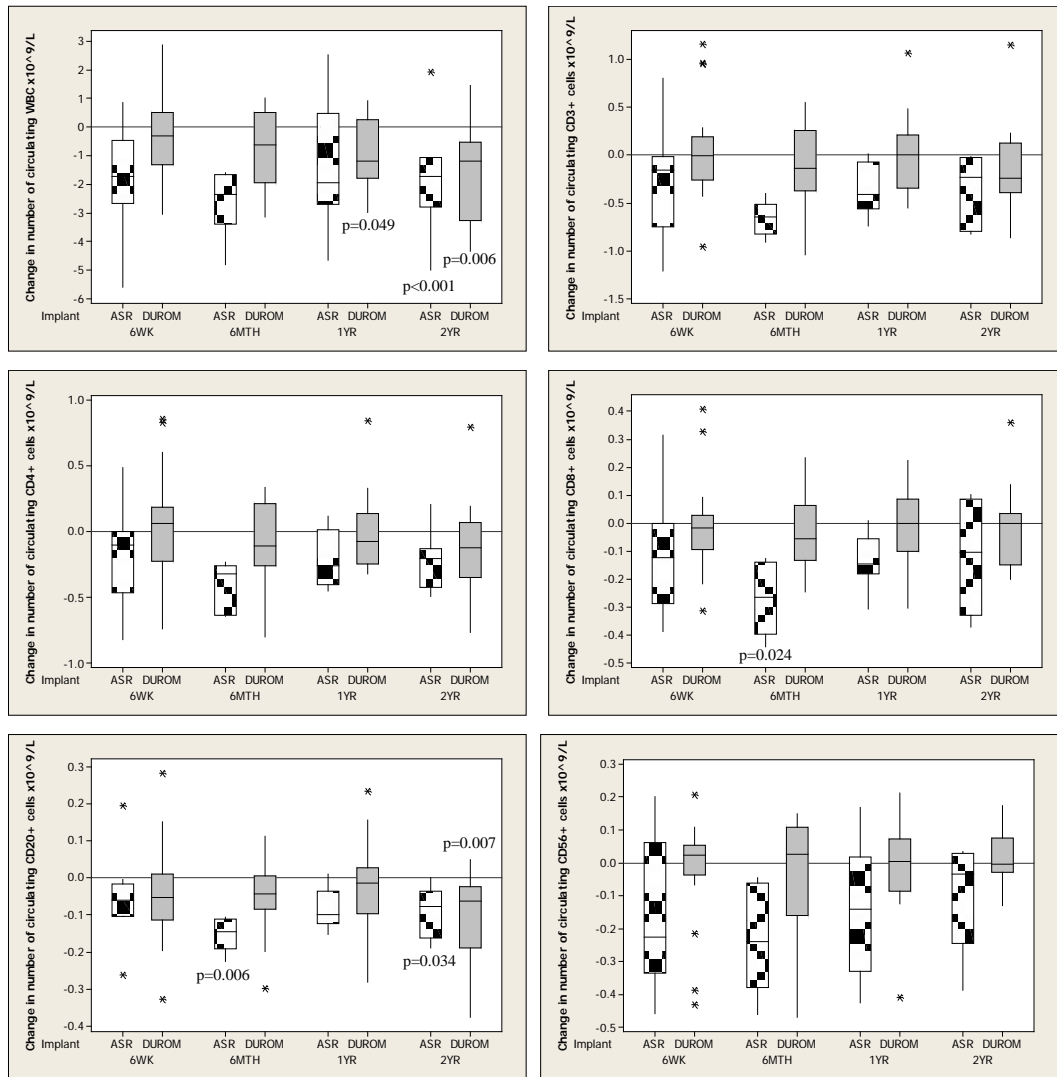
### **6.4.1 Effects of MoM resurfacing on lymphocyte numbers**

Figure 6.1 displays the changes in WBC and lymphocyte number following MoM hip resurfacing arthroplasty. It was observed that DUROM patients had significantly less circulating WBCs 1 and 2 years following resurfacing surgery compared to pre-operative values. ASR patients were found to have significantly reduced numbers of circulating WBCs 2 years following hip arthroplasty.

Although ASR subjects had lower numbers of circulating  $\text{CD3}^{+}$  cells (T-lymphocytes) compared to pre-operative levels, these changes are not significant. This was also the case for a subset of these cells,  $\text{CD4}^{+}$  cells (helper T-lymphocytes). The other subset of  $\text{CD3}^{+}$  cells,  $\text{CD8}^{+}$  cells (cytotoxic T-lymphocytes), were found to be reduced at 6 weeks following resurfacing surgery with an ASR implant. No changes were observed in any T-lymphocyte populations in patients who had received a DUROM implant.

Figure 6.1 also shows that the number of CD20<sup>+</sup> cells (B-lymphocytes) were reduced from pre-operative values in ASR patients 6 weeks and 2 years post resurfacing arthroplasty. These cells were also found to be reduced in DUROM patients 2 years following surgery.

No changes in CD56<sup>+</sup> cells (NK cells) were observed at any time point following hip resurfacing with either MoM prostheses.



**Figure 6.1** Change in number of circulating white blood cells and different lymphocyte subsets following MoM hip resurfacing arthroplasty surgery using the ASR and Durom implants. Y-axis indicates change from pre-operative levels; \* indicates outliers; significantly different levels marked with p-values by repeated measures analysis of variance ( $p < 0.05$ ) with respect to preoperative values.

Table 6.2 shows the percentage of patients at 1 and 2 years post hip resurfacing arthroplasty who were lymphopenic. As can be seen, the percentage of patients that were lymphopenic was higher in the ASR group than DUROM group, 1 year post surgery. The percentage of patients with a DUROM implant that were lymphopenic was relatively low at 1 year but this increased at 2 years post surgery. At two years

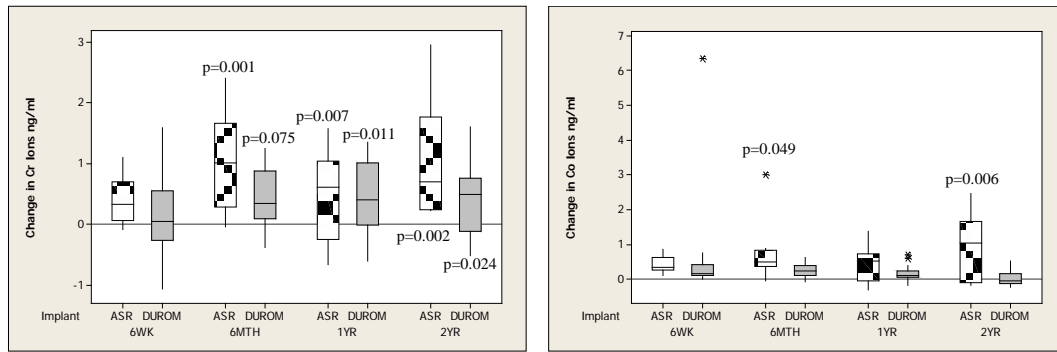
post surgery, a higher percentage of DUROM patients had CD3 and CD8 lymphopenia than ASR patients.

	1 Year		2 Year	
	ASR (%)	DUROM (%)	ASR (%)	DUROM (%)
<b>CD3</b>	44	7	29	36
<b>CD4</b>	33	11	43	18
<b>CD8</b>	22	20	0	27
<b>CD20</b>	7	0	29	9

**Table 6.2 Percentage of patients with laboratory defined lymphopenia following MoM hip resurfacing.** Patients received either an ASR or Durom implant. CD3<sup>+</sup> lymphopenia is defined as absolute counts of  $<0.8 \times 10^9/l$ ; CD4<sup>+</sup> lymphopenia as absolute counts of  $<0.5 \times 10^9/l$ ; CD8<sup>+</sup> lymphopenia as absolute counts of  $<0.2 \times 10^9/l$  and CD20<sup>+</sup> lymphopenia as absolute counts of  $<0.08 \times 10^9/l$ .

#### **6.4.2 Effect of blood metal ion concentrations on lymphocyte numbers following MoM arthroplasty**

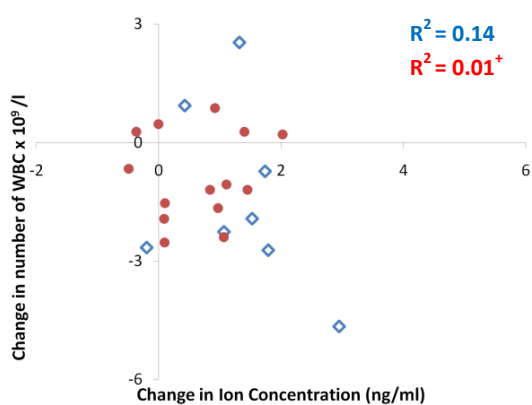
Figure 6.2 shows that blood chromium ion levels are higher at 6 months and 1 and 2 years following MoM hip resurfacing compared with pre-operative values. This is the case in both ASR and DUROM patients. This figure also indicates that ASR patients have higher levels of cobalt ions in blood at 6 months and 1 year following hip resurfacing. No significant alterations in blood cobalt levels were observed in patients who received a DUROM implant. Additionally, it was found that the increase in Co levels in ASR patients' blood was significantly higher at each time-point compared with DUROM patients ( $p < 0.05$ , Mann-Whitney test). However, no differences were observed between the two patients groups with respect to whole blood Cr ions.



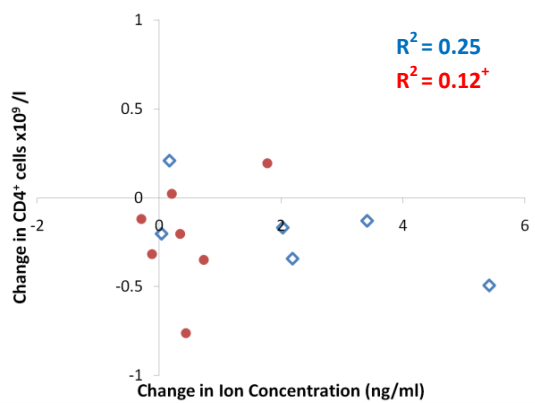
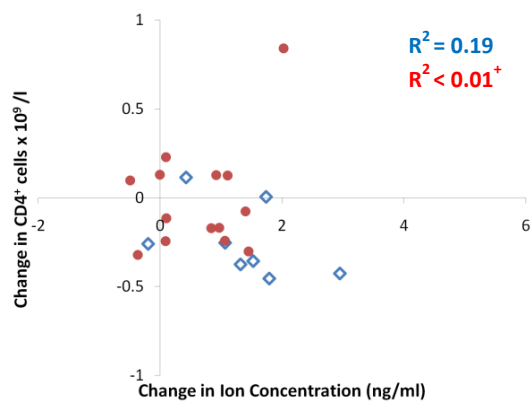
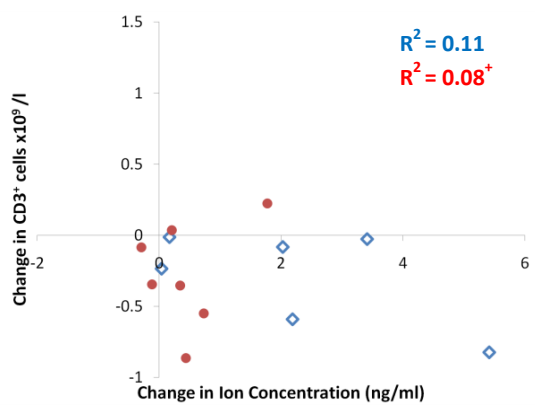
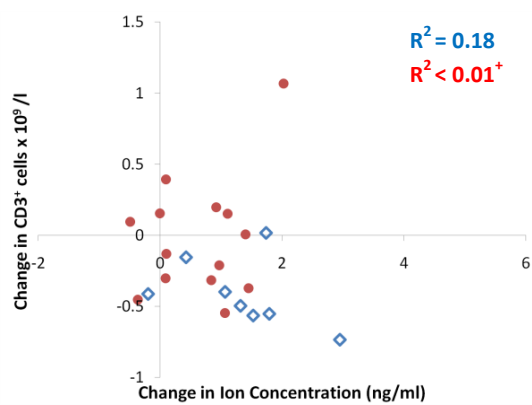
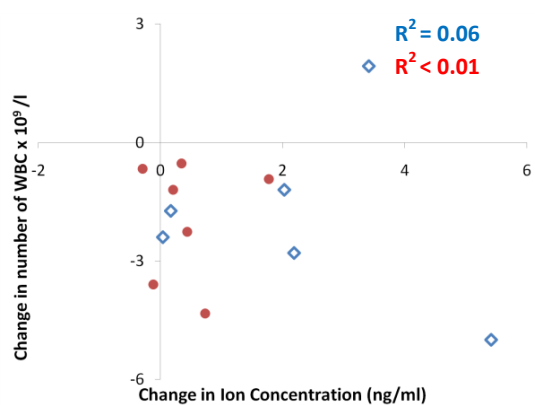
**Figure 6.2 Change in whole blood chromium and cobalt levels following MoM hip resurfacing arthroplasty surgery using the ASR and Durom implants.** Y-axis indicates change from pre-operative levels; \* indicates outliers; significantly different levels marked with p-values by repeated measures analysis of variance ( $p \leq 0.05$ ) with respect to preoperative values.

Figure 6.3 displays the change in the numbers of WBCs, T-lymphocyte subsets and B-lymphocytes plotted against changes in blood metal ion levels (Cr + Co) 1 and 2 years post MoM hip resurfacing arthroplasty. There was little evidence of an inverse correlation between the changes in individual ions and changes in the number of different WBCs (Appendix 2), hence the changes in combined ions was applied to determine any relationship. There appears to be no clear inverse relationship between changes in metal ion levels and the numbers of these cells. The  $r^2$  values were very low when attempting to correlate these parameters at 1 year post arthroplasty and, in some cases DUROM patients showed a very weak positive correlation. The correlation was strengthened when assessing an inverse relationship between changes in metal ion levels and lymphocyte number at 2 years post arthroplasty surgery.  $CD4^+$  T-helper cells and B-lymphocytes show a moderate inverse relationship compared with changes in metal ions following ASR hip arthroplasty 2 years post surgery. As at 1 year, there was little evidence of an inverse relationship following DUROM implantation.

### 1 YEAR



### 2 YEAR



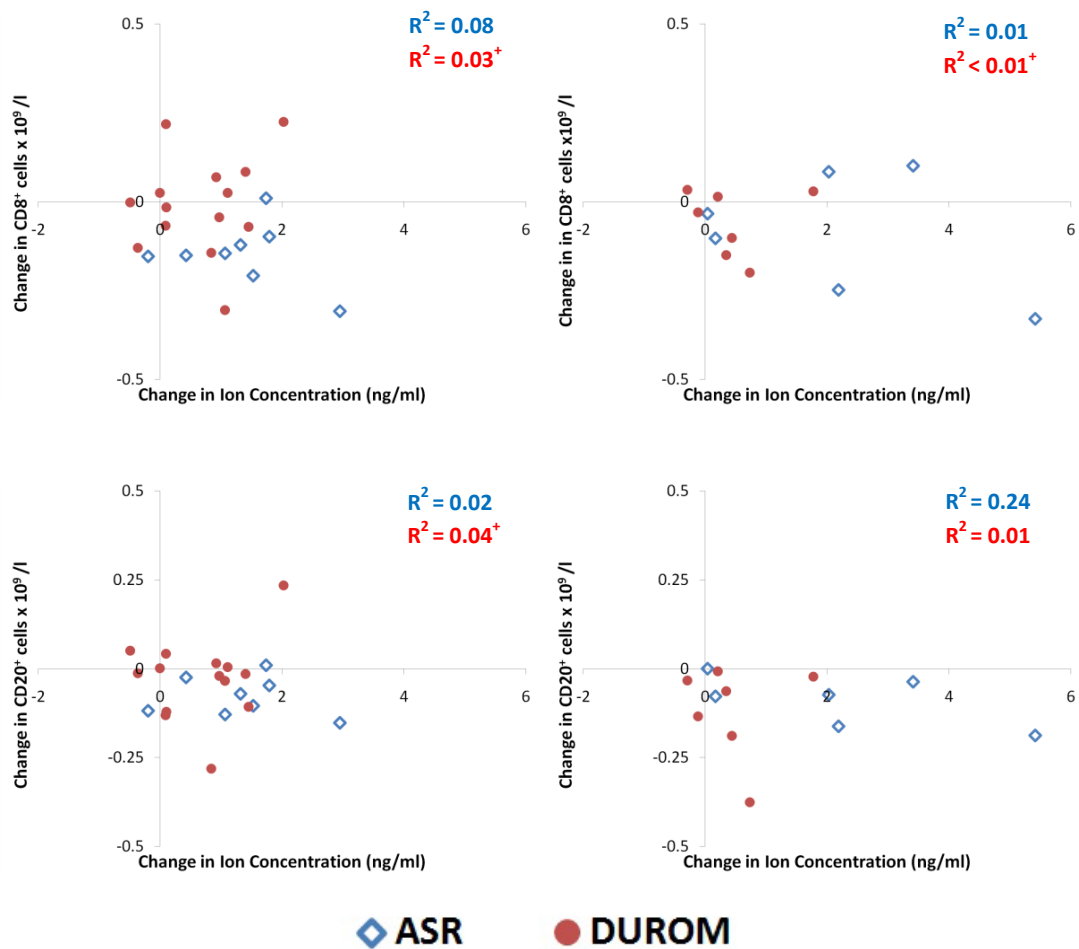


**Figure 6.3 Correlation between changes in whole blood metal ion levels (Cr + Co) and changes in WBCs and lymphocyte populations at 1 and 2 years post MoM arthroplasty using either ASR or Durom implants.** R<sup>2</sup> values indicate the inverse correlation between changes in metal ions and changes in the different WBCs. +Indicates a positive correlation between the two parameters.

### 6.4.3 Effects of THR on lymphocyte numbers

The boxplots in Figure 6.4 show the changes in WBC, T and B-lymphocytes and, NK cells following THR with either CoM or MoM implants at 6 weeks, 6 months and 1 year post surgery. No significant changes were measured in any of these cells,

compared to pre-operative values, at any of the time-points within either patient group.

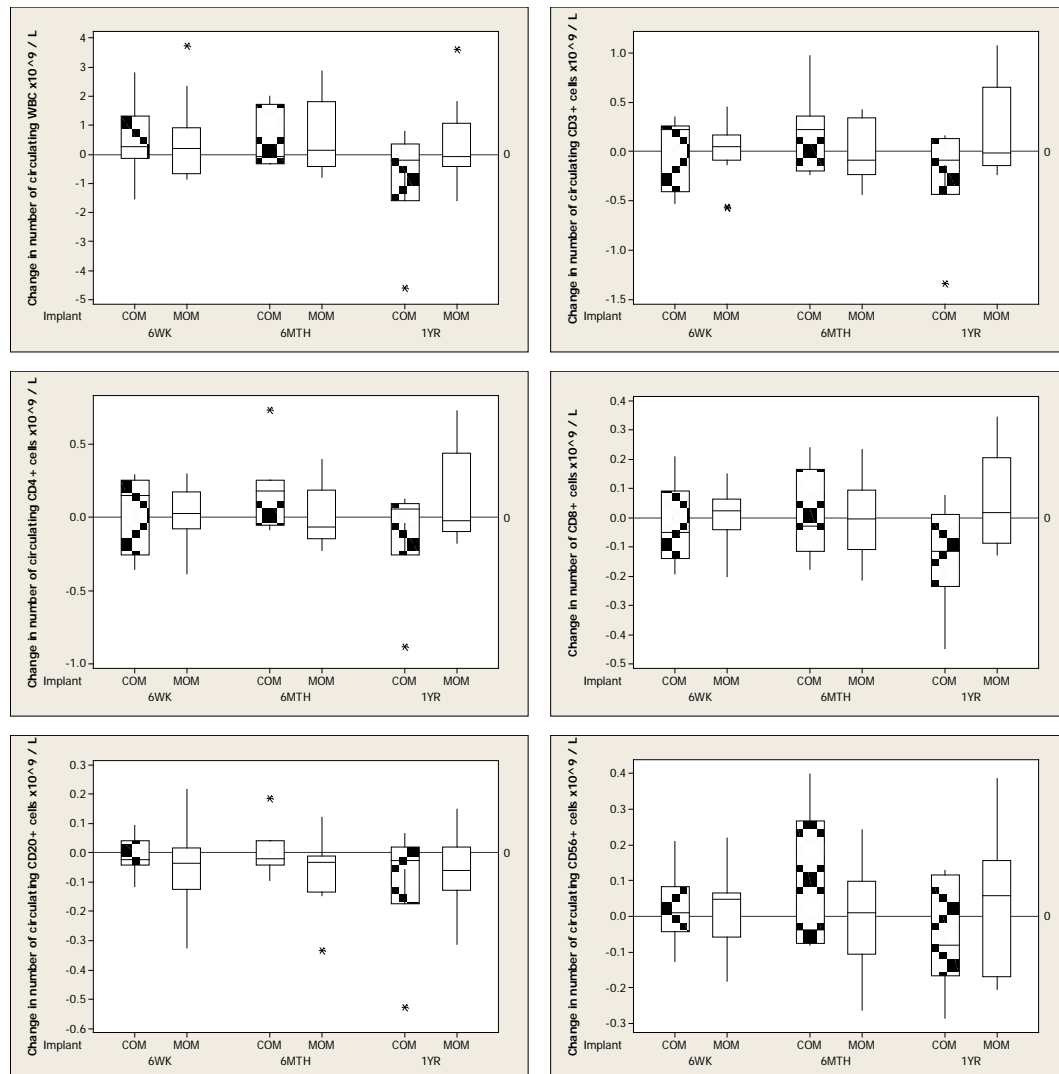


**Figure 6.4** Change in number of circulating white blood cells and different lymphocyte subsets following CoM or MoM THR. Y-axis indicates change from pre-operative levels; \* indicates outliers. No significant changes were observed values by repeated measures analysis of variance ( $p \leq 0.05$ ) with respect to preoperative values.



#### 6.4.4 Correlation between blood metal ion concentrations and lymphocyte number

No significant changes were observed in blood metal ion levels following CoM or MoM THR (Figure 6.5). There did appear to be a gradual increase over time in the level of blood Cr and Co in THR patients, this increase was more evident in MoM patients. However, as mentioned, no significant changes were measured.

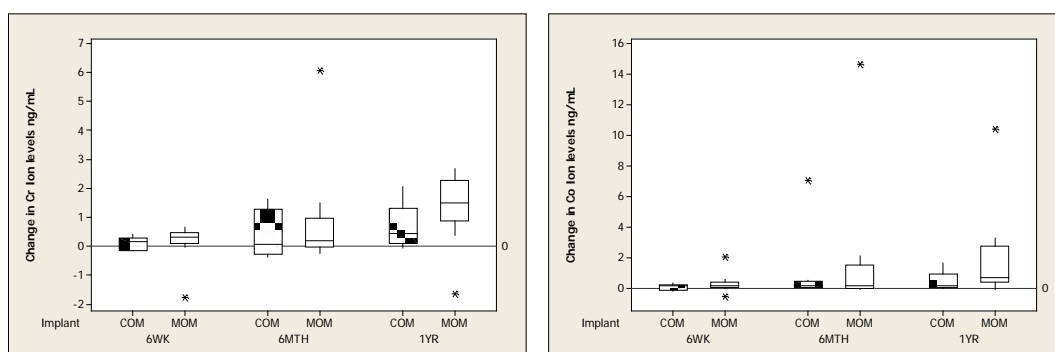


**Figure 6.5 Change in whole blood chromium and cobalt levels following CoM or MoM THR.** Y-axis indicates change from pre-operative levels; \* indicates outliers. No significant changes were observed values by repeated measures analysis of variance ( $p \leq 0.05$ ) with respect to preoperative values.

### 6.5 Discussion

The current chapter has primarily focussed on the effect of MoM hip arthroplasty on circulating lymphocyte numbers. Initially this study concentrated on comparing the alterations in lymphocyte numbers following MoM hip resurfacing arthroplasty with either an ASR prosthesis or DUROM prosthesis. Previous studies have shown that MoM resurfacing leads to a lower number of circulating WBCs, particularly lymphocytes, compared with patients who received a different type of implant such as MoP or CoM (Savarino et al., 1999, Hart et al., 2009). However, in this current study we chose to compare the changes from each individual's pre-operative value

therefore tracking changes within each patient, thus reducing the effects of inter-individual variability. The data from the present study show that the number of circulating WBCs is significantly reduced 2 years following hip resurfacing arthroplasty with an ASR implant. The only WBC sub-population which was significantly reduced at this time-point was CD20<sup>+</sup> B-lymphocytes, which is in keeping with previous findings (Hart et al., 2009). The other WBC sub-populations are also reduced in number at this time-point, however, these reductions are not significant. This may be as a result of the small sample size within this cohort of patients where the small reductions observed at both 1 and 2 years, post ASR implantation, within the subsets of WBCs are not significant. Interestingly, patients with a DUROM implant also have significantly reduced numbers of circulating WBCs at 1 and 2 years post-surgery. Again, the only significant decrease in any subset of WBCs was found to be in CD20<sup>+</sup> B-lymphocytes 2 years following arthroplasty. These cells are extremely important in the humoral immune response and their reduction within the circulation could leave the subject vulnerable to foreign bodies such as bacteria and viruses.

Although B-lymphocytes are extremely important, these cells are only a small proportion (1-5%) of the total WBC numbers therefore a decrease in their number alone does not account for the reduction in circulating WBC numbers. The results show that, barring B-lymphocytes at 2 years, there is very little variation in the other lymphocytes or NK cells in DUROM patients at 1 or 2 years following hip resurfacing. This implies that a reduction in another major subset of cells not analysed in the current study, such as neutrophils or monocytes/macrophages may contribute to the reduction in total WBC numbers. This may also be the case following hip resurfacing arthroplasty with an ASR. Infiltrates of CD3<sup>+</sup> T-lymphocytes and B-lymphocytes, as well as macrophages, have been reported around the joint (Willert et al., 2005, Counsell et al., 2008, Mahendra et al., 2009). This is said to be specific to MoM and distinctly different from the observations following MoP arthroplasty (Boardman et al., 2006, Pandit et al., 2008). It is postulated that the decreased number of WBCs previously reported may be as a result of cells being drawn from the circulation and accumulating around the joint (Langton et al., 2008,

Hart et al., 2009). Therefore, the reductions in WBCs may be a result of B- and T-lymphocytes as well as monocytes migrating from the circulation to the local area around the prosthesis.

It has also been suggested that changes in the number of the subsets of WBCs following MoM hip arthroplasty is as a result of increasing levels of circulating metal ions (Case et al., 2000). Data from earlier chapters (1 and 2) have shown metal ions to be toxic to lymphocytes and monocytes, *in vitro*. The present study found that Cr levels were significantly increased following MoM hip resurfacing, irrespective of which implant was used. However, only patients with an ASR implant showed increased levels of Co. Further to this, comparing the whole blood Co ion levels at different time points, it was found that ASR patients had significantly higher levels than patients with a Durom implant. Interestingly, when the current author investigated any inverse relationship with levels of metal ions and changes in numbers of WBCs or lymphocytes, very little correlation was found at 1 year. In fact, patients with a Durom implant actually showed a positive correlation, although very weak, between metal ion concentrations and numbers of WBCs or subsets of lymphocytes at 1 and 2 year post hip arthroplasty. However, patients do show a moderate inverse relationship between changes in metal ions and changes in T-lymphocyte numbers, in particular CD4<sup>+</sup> T-helper cells, and B-lymphocyte numbers at 1 year post ASR implantation. This inverse relationship is strengthened at 2 years post surgery for T-helper cells and B-lymphocytes. When attempting to correlate changes in individual ions and WBCs or lymphocyte number, the correlation was weaker (Appendix 2). Therefore, should there be any relationship with metal ions and WBC or lymphocyte numbers it is likely to be as a consequence of both metal ions. At present, however, it is difficult to claim that metal ion release from hip resurfacing implants leads to a reduction in the number of WBCs or lymphocytes. Although a number of patients in both cohorts were lymphopenic, we see no clear relationship between metal ions and WBC levels. Additionally, the vast majority of patients in both groups had blood ion levels well below the MHRA recommended 7 ng/ml and even the 5 ng/ml described by (Hart et al., 2009). Further to this, the metal ions levels measured within whole blood of patients in the present study were

lower than those which induce cytotoxicity *in vitro*. Therefore, it is possible that should the implant remain *in situ* for a longer period, metal ion levels may increase to levels which may adversely affect the immune system. However, evidence from the present study makes it difficult to suggest metal ions are the cause, or sole cause, for the decrease in WBC and lymphocyte numbers. Therefore, it is likely that the decreases measured in the number of circulating WBCs and lymphocytes following hip resurfacing arthroplasty are due to factors other than high levels of metal ions within the circulation.

The postulation that circulating WBC and lymphocyte number may not be solely related to whole blood metal ion levels is strengthened by initial findings from the second clinical trial which compared CoM and MoM THR. No significant changes in circulating WBC or lymphocyte number were observed following CoM or MoM THR. Over the course of 1 year, the subjects in both groups showed a clear small gradual increase in blood metal ion levels following THR, however, due to the small sample number at this time point, the increases did not show any significance. Also, at present, the increase in ion levels is more apparent following MoM THR than post CoM THR, however, when assessing changes in lymphocyte numbers it was found that the reduction in CD8<sup>+</sup> cytotoxic T-lymphocytes in CoM subjects 1 year post THR was the closest to significance ( $p=0.06$ ). Overall, no reductions are observed in circulating WBC or lymphocyte number following MoM THR even though there is a small increase in whole blood ion levels. However, it is conceivable, as with the resurfacing study, that the blood metal ion levels are not high enough to be detrimental for patients. However, this may change as the duration of implant presence *in situ* increases.

Previous data had showed a decrease in WBCs along with an increase in blood metal ion levels following THR, however, this was in patients with a failed joint arthroplasty (Savarino et al., 1999). In addition, the studies by Hart and colleagues (Hart et al., 2006, Hart et al., 2009) compared ion levels and lymphocyte numbers between patients with MoM or MoP implants rather than changes within individuals. Further to this, there are a number of reports which show an increase in lymphocyte

numbers following MoM hip replacement. Studies have demonstrated an increased proportion of cytotoxic T-lymphocytes and NK cells in patients with a failed metal orthopaedic implant (Case et al., 2000). In addition, a recent study showed that cytotoxic T-lymphocytes increase in number along with blood metal ion levels 6 years following MoM hip arthroplasty (Hailer et al., 2011). This further strengthens the current author's belief that metal ions may not directly cause a decrease in circulating WBC or lymphocyte numbers.

Data from the current chapter has demonstrated that numbers of circulating WBCs and lymphocytes are decreased following MoM hip resurfacing but no change is observed following THR even though there is an apparent increase in levels of metal ions within whole blood following both types of hip arthroplasty. It is possible that effects observed within the current study, as well as the general adverse effects previously reported, may be the result of the functioning and wear properties of the prosthesis. Metal ion release has been correlated with MoM wear debris generation (De Smet et al., 2008), and it has been stated that mechanical wear is the predominant process which drives the production of metal ions (Langton et al., 2008). Certain MoM resurfacing and large-diameter THR joints have greater wear than expected for the duration *in situ*, and this is accompanied by higher levels of blood metal ions (Langton et al., 2010, Matthies et al., 2011). In particular, the ASR implant has higher wear rates than other resurfacing implants such as BHR (Birmingham Hip Resurfacing; Smith & Nephew, Memphis, Tennessee, US) (Matthies et al., 2011). Also, MoM hip resurfacing, particularly using smaller ASR components, is sensitive to positioning *in situ* and high inclination angles can lead to high levels of wear debris and ion release (Langton et al., 2008, De Haan et al., 2008). Although all the hip resurfacing patients within the current study had inclination angles within the optimal region to minimise wear debris formation (Grammatopoulos et al., 2010), wear debris formation is still possible. In addition, ASR also had a higher cumulative revision rate (10.9%) at 5 years compared with Durom resurfacing (7.6%) according to the Australian National Joint register (2010). As such, the current author suggests that the reduced numbers of WBC and lymphocytes subsets observed following MoM resurfacing are likely to be due to

high levels of wear debris production from the implant rather than a direct effect of high metal ion levels. In addition, the author believes that wear debris formation is the result of a poorly implanted prosthesis. As such, the limited adverse effects observed within the patients of the current study may represent well fitted implants.

Data from the earlier chapter (section 5.3.4) has shown that implantation of ASR debris in mice leads to higher levels of Co than Cr within whole blood. Higher levels of Co were also measured in ASR patients compared with those with DUROM prosthesis and this may be related to the debris released from the implant as the composition of this debris was primarily Co (section 5.4.1). In addition to this, explant data have shown that implants which are revised due to ARMD or pseudotumour presence have higher wear compared with those revised due to other causes (Kwon et al., 2010, Langton et al., 2010). The previous chapter also showed that implantation of ASR wear debris, *in vivo*, in mice leads to a local immune response around the debris. This is supported by the view that the reaction to MoM wear debris exists as a chronic local immune response (Jameson et al., 2008), and recent *in vitro* data implicate CoCr particles as mediating the immune effects (Allen et al., 1997, Caicedo et al., 2009). The fact that no significant changes were observed in blood metal ion levels or WBC numbers following THR in our studies may be a result of a well-implanted small diameter implant. Therefore, it is hypothesised that wear debris from MoM resurfacing implants lead to the reduction of circulating WBCs due to a local immune response in which these cells accumulate locally (Caicedo et al., 2009, Hart et al., 2009). Also, high levels of circulating metal ions may be as a result of increased wear debris formation and its corrosion, and thus it may be used as a diagnostic tool to assess the functioning of the prosthesis (De Smet et al., 2008).

# Chapter 7

## 7. Summary and future work

### 7.1 Summary of the thesis findings

#### 7.1.1 Effects of chromium and cobalt on U937 cells *in vitro*

U937 monocyte-like cells were exposed to  $\text{Cr}^{6+}$  and  $\text{Co}^{2+}$ , individually or in combination, for 24 and 48 hours *in vitro*. These cells were treated with ion concentrations that had previously been reported in the blood of patients with a metal implant: 0.1, 1, 10  $\mu\text{M}$ . It was observed that exposure to all concentrations of  $\text{Cr}^{6+}$  decreased viability of these cells. Following exposure to the highest concentration of  $\text{Cr}^{6+}$ , 10  $\mu\text{M}$ , for 24 hours, cell viability was as low as 11.59% of control values. In addition, flow cytometric and microscopy data showed that  $\text{Cr}^{6+}$  exposure induced apoptosis of U937 cells, particularly at higher concentrations.

This study also demonstrated that  $\text{Cr}^{6+}$  is more toxic than  $\text{Co}^{2+}$ , *in vitro*. The data showed that  $\text{Cr}^{6+}$  exposure led to a greater reduction in cell viability and induced more cell death than  $\text{Co}^{2+}$  at all concentrations tested. There was minimal evidence of any toxicity of 0.1  $\mu\text{M}$   $\text{Co}^{2+}$ , and following exposure to 10  $\mu\text{M}$ , cell viability was still 69.90% of control values. In contrast to  $\text{Cr}^{6+}$  which primarily initiated apoptosis, the data indicate that high concentrations of  $\text{Co}^{2+}$  may induce necrosis as well as apoptosis. It is postulated that  $\text{Cr}^{6+}$  is more toxic than  $\text{Co}^{2+}$  because the intermediates formed as it is reduced to  $\text{Cr}^{3+}$  have adverse effects on cells

Although individual exposure of  $\text{Cr}^{6+}$  or  $\text{Co}^{2+}$  led to decreased viability of U937 cells, there was little evidence of any synergy when cells were exposed to both ions in combination. Only exposure to 1  $\mu\text{M}$   $\text{Cr}^{6+}$  and 10  $\mu\text{M}$   $\text{Co}^{2+}$  together for 24 hours showed a greater effect on cell viability than either of the individual exposures. This synergy was not observed following 48 hours of exposure. These ions may indeed be able to act in synergy but due to the cytotoxic nature of these ions, especially  $\text{Cr}^{6+}$ , it may be difficult to identify any synergy at high concentrations or at the longer durations of exposure. Overall, it was found that clinically recorded concentrations of  $\text{Cr}^{6+}$  and  $\text{Co}^{2+}$  led to cell death. The exact intracellular mechanism by which this



occurs in U937 cells was not elucidated but the author believes that it is as a result of ROS formation.

### **7.1.2 Effects of chromium and cobalt on primary human lymphocytes *in vitro***

Primary cultures of human lymphocytes were exposed to Cr<sup>6+</sup> and Co<sup>2+</sup> ions *in vitro*. These experiments were carried out to investigate mechanisms responsible for observed decreases in numbers of circulating lymphocytes in patients with MoM implants (Savarino et al., 1999, Hart et al., 2006). Resting and anti-CD3 ± anti-CD28 activated lymphocytes were exposed 0.1, 1, 10 and 100 µM Cr<sup>6+</sup> and Co<sup>2+</sup>, individually and in combination *in vitro*.

It was observed that Cr<sup>6+</sup> exposure led to a decrease of lymphocyte viability in resting and anti-CD3 activated lymphocytes to a similar extent with respect to their unexposed controls. This was particularly evident at 10 and 100 µM, and these concentrations of Cr<sup>6+</sup> also significantly decreased cell proliferation following activation. Flow cytometric data demonstrated that the reduced cell viability and proliferation of lymphocytes was due to the initiation of apoptosis following chromium exposure. Pre-treatment of lymphocytes with a caspase-3 inhibitor did not inhibit the apoptosis induced following metal ion exposure. Exposure to high levels of Cr<sup>6+</sup> led to MOMP. This occurred irrespective of caspase inhibition. Therefore, attempting to inhibit the induced apoptosis by inhibiting caspase-3 activity was unlikely to work as the mitochondrial damage occurs upstream from caspase activation.

As with the U937 cell line, Cr<sup>6+</sup> was more toxic to primary human lymphocytes than Co<sup>2+</sup>. Exposure to chromium ions consistently had a greater negative effect on the viability and function of lymphocytes compared with cobalt ion exposure. Only exposure to 100 µM Co<sup>2+</sup> led to a significant decrease in cell viability of resting lymphocytes; this was also accompanied by an increase in mitochondrial damage and

apoptosis. However, in activated lymphocytes 10 and 100  $\mu\text{M}$   $\text{Co}^{2+}$  treatment led to reduced viability and proliferation, but an increase in apoptosis was only measured in cells exposed to 100  $\mu\text{M}$   $\text{Co}^{2+}$ . The greater decrease in viability of activated lymphocytes (at 10 $\mu\text{M}$   $\text{Co}^{2+}$ ) indicates that  $\text{Co}^{2+}$  may be acting through additional mechanisms, which also reduce cell proliferation, rather than simply initiating apoptosis. It is postulated that  $\text{Co}^{2+}$  may also inhibit intracellular processes such as calcium trafficking. Through this mechanism,  $\text{Co}^{2+}$  concentrations that are not directly cytotoxic to lymphocytes may affect events at a molecular level impeding lymphocyte activation and proliferation.

$\text{IFN}\gamma$ , IL-2 and  $\text{TNF}\alpha$ , release was inhibited following metal ion exposure to activated lymphocytes. The reduction in  $\text{IFN}\gamma$  and  $\text{TNF}\alpha$  release occurred following exposure to concentrations of metal ions which also led to a reduction in cell viability and proliferation. Hence, it was concluded that production of these two cytokines was reduced because the activated lymphocytes became apoptotic and non-viable, and thus unable to produce these key cytokines. In contrast, IL-2 release was reduced at the lowest concentrations of metal ions where no other adverse effects were measured. In addition, IL-2 supplementation to metal ion exposed activated lymphocytes did not increase cell proliferation. As well as this, co-stimulation (with anti-CD28), which enhances IL-2 release and other survival factors in lymphocytes, did not reverse any of the adverse effects observed following metal ion exposure. This indicates that although the metal ions inhibited IL-2 release, this was not directly involved in the mechanism by which these two metal ions affected proliferation or induced apoptosis in lymphocytes.

Although high concentrations of  $\text{Cr}^{6+}$  and  $\text{Co}^{2+}$  are cytotoxic, exposure to both ions in combination did not lead to any significant synergistic effects. This again may be due the extreme toxicity of these ions, and exposure to lower concentrations may have been able to identify synergy.

### 7.1.3 *In vivo* response to CoCr implant wear debris

The initial stages of this thesis have dealt with the *in vitro* toxicity from metal ions released from MoM hip implants. Despite providing valuable data, the limitations of *in vitro* models have led the author to develop an *in vivo* model of host interactions with CoCr wear debris that could provide more useful information. A rodent air-pouch model was modified to assess the distribution of metal ions in blood and organs in addition to assessing the local and systemic immunological effects of the CoCr wear debris generated from a hip implant by a mechanical simulator.

We observed increased levels of Co, Cr and Mo in blood for up to 72 hours following the introduction of CoCr wear debris into the mouse air-pouch; the levels of Co were highest and remained elevated for 7 days. Co levels were elevated in all organs studied (liver, kidney, spleen, lung, heart, brain and testes), with the peak at 48h, and the highest levels measured in liver and kidney ( $838.94 \pm 223.66$  ng/g in liver, and  $938.79 \pm 131.61$  ng/g in kidney). Levels of Cr in organs were considerably lower than those for Co, for example, Cr in kidney was  $117.24 \pm 12.61$  ng/g tissue at 48 h. Co ions were more mobile than Cr, reaching higher levels at earlier time points. This could be a reflection of the debris composition (which was primarily Co), the valency of Cr ion released ( $\text{Cr}^{3+}$  may be released from the CoCr debris rather than the more mobile  $\text{Cr}^{6+}$ ) or local tissue binding of Cr ions as discussed by Langton et al (2010).

Analysis of the inflammatory exudates showed that CoCr wear debris induced a different inflammatory pattern compared with LPS, which was used as a positive control to induce an inflammatory response. LPS induced a strong early (at 4 hours) neutrophil influx into the pouch with monocyte/macrophage influx peaking at 24 hours, whereas CoCr wear debris initiated almost equal numbers of early monocyte/macrophage and neutrophil recruitment. Histological analysis also showed that CoCr debris which became embedded deep within the pouch tissue was surrounded by a vast cellular infiltration, with fibrosis and granuloma formation around the debris. The majority of the cells which encircled the debris had a monocytic morphology. The encapsulation of CoCr debris within fibrous tissue and

monocytes remained in place for the duration of the experiment, whereas the number of cells within the tissue of LPS-treated pouches was reduced at 7 days.

Assessment of inflammatory gene transcripts from air-pouch tissue, excised at 24 hours, showed that CoCr wear debris increased expression of cytokines involved in promoting inflammation and fibrosis (IL-1 $\beta$ , TGF- $\beta$ ) and chemokines which promote recruitment of neutrophils and monocytes/macrophages (CXCL2, CCL2). Although LPS treatment also led to an upregulation of these gene transcripts, in addition it caused pronounced up-regulation of certain chemokines such as CCL4 and CXCL13, which were not as up-regulated by CoCr stimulation. This demonstrates that CoCr debris provokes a specific inflammatory response which is distinct from LPS.

In addition, there was little evidence demonstrating significant effects, in terms of viability and apoptosis, on lymphocytes isolated from the draining lymph nodes of CoCr treated mice, either in their resting or activated states.

It is clear that the current *in vivo* model simulates processes in the pathology of adverse effects from MoM hip implants described in the literature. In addition, implantation of CoCr wear debris from a MoM hip resurfacing implant lead to an inflammatory process which is distinct from that induced by LPS. The process involves infiltration of inflammatory cells, primarily monocytes/macrophages, as well as granuloma and fibrous capsule formation around the debris. Monocytes/macrophages not only have a key role in the above processes in the *in vivo* mouse model, but may also be highly significant in the chronic inflammatory response observed following MoM hip arthroplasty. The author believes that the data presented indicate that the adverse effects of MoM implants are a result of a sterile inflammatory response that is mediated via monocytes/macophages. The release of wear debris *in situ* is continuous for the life-time of an implant, whereas the current model only provides the equivalent of a single release of wear debris leading to a transient response. Therefore, it is suggested that this *in vivo* air-pouch model would need modification such that additional serial doses could be introduced into the pouch to simulate continuous release of wear debris.

#### **7.1.4 Effects of metal-on-metal arthroplasty on lymphocytes *in vivo* in patients**

Reduced levels of white blood cells, particularly lymphocytes, have been reported following MoM hip arthroplasty. Two clinical studies were implemented in order to assess whether levels of circulating lymphocytes were altered following MoM hip arthroplasty with different types of implant. The first prospective study compared the levels of WBCs following hip resurfacing using either DePuy ASR prostheses or Zimmer Durom prostheses. The second study compared WBCs following hip THR using either CoM or MoM bearing surfaces. The Cr and Co ions levels within whole blood were also determined to identify any correlations between WBC levels and ion concentration.

In the first study it was shown that in patients 2 years post-operative, using either hip resurfacing implant, there was a significant reduction in the number of circulating WBCs and B-lymphocytes. The significant reduction in circulating WBCs following DUROM resurfacing was also measured at 1 year post arthroplasty. No significant effects were observed in T-lymphocyte number following either MoM hip resurfacing arthroplasty. However, there was a consistent insignificant decrease in T-lymphocyte numbers following ASR implantation at all time points, and this may not have reached statistical significance due to the small sample size. Although whole blood levels of Cr were significantly increased following MoM hip resurfacing arthroplasty and Co levels were observed to increase following ASR implantation, there was minimal evidence of any correlation between the changes in numbers of WBCs (and lymphocytes) and whole blood ion levels in this study.

It was demonstrated from the second clinical study that THR, using either CoM or MoM bearing surfaces, did not lead to any significant changes in the numbers of circulating WBC or lymphocytes despite a small incremental increase in whole blood Cr and Co ion levels. It is the author's belief that circulating WBCs and lymphocyte numbers are reduced due to the type of prostheses and its clinical performance rather than to a direct relationship with whole blood ion levels. In addition, the author

supports the view that metal ion levels may be raised as a consequence of excessive wear from the bearing surfaces and could be used a surrogate for clinical performance (De Smet et al., 2008). It is the author belief that although MoM implants may lead to increased levels of circulatory metal ions, a well designed and correctly implanted MoM prosthesis does not have any shortcomings compared to other bearing surface couples such as CoM.

### **7.1.5 Major findings of thesis**

The major findings of this thesis are:

- Clinically relevant concentrations of  $\text{Cr}^{6+}$  and  $\text{Co}^{2+}$  induce apoptosis in U937 cells, *in vitro*.
- Exposure of primary human lymphocytes to  $\text{Cr}^{6+}$  and  $\text{Co}^{2+}$  at clinically relevant concentrations, *in vitro*, results in mitochondrial damage leading to apoptosis.
- *In vivo* implantation of CoCr wear debris from a MoM hip resurfacing prosthesis into mice leads to an inflammatory process in which monocytes/macrophage have a central role.
- CoCr wear debris implantation results in the accumulation of Cr and, in particularly, Co ions within the circulation and distant organs.
- MoM hip resurfacing arthroplasty results in increased levels of Cr and Co ions within whole blood.
- WBC and B-lymphocyte numbers within peripheral blood are reduced following MoM hip resurfacing implant.
- No change in whole blood metal ions or levels of WBCs are observed following THR with either CoM or MoM implants

## 7.2 Limitations of studies

Although the current thesis has demonstrated that metal ions and debris released from MoM hip implants can have detrimental effects, there are a number of limitations within each of the individual studies. Firstly, the *in vitro* data from chapters 3 and 4 have shown that high concentrations of Cr<sup>6+</sup> or Co<sup>2+</sup> are toxic to U937 cells and T-lymphocytes. However, the *in vitro* environment may not be reflective of the *in vivo* setting and it can be difficult to extrapolate *in vitro* findings to the mechanism *in vivo*, particularly in the case of immune responses as the isolated *in vitro* environment, as in chapters 3 and 4, is not reflective of the immune response *in vivo*. For instance, T-lymphocytes are unable to identify and respond to foreign or infectious bodies on their own and require interaction and cooperation with other WBCs in order to activate and produce a response. In addition to this, as the donors of the buffy coat were anonymous it was not possible to determine whether there was any previous exposure to metal debris or ions (e.g. currently having a MoM prosthesis or industrial exposure to metals). This could alter the responses *in vitro* after lymphocyte isolation. However, as the experiments were repeated with different donors of buffy coat it would be unlikely that all donors would have had a previous exposure to high levels of metal ions.

In addition to the above, the concentrations at which metal ions had a toxic effect on cells were relatively high. As described in section 1.4.2, the exact level of metal ions following MoM hip arthroplasty can vary substantially. The data showed that high concentrations induce toxic effects *in vitro*, whereas there was little effect observed following exposure to the lower concentrations. The metal ion concentrations within the blood of MoM arthroplasty patients tend to be around 0.02-0.07 µM. This is lower than smallest concentration used within the *in vitro* studies. Therefore, it could be argued that the data has little or no clinical relevance. Although the current author does acknowledge that the concentrations used were high there are also cases of high blood metal ions as well as extremely high concentrations measured around failed prostheses (described in section 1.4.2).

Further to the concentration, the duration of *in vitro* exposure also differs to the *in vivo* situation. Cells were exposed acutely to metal ions *in vitro*, however, the evidence presented in chapter 1 indicates that the adverse effects are due to a chronic exposure of high levels of metal. Hence, it may be difficult to extrapolate the effects of a large acute dose *in vitro* to a smaller chronic dose *in vivo*.

Although it is difficult to extrapolate *in vitro* data to *in vivo* settings, there are also limitations in relating data from an *in vivo* animal model to the findings in patients following MoM hip arthroplasty. As discussed in section 5.5 the dose of CoCr wear debris administered to the animals was higher than a lifetime of debris produced from a MoM implant. Even though the findings from the animal model displayed similarities with data from MoM hip arthroplasty patients, the author acknowledges that the effects observed with the animal model may have been different had a lower dose been administered. In addition to this, animals were only given a single dose of wear debris and it was assumed that the debris would be contained within the air-pouch and any migration of wear debris and ions would occur slowly. However, this was not the case and it is evident that the administered dose migrates rapidly and produces an acute effect where the majority of responses cease at 7 days post CoCr debris administration. As mentioned previously, this is not the case in MoM hip arthroplasty patients, metal wear debris and ions are continuously released from the implant. This leads to a chronic response and as with the *in vitro* studies a large acute dose may not produce the same effects as smaller more chronic doses.

There were also a number of limitations with regards to the clinical studies presented in chapter 6. Firstly, it is evident that the number of patients in certain groups was low, particularly in the ASR group of patients. This primarily led to data which showed small changes over time that were statistically not significant. In addition, the low number of patients, particularly at 1 and 2 years post surgery, also made it difficult to identify any significant changes in WBC numbers at any stage where metal wear or ions could induce an effect. In addition, although the patients were relatively healthy upon receiving the prosthesis it was not ascertained whether there were any previous environmental or industrial exposures to metals that may have



affected the levels of metal ions or WBCs. Finally, it was also not established whether the patients were taking any dietary supplements post surgery that may have altered the level of metal ions determined.

## **7.3 Future work**

### **7.3.1 Mechanism of CoCr debris induced inflammation**

The results indicate that CoCr wear debris leads to an inflammatory process in which monocytes/macrophages have a central role. In addition, there have been reports that chromium and cobalt ions as well as engineered CoCr microparticles can induce an inflammatory process, resulting in IL-1 $\beta$  secretion, that is mediated via the NLRP3 (NOD-like receptor family, pyrin domain containing 3) inflammasome (Caicedo et al., 2009). The NLRP3 inflammasome is a multi-protein that forms a complex with ASC (apoptosis-associated speck-like protein containing a CARD) which in turn binds to pro-caspase-1 to activate caspase-1 (Chen et al., 2011). Proteins containing the caspase recruitment domain (CARD) are reported to be involved in inflammation and the immune response. This leads to a cascade of events that result in IL-1 $\beta$  and IL-18 secretion.

It would be beneficial to determine whether the inflammatory process following CoCr wear debris implantation is mediated via the NLRP3 inflammasome. It is proposed to expose NLRP3 deficient mice to CoCr wear debris as in chapter 6 and compare the response with exposed wild-type mice. This could identify the processes which lead to the adverse effects following MoM arthroplasty. In addition, the findings from this may be validated by analyzing the expression of NLRP3, ASC, caspase-1 and IL-1 $\beta$  from tissue excised from patients with a failed MoM hip implant prior to revision surgery.

Further to this, should the results be positive from the above proposed studies, mice implanted with CoCr wear debris could be treated with IL-1 receptor antagonists, i.e.

Anakinra, or caspase-1 inhibitor as a possible therapeutic intervention to wear debris induced inflammation.

### **7.3.2 Chronic *in vivo* experiment**

Although the current study has found CoCr wear debris to elicit an inflammatory process which results in cellular infiltration and fibrosis, the response appears to be acute unlike the chronic response observed in MoM arthroplasty patients. It is suggested that the *in vivo* model described earlier only mimics a single release of wear debris *in situ*. It would be valuable to develop this model such that a chronic inflammatory response is induced. It is proposed that repeated lower doses of CoCr be introduced into the pouch, e.g. 0.05mg every 72 hours. This may mimic the continuous wear of a MoM hip implant *in situ* more accurately.

### **7.3.3 Specificity of wear debris effects**

It has previously been stated that MoM hip implants produce a distinct inflammatory process which differs from that which is induced following MoP implantation (Doorn et al., 1996). Due to the adverse effects of MoM bearing surfaces and the accompanying negative publicity, many manufacturers and clinicians have shifted toward other bearing couples such CoM. The author proposes a comparative study which would assess the effects of CoM wear debris and MoM wear debris. This would be assessed using existing *in vitro* and *in vivo* methods.

*In vitro* study: Primary human lymphocytes and monocytes would be exposed *in vitro*, to the wear debris at a range of concentrations to assess any cytotoxic and/or stimulatory effects of these two different wear particles by initially measuring cell viability, apoptosis, cell activation, proliferation and secretion of cytokines. Dependent on these findings, mechanisms of toxicity and/or stimulatory effects would be further determined.

*In vivo* study: Using a concentration determined from the *in vitro* study, CoM wear debris would be implanted into mice using methods similar to those in Chapter 5. As in this chapter the inflammatory process could be assessed via analysis of the inflammatory exudate, histological analysis of implant tissue and effects on the draining lymph nodes. This could be followed up by examining the expression of inflammatory chemokines and cytokines in the implantation site.

## **7.4 Implications for the safety and future development of hip implants**

The current thesis has shown that  $\text{Cr}^{6+}$  and  $\text{Co}^{2+}$  ions are toxic to primary human lymphocytes. However, the concentrations at which these ions became toxic was higher than the levels measured within the whole blood of MoM hip arthroplasty patients. At present the MHRA has set a metal ion concentration safety threshold of  $7 \mu\text{g/l}$  within the whole blood of patients following hip arthroplasty. Although this is substantially lower than the toxic concentration *in vitro*, it has been shown that metal ion concentrations around the hip prosthesis are higher than those recorded within the circulation. Therefore, the author believes that the MHRA safety level is adequate, and that circulatory metal ion concentrations should be regularly analysed following MoM hip arthroplasty as an indicator for implant performance.

Although  $\text{Cr}^{6+}$  ions are more toxic than  $\text{Co}^{2+}$  *in vitro*, the data from the *in vivo* and clinical studies suggest that cobalt ions are more mobile and disseminate through the circulation and into the organs to a greater extent than chromium ions. It is possible that this could be as a result of the formation of chromium complexes locally around the prosthesis, as mentioned earlier. Whilst low levels of circulating metal ions could be indicative of a well functioning implant, it may not completely reflect the local environment. Therefore, the author believes that additional clinical diagnostics should be utilised to ensure safe functioning of the prostheses.

Furthermore, the authors believes that although increasing the follow-up checks in patients with MoM hip prosthesis could identify any adverse effects from the implant before they become severe, more stringent safety testing procedures are required prior to new implants being introduced into the market. Despite, *in vitro* simulator testing which demonstrated that MoM articulations were superior to MoP in terms of wear, there was no indication of the problems that would arise from the larger surface area of the nano-particulate debris produced from MoM implants. This current thesis has used *in vitro and in vivo* studies to demonstrate that metal ions and debris from MoM implants can lead to adverse immunological changes. Since the problems with MoM articulations have arisen and come to public knowledge, the hip implant industry have made a shift from MoM to other supposed 'superior' bearing couples such as CoM and CoC with little more solid data available than was available previously when MoM was stated to be superior to MoP. The author believes that bodies such as the MHRA need to create more stringent safety testing procedures to ensure that information on the release of ions/debris by corrosion/wear, their dissemination and fate in the body, and both short and long term effects on body systems are in place before orthopaedic implants are released for widespread implantation rather than seek a remedy or shift to another material once these implants fail.

# APPENDIX

## Appendix 1. List of TLDA gene targets

Comments	Detector	Comments	Detector
Eukaryotic 18S rRNA	Hs99999901_s1	chemokine (C-X-C motif) ligand 2	Mm00436450_m1
interleukin 1 beta	Mm00434228_m1	chemokine (C-X-C motif) ligand 5	Mm00436451_g1
tumor necrosis factor	Mm00443258_m1	chemokine (C-X-C motif) ligand 10	Mm00445235_m1
interferon gamma	Mm00801778_m1	chemokine (C-X-C motif) ligand 11	Mm00444662_m1
chemokine (C-X3-C motif) ligand 1	Mm00436454_m1	chemokine (C-X-C motif) ligand 12	Mm00445553_m1
chemokine (C-C motif) ligand 2	Mm00441242_m1	chemokine (C-X-C motif) ligand 13	Mm00444534_m1
chemokine (C-C motif) ligand 3	Mm00441258_m1	chemokine (C-X-C motif) ligand 14	Mm00444699_m1
chemokine (C-C motif) ligand 5	Mm01302427_m1	interleukin 4	Mm00445259_m1
chemokine (C-C motif) ligand 6	Mm01302419_m1	interleukin 12b	Mm01288990_m1
chemokine (C-C motif) ligand 7	Mm00443113_m1	interleukin 13	Mm00434204_m1
chemokine (C-C motif) ligand 17	Mm00516136_m1	interleukin 17A	Mm00439619_m1
chemokine (C-C motif) ligand 19	Mm00839967_g1	interleukin 22	Mm00444241_m1
chemokine (C-C motif) ligand 20	Mm00444228_m1	interleukin 10	Mm00439616_m1
chemokine (C-C motif) ligand 21A,B,C	Mm03646971_gH	transforming growth factor, beta 1	Mm00441724_m1
chemokine (C-C motif) ligand 22	Mm00436439_m1	TATA box binding protein	Mm00446971_m1
chemokine (C-C motif) ligand 4	Mm00443111_m1		
chemokine (C-C motif) ligand 27A	Mm01215829_m1		

**Appendix 1. List of TLDA gene targets used in the assay.** All genes are shown with accession code taken from ABI website (which contains full primer sequences). Genes with the post-script \_m1 are primers which cross introns (and will not target genomic DNA). Genes with the post-script \_s1, g1 or gH may detect genomic DNA, which is why a DNase step is included in the preparation of cDNA used in the assay.

## Appendix 2. Correlation between changes in Cr or Co ion blood metal levels and changes in WBCs and lymphocyte following MoM hip resurfacing

	ASR				DUROM			
	1 YR		2 YR		1 YR		2YR	
	Cr	Co	Cr	Co	Cr	Co	Cr	Co
<b>WBC</b>	0.12	0.13	0.048	0.05	0.03 <sup>+</sup>	0.01	<0.01 <sup>+</sup>	0.01
<b>CD3</b>	0.17	0.17	0.13	0.08	0.04	0.22 <sup>+</sup>	0.05 <sup>+</sup>	0.19 <sup>+</sup>
<b>CD4</b>	0.20	0.15	0.24	0.20	0.04 <sup>+</sup>	0.03 <sup>+</sup>	0.08 <sup>+</sup>	0.13 <sup>+</sup>
<b>CD8</b>	0.05	0.11	0.01	<0.01	0.02 <sup>+</sup>	0.06 <sup>+</sup>	0.01 <sup>+</sup>	0.04 <sup>+</sup>
<b>CD20</b>	<0.01	0.03	0.18	0.24	<0.01 <sup>+</sup>	0.06 <sup>+</sup>	<0.01	0.01

Appendix 2. R<sup>2</sup> values demonstrating correlation between changes in Cr or Co ion blood metal levels and changes in WBCs and lymphocyte populations at 1 and 2 years post MoM arthroplasty using either ASR or Durom implants. r<sup>2</sup> values indicate the inverse correlation between changes in metal ions and changes in the different WBCs. <sup>+</sup>Indicates a positive correlation between the two parameters.

## Appendix 3. List of publications

### Published papers.

Akbar M, Brewer J, Grant MH, Effect of Chromium and Cobalt Ions on Primary Human Lymphocytes *In Vitro*, *The Journal of Immunotoxicology*, 8: 140-9, 2011

### Papers submitted for publication

Akbar M, Fraser A, G Graham, Brewer J, Grant MH, Inflammatory Response to Cobalt Chromium Orthopaedic Wear Debris in a Rodent Air-pouch Model, *Journal of the Royal Society Interface*, Submitted for publication, August 2011

Afolaranmi GA, Akbar M, Brewer J, Grant MH, Distribution of ions released from cobalt chromium (Co-Cr) alloy orthopaedic wear particles implanted into air pouches in mice. *Journal of Biomedical Materials Research Part A*, Submitted for publication, July 2011

Afolaranmi GA, Akbar M, Farmer JG, Brewer J, Grant MH, Meek RMD, Blood Metal Ion Levels after Hip resurfacing Arthroplasty using Durom or ASR Implants, *The Journal of Bone and Joint Surgery (British Volume)*, April 2011

### **Conference proceedings.**

Akbar M, Brewer J, Grant MH, Interaction of Metal Ions with Human Lymphocytes. Poster Communication at the 12<sup>th</sup> Combined Meeting of the Orthopaedic Associations, Glasgow, UK, September 2010.

Akbar M, Brewer J, Grant MH, Inflammatory response to orthopaedic cobalt chromium alloy wear debris in a rodent air pouch model. Poster communication at the XII International Congress of Toxicology, Barcelona, Spain, July 2010. *Toxicology Letters* 196S:199

Akbar M, Brewer J, Grant MH, Chromium and Cobalt Ions Cause Apoptosis in Human Lymphocytes *In Vitro*. Oral communication presented at the British Toxicology Society Autumn Meeting, Durham, UK, September 2009. This abstract has been reviewed and accepted for publication in '*Toxicology*'.

## REFERENCES

- No author listed. (2005) Table 1: List of approved workplace exposure limits (as consolidated with amendments October 2007).
- No author listed. (2008) Fifth Annual Report. National Joint Registry for England and Wales.
- No author listed. (2010) Australian National Joint Replacement Registry. *Annual Report*.
- No author listed. (2010) Seventh Annual Report. National Joint Registry for England and Wales.
- AL-SAFFAR, N., KADOYA, Y. & REVELL, P. (1994) The role of newly formed vessels and cell adhesion molecules in the tissue response to wear products from orthopaedic implants. *Journal of Materials Science: Materials in Medicine*, 5, 813-818.
- ALLEN, M. J., MYER, B. J., MILLETT, P. J. & RUSHTON, N. (1997) The effects of particulate cobalt, chromium and cobalt-chromium alloy on human osteoblast-like cells in vitro. *Journal of Bone and Joint Surgery - British Volume*, 79-B, 475-482.
- AMSTUTZ, H. C. & GRIGORIS, P. (1996) Metal on Metal Bearings in Hip Arthroplasty. *Clinical Orthopaedics and Related Research*, 329S, 11-34.
- ANDERSON, J. M. (1994) In vivo biocompatibility of implantable delivery systems and biomaterials. *European Journal of Pharmaceutics and Biopharmaceutics*, 40, 1-8.
- ANDERSON, R. A. (1989) Essentiality of chromium in humans. *Science of The Total Environment*, 86, 75-81.
- ANDERSON, R. A. (1997) Chromium as an Essential Nutrient for Humans. *Regulatory Toxicology and Pharmacology*, 26, S35-S41.
- ANDRIS, F., DENANGLAIRE, S., DE MATTIA, F., URBAIN, J. & LEO, O. (2004) Naive T Cells Are Resistant to Anergy Induction by Anti-CD3 Antibodies. *The Journal of Immunology*, 173, 3201-3208.
- AYALA-FIERRO, F., FIRRIOLO, J. M. & CARTER, D. E. (1999) Disposition, Toxicity, and Intestinal Absorption of Cobaltous Chloride in Male Fischer 344 Rats. Taylor & Francis.
- BACK, D. L., YOUNG, D. A. & SHIMMIN, A. J. (2005) How do serum cobalt and chromium levels change after metal-on-metal hip resurfacing? *Clinical orthopaedics and related research*, 438, 177-181.
- BAGCHI, D., JOSHI, S. S., BAGCHI, M., BALMOORI, J., BENNER, E. J., KUSZYNSKI, C. A. & STOHS, S. J. (2000) Cadmium- and chromium-induced oxidative stress, DNA damage, and apoptotic cell death in cultured human chronic myelogenous leukemic K562 cells, promyelocytic leukemic HL-60 cells, and normal human peripheral blood mononuclear cells. *Journal of Biochemical and Molecular Toxicology*, 14, 33-41.
- BARATZ, M., IMBRIGLIA, J. E. & WATSON, A. D. (1999) Biomaterials. *Orthopedic Surgery: The Essentials* New York, Thieme.
- BARBOSA, J. N., BARBOSA, M. A. & ÁGUAS, A. P. (2004) Inflammatory responses and cell adhesion to self-assembled monolayers of alkanethiolates on gold. *Biomaterials*, 25, 2557-2563.



- BIRX, D. L., BERGER, M. & FLEISHER, T. A. (1984) The interference of T cell activation by calcium channel blocking agents. *The Journal of Immunology*, 133, 2904-2909.
- BLANK, C. & MACKENSEN, A. (2007) Contribution of the PD-L1/PD-1 pathway to T-cell exhaustion: an update on implications for chronic infections and tumor evasion. *Cancer Immunology, Immunotherapy*, 56, 739-745.
- BLASIAK, J. & KOWALIK, J. (2000) A comparison of the in vitro genotoxicity of tri- and hexavalent chromium. *Mutation Research/Genetic Toxicology and Environmental Mutagenesis*, 469, 135-145.
- BOARDMAN, D. R., MIDDLETON, F. R. & KAVANAGH, T. G. (2006) A benign psoas mass following metal-on-metal resurfacing of the hip. *Journal of Bone and Joint Surgery - British Volume*, 88-B, 402-404.
- BOEHLER, M., KNAHR, K., PLENK, H., JR., WALTER, A., SALZER, M. & SCHREIBER, V. (1994) Long-term results of uncemented alumina acetabular implants. *Journal of Bone and Joint Surgery - British Volume*, 76-B, 53-59.
- BOISE, L. H., MINN, A. J., NOEL, P. J., JUNE, C. H., ACCAVITTI, M. A., LINDSTEN, T. & THOMPSON, C. B. (1995a) CD28 costimulation can promote T cell survival by enhancing the expression of Bcl-xL. *Immunity*, 3, 87-98.
- BOISE, L. H., NOEL, P. J. & THOMPSON, C. B. (1995b) CD28 and apoptosis. *Current Opinion in Immunology*, 7, 620-625.
- BOSS, J. H., SHAJRAWI, I., SOUDRY, M. & MENDES, D. G. (1990) Histological features of the interface membrane of failed isoelastic cementless prostheses. *International Orthopaedics*, 14, 399-403.
- BRAVO, I., CARVALHO, G. S., BARBOSA, M. A. & DE SOUSA, M. (1990) Differential effects of eight metal ions on lymphocyte differentiation antigens in vitro. *J Biomed Mater Res*, 24, 1059-68.
- BRENNER, D., KRAMMER, P. H. & ARNOLD, R. (2008) Concepts of activated T cell death. *Critical Reviews in Oncology/Hematology*, 66, 52-64.
- BRINK, N. G., KUEHL, F. A., JR. & FOLKERS, K. (1950) Vitamin B12: the identification of vitamin B12 as a cyano-cobalt coordination complex. *Science*, 112, 354-360.
- BROWN, S. A., FARNSWORTH, L. J., MERRITT, K. & CROWE, T. D. (1988) In vitro and in vivo metal ion release. *Journal of Biomedical Materials Research*, 22, 321-338.
- BROWN, S. R., DAVIES, W. A., DEHEER, D. H. & SWANSON, A. B. (2002) Long-Term Survival of McKee-Farrar Total Hip Prostheses. *Clinical Orthopaedics and Related Research*, 402, 157-163.
- BRUNE, D. A. G., KJÆRHEIM, A., PAULSEN, G. & BELTESBREKKE, H. (1980) Pulmonary deposition following inhalation of chromium-cobalt grinding dust in rats and distribution in other tissues. *European Journal of Oral Sciences*, 88, 543-551.
- CAICEDO, M. S., DESAI, R., MCALLISTER, K., REDDY, A., JACOBS, J. J. & HALLAB, N. J. (2009) Soluble and particulate Co-Cr-Mo alloy implant metals activate the inflammasome danger signaling pathway in human macrophages: A novel mechanism for implant debris reactivity. *Journal of Orthopaedic Research*, 27, 847-854.

- CAICEDO, M. S., PENNEKAMP, P. H., MCALLISTER, K., JACOBS, J. J. & HALLAB, N. J. (2010) Soluble ions more than particulate cobalt-alloy implant debris induce monocyte costimulatory molecule expression and release of proinflammatory cytokines critical to metal-induced lymphocyte reactivity. *Journal of Biomedical Materials Research Part A*, 93A, 1312-1321.
- CAMPBELL, P., DOORN, P., DOREY, F. & AMSTUTZ, H. C. (1996) Wear and morphology of ultrahigh molecular weight polyethylene wear particles from total hip replacements. *Journal of Engineering in Medicine*, 210, 167-174.
- CARLISLE, D. L., PRITCHARD, D. E., SINGH, J., OWENS, B. M., BLANKENSHIP, L. J., ORENSTEIN, J. M. & PATIERNO, S. R. (2000) Apoptosis and P53 Induction in Human Lung Fibroblasts Exposed to Chromium (VI): Effect of Ascorbate and Tocopherol. *Toxicological Sciences*, 55, 60-68.
- CARMO PEREIRA, M. D., DE LOURDES PEREIRA, M. & SOUSA, J. P. (1999) Individual study of chromium in the stainless steel implants degradation: An experimental study in mice. *BioMetals*, 12, 277-282.
- CARTER, D. E. (1995) Oxidation-reduction reactions of metal ions. *Environmental Health Perspectives*, 103, 17-9.
- CASE, C. P., LANGKAMER, V. G., JAMES, C., PALMER, M. R., KEMP, A. J., HEAP, P. F. & SOLOMON, L. (1994) Widespread dissemination of metal debris from implants. *Journal of Bone and Joint Surgery - British Volume*, 76-B, 701-712.
- CASE, C. P., LANGKAMER, V. G., LOCK, R. J., PERRY, M. J., PALMER, M. R. & KEMP, A. J. (2000) Changes in the proportions of peripheral blood lymphocytes in patients with worn implants. *Journal of Bone and Joint Surgery - British Volume*, 82-B, 748-754.
- CATELAS, I., PETIT, A., VALI, H., FRAGISKATOS, C., MEILLEUR, R., ZUKOR, D. J., ANTONIOU, J. & HUK, O. L. (2005) Quantitative analysis of macrophage apoptosis vs. necrosis induced by cobalt and chromium ions in vitro. *Biomaterials*, 26, 2441-2453.
- CHEN, G. Y. & NUNEZ, G. (2010) Sterile inflammation: sensing and reacting to damage. *Nat Rev Immunol*, 10, 826-837.
- CHEN, M., WANG, H., CHEN, W. & MENG, G. (2011) Regulation of adaptive immunity by the NLRP3 inflammasome. *International Immunopharmacology*, 11, 549-554.
- CLARKE, M. T., LEE, P. T. H., ARORA, A. & VILLAR, R. N. (2003) Levels of metal ions after small- and large-diameter metal-on-metal hip arthroplasty. *Journal of Bone & Joint Surgery, British Volume* 85-B, 913-917.
- COBB, A. & SCHMALZREID, T. (2006) The clinical significance of metal ion release from cobalt-chromium metal-on-metal hip joint arthroplasty. *Proceedings of the Institution of Mechanical Engineers, Part H: Journal of Engineering in Medicine*, 220, 385-398.
- COOGAN, T. P., SQUIBB, K. S., MOTZ, J., KINNEY, P. L. & COSTA, M. (1991) Distribution of chromium within cells of the blood. *Toxicology and Applied Pharmacology*, 108, 157-166.
- COSTA, M. (1997) Toxicity and Carcinogenicity of Cr(VI) in Animal Models and Humans. *Critical Reviews in Toxicology*, 27, 431-442.

- COUNSELL, A., HEASLEY, R., ARUMILLI, B. & PAUL, A. (2008) A groin mass caused by metal particle debris after hip resurfacing. *Acta Orthopaedica Belgica*, 74, 870-874.
- DANIEL, J., ZIAEE, H., PRADHAN, C., PYNSENT, P. B. & MCMINN, D. J. W. (2007) Blood and urine metal ion levels in young and active patients after Birmingham hip resurfacing arthroplasty: FOUR-YEAR RESULTS OF A PROSPECTIVE LONGITUDINAL STUDY. *Journal of Bone and Joint Surgery - British Volume*, 89-B, 169-173.
- DANIEL, J., ZIAEE, H., SALAMA, A., PRADHAN, C. & MCMINN, D. J. W. (2006) The effect of the diameter of metal-on-metal bearings on systemic exposure to cobalt and chromium. *Journal of Bone and Joint Surgery*, 88-B, 443-448.
- DAVIES, A. P., WILLERT, H. G., CAMPBELL, P. A., LEARMONTH, I. D. & CASE, C. P. (2005) An Unusual Lymphocytic Perivascular Infiltration in Tissues Around Contemporary Metal-on-Metal Joint Replacements. *The Journal of Bone and Joint Surgery (American)*, 87, 18-27.
- DE HAAN, R., PATTYN, C., GILL, H. S., MURRAY, D. W., CAMPBELL, P. A. & DE SMET, K. (2008) Correlation between inclination of the acetabular component and metal ion levels in metal-on-metal hip resurfacing replacement. *Journal of Bone and Joint Surgery - British Volume*, 90-B, 1291-1297.
- DE SMET, K., DE HAAN, R., CALISTRI, A., CAMPBELL, P. A., EBRAMZADEH, E., PATTYN, C. & GILL, H. S. (2008) Metal Ion Measurement as a Diagnostic Tool to Identify Problems with Metal-on-Metal Hip Resurfacing. *The Journal of Bone and Joint Surgery*, 90, 202-208.
- DEARNLEY, P. (1999) A review of metallic, ceramic and surface-treated metals used for bearing surfaces in human joint replacements. *Proceedings of the Institution of Mechanical Engineers, Part H: Journal of Engineering in Medicine*, 213, 107-135.
- DELAUNAY, C., PETIT, I., LEARMONTH, I. D., OGER, P. & VENDITTOLI, P. A. (2010) Metal-on-metal bearings total hip arthroplasty: The cobalt and chromium ions release concern. *Orthopaedics & Traumatology: Surgery & Research*, 96, 894-904.
- DESHMANE, S. L., KREMLEV, S., AMINI, S. & SAWAYA, B. E. (2009) Monocyte Chemoattractant Protein-1 (MCP-1): An Overview. *Journal of Interferon & Cytokine Research*, 29, 313-326.
- DOORN, P. F., MIRRA, J. M., CAMPBELL, P. A. & AMSTUTZ, H. C. (1996) Tissue Reaction to Metal on Metal Total Hip Prostheses. *Clinical Orthopaedics and Related Research*, 329s, 187-205.
- DUNSTAN, E., LADON, D., WHITTINGHAM-JONES, P., CARRINGTON, R. & BRIGGS, T. W. R. (2008) Chromosomal Aberrations in the Peripheral Blood of Patients with Metal-on-Metal Hip Bearings. *Journal of Bone and Joint Surgery*, 90, 517-522.
- FIFE, B. T. & BLUESTONE, J. A. (2008) Control of peripheral T-cell tolerance and autoimmunity via the CTLA-4 and PD-1 pathways. *Immunological Reviews*, 224, 166-182.
- FIRKINS, P. J., TIPPER, J. L., SAADATZADEH, M. R., INGHAM, E., STONE, M. H., FARRAR, R. & FISHER, J. (2001) Quantitative analysis of wear and

- wear debris from metal-on-metal hip prostheses tested in a physiological hip joint simulator. *Bio-Medical Materials and Engineering*, 11, 143-157.
- FLEURY, C., PETIT, A., MWALE, F., ANTONIOU, J., ZUKOR, D. J., TABRIZIAN, M. & HUK, O. L. (2006) Effect of cobalt and chromium ions on human MG-63 osteoblasts in vitro: Morphology, cytotoxicity, and oxidative stress. *Biomaterials*, 27, 3351-3360.
- FREEMAN, G. J., LONG, A. J., IWAI, Y., BOURQUE, K., CHERNOVA, T., NISHIMURA, H., FITZ, L. J., MALENKOVICH, N., OKAZAKI, T., BYRNE, M. C., HORTON, H. F., FOUSSER, L., CARTER, L., LING, V., BOWMAN, M. R., CARRENO, B. M., COLLINS, M., WOOD, C. R. & HONJO, T. (2000) Engagement of the Pd-1 Immunoinhibitory Receptor by a Novel B7 Family Member Leads to Negative Regulation of Lymphocyte Activation. *The Journal of Experimental Medicine*, 192, 1027-1034.
- GAVIN, I. M., GILLIS, B., ARBIEVA, Z. & PRABHAKAR, B. S. (2007) Identification of human cell responses to hexavalent chromium. *Environmental and Molecular Mutagenesis*, 48, 650-657.
- GLAHN, F., SCHMIDT-HECK, W., ZELLMER, S., GUTHKE, R., WIESE, J., GOLKA, K., HERGENRÖDER, R., DEGEN, G., LEHMANN, T., HERMES, M., SCHORMANN, W., BRULPORT, M., BAUER, A., BEDAWY, E., GEBHARDT, R., HENGSTLER, J. & FOTH, H. (2008) Cadmium, cobalt and lead cause stress response, cell cycle deregulation and increased steroid as well as xenobiotic metabolism in primary normal human bronchial epithelial cells which is coordinated by at least nine transcription factors. *Archives of Toxicology*, 82, 513-524.
- GLASER, U., HOCHRAINER, D., KLÖPPEL, H. & OLDIGES, H. (1986) Carcinogenicity of sodium dichromate and chromium (VI/III)oxide aerosols inhaled by male wistar rats. *Toxicology*, 42, 219-232.
- GOLDSMITH, A., DOWSON, D., ISAAC, G. & LANCASTER, J. (2000) A comparative joint simulator study of the wear of metal-on-metal and alternative material combinations in hip replacements. *Proceedings of the Institution of Mechanical Engineers, Part H: Journal of Engineering in Medicine*, 214, 39-47.
- GOMEZ, P. F. & MORCUENDE, J. A. (2005) Early attempts at hip arthroplasty--1700s to 1950s. *The Iowa Orthopaedic Journal*, 25, 25-9.
- GOODMAN, S. B. (2007) Wear particles, periprosthetic osteolysis and the immune system. *Biomaterials*, 28, 5044-5048.
- GRAMMATOPOULOS, G., PANDIT, H., GLYN-JONES, S., MCLARDY-SMITH, P., GUNDLE, R., WHITWELL, D., GILL, H. S. & MURRAY, D. W. (2010) Optimal acetabular orientation for hip resurfacing. *Journal of Bone and Joint Surgery - British Volume*, 92-B, 1072-1078.
- GRANCHI, D., CENNI, E., CIAPETTI, G., SAVARINO, L., STEA, S., GAMBERINI, S., GORI, A. & PIZZOFERRATO, A. (1998a) Cell death induced by metal ions: necrosis or apoptosis? *Journal of Materials Science: Materials in Medicine*, 9, 31-37.
- GRANCHI, D., CIAPETTI, G., SAVARINO, L., STEA, S., FILIPPINI, F., SUDANESE, A., ROTINI, R. & GIUNTI, A. (2000) Expression of the CD69 activation antigen on lymphocytes of patients with hip prosthesis. *Biomaterials*, 21, 2059-2065.

- GRANCHI, D., VERRI, E., CIAPETTI, G., SAVARINO, L., CENNI, E., GORI, A. & PIZZOFERRATO, A. (1998b) Effects of chromium extract on cytokine release by mononuclear cells. *Biomaterials*, 19, 283-291.
- GREENHALGH, D. G. (1998) The role of apoptosis in wound healing. *The International Journal of Biochemistry & Cell Biology*, 30, 1019-1030.
- GREGUS, Z. & KLAASSEN, C. D. (1986) Disposition of metals in rats: A comparative study of fecal, urinary, and biliary excretion and tissue distribution of eighteen metals. *Toxicology and Applied Pharmacology*, 85, 24-38.
- GRETZER, C., EMANUELSSON, L., LILJENSTEN, E. & THOMSEN, P. (2006) The inflammatory cell influx and cytokines changes during transition from acute inflammation to fibrous repair around implanted materials. *Journal of Biomaterials Science, Polymer Edition*, 17, 669-687.
- GROENEVELD, P. W., KWOH, C. K., MOR, M. K., APPELT, C. J., GENG, M., GUTIERREZ, J. C., WESSEL, D. S. & IBRAHIM, S. A. (2008) Racial differences in expectations of joint replacement surgery outcomes. *Arthritis Care & Research*, 59, 730-737.
- HAILER, N. P., BLAHETA, R. A., DAHLSTRAND, H. & STARK, A. (2011) Elevation of circulating HLA DR+ CD8+ T-cells and correlation with chromium and cobalt concentrations 6 years after metal-on-metal hip arthroplasty. *Acta Orthopaedica*, 82, 6-12.
- HALLAB, N., CAICEDO, M., FINNEGAN, A. & JACOBS, J. (2008) Th1 type lymphocyte reactivity to metals in patients with total hip arthroplasty. *Journal of Orthopaedic Surgery and Research*, 3, 6.
- HALLAB, N. J., MIKECZ, K., VERMES, C., SKIPOR, A. & JACOBS, J. J. (2001) Differential lymphocyte reactivity to serum-derived metal-protein complexes produced from cobalt-based and titanium-based implant alloy degradation. *Journal of Biomedical Materials Research*, 56, 427-436.
- HART, A. J., HESTER, T., SINCLAIR, K., POWELL, J. J., GOODSHIP, A. E., PELE, L., FERSHT, N. L. & SKINNER, J. (2006) The association between metal ions from hip resurfacing and reduced T-cell counts. *Journal of Bone & Joint Surgery - British Volume*, 88-B, 449-454.
- HART, A. J., SKINNER, J. A., WINSHIP, P., FARIA, N., KULINSKAYA, E., WEBSTER, D., MUIRHEAD-ALLWOOD, S., ALDAM, C. H., ANWAR, H. & POWELL, J. J. (2009) Circulating levels of cobalt and chromium from metal-on-metal hip replacement are associated with CD8+ T-cell lymphopenia. *Journal of Bone and Joint Surgery - British Volume*, 91-B, 835-842.
- HAYASHI, Y., KONDO, T., ZHAO, Q.-L., OGAWA, R., CUI, Z.-G., FERIL, L. B., TERANISHI, H. & KASUYA, M. (2004) Signal transduction of p53-independent apoptotic pathway induced by hexavalent chromium in U937 cells. *Toxicology and Applied Pharmacology*, 197, 96-106.
- HUK, O. L., CATELAS, I., MWALE, F., ANTONIOU, J., ZUKOR, D. J. & PETIT, A. (2004) Induction of apoptosis and necrosis by metal ions in vitro. *The Journal of Arthroplasty*, 19, 84-87.
- HUMMER, C. D., ROTHMAN, R. H. & HOZACK, W. J. (1995) Catastrophic failure of modular Zirconia-Ceramic femoral head components after total hip arthroplasty. *The Journal of arthroplasty*, 10, 848-850.

- Iavicoli, I., Falcone, G., Alessandrelli, M., Cresti, R., De Santis, V., Salvatori, S., Alimonti, A. & Carelli, G. (2006) The release of metals from metal-on-metal surface arthroplasty of the hip. *Journal of Trace Elements in Medicine and Biology*, 20, 25-31.
- Ichikawa, Y., Kusaka, Y. & Goto, S. (1985) Biological monitoring of cobalt exposure, based on cobalt concentrations in blood and urine. *International Archives of Occupational and Environmental Health*, 55, 269-276.
- Ingham, E. & Fisher, J. (2000) Biological reactions to wear debris in total joint replacement. *Proceedings of the Institution of Mechanical Engineers, Part H: Journal of Engineering in Medicine*, 214, 21-37.
- Jacobsson, S.-A., Djurf, K. & Wahlstrom, O. (1996) 20-Year Results of McKee-Farrar Versus Charnley Prosthesis. *Clinical Orthopaedics and Related Research*, 329, 60-68.
- Jakobsen, S. S., Danscher, G., Stoltenberg, M., Larsen, A., Bruun, J. M., Mygind, T., Kemp, K. & Soballe, K. (2007) Cobalt-Chromium-Molybdenum Alloy Causes Metal Accumulation and Metallothionein Up-Regulation in Rat Liver and Kidney. *Basic and Clinical Pharmacology and Toxicology*, 101, 441-446.
- Jameson, S. S., Langton, D. J., Natu, S. & Nargol, T. V. F. (2008) The Influence of Age and Sex on Early Clinical Results After Hip Resurfacing: An Independent Center Analysis. *The Journal of Arthroplasty*, 23, 50-55.
- Jansen, H. M. L., Knollema, S., Van der Duin, L. V., Willemssen, A. T. M., Wiersma, A., Franssen, E. J. F., Russel, F. G. M., Korf, J. & Paans, A. M. J. (1996) Pharmacokinetics and Dosimetry of Cobalt-55 and Cobalt-57. *Journal of Nuclear Medicine*, 37, 2082-2086.
- Jarrett, C. A., Ranawat, A. S., Bruzzone, M., Blum, Y. C., Rodriguez, J. A. & Ranawat, C. S. (2009) The Squeaking Hip: A Phenomenon of Ceramic-on-Ceramic Total Hip Arthroplasty. *Journal of Bone and Joint Surgery*, 91, 1344-1349.
- Jenkins, M. K. (1994) The ups and downs of T cell costimulation. *Immunity*, 1, 443-446.
- Kadl, A., Galkina, E. & Leitinger, N. (2009) Induction of CCR2-dependent macrophage accumulation by oxidized phospholipids in the air-pouch model of inflammation. *Arthritis Rheum*, 60, 1362-71.
- Katiyar, S., Awasthi, S. K. & Sahu, R. K. (2008) Suppression of IL-6 level in human peripheral blood mononuclear cells stimulated with PHA/LPS after occupational exposure to chromium. *Science of The Total Environment*, 390, 355-361.
- Kawanishi, S., Hiraku, Y., Murata, M. & Oikawa, S. (2002) The role of metals in site-specific DNA damage with reference to carcinogenesis. *Free Radical Biology and Medicine*, 32, 822-832.
- Keegan, G. M., Learmonth, I. D. & Case, C. P. (2007) Orthopaedic metals and their potential toxicity in the arthroplasty patient: A REVIEW OF CURRENT KNOWLEDGE AND FUTURE STRATEGIES. *Journal of Bone & Joint Surgery, British Volume*, 89-B, 567-573.
- Keegan, G. M., Learmonth, I. D. & Case, C. P. (2008) A Systematic Comparison of the Actual, Potential, and Theoretical Health Effects of Cobalt

- and Chromium Exposures from Industry and Surgical Implants. *Critical Reviews in Toxicology*, 38, 645 - 674.
- KERSTAN, A., ARMBRUSTER, N., LEVERKUS, M. & HUNIG, T. (2006) Cyclosporin A Abolishes CD28-Mediated Resistance to CD95-Induced Apoptosis via Superinduction of Caspase-3. *The Journal of Immunology*, 177, 7689-7697.
- KEURENTJES, J., KUIPERS, R., WEVER, D. & SCHREURS, B. (2008) High Incidence of Squeaking in THAs with Alumina Ceramic-on-ceramic Bearings. *Clinical Orthopaedics and Related Research*®, 466, 1438-1443.
- KRISHAN, A. (1975) Rapid flow cytofluorometric analysis of mammalian cell cycle by propidium iodide staining. *The Journal of Cell Biology*, 66, 188-193.
- KROEMER, G. & MARTIN, S. J. (2005) Caspase-independent cell death. *Nat Med*, 11, 725-730.
- KURTZ, S., LAU, E., ONG, K., ZHAO, K., KELLY, M. & BOZIC, K. (2009) Future Young Patient Demand for Primary and Revision Joint Replacement: National Projections from 2010 to 2030. *Clinical Orthopaedics and Related Research*, 467, 2606-2612.
- KWON, Y.-M., THOMAS, P., SUMMER, B., PANDIT, H., TAYLOR, A., BEARD, D., MURRAY, D. W. & GILL, H. S. (2009a) Lymphocyte proliferation responses in patients with pseudotumors following metal-on-metal hip resurfacing arthroplasty. *Journal of Orthopaedic Research*, 28, 444-450.
- KWON, Y.-M., XIA, Z., GLYN-JONES, S., BEARD, D., GILL, H. S. & MURRAY, D. W. (2009b) Dose-dependent cytotoxicity of clinically relevant cobalt nanoparticles and ions on macrophages in vitro. *Biomedical Materials*, 4, 025018.
- KWON, Y. M., GLYN-JONES, S., SIMPSON, D. J., KAMALI, A., MCLARDY-SMITH, P., GILL, H. S. & MURRAY, D. W. (2010) Analysis of wear of retrieved metal-on-metal hip resurfacing implants revised due to pseudotumours. *The Journal of Bone and Joint Surgery, British Volume*, 92-B, 356-361.
- LADON, D., DOHERTY, A., NEWSON, R., TURNER, J., BHAMRA, M. & CASE, C. P. (2004) Changes in metal levels and chromosome aberrations in the peripheral blood of patients after metal-on-metal hip arthroplasty. *The Journal of Arthroplasty*, 19, 78-83.
- LALAOUNI, A., HENDERSON, C., KUPPER, C. & GRANT, M. H. (2007) The interaction of chromium (VI) with macrophages: Depletion of glutathione and inhibition of glutathione reductase. *Toxicology*, 236, 76-81.
- LALOR, P. A. & REVELL, P. A. (1993) T-lymphocytes and titanium aluminium vanadium (TiAlV) alloy: Evidence for immunological events associated with debris deposition. *Clinical Materials*, 12, 57-62.
- LANGKAMER, V. G., CASE, C. P., HEAP, P., TAYLOR, A., COLLINS, C., PEARSE, M. & SOLOMON, L. (1992) Systemic distribution of wear debris after hip replacement. A cause for concern? *Journal of Bone and Joint Surgery - British Volume*, 74-B, 831-839.
- LANGTON, D. J., JAMESON, S. S., JOYCE, T. J., HALLAB, N. J., NATU, S. & NARGOL, A. V. F. (2010) Early failure of metal-on-metal bearings in hip resurfacing and large-diameter total hip replacement: A CONSEQUENCE

- OF EXCESS WEAR. *Journal of Bone and Joint Surgery - British Volume*, 92-B, 38-46.
- LANGTON, D. J., JAMESON, S. S., JOYCE, T. J., WEBB, J. & NARGOL, A. V. F. (2008) The effect of component size and orientation on the concentrations of metal ions after resurfacing arthroplasty of the hip. *Journal of Bone and Joint Surgery - British Volume*, 90-B, 1143-1151.
- LANGTON, D. J., SPROWSON, A. P., JOYCE, T. J., REED, M., CARLUKE, I., PARTINGTON, P. & NARGOL, A. V. F. (2009) Blood metal ion concentrations after hip resurfacing arthroplasty: A COMPARATIVE STUDY OF ARTICULAR SURFACE REPLACEMENT AND BIRMINGHAM HIP RESURFACING ARTHROPLASTIES. *Journal of Bone and Joint Surgery - British Volume*, 91-B, 1287-1295.
- LAUWERYS, R. & LISON, D. (1994) Health risks associated with cobalt exposure - an overview. *Science of The Total Environment*, 150, 1-6.
- LEARMONTH, I. D. & CASE, C. P. (2007) Metallic debris from orthopaedic implants. *The Lancet*, 369, 542-544.
- LEARMONTH, I. D., YOUNG, C. & RORABECK, C. (2007) The operation of the century: total hip replacement. *The Lancet*, 370, 1508-1519.
- LEGLER, D. F., LOETSCHER, M., ROOS, R. S., CLARK-LEWIS, I., BAGGIOLINI, M. & MOSER, B. (1998) B Cells-attracting Chemokine 1, a Human CXC Chemokine Expressed in Lymphoid Tissues, Selectively Attracts B Lymphocytes via BLR1/CXCR5. *The Journal of Experimental Medicine*, 187, 655-660.
- LENSCHOW, D. J., WALUNAS, T. L. & BLUESTONE, J. A. (1996) CD28/B7 SYSTEM OF T CELL COSTIMULATION. *Annual Review of Immunology*, 14, 233-258.
- LEONARD, S., M. GANNETT, P., ROJANASAKUL, Y., SCHWEGLER-BERRY, D., CASTRANOVA, V., VALLYATHAN, V. & SHI, X. (1998) Cobalt-mediated generation of reactive oxygen species and its possible mechanism. *Journal of Inorganic Biochemistry*, 70, 239-244.
- LESLIE, I., WILLIAMS, S., BROWN, C., ISAAC, G., JIN, Z., INGHAM, E. & FISHER, J. (2008) Effect of bearing size on the long-term wear, wear debris, and ion levels of large diameter metal-on-metal hip replacements—An in vitro study. *Journal of Biomedical Materials Research Part B: Applied Biomaterials*, 87B, 163-172.
- LHOTKA, C., SZEKERES, T., STEFFAN, I., ZHUBER, K. & ZWEYMÜLLER, K. (2003) Four-year study of cobalt and chromium blood levels in patients managed with two different metal-on-metal total hip replacements. *Journal of Orthopaedic Research*, 21, 189-195.
- LONG, P. H. (2008) Medical Devices in Orthopedic Applications. *Toxicologic Pathology*, 36, 85-91.
- LUTZ, M. B., KUKUTSCH, N., OGILVIE, A. L. J., RÖßNER, S., KOCH, F., ROMANI, N. & SCHULER, G. (1999) An advanced culture method for generating large quantities of highly pure dendritic cells from mouse bone marrow. *Journal of Immunological Methods*, 223, 77-92.
- MABILLEAU, G., KWON, Y.-M., PANDIT, H., MURRAY, D. W. & SABOKBAR, A. (2008) Metal-on-metal hip resurfacing arthroplasty: A



- review of periprosthetic biological reactions. *Acta Orthopaedica*, 79, 734-747.
- MACDONALD, S. J., BRODNER, W. & JACOBS, J. J. (2004) A consensus paper on metal ions in metal-on-metal hip arthroplasties. *The Journal of arthroplasty*, 19, 12-16.
- MACDONALD, S. J., MCCALDEN, R. W., CHESS, D. G., BOURNE, R. B., RORABECK, C. H., CLELAND, D. & LEUNG, F. (2003) Metal-on-Metal Versus Polyethylene in Hip Arthroplasty: A Randomized Clinical Trial. *Clinical Orthopaedics and Related Research*, 406.
- MACPHERSON, G. & BREUSCH, S. (2010) Metal-on-metal hip resurfacing: a critical review. *Archives of Orthopaedic and Trauma Surgery*, 1-10.
- MADAN, S., JOWETT, R. L. & GOODWIN, M. I. (2000) Recurrent intrapelvic cyst complicating metal-on-metal cemented total hip arthroplasty. *Archives of Orthopaedic and Trauma Surgery*, 120, 508-510.
- MAEZAWA, K., NOZAWA, M., MATSUDA, K., SUGIMOTO, M., SHITOTO, K. & KUROSAWA, H. (2009) Serum Chromium Levels Before and After Revision Surgery for Loosened Metal-On-Metal Total Hip Arthroplasty. *The Journal of arthroplasty*, 24, 549-553.
- MAHENDRA, G., PANDIT, H., KLISKEY, K., MURRAY, D., GILL, H. S. & ATHANASOU, N. (2009) Necrotic and inflammatory changes in metal-on-metal resurfacing hip arthroplasties. *Acta Orthopaedica*, 80, 653-659.
- MALEK, T. R. (2008) The Biology of Interleukin-2. *Annual Review of Immunology*, 26, 453-479.
- MARTÍN-ROMERO, C., SANTOS-ALVAREZ, J., GOBERNA, R. & SÁNCHEZ-MARGALET, V. (2000) Human Leptin Enhances Activation and Proliferation of Human Circulating T Lymphocytes. *Cellular Immunology*, 199, 15-24.
- MARX, M., WEBER, M., MERKEL, F., BUSCHENFELDE, M. Z. K. H. & KOHLER, H. (1990) Additive Effects of Calcium Antagonists on Cyclosporin A-Induced Inhibition of T-Cell Proliferation. *Nephrology Dialysis Transplantation*, 5, 1038-1044.
- MATTHIES, A., UNDERWOOD, R., CANN, P., ILO, K., NAWAZ, Z., SKINNER, J. & HART, A. J. (2011) Retrieval analysis of 240 metal-on-metal hip components, comparing modular total hip replacement with hip resurfacing. *Journal of Bone and Joint Surgery - British Volume*, 93-B, 307-314.
- MCCOY, K. M. & LE GROS, G. (1999) The role of CTLA-4 in the regulation of T cell immune responses. *Immunol Cell Biol*, 77, 1-10.
- MCMINN, D., TREACY, R., LIN, K. & PYNSENT, P. (1996) Metal on Metal Surface Replacement of the Hip: Experience of the McMinn Prosthesis. *Clinical Orthopaedics and Related Research*, 329, 89-98.
- MDA/2010/033 (2010) Medical Device Alert: All metal-on-metal (MoM) hip replacements (MDA/2010/033). IN MHRA (Ed.).
- MEDLEY, J. B., CHAN, F. W., KRYGIER, J. J. & BOBYN, J. D. (1996) Comparison of Alloys and Designs in a Hip Simulator Study of Metal on Metal Implants. *Clinical Orthopaedics and Related Research*, 329, 148-159.
- MEROLLA, L. & RICHARDS, R. J. (2005) IN VITRO EFFECTS OF WATER-SOLUBLE METALS PRESENT IN UK PARTICULATE MATTER. *Experimental Lung Research*, 31, 671-683.

- MERRITT, K. & BROWN, S. A. (1995) Release of hexavalent chromium from corrosion of stainless steel and cobalt—chromium alloys. *Journal of Biomedical Materials Research*, 29, 627-633.
- MERRITT, K. & BROWN, S. A. (1996) Distribution of Cobalt Chromium Wear and Corrosion Products and Biologic Reactions. *Clinical Orthopaedics and Related Research*, 329, 233-243.
- MERRITT, K. & RODRIGO, J. J. (1996) Immune Response to Synthetic Materials: Sensitization of Patients Receiving Orthopaedic Implants. *Clinical Orthopaedics and Related Research*, 326, 71-79.
- MIKSCH, L. W. & LEWALTER, J. (1997) Health Surveillance and Biological Effect Monitoring for Chromium-Exposed Workers. *Regulatory Toxicology and Pharmacology*, 26, S94-S99.
- MILOSEV, I., TREBSE, R., KOVAC, S., COR, A. & PISOT, V. (2006) Survivorship and Retrieval Analysis of Sikomet Metal-on-Metal Total Hip Replacements at a Mean of Seven Years. *Journal of Bone and Joint Surgery*, 88, 1173-1182.
- MORONI, A., SAVARINO, L., CADOSSO, M., BALDINI, N. & GIANNINI, S. (2008) Does Ion Release Differ Between Hip Resurfacing and Metal-on-metal THA? *Clinical Orthopaedics and Related Research*, 466, 700-707.
- MOSMANN, T. (1983) Rapid colorimetric assay for cellular growth and survival: Application to proliferation and cytotoxicity assays. *Journal of Immunological Methods*, 65, 55-63.
- MURPHY, K., TRAVERS, P. & MARK, W. (2007) *Janeway's Immunobiology*, Garland Science.
- NOEL, P. J., BOISE, L. H., GREEN, J. M. & THOMPSON, C. B. (1996) CD28 costimulation prevents cell death during primary T cell activation. *The Journal of Immunology*, 157, 636-642.
- O'BRIEN, T., MANDEL, H. G., PRITCHARD, D. E. & PATIERNO, S. R. (2002a) Critical Role of Chromium (Cr)<sup>6+</sup> DNA Interactions in the Formation of Cr-Induced Polymerase Arresting Lesions. *Biochemistry*, 41, 12529-12537.
- O'BRIEN, T. J., FORNSAGLIO, J. L., CERYAK, S. & PATIERNO, S. R. (2002b) Effects of hexavalent chromium on the survival and cell cycle distribution of DNA repair-deficient *S. cerevisiae*. *DNA Repair*, 1, 617-627.
- PANDIT, H., GLYN-JONES, S., MCLARDY-SMITH, P., GUNDLE, R., WHITWELL, D., GIBBONS, C. L. M., OSTLER, S., ATHANASOU, N., GILL, H. S. & MURRAY, D. W. (2008) Pseudotumours associated with metal-on-metal hip resurfacings. *Journal of Bone and Joint Surgery - British Volume*, 90-B, 847-851.
- PARK, Y.-S., HWANG, S.-K., CHOY, W.-S., KIM, Y.-S., MOON, Y.-W. & LIM, S.-J. (2006) Ceramic Failure After Total Hip Arthroplasty with an Alumina-on-Alumina Bearing. *Journal of Bone and Joint Surgery*, 88, 780-787.
- PETIT, A., MWALE, F., TKACZYK, C., ANTONIOU, J., ZUKOR, D. J. & HUK, O. L. (2006) Cobalt and chromium ions induce nitration of proteins in human U937 macrophages in vitro. *J Biomed Mater Res A*, 79, 599-605.
- POITOUT, D. G. & KOTZ, R. (2004) Biomaterials for Total Joint Replacements. *Biomechanics and Biomaterials in Orthopedics*. New York, Springer.
- POYNER, D. R., COOKE, F., HANLEY, M. R., REYNOLDS, D. J. & HAWKINS, P. T. (1993) Characterization of metal ion-induced [3H]inositol

- hexakisphosphate binding to rat cerebellar membranes. *The Journal of Biological Chemistry*, 268, 1032-1038.
- PRITCHARD, D. E., CERYAK, S., HA, L., FORNSAGLIO, J. L., HARTMAN, S. K., O'BRIEN, T. J. & PATIERNO, S. R. (2001) Mechanism of apoptosis and determination of cellular fate in chromium(VI)-exposed populations of telomerase-immortalized human fibroblasts. *Cell Growth Differ*, 12, 487-96.
- PRITCHARD, D. E., SINGH, J., CARLISLE, D. L. & PATIERNO, S. R. (2000) Cyclosporin A inhibits chromium(VI)-induced apoptosis and mitochondrial cytochrome c release and restores clonogenic survival in CHO cells. *Carcinogenesis*, 21, 2027-2033.
- PULIDO, M. D. & PARRISH, A. R. (2003) Metal-induced apoptosis: mechanisms. *Mutation Research/Fundamental and Molecular Mechanisms of Mutagenesis*, 533, 227-241.
- QUIEVRYN, G., PETERSON, E., MESSER, J. & ZHITKOVICH, A. (2003) Genotoxicity and Mutagenicity of Chromium(VI)/Ascorbate-Generated DNA Adducts in Human and Bacterial Cells. *Biochemistry*, 42, 1062-1070.
- RAFFN, E., MIKKELSEN, S., ALTMAN, D. G., CHRISTENSEN, J. M. & GROTH, S. (1988) Health effects due to occupational exposure to cobalt blue dye among plate painters in a porcelain factory in Denmark. *Scand J Work Environ Health*, 14, 378-84.
- RAGHUNATHAN, V. K., TETTEY, J. N. A., ELLIS, E. M. & GRANT, M. H. (2009) Comparative chronic in vitro toxicity of hexavalent chromium to osteoblasts and monocytes. *Journal of Biomedical Materials Research Part A*, 88A, 543-550.
- RASQUINHA, V. J., RANAWAT, C. S., WEISKOPF, J., RODRIGUEZ, J. A., SKIPOR, A. K. & JACOBS, J. J. (2006) Serum Metal Levels and Bearing Surfaces in Total Hip Arthroplasty. *The Journal of arthroplasty*, 21, 47-52.
- RATNER, B. D., HOFFMAN, A. S., SCHOEN, F. J. & LEMONS, J. E. (2004 ) *Biomaterials Science: An Introduction to Materials in Medicine*
- REPETTO, G., DEL PESO, A. & ZURITA, J. L. (2008) Neutral red uptake assay for the estimation of cell viability/cytotoxicity. *Nat. Protocols*, 3, 1125-1131.
- REUTER, H. (1983) Calcium-Channel Modulation by Neurotransmitters, Enzymes and Drugs. *Nature*, 301, 569-574.
- ROCK, K. L., LATZ, E., ONTIVEROS, F. & KONO, H. (2010) The Sterile Inflammatory Response. *Annual Review of Immunology, Vol 28*. Palo Alto, Annual Reviews.
- ROESEMS, G., HOET, P. H. M., DINSDALE, D., DEMEDTS, M. & NEMERY, B. (2000) In Vitro Cytotoxicity of Various Forms of Cobalt for Rat Alveolar Macrophages and Type II Pneumocytes. *Toxicology and Applied Pharmacology*, 162, 2-9.
- RÜDIGER, A., DIRK, B., MAREIKE, B., CHRISTIAN, R. F. & PETER, H. K. (2006) How T lymphocytes switch between life and death. *European Journal of Immunology*, 36, 1654-1658.
- RUSSO, P., CATASSI, A., CESARIO, A., IMPERATORI, A., ROTOLO, N., FINI, M., GRANONE, P. & DOMINIONI, L. (2005) Molecular Mechanisms of Hexavalent Chromium-Induced Apoptosis in Human Bronchoalveolar Cells. *American Journal of Respiratory Cell and Molecular Biology*, 33, 589-600.

- SANDERS, C., DONOVAN, J. L. & DIEPPE, P. A. (2004) Unmet need for joint replacement: a qualitative investigation of barriers to treatment among individuals with severe pain and disability of the hip and knee. *Rheumatology*, 43, 353-357.
- SARGEANT, A. & GOSWAMI, T. (2007) Hip implants - Paper VI - Ion concentrations. *Materials & Design*, 28, 155-171.
- SAUVE, P., MOUNTNEY, J., KHAN, T., DE BEER, J., HIGGINS, B. & GROVER, M. (2007) Metal ion levels after metal-on-metal Ring total hip replacement: A 30-YEAR FOLLOW-UP STUDY. *Journal of Bone and Joint Surgery - British Volume*, 89-B, 586-590.
- SAVARINO, L., GRANCHI, D., CIAPETTI, G., CENNI, E., NARDI PANTOLI, A., ROTINI, R., VERONESI, C. A., BALDINI, N. & GIUNTI, A. (2002) Ion release in patients with metal-on-metal hip bearings in total joint replacement: A comparison with metal-on-polyethylene bearings. *Journal of Biomedical Materials Research*, 63, 467-474.
- SAVARINO, L., GRANCHI, D., CIAPETTI, G., STEA, S., DONATI, M. E., ZINGHI, G., FONTANESI, G., ROTINI, R. & MONTANARO, L. (1999) Effects of metal ions on white blood cells of patients with failed total joint arthroplasties. *Journal of Biomedical Materials Research Part A*, 47, 543-550.
- SCHAFFER, A. W., SCHAFFER, A., PILGER, A., ENGELHARDT, C., ZWEYMUELLER, K. & RUEDIGER, H. W. (1999) Increased Blood Cobalt and Chromium After Total Hip Replacement. *Clinical Toxicology*, 37, 839-844.
- SCHMALZRIED, T. P., SZUSZCZEWICZ, E. S., NORTHFIELD, M. R., AKIZUKI, K. H., FRANKEL, R. E., BELCHER, G. & AMSTUTZ, H. C. (1998) Quantitative assessment of walking activity after total hip or knee replacement. *The Journal of Bone & Joint Surgery*, 80, 54-59.
- SEDGWICK, A. D., SIN, Y. M., EDWARDS, J. C. W. & WILLOUGHBY, D. A. (1983) Increased inflammatory reactivity in newly formed lining tissue. *The Journal of Pathology*, 141, 483-495.
- SEMLITSCH, M. & WILLERT, H. (1997) Clinical wear behaviour of ultra-high molecular weight polyethylene cups paired with metal and ceramic ball heads in comparison to metal-on-metal pairings of hip joint replacements. *Proceedings of the Institution of Mechanical Engineers, Part H: Journal of Engineering in Medicine*, 211, 73-88.
- SHETTLEMORE, M. G. & BUNDY, K. J. (1999) Toxicity measurement of orthopedic implant alloy degradation products using a bioluminescent bacterial assay. *Journal of Biomedical Materials Research*, 45, 395-403.
- SHIMMIN, A., BEAULE, P. E. & CAMPBELL, P. (2008) Metal-on-Metal Hip Resurfacing Arthroplasty. *The Journal of Bone and Joint Surgery*, 90, 637-654.
- SIEBER, H. P., RIEKER, C. B. & KOTTIG, P. (1999) Analysis of 118 second-generation metal-on-metal retrieved hip implants. *Journal of Bone and Joint Surgery - British Volume*, 81-B, 46-50.
- SIPOWICZ, M. A., ANDERSON, L. M., UTERMAHLEN, W. E., ISSAQ, H. J. & KASPRZAK, K. S. (1997) Uptake and tissue distribution of chromium(III) in

- mice after a single intraperitoneal or subcutaneous administration. *Toxicology Letters*, 93, 9-14.
- SMITH-GARVIN, J. E., KORETZKY, G. A. & JORDAN, M. S. (2009) T Cell Activation. *Annual Review of Immunology*, 27, 591-619.
- SMITH, S. L., ELFICK, A. P. D. & UNSWORTH, A. (1999) An evaluation of the tribological performance of zirconia and CoCrMo femoral heads. *Journal of Materials Science*, 34, 5159-5162.
- SONG, E., OUYANG, N., HÖRBEIT, M., ANTUS, B., WANG, M. & EXTON, M. S. (2000) Influence of Alternatively and Classically Activated Macrophages on Fibrogenic Activities of Human Fibroblasts. *Cellular Immunology*, 204, 19-28.
- TIPPER, J. L., INGHAM, E., JIN, Z. M. & FISHER, J. (2005) (iv) The science of metal-on-metal articulation. *Current Orthopaedics*, 19, 280-287.
- TKACZYK, C., HUK, O. L., MWALE, F., ANTONIOU, J., ZUKOR, D. J., PETIT, A. & TABRIZIAN, M. (2009) The molecular structure of complexes formed by chromium or cobalt ions in simulated physiological fluids. *Biomaterials*, 30, 460-467.
- TODD, I. & SPIKETT, G. (2010) *Immunology*, Wiley-Blackwell.
- TOMS, A. P., MARSHALL, T. J., CAHIR, J., DARRAH, C., NOLAN, J., DONELL, S. T., BARKER, T. & TUCKER, J. K. (2008) MRI of early symptomatic metal-on-metal total hip arthroplasty: a retrospective review of radiological findings in 20 hips. *Clinical Radiology*, 63, 49-58.
- TORTORA, G. J. & GRABOWSKI, S. R. (2010) *Principles of anatomy and physiology*, John Wiley.
- TSAPAKOS, M. J., HAMPTON, T. H. & WETTERHAHN, K. E. (1983) Chromium(VI)-induced DNA Lesions and Chromium Distribution in Rat Kidney, Liver, and Lung. *Cancer Research*, 43, 5662-5667.
- VASANT, C., BALAMURUGAN, K., RAJARAM, R. & RAMASAMI, T. (2001) Apoptosis of Lymphocytes in the Presence of Cr(V) Complexes: Role in Cr(VI)-Induced Toxicity. *Biochemical and Biophysical Research Communications*, 285, 1354-1360.
- VASANT, C., RAJARAM, R. & RAMASAMI, T. (2003) Apoptosis of lymphocytes induced by chromium(VI) is through ROS-mediated activation of Src-family kinases and caspase-3. *Free Radical Biology and Medicine*, 35, 1082-1100.
- VENDITTOLI, P. A., MOTTARD, S., ROY, A. G., DUPONT, C. & LAVIGNE, M. (2007) Chromium and cobalt ion release following the Durom high carbon content, forged metal-on-metal surface replacement of the hip. *Journal of Bone and Joint Surgery - British Volume*, 89-B, 441-448.
- VERMES, I., HAANEN, C., STEFFENS-NAKKEN, H. & REUTELLINGSPERGER, C. (1995) A novel assay for apoptosis Flow cytometric detection of phosphatidylserine expression on early apoptotic cells using fluorescein labelled Annexin V. *Journal of Immunological Methods*, 184, 39-51.
- WANG, J. Y., TSUKAYAMA, D. T., WICKLUND, B. H. & GUSTILO, R. B. (1996a) Inhibition of T and B cell proliferation by titanium, cobalt, and chromium: Role of IL-2 and IL-6. *Journal of Biomedical Materials Research Part A*, 32, 655-661.

- WANG, J. Y., WICKLUND, B. H., GUSTILO, R. B. & TSUKAYAMA, D. T. (1996b) Titanium, chromium and cobalt ions modulate the release of bone-associated cytokines by human monocytes/macrophages in vitro. *Biomaterials*, 17, 2233-2240.
- WEHNER, A. P. & CRAIG, D. K. (1972) Toxicology of Inhaled NiO and CoO in Syrian Golden Hamsters. Taylor & Francis.
- WILLERT, H.-G., BUCHHORN, G. H., FAYYAZI, A., FLURY, R., WINDLER, M., KOSTER, G. & LOHMANN, C. H. (2005) Metal-on-Metal Bearings and Hypersensitivity in Patients with Artificial Hip Joints. A Clinical and Histomorphological Study. *The Journal of Bone and Joint Surgery*, 87, 28-36.
- WILLIAMS, S., LESLIE, I., ISAAC, G., JIN, Z., INGHAM, E. & FISHER, J. (2008) Tribology and Wear of Metal-on-Metal Hip Prostheses: Influence of Cup Angle and Head Position. *The Journal of Bone & Joint Surgery*, 90, 111-117.
- WITKIEWICZ-KUCHARCZYK, A. & BAL, W. (2006) Damage of zinc fingers in DNA repair proteins, a novel molecular mechanism in carcinogenesis. *Toxicology Letters*, 162, 29-42.
- WITZLEB, W.-C., ZIEGLER, J., KRUMMENAUER, F., NEUMEISTER, V. & GUENTHER, K.-P. (2006) Exposure to chromium, cobalt and molybdenum from metal-on-metal total hip replacement and hip resurfacing arthroplasty. *Acta Orthopaedica*, 77, 697-705.
- WOLPE, S. D., SHERRY, B., JUERS, D., DAVATELIS, G., YURT, R. W. & CERAMI, A. (1989) Identification and characterization of macrophage inflammatory protein 2. *Proceedings of the National Academy of Sciences*, 86, 612-616.
- WOOLEY, P. H., MORREN, R., ANDARY, J., SUD, S., YANG, S.-Y., MAYTON, L., MARKEL, D., SIEVING, A. & NASSER, S. (2002) Inflammatory responses to orthopaedic biomaterials in the murine air pouch. *Biomaterials*, 23, 517-526.
- WULFING, C., RABINOWITZ, J. D., BEESON, C., SJAASTAD, M. D., MCCONNELL, H. M. & DAVIS, M. M. (1997) Kinetics and Extent of T Cell Activation as Measured with the Calcium Signal. *The Journal of Experimental Medicine*, 185, 1815-1825.
- YANG, J. & BLACK, J. (1994) Competitive binding of chromium, cobalt and nickel to serum proteins. *Biomaterials*, 15, 262-268.
- YE, J. & SHI, X. (2001) Gene expression profile in response to chromium-induced cell stress in A549 cells. *Molecular and Cellular Biochemistry*, 222, 189-197.
- YE, J., WANG, S., LEONARD, S. S., SUN, Y., BUTTERWORTH, L., ANTONINI, J., DING, M., ROJANASAKUL, Y., VALLYATHAN, V., CASTRANOVA, V. & SHI, X. (1999) Role of Reactive Oxygen Species and p53 in Chromium(VI)-induced Apoptosis. *The Journal of Biological Chemistry*, 274, 34974-34980.
- ZHANG, X.-H., ZHANG, X., WANG, X.-C., JIN, L.-F., YANG, Z.-P., JIANG, C.-X., CHEN, Q., REN, X.-B., CAO, J.-Z., WANG, Q. & ZHU, Y.-M. (2011) Chronic occupational exposure to hexavalent chromium causes DNA damage in electroplating workers. *BMC Public Health*, 11, 224-231.
- ZHENG, Y. & RUDENSKY, A. Y. (2007) Foxp3 in control of the regulatory T cell lineage. *Nat Immunol*, 8, 457-462.